GROUNDWATER CHARACTERISATION AND DISPOSAL MODELLING FOR COAL SEAM GAS RECOVERY

A thesis submitted in partial fulfilment of

the requirements for the Degree of PhD in

Environmental Engineering in the

University of Canterbury

by Mauricio Taulis

University of Canterbury

2007

Contents

List of Tables

List of Figures

Acknowledgements

This thesis was carried out at the Civil Engineering Department, University of Canterbury and CRL Energy Ltd in conjunction with L&M Mining Ltd, with funding from the New Zealand Foundation for Science and Technology (Technology for Industry Fellowship). Special thanks to CRL Energy Ltd for their support while carrying out this work.

Throughout this thesis, several people provided help and advice for carrying out this work and so they disserve special thanks. First and foremost I would like to thank my main supervisor, Dr Mark Milke (University of Canterbury), for his help, advice, and support while carrying out this work. Mark not only gave me invaluable guidance and insight throughout this thesis, but he also motivated me beyond normal limits, transmitting me his optimism and always offering me his encouragement. Without Mark's help, this research would not have been possible. I would also like to thank David Trumm (CRL Energy Ltd) who, since the beginning, offered me his valuable help. Dave's friendly advice never failed to cheer me up and provide me with a fresh new perspective. Thank you Dave. Also, I am very grateful to Professor James Bauder (Montana State University) and his team for extending me his help. Jim's help came at a critical time and his advice gave me much needed direction.

Many thanks to Dr David Nobes (University of Canterbury) for his help and advice throughout this work. Dr Tom Cochrane disserves a special thank you for his help with GIS modelling. Also, I would like to thank Dr Aisling O'Sullivan (University of Canterbury) for her advice. Ron Drake (Drake Engineering Incorporated) disserves a special mention for meeting with me and discussing ion exchange technology. Thanks to Mick Ryan (L&M Mining Ltd) for his help in collecting samples. Finally, personal thanks to my friends and family who have helped me with their unconditional love and support throughout the completion of this thesis.

Abstract

Coal Seam Gas (CSG) is a form of natural gas (mainly methane) sorbed in underground coal deposits. Mining this gas involves drilling a well directly into an underground coal seam, and pumping out the water (CSG water) flowing through it. Presently, CSG is under exploration in New Zealand (NZ); however, there is concern about CSG water disposal in NZ mainly because of the controversy that this activity has generated in some basins in the United States (US).

The first part of this thesis studies CSG water from a well in Maramarua (NZ) and compares it to water from US basins. The NZ CSG water from this well had high pH (7.8), alkalinity in the order of 360 mg/l as $CaCO_3$, high sodium (334 mg/l), bicarbonate (435 mg/l), and chloride (146 mg/l). These ions also occur in US CSG waters, and their concentrations follow the same trend – high sodium, bicarbonate, and chloride with low calcium, magnesium, and sulphate concentrations. Prior to this work, little detailed analyses of CSG water quality variability from a well had been carried out. A Factor Analysis of 33 Maramarua samples was conducted and revealed that about one third of the variations were due to sample degassing, which induced calcium carbonate precipitation - this was supported by experimental work (sample sparging) and geochemical modelling (MINTEQA2). This finding is important for CSG water management because, as calcium concentrations decrease, higher SAR values are generated, and this can cause problems if CSG waters are disposed on land.

In the second part, this thesis assesses the potential environmental effects of disposing CSG waters in NZ by formulating management options and a simple wastewater treatment system. This was carried out by studying the ecological response (soils, plant, and aquatic life) resulting from CSG water disposal operations in the US, and by applying relevant salinity and sodicity guidelines to the interaction between soils and CSG waters from Maramarua. This work showed that similar problems are likely to occur in NZ if CSG water disposal takes place without proper controls. Such a study has never been carried out in a region before actual CSG development has taken place, so this work shows how to quantify the effects arising from CSG water disposal prior to full scale production. This can be particularly useful for CSG stakeholders wanting to develop this resource in other regions around the world.

A simple treatment system using Ngakuru zeolites has proven effective in reducing the SAR of Maramarua CSG water. Laboratory results indicate that these zeolites work by exchanging sodium cations in the water by other cations contained within the zeolite structure but with slow ion exchange kinetics. The calculated sodium absorption capacity for these natural zeolites ranged from 11.3 meq/100g to 16.7 meq/100g (flow-through conditions without previous regeneration). In addition, these experiments showed that the ion exchange process is accompanied by some dissolution (sulphate, boron, TOC, sodium, calcium, magnesium, potassium and reactive silica), but mainly at the beginning of the treatment process. Nevertheless, using this system, 180 grams of zeolite material were used to treat an initial 1.83 litres of Maramarua CSG water thus reducing potential soil infiltration problems to nil. As more CSG water was treated, the zeolites kept reducing SAR values but at a lesser rate until 4.53 litres of CSG water had been treated. A step-by-step methodology to assess treatment design options for these materials has been developed and will aid future researchers and engineers

This thesis presents the first comprehensive study of CSG water management in NZ. It also presents an ion exchange treatment system using natural zeolites already available in NZ. In conclusion, the research finds that, whether through adequate management or active treatment, CSG waters can be safely disposed without creating major environmental problems, and can even be used in beneficial applications.

Chapter 1

General Introduction

Objective

Coal Seam Gas (CSG) exploration is currently taking place in New Zealand, and there is a reasonable expectation about the opportunities this new energy source will create. Also, there is concern about the potential environmental effects arising from CSG extraction and, in this context, the main issue is having to deal with large amounts of co-produced water (CSG water). Therefore, questions about this issue immediately spring to mind. For example, what will be the nature of CSG waters arising from CSG production operations in New Zealand? Are NZ CSG stakeholders bound to experience the same problems as other CSG stakeholders have encountered in the US? What sort of environmental issues will take place in relation to CSG water disposal? Can these problems be prevented or reduced using cost effective methods? These and other questions are answered throughout this thesis whilst taking a closer look at CSG water quality issues in context with New Zealand conditions.

Full scale CSG production has not started yet in New Zealand, so the environmental problems that could arise due to CSG water disposal have never existed in this country. Coal Seam Gas is such a new resource in New Zealand that, before this thesis was started, nothing was known about the quality of CSG co-produced waters in New Zealand or the potential environmental problems arising from their disposal. Therefore, rather than focusing on one particular aspect, this thesis focuses on the whole range of issues related to CSG water in New Zealand. Each one of this thesis' chapters is an independent study, but the later chapters heavily rely on the findings from the first chapters. The first chapters (2-3) include a study on the origins and nature of CSG water in New Zealand, while the potential environmental problems related to CSG water disposal, management and treatment options are accounted in subsequent chapters (4-5).

Thesis outline

A description of each of the chapters is as follows:

1) Chapter 1. “Introduction”. In this chapter the objectives are laid out and the thesis outline is described.
2) Chapter 2. “Identification of Coal Seam Gas waters in New Zealand”. This chapter describes the origins and defining characteristics of CSG waters. It also presents a methodology for analysing New Zealand CSG water samples, and presents actual CSG water quality data from a well in Maramarua.
3) Chapter 3. “Coal Seam Gas water quality variability”. By using a factor analysis, the major sources of water quality variations are identified and explained in this chapter. These findings are further supported by experimental work and geochemical modelling.
4) Chapter 4. “Potential environmental impacts associated with coal seam gas water management in New Zealand”. In this chapter, a methodology for assessing the potential environmental effects arising from CSG water disposal is developed.
5) Chapter 5. “Sodium removal from Maramarua coal seam gas waters using Ngakuru zeolites”. Here, a specific wastewater treatment method using readily available materials in New Zealand (Ngakuru zeolites) is explored.
6) Chapter 6. “General conclusions”.

Chapters 2-5 were written as individual pieces of work to facilitate their publication. As such, all of these chapters have their own introductions, methodologies, results, discussions, conclusions, and lists of references. However, these chapters follow a chronological line of thought with the first chapters providing support and information to subsequent ones. As a whole, this thesis constitutes an integral piece of work dealing with the origin and fate of CSG water - CSG water production, CSG water quality, disposal, potential environmental problems arising from its disposal, and possible solutions (including treatment). Consequently, this thesis can be a useful piece of research, which can help CSG stakeholders assess best practice options for managing CSG waters in New Zealand.

Chapter 2

Identification of Coal Seam Gas waters in New Zealand

Introduction

Coal Seam Gas (CSG) is mainly methane gas sorbed (absorbed and adsorbed) in underground coal beds. The procedure for mining this gas involves drilling a hole that directly targets one or more coal seams and pumping out groundwater in order to recover methane gas. This gas is generated in the coal through biogenic and thermogenic processes, and is sorbed into the coal's micropores; it will remain in the micropores as long as there is enough piezometric energy pushing it into the coal matrix. When the piezometric surface is lowered by artificial means (e.g. pumping), methane gas is released from the micropores and flows out of the well. However to achieve this, large quantities of groundwater have to be pumped out to the surface. Therefore, CSG waters need to be properly disposed of to safeguard the environment without compromising other natural resources.

Before CSG extraction takes place in New Zealand, it is essential to understand the nature of these waters and their environment. In doing so, a conceptual model for the formation of CSG is presented and corroborated with actual water quality data from known CSG generating basins in the United States. Subsequently, water quality data from potential CSG sites in NZ are presented and compared against the geochemical signature for CSG waters. These data will constitute the basis for evaluating the potential environmental problems that would arise when dealing with water co-produced with CSG once production is underway.

The term "CBM" is used as an acronym for Coalbed Methane, which is the term used in the United States to refer to this natural resource. In New Zealand, however, the term Coal Seam Gas is used instead to better reflect its source and gaseous state. In this paper, the term "CSG" will be used as an acronym for Coal Seam Gas, and "CSG water(s)" will be used to refer to the waters co-produced with CSG. Occasionally, the term "CBM" and "CBM water(s)" will be used to refer to CSG and CSG waters in the United States.

The genesis of coal seam gas

Coal seam gas is a product of the anaerobic processes (biogenic) and temperature transformations (thermogenic) associated with the formation of coal. This gas consists mainly of methane, carbon dioxide and sometimes other hydrocarbon gases.

Initially, plant detritus is deposited as peat and then buried by the deposition of sediments of marine or terrestrial origin. This organic matter is first decomposed by aerobic respiration as oxygen is readily available in voids and dissolved in water, which has been in contact with the atmosphere. However, as the burial process continues and oxygen is depleted, these organisms are unable to function aerobically. At the end of this process, the pH of the water contained in these voids tends to be neutral.

At this point the biodegradation process turns from aerobic respiration to anaerobic respiration or fermentation. Anaerobic decomposition is well documented as it normally takes place in anoxic environments such as the digestive tracks of animals, swamps, and landfills to mention a few. In buried coal seams the same processes of anaerobic decomposition occur. Here, facultative anaerobic bacteria breakdown organic matter in a series of redox chemical reactions (Bartos et al., 2002). These reactions take place in succession (4 phases) under different conditions as different types of bacteria consume available organic matter. The first of these reactions is *sulphate reduction* which becomes the dominant form of respiration especially in depositions of marine association where large concentrations of sulphate are available (Rice, 1993).

After sulphate reduction has finalised, the decomposition process continues with an *acidic stage*. Here, the process is taken over by hydrolytic, fermentative, and acetogenic bacteria which can thrive in the absence of oxygen. This results in the production of carbon dioxide and the accumulation of carboxylic acids, which causes a decrease in pH (Kjeldsen et al., 2002). This leads to a third phase of decomposition which is an *initial methanogenic phase*. During this phase, the acids generated in the acidic stage are converted into methane and carbon dioxide by methanogenic bacteria, therefore pH values increase considerably (Kjeldsen et al., 2002). The fourth and last phase can be referred to as *methanogenesis*. Here, methane production reaches its

maximum but then decreases after the carboxylic acids are consumed, which makes pH values increase even further (Kjeldsen et al., 2002). In this way, after the end of the first phase when sulphate reduction has finalised, the methane generation process can take place through two different pathways: carbon dioxide reduction and methyl-type fermentation (Jenden and Kaplan, 1986; Schoell, 1980; Whiticar et al., 1986; Woltemate et al., 1984). Chapelle (2001) has presented two generalised reactions (Eq 2.1 and Eq 2.2) showing the two pathways for methane generation from the biodegradation of organic matter:

Methyl-group fermentation:

$$CH_3COOH \rightarrow CH_4 + CO_2$$

(acetic acid or carboxylic acids)

Eq 2.1

Carbon dioxide reduction:

$$CO_2 + 4H_2 \rightarrow CH_4 + 2H_2O$$

Eq 2.2

Decker et al. (1987) have summarised the methanation process occurring in coal seams using equations for different steps in the process (Eq 2.3 - Eq 2.5). In this model, "CH_2O" represents organic matter which is transformed into H_2O, H_2S, HS^-, and CO_2 while at the same time reducing sulphate (SO_4^{2-}) to H_2S and HS^-. Because of carbonate equilibrium, CO_2 can be expressed in terms of HCO_3^- and H^+ ions. At this stage, methyl-group fermentation and carbon dioxide reduction are responsible for methane (CH_4) being generated (Eq 2.5). Not all the CO_2 is transformed into methane, some of it dissociates into bicarbonate (HCO_3^-), and some of it stays dissolved in the water.

$$SO_4^{2-} + 2CH_2O + 2H^+ \leftrightarrows H_2S + 2H_2O + 2CO_2 \qquad pH < 7.0$$

Eq 2.3

$$SO_4^{2-} + 2CH_2O + H^+ \leftrightarrows HS^- + 2H_2O + 2CO_2 \qquad pH > 7.0$$

Eq 2.4

$$2CH_2O + H_2O \leftrightarrows CH_4 + HCO_3^- + H^+$$

Eq 2.5

Summarising, the anaerobic decomposition of organic matter yields low SO_4^{2-} concentrations but high CO_2^{2-} and HCO_3^- concentrations with increasing methanation. It is important to note that, in these equations, the actual methane generation process

takes place only after sulphate reduction has taken place. This is because sulphate reduction is the dominant form of anaerobic respiration for non-methane-producing bacteria. Also for this reason "biogenic methane does not accumulate in significant amounts in the presence of high concentrations of dissolved sulphate" (Rice and Claypool, 1981). Biogenic methane generated like this is normally referred to as early stage. It estimated that most of the ancient biogenic gas accumulations took place in this early stage (Rice, 1992; Rice and Claypool, 1981) over a period of tens of thousands of years after burial (Claypool and Kaplan, 1974).

Gas and water production are directly related to the coal maturation process, which is described by coal rank. Vitrinite is a type of organic material which is the primary component of coal, and vitrinite reflectance is a parameter normally used to establish the thermal maturity of coals (coal rank). Figure 2.1 presents the different types of coal rank with matching vitrinite reflectance values. In terms of CSG generation, thermogenic gas is formed when coals reach a certain level of thermal maturity, which generally corresponds to high-volatile A bituminous coal (Scott, 2000). Low rank coals (peat, lignites, and sub-bituminous) have high porosities, high water content, and low temperature biogenic methane (ALL-Consulting, 2003). As the burial process continues, higher temperatures and pressures develop, making it difficult for bacteria to survive (Nuccio, 2002). Thus biogenesis ceases and thermogenesis begins. The thermogenic process is not just a temperature transformation; it also involves chemical and physical transformations that result in further coalification of the organic matter. In coalification, "coals become enriched with carbon as large amounts of volatile organic matter rich in hydrogen and oxygen are released" (Rice, 1993).

Coal Rank

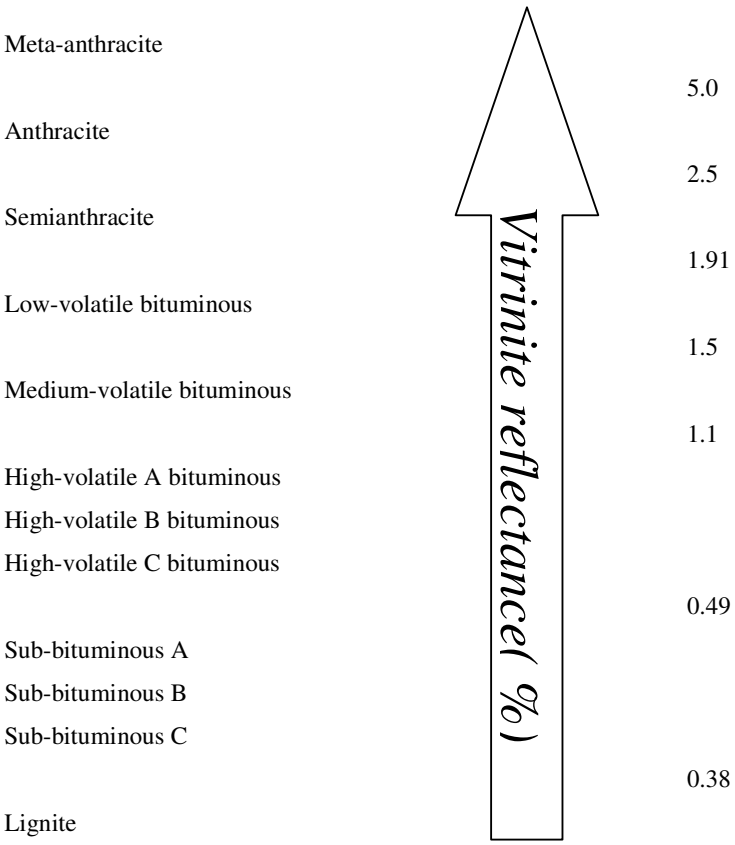

Figure 2.1. Coal Rank according to vitrinite reflectance (ASTM, 1983)

The released volatile organic matter is mainly methane, carbon dioxide, and water. In addition, depending on the composition of the peat, some heavier hydrocarbon gases and even oil may be released (Nuccio, 2002). With increasing coalification (bituminous types), porosity decreases, water is expelled, and temperature increases (ALL-Consulting, 2003). Therefore, the generation of thermogenic methane occurs at high-volatile bituminous ranks and higher (Rice, 1993). This process can carry on until the coal is entirely transformed into anthracite; as this takes place, less methane is generated , the coal porosity becomes even lower, and most of the water is expelled (ALL-Consulting, 2003). Biogenic and thermogenic processes can take place independently, in succession, or overlapping in time. For example for sub-bituminous coals, biogenic methane generation rates decrease with increasing temperatures and exhaustion of methanogenic bacteria. However, before all methane-generating bacteria have died, some thermogenic methane is released from

the coal material thus overlapping these two processes. If the organic-rich matter (i.e. coal or organic matter undergoing coalification) is uplifted through tectonic forces, then pressure and temperature are reduced thereby stopping the thermogenic transformation and once again favouring biogenic generation.

Biogenic gas can be further generated in the Pleistocene or the Holocene periods (tens of thousands to a few million years ago) long after the initial biogenic or thermogenic processes (Rice, 1993). This can take place because coal seams can act as regional aquifers with specific recharge zones and groundwater flowing through the coal seams. Water can flow through coal seams because the coal material has a network of fractures known as cleats, which give the coal adequate permeability for water and natural gas flow. These cleats are formed in the coal maturation process (coal dehydration, local and regional stresses, and changes in pressure) and they control the directional permeability of coals (ALL-Consulting, 2003).

The new waters introduced into the system are loaded with microbes and may have a high oxygen content. Figure 2.2 shows the recharge and water flow through a generic coal aquifer. The hydraulic conductivity of such a coal aquifer system is not necessarily low at shallow depths (10^{-6}-10^{-4} m/s), but can decrease significantly at depths greater than 100 m (Van Voast and Hedges, 1975). As these new oxygen charged waters enter the recharge area and flow through the coal aquifer, the aerobic decomposition process starts all over again. At this point, if there is a methane generation process taking place then this process is interrupted because "methane-producing micro organisms are strictly anaerobic and cannot tolerate even traces of oxygen" (Rice and Claypool, 1981). However, additional oxidation of organic matter will occur because organic matter (i.e. coal material undergoing further coalification) is more degradable under aerobic conditions than under anaerobic environments (Kjeldsen et al., 2002). This process results in the generation of a new food supply and hydrogen ions, but finishes soon after the dissolved oxygen in the water is depleted. This new food supply is basically anaerobically degradable organic matter which can now get transformed into methane either by methyl-fermentation (Eq 2.1) or by carbon dioxide reduction (Eq 2.2). Additionally, the new hydrogen ions (protons) combine with bicarbonate generated in the early stage to form more carbon dioxide, and more methane gas is generated through carbon dioxide reduction (Rice, 1993). It is estimated that this process could take place in thousands of years depending on specific conditions (Rice, 1993). In this way, CO_2 reduction (Eq 2.2) is the main

process responsible for methane generation in coal seams acting as active aquifer systems.

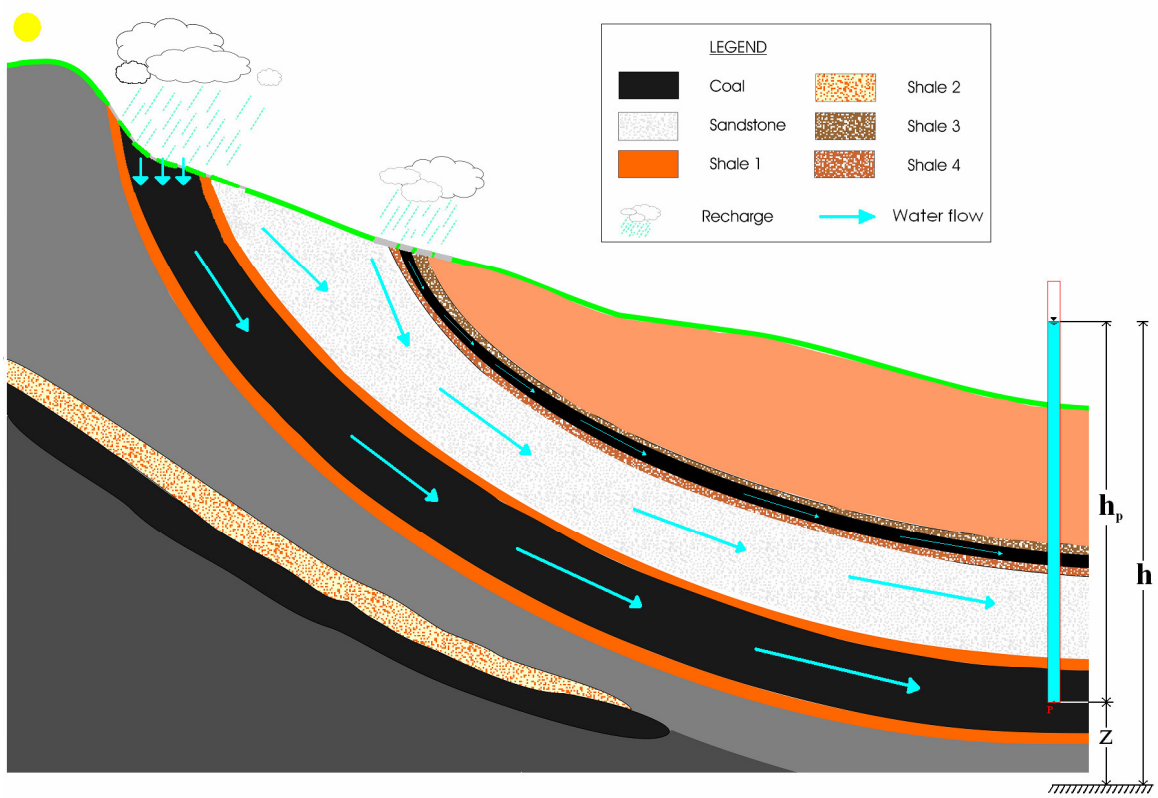

Figure 2.2. Water flow through coal aquifer system.

Coal seam gas storage and migration

The storage and migration of CSG is directly related to the flow of water in coal seams, and to the physical and chemical structure of the coal. This structure is often described as a block matrix containing micropores or internal coal surfaces (Figure 2.3). This matrix is divided by a natural fracture or cleat system which is generally saturated with water. The cleats form an orthogonal arrangement and can be divided into face cleats and butt cleats. Face cleats (Figure 2.3) are dominant cleats parallel to the maximum compressive stress and perpendicular to the fold axes. Secondary cleats or butt cleats (Figure 2.3) are formed parallel to the fold axes and terminate against face cleats (ALL-Consulting, 2003). In addition, the coal structure may also include non-orthogonal cleats referred to as curvilinear cleats.

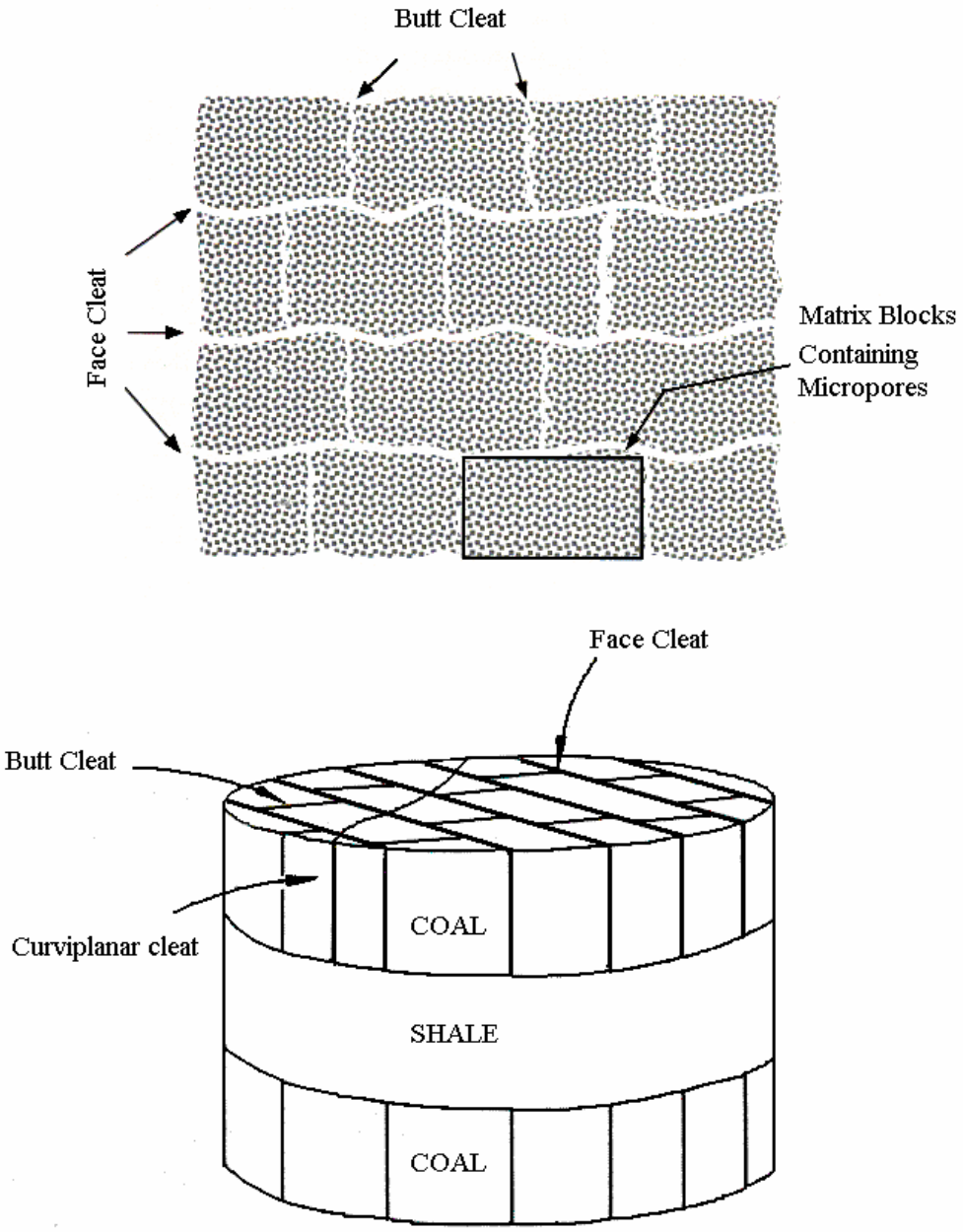

Figure 2.3. Cleat system and matrix blocks in coal (Gamson et al., 1996).

Therefore, gas storage and migration take place both at micro and macro levels. At the micro level, the molecular structure of the coal acts as a virtual chemical cage (Krevelen, 1961) capable of storing methane molecules. Therefore, gas is stored in the coal's micropores by means of absorption and adsorption. Because coal has a large and complex internal surface area, large quantities of coal seam gas can be stored within these surfaces by absorption (Rice, 1993). However, methane gas mainly resides on the internal surfaces of coal (adsorption).

The combination of absorption and adsorption processes is often referred to as sorption, and the reverse process is referred to as desorption. For the gas to remain sorbed in the micro molecular cage, an external force (i.e. water pressure) must constantly push the gas molecules into the coal micro structure, and the coal seam must remain mostly confined. In coal seams, this is possible because groundwater saturates and flows through the cleat system building up reservoir pressure, and thus preventing the gas from escaping the coal microstructure (Rice, 1993). Impermeable layers (clays, shales or mudstones) immediately on top or underneath the coal seam can effectively act as confining layers for the coal seam aquifer. Thus, water is prevented from escaping the coal seam and pressure increases as water flows through the cleats.

Reservoir pressure at a given point (P) in the aquifer (Figure 2.5) can be expressed as a function of hydraulic head, elevation, and water velocity (Eq 2.6). Since water velocity (v) is extremely low for porous-media flow then the second term of Eq 2.6 can almost always be neglected (Freeze and Cherry, 1979). For the aquifer pressure to drop at point P, the hydraulic head value (h) or h_p would have to drop accordingly. When this happens (naturally or artificially), methane gas desorbs from the internal surfaces of the coal. Methane gas then diffuses through the coal matrix (micropores) until it reaches a cleat. At this point, the gas has reached the coal macro structure (large pores and fractures or cleats) where it is stored and transported. Diffusion from the coal matrix and gas flow through fractures can be modelled using basic physical laws. The diffusion process is modelled according to Fick's Law while the free flow of gas and water through cleats is modelled using Darcy's Law (Gamson et al., 1996). Figure 2.4 shows the gas pathway after desorption and the procedure normally used for modelling its flow. It has been estimated that coal can store biogenic gas in this way up to "six or seven times the volume that can be stored in a conventional natural gas reservoir of equal rock volume" (Nuccio, 2002). However, as mentioned before, gas flow occurs only after fluid pressure acting on the internal coal surface is reduced. This can take place naturally over time if there is tectonic movement or uplifting of gas bearing coal seams, and water has "leaked" from the coal aquifer or water flow is reduced. On the other hand, this can take place artificially by human intrusion when water is pumped out at high rates from the coal aquifer.

$$P_p = \rho \cdot g \cdot (h - z) - \frac{\rho \cdot v^2}{2}$$

Eq 2.6. (Freeze and Cherry, 1979)

where:

Pp = gage pressure at point p in the coal aquifer system

ρ = density of water
g = acceleration of gravity
h = hydraulic head
z = elevation of point z with respect to a given datum
v = groundwater velocity

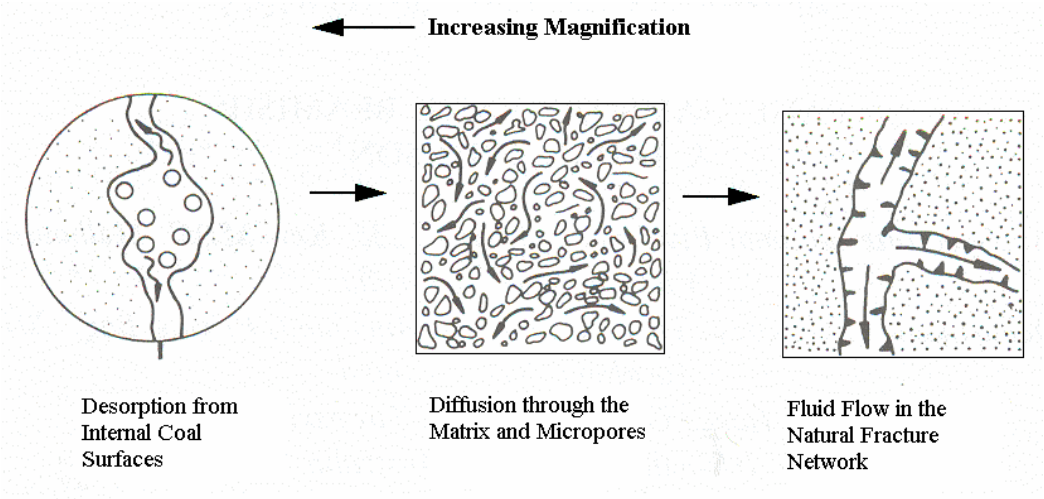

Figure 2.4. Coal Seam Gas pathway and processes involved in its transport modelling. Adapted from Gamson et al (1993).

CSG mining procedure

Coal seam gas is typically mined by drilling a hole right into the coal seam and then dewatering the coal aquifer to lower the hydraulic head, thus reducing the aquifer pressure in the vicinity of the well (Figure 2.2 and Eq 2.6). Figure 2.5 shows a typical production pod used in the Powder River Basin, located in the USA (ALL-Consulting, 2003). The well is cased all the way down to the coal seam to effectively isolate the coal seam and to prevent well collapse. In this schematic, a submersible pump is used to dewater the coal seam, but other pumps can also be used (i.e. sucker rod pumps). Because the well is cased all the way down to the coal seam, no energy is wasted by lifting water from adjacent units. In principle, only CSG waters are being

pumped up to the surface, and no mixing with waters from other units can take place. As the aquifer is dewatered, and the aquifer pressure drops, gas starts to diffuse from the micropores. This gas can then flow from the coal matrix into the well cavity where it then separates from the water. This gas flows through an outer pipe and is then fed to a gas separator and compressor, while the CSG water flows through an inner pipe into an impoundment or holding facility for its subsequent treatment and disposal.

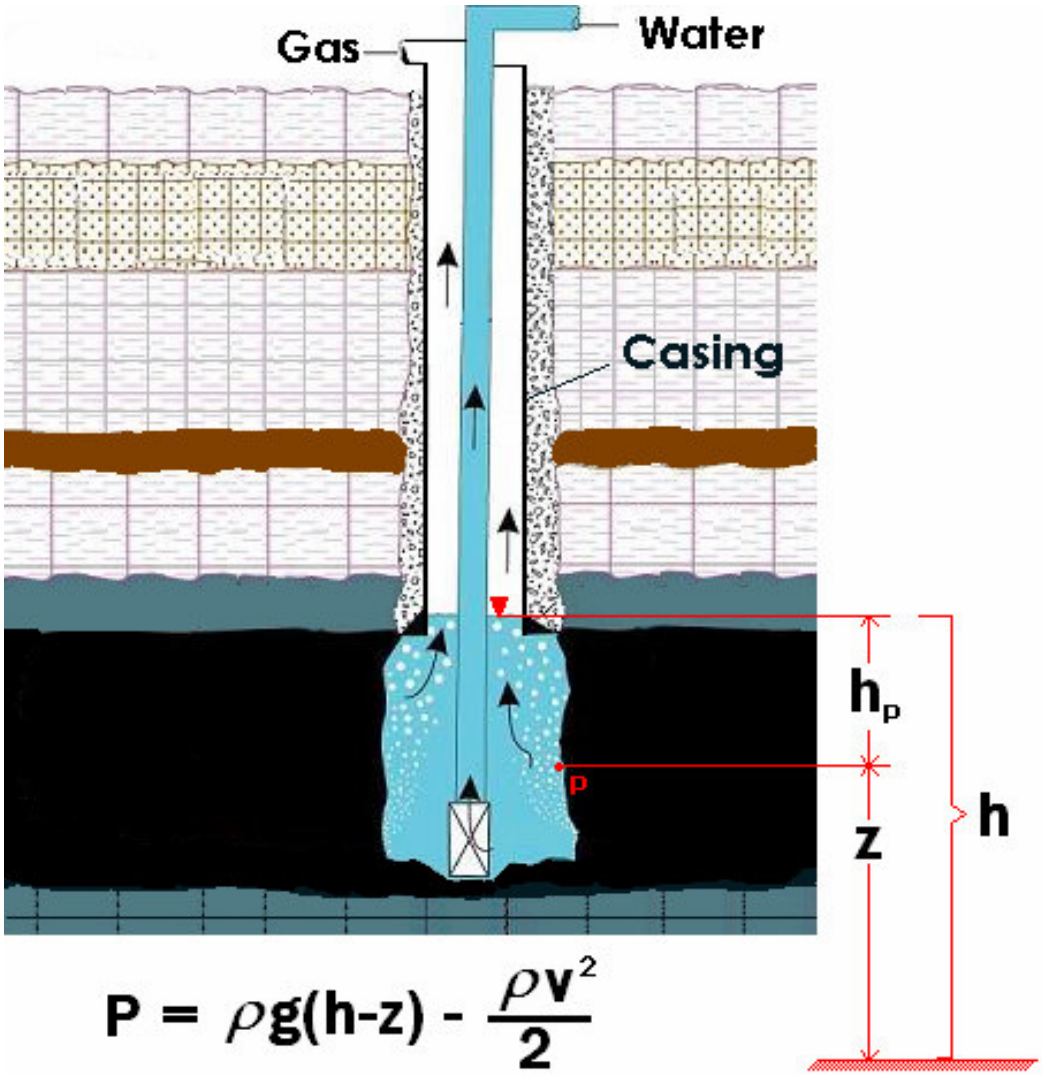

Figure 2.5. Schematic of CSG production pod in the Powder River Basin (Wyoming State Engineers Office and Wyoming State Geological Survey, 2005).

Chemistry of waters associated with coal seam gas

Coal seam gas bearing aquifers have a specific water chemistry that relates to geological, geochemical, physical, and biological processes. Underground, coal seams are interbedded with other layers or units which can be mudstones, shales, or clays. The geological and geochemical processes relate to the arrangement and characteristics of adjoining units, while the physical processes relate to depth of burial, potential tectonic uplifting, possible erosion (due to pumping for example), and mixing of waters from other units. The biological factors affecting the chemistry of these waters pose major implications particularly when the gas is of biogenic origin. In essence, whether the processes involved are biogenic or thermogenic depends on the depth of burial. The deeper the coal seam, the higher the temperatures and pressures acting on it. On the one hand coal temperatures may be above the limit at which methanogenic bacteria are able to survive, but on the other hand higher temperatures and pressures increase the level of coalification in the seam. Coalification is directly related to coal rank, which is a classification of coals mainly relying on its moisture content, volatile matter, and calorific value. Low rank coals comprise lignite and subbituminous coals having a low calorific value and a low carbon content. High rank coals are bituminous or anthracitic coals which have a higher calorific value and carbon content than lower rank coals.

In general, biogenic methane is associated with low rank coals, whereas thermogenic methane is most likely linked to high rank coals. Most of the coal seam gas (or coal bed methane) projects around the world are mining biogenic methane. Normally, higher hydrocarbon gases (ethane and butane for example) and even oil are produced with thermogenic gas. Therefore, thermogenic coal seam gas is generally classified under a different category and referred to using a different name. Nevertheless, most of the water quality properties associated with biogenic gas are still applicable to waters associated with thermogenic gas.

In most biogenic CSG producing basins, coal seams act as regional aquifers which are confined by nearly impermeable units (mudstones or shales). As recharge water enters the coal seam, it flows very slowly and undergoes chemical and biological transformations over the course of time. In addition, depending on each particular scenario there may be infiltration from other units and some mixing may

occur. Nevertheless, tritium analyses of CSG water samples in the Powder River Basin (Bartos et al., 2002) suggest that coal seam waters in coal aquifers are at least submodern or pre 1950s. The different processes responsible for shaping the chemistry of coal seam gas waters will be explained in the next paragraphs. Knowing the conceptual chemical characterisation of these waters is important for the correct interpretation of water quality samples taken from CSG bearing aquifers and for their subsequent treatment and disposal.

Dissolution of Sodium Feldspars and Similar Minerals. As fresh water seeps through recharge areas and flows through the coal aquifer, it encounters different minerals along its path of flow. One of these minerals is sodium feldspar, which can dissolve with recharge water (Figure 2.6) and increase Na^+ concentrations (Lee, 1981). When these minerals are of marine origin (albite and halite for example), chloride concentrations can also increase with mineral dissolution.

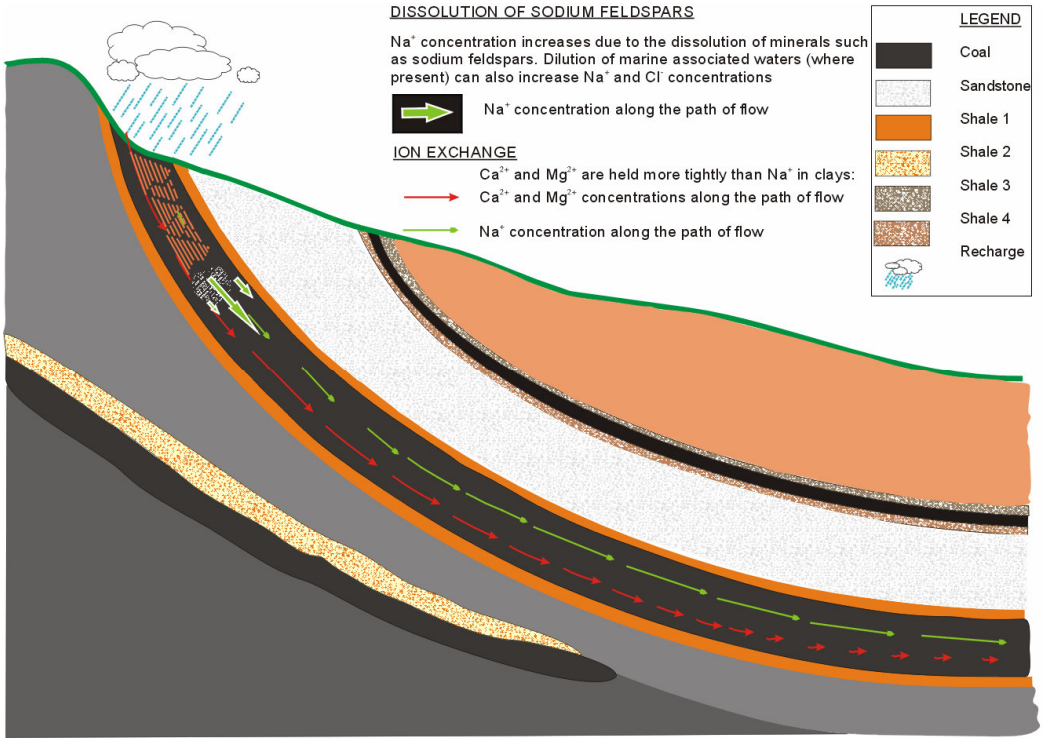

Figure 2.6. Dissolution of sodium feldspars and ion exchange process in coal seam aquifers.

Bicarbonate concentrations. Coal seam gas waters always have a high bicarbonate (HCO_3^-) content, which can be accounted for by two processes in the aquifer. The first of these processes is the dissolution of carbonate by oxygenated recharge waters (Freeze and Cherry, 1979). However, this process is not the primary cause for the high HCO_3^- content in CSG aquifers. The second and primary process accounting for high HCO_3^- content in CSG aquifers is methanation (Eq 2.5). As the sulphate reduction process takes place, large amounts of HCO_3^- are produced and this gives way to methanation. Other products of methanation include the generation of aqueous carbon dioxide ($CO_{2\ (aq)}$) and a fairly alkaline pH. Therefore, the concentrations of HCO_3^- in the aquifer will follow the speciation rules for a closed aqueous carbonate system. The possible species available are CO_3^{2-}, $CO_{2\ (aq)}$, H_2CO_3, and HCO_3^-. However, the fairly alkaline pH falls between 6.3 and 10.3 and, in this range of values, HCO_3^- will be the dominant species according to carbonate chemistry (Decker et al., 1987). Also, high pressure develops in the aquifer with increasing depth, and this keeps CO_3^{2-} in the HCO_3^- form along with dissolved $CO_{2\ (aq)}$. Figure 2.7 shows the evolution of recharge waters as these enter and flow through the coal aquifer. When fresh water enters deeper parts of the coal aquifer, oxygen is depleted, and anaerobic respiration takes place with increasing methanation and high bicarbonate concentrations.

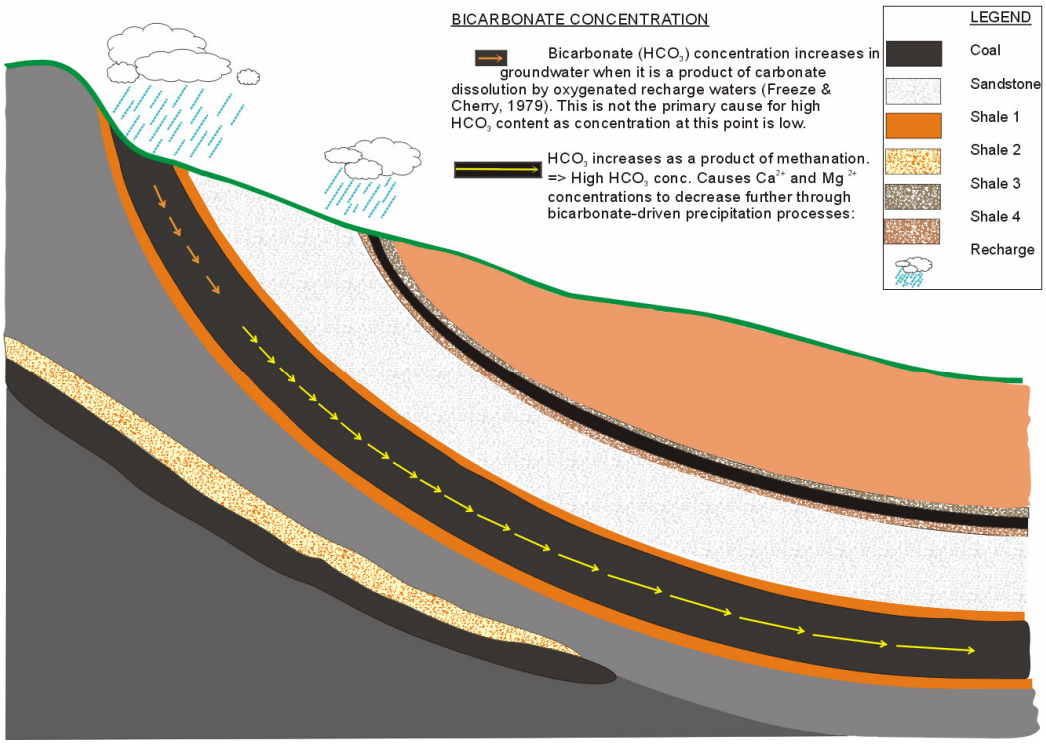

Figure 2.7. Evolution of bicarbonate concentration in coal seam gas waters.

Calcium and Magnesium depletion with ion exchange. Van Voast (2003) has identified high HCO_3^- concentrations as the main cause for low Ca^{2+} and Mg^{2+} concentrations in CSG waters. This is because the solubility of Ca^{2+} and Mg^{2+} decreases with high bicarbonate concentrations, which causes precipitation of calcite ($CaCO_3$) and dolomite ($CaMg(CO_3)_2$) in the aquifer. Another source of calcium and magnesium depletion is given by the process of ion exchange. In coal aquifers, groundwater may encounter clays or shales in adjoining units or in lenses or pockets as it flows through the coal seam. Therefore, an ion exchange process takes place between these minerals and the water itself. In this process, Ca^{2+} and Mg^{2+} are held more tightly than Na^+ in clays (especially in shales from marine origin with high adsorbed Na^+ ions). Therefore, the outcome of this exchange is a soft groundwater (low Ca^{2+} and Mg^{2+}) with an enhanced Na^+ concentration. This process accounts for the high Na^+ and low Ca^{2+} and Mg^{2+} concentrations in CSG waters from the Powder River Basin (Bartos et al., 2002), and it can be explained using the reactions in equations Eq 2.7 and Eq 2.8 (Hem, 1985).

$$Na_2X + Ca^{2+} \leftrightarrows CaX + 2\,Na^+$$

Eq 2.7

$$Na_2X + Mg^{2+} \leftrightarrows MgX + 2\,Na^{+}$$
Eq 2.8

where Na^{+} = sodium ion
Ca^{2+} = calcium ion
Mg^{2+} = magnesium ion
X = clay or shale

Studies by Hagmaier (1971), Lee (1981), and Hamilton (1970) suggest that this process is more pronounced with increasing depth and away from sources of recharge. Therefore as aquifer water flows into deeper parts of the basin, calcium and magnesium concentrations gradually decrease due to ion exchanges with clays. The same inversely holds true for sodium concentrations which would increase even further with increasing aquifer depth (Figure 2.6).

Sulphate reduction. Sulphate (SO_4^{2-}) increases when fresh recharge water encounters and dissolves sulphate minerals ($CaSO_4$, gypsum and anhydrite) along the path of flow, or through the weathering and oxidation of pyrite and marcasite (FeS_2) (Bartos et al., 2002) and similar sulphide minerals. Sulphate is also present in sea spray (Rosen et al., 2001) and, if coal seams are near the sea, it may deposit on recharge areas and infiltrate into the aquifer. Organic matter (i.e. coal) first decomposes aerobically with oxygenated recharge waters. However, as these waters enter deeper parts of the aquifer, oxygen replenishment is no longer possible. The process then turns to anaerobic decomposition as described by equations Eq 2.1- Eq 2.4. In the first phase of anaerobic decomposition (sulphate reduction), anaerobic bacteria consume the available organic matter thus reducing sulphate concentrations. A by product of the sulphate reduction process is the generation of dissolved hydrogen sulphide (H_2S); however, the presence of small traces of iron (Fe^{2+}) will cause hydrogen sulphide precipitation as black iron sulphides (Decker et al., 1987). Once the majority of the sulphate is reduced, the anaerobic process can carry on to the acidic and methanogenic phases (Rice and Claypool, 1981). In addition, depending on the methanogenic species present in the aquifer, methane generation can take place simultaneously with the sulphate reduction process (Oremland et al., 1982). However, at high sulphate concentrations methane generation does not occur because, in this situation, sulphate reduction becomes the dominant form of respiration.

With thermogenesis, sulphate reduction can take place with increasing coalification, because coalification is basically a “metamorphism by pressure and heat

of burial" (Van Voast, 2003). Also, thermogenesis occurs in the absence of oxygen because at the depths where this takes place, air or oxygenated water are not available. Since there is no oxygen available, sulphide minerals are not able to oxidise and generated sulphate ions.

Therefore, whether biogenic or thermogenic, CSG waters exhibit very low sulphate concentrations (Figure 2.8). Van Voast (2003) has presented an upper limit of 10 meq/l (~500 mg/l) for sulphate concentrations in co-produced water from methane-producing wells in the US, which has useful exploration implications. The 10 meq/l upper limit was selected by Van Voast (2003) because this concentration corresponds to the sulphate concentration of coal seam gas waters which are not associated with the production of methane.

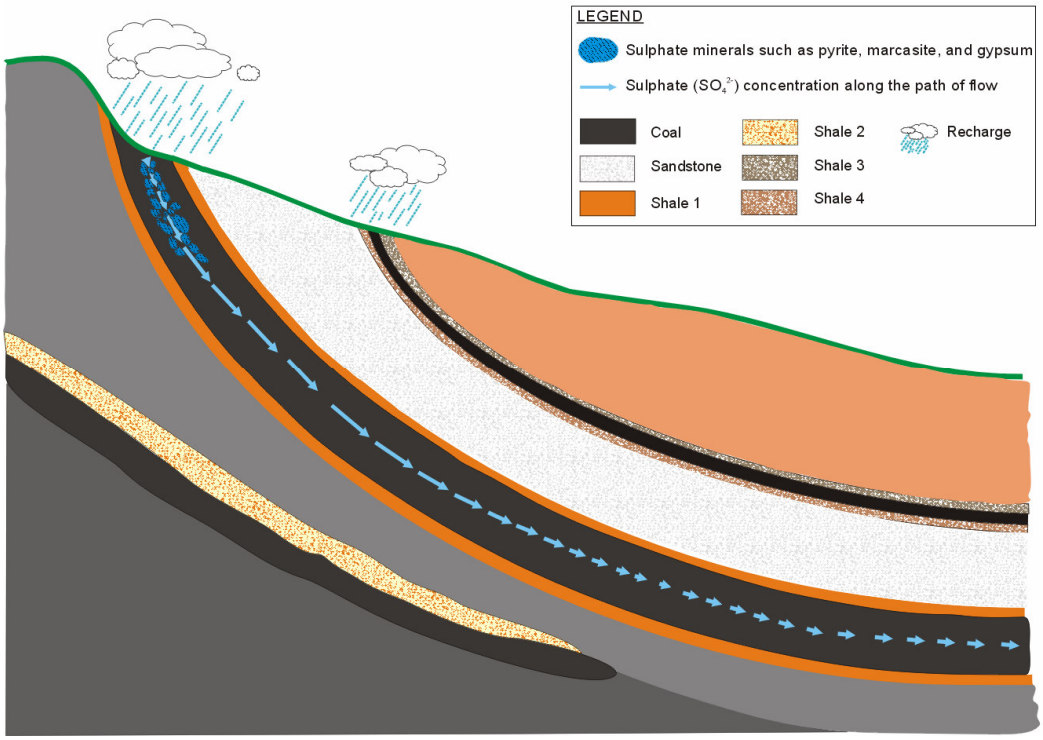

Figure 2.8. Sulphate reduction in CSG aquifers

Summarizing, the chemical signature of CSG waters can be described as high-bicarbonate, high-sodium, low-calcium, low-magnesium, and low-sulphate. As demonstrated by Van Voast (2003), different CSG producing basins in the United States have approximately the same previously-stated chemical signature and almost negligible sulphate concentrations (in many cases nil). This particular chemical

signature is useful for identifying CSG waters, which is useful during the exploration phase. For example, if the abstracted water has a completely different signature than the previously stipulated CSG water signature, and sulphate concentrations are higher than 500 mg/l (Van Voast, 2003), then that well will most likely not produce methane gas.

Differences with Acid Mine Drainage (AMD)

When certain minerals like pyrite and marcasite come in contact with water and air (oxygen), oxidation reactions take place which result in the dissolution of iron, sulphate, and a net increase in acidity. When this process occurs naturally, it is referred to as Acid Rock Drainage, but when it is anthropogenic it is termed Acid Mine Drainage. Equations Eq 2.9-Eq 2.12 are generally used to explain this process (Stumm and Morgan, 1996). The oxidation of pyrite can be further increased with the aid of iron-oxidising bacteria which can increase the oxidation rate of these minerals. However, these bacteria operate only in Eq 2.10, at pH levels of below or around 3, and the reaction is mostly abiotic.

$$FeS_{2\,(s)} + \frac{7}{2}O_2 + H_2O \rightarrow Fe^{2+} + 2SO_4{}^{2-} + 2H^+$$

Eq 2.9

$$Fe^{2+} + \frac{1}{4}O_2 + H^+ \rightarrow Fe^{3+} + \frac{1}{2}H_2O$$

Eq 2.10

$$Fe^{3+} + 3H_2O \rightarrow Fe(OH)_{3\,(s)} + 3H^+$$

Eq 2.11

$$FeS_{2\,(s)} + 14Fe^{3+} + 8H_2O \rightarrow 15Fe^{2+} + 2SO_4{}^{2-} + 16H^+$$

Eq 2.12

Coal seams can have sulphur-bearing minerals such as iron sulphide, pyrite ($FeS_{2(s)}$), and marcasite, therefore they have acid producing potential. In this way, water that has come in contact with coal under oxidising conditions, has generally a low pH, metals dissolved in solution (iron, manganese, and aluminium), iron hydroxide, and sulphate.

AMD waters in New Zealand have traditionally been associated with coal mining operations. Therefore, people not familiar with CSG waters sometimes tend to associate these waters to AMD. Coal seam gas waters are generated in an anoxic environment therefore they do not oxidise sulphur-bearing minerals within the coal

seam. The biogenic processes of CSG formation produce water with a fairly neutral pH, little or no dissolved metals, and very low sulphate concentrations. In this way AMD and CSG are completely different processes yielding completely different results. Table 2.1 shows two water quality samples from two NZ mines experiencing AMD problems. These samples have a very acidic pH (below 3) and exhibit various metals dissolved in solution (ferrous iron, manganese, aluminium, nickel, and zinc to mention a few). Sulphate concentrations are also fairly high particularly in the Castle Point Mine sample (829 mg/l). Other parameters of importance are total acidity and specific conductance which are also high in both samples. These water samples do not exhibit the geochemical signature for coal seam gas waters. In fact, they exhibit quite the opposite chemistry: low pH, high calcium and magnesium in comparison to sodium and chloride, high sulphate, and almost zero bicarbonate (Figure 2.9).

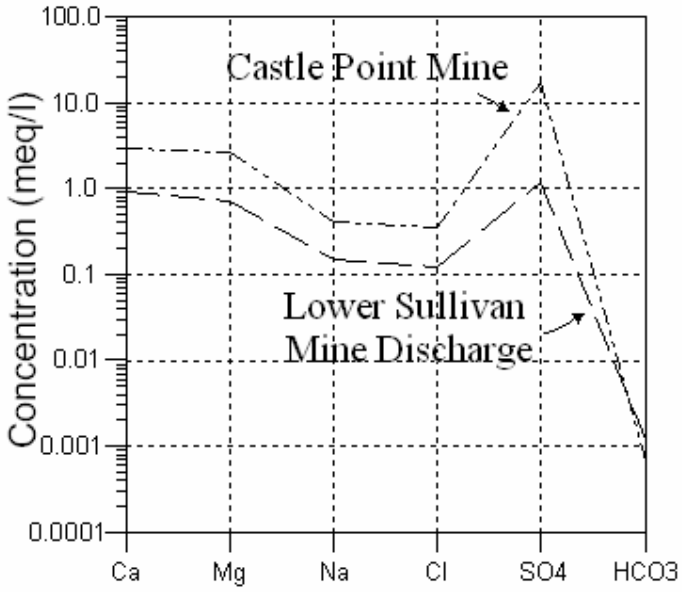

Figure 2.9. Schoeller diagram for NZ AMD samples.

Table 2.1. AMD water samples from two NZ mines.

Dissolved constituents		Lower Sullivan Mine Discharge 22/02/2001	Castle Point Mine 02/04/2001
pH		2.86	2.53
Specific Conductance	µS/cm	9770	20100
Total Acidity [(a)]	mg/l $CaCO_3$	339	505
Sodium (Na^+)	mg/l	3.41	9.6
Potassium (K)	mg/l	3.59	3.62
Calcium (Ca^{2+})	mg/l	18.2	59.7
Magnesium (Mg^{2+})	mg/l	8.74	33.1
Total Iron	mg/l	83.7	15.4
Ferrous Iron (Fe^{2+})	mg/l	47.1	14.5
Ferric Iron (Fe^{3+})	mg/l	36.6	0.9
Manganese (Mn^{2+})	mg/l	0.57	0.88
Barium (Ba^{2+})	mg/l	0.01	0.01
Copper (Cu^{2+})	ug/l	24.3	13.3
Nickel (Ni^{2+})	ug/l	130	192
Zinc (Zn^{2+})	ug/l	718	634
Aluminium (Al^{3+})	ug/l	14300	58900
Arsenic (As^{3+})	ug/l	3	< 0.001
Chromium (Cr^{2+})	ug/l	3.3	25.5
Rubidium (Rb^{2+})	ug/l	37.3	33.2
Lead (Pb)	ug/l	1.2	1.9
Strontium (Sr^{2+})	mg/l	0.09	0.36
Chloride (Cl^-)	mg/l	4.3	12.8
Boron (B)	mg/l	< 0.005	0.11
Bicarbonate (HCO_3^-) [(b)]	mg/l	0.07	0.04
Sulphate (SO_4^{2-})	mg/l	56.9	829
Silica (SiO_2)	mg/l	34.4	NA
Carbon dioxide ($CO_{2\,(aq)}$) [(b)]	mg/l	256.7	297.24
Total Phosphorus (P)	mg/l	2.33	< 0.004
Selenium (Se)	mg/l	< 0.001	< 0.001
Cobalt (Co)	mg/l	0.0634	0.0629

Data supplied by CRL Energy. Sullivan Mine and Castle Point Mine are located in the West Coast, South Island (NZ).
[(a)] Calculated from ferrous and ferric iron concentrations, aluminium, manganese, and pH.
[(b)] Calculated from total acidity and carbonate equilibrium.

CSG water quality from US basins

In the 1980's coal seam gas (or coal bed methane) began in the United States with the government's endorsement of tax credits for non-conventional energy production. CSG production bloomed in the 1990's, and by the end of 2000, CSG

production in the US totalled 3.831 trillion cubic metres (US Environmental Protection Agency, 2004). The most important basins in the US include the Black Warrior, San Juan, Raton, Piceance, Uinta, and the Powder River (Figure 2.10). This last basin is important because it produces biogenic gas from low rank coals, which is a similar scenario to the one in New Zealand. Nowadays, coal bed methane in the United States plays a significant role in the energy market sector; in 2003 coal bed methane accounted for about 8% of the US total methane production and proved reserves for this resource increase at a rate of about 1% per year (Energy Information Administration, 2004).

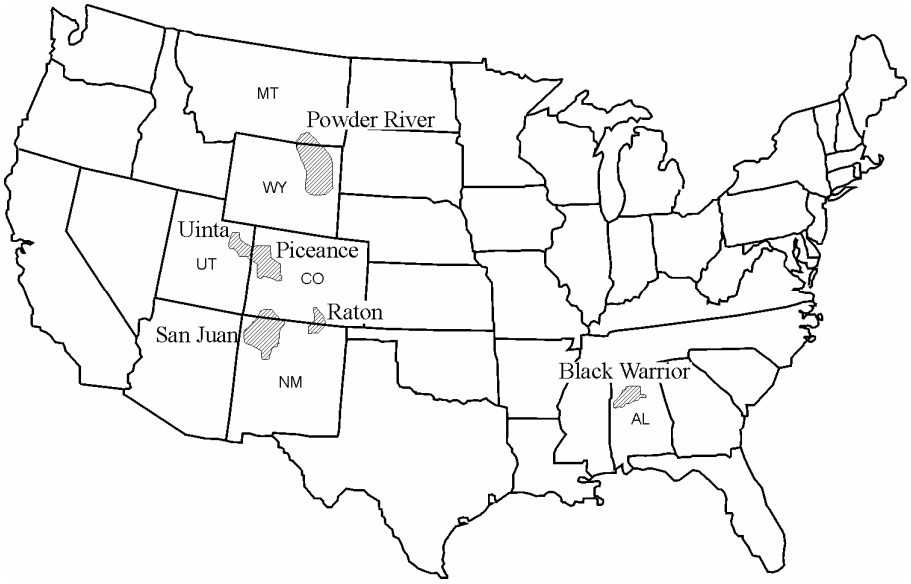

Figure 2.10. Major CSG producing basins in the United States. Adapted from Van Voast (2003).

Water quality from CSG producing basins has similar characteristics in terms of geochemical signature (Na^+ being the major ion), but can vary considerably in terms of quantities produced and concentration of specific constituents. Table 2.2 summarises the water quality and quantity for six major CSG producing basins in the United States. Water production across the different basins varies considerably. For example, water production (per well) in the Black Warrior Basin is approximately 7.5 m^3/day (Alabama State Oil and Gas Board (AOGB), 2003), whereas in the Powder River Basin this figure reaches 63.6 m^3/day (ALL-Consulting and Montana Board of Oil and Gas Conservation, 2004). This is because CSG in the Black Warrior Basin is of thermogenic origin, therefore coal porosity in this basin is low in comparison to coal porosity from biogenic origin reserves such as the one in the Powder River Basin.

Low rank coal and lignites (biogenic methane) have high porosities whereas high rank (thermogenic origin) have low porosity and lower water content (ALL-Consulting, 2003). Therefore, a larger quantity of CSG waters is expected from biogenic methane reservoirs which needs to be managed accordingly. This can be observed by analysing the differences in the Water/Gas ratio presented in Table 2.2. Here, the Powder River Basin presents an impressive 17.33 m^3/TCM ratio (ALL-Consulting and Montana Board of Oil and Gas Conservation, 2004), which is a good indicator of the number of issues that arise from water disposal operations associated with CSG extraction. This is exacerbated when considering the salinity of these waters; in CSG waters the major ion present in solution is sodium, which can have detrimental effects to soils and surface waters if not adequately disposed. Another chemical property presenting significant variations is TDS. In general, this value increases with coal rank, depth, and distance from main recharge areas. In sites like the Powder River Basin this value does not seem very high; however, due to the large quantities of water involved, this parameter can pose serious risks when managing CSG waters. These variations suggest carrying out an in-depth study of the chemical nature and signature of CSG waters.

The study of CSG waters involves the determination of important chemical properties like pH, TDS, and the concentration of major and minor ions. Once this information is collected, it needs to be put in context or compared against the composition of surface waters and other CSG waters. For example, Piper diagrams (Freeze and Cherry, 1979) are used for grouping and presenting samples according to their major ion composition, and Schoeller diagrams (Freeze and Cherry, 1979) are used for comparing samples in a quantitavely manner. The chemical signature for these six major producing basins has been presented by Van Voast (2003) using the Schoeller diagram representation (Figure 2.11). Figure 2.11 shows the geochemical signature for CSG waters (defined in the previous section) which corresponds to the outcome of the conceptual model for the genesis of coal seam gas waters. In this figure, it is possible to compare the proportion of ions for individual water samples within (and between) basins. In this way, calcium and magnesium concentrations are low in comparison to sodium and bicarbonate ones. In addition, sulphate concentrations are always low as a result of the sulphate reduction process prior to methogenesis; sulphate concentrations are always below the previously defined

Table 2.2. CSG water quantity and quality from selected US basins.

Basin	State	N° Wells	Average Water Production m^3/day /well	Gas TCM/day/well	Water/Gas m^3/TCM	Water type [c]	pH[c]	TDS[c] mg/l	TDS mg/TCM/well
Black Warrior	AL	3423 [a]	7.5 [a]	2.6 [a]	2.86	Na-Cl-HCO_3	5.4-9.9	160-31,000	134-25901
Powder River	WY, MT	13880 [b]	32.9 [b]	1.9 [b]	17.33	Na-HCO_3	6.8-8.0	270-3,010	337-3758
Raton	CO	694 [c]	42.3 [c]	8.5 [c]	4.98	Na-HCO_3	6.0-7.9 [e]	86-2,582 [e]	617-18527
San Juan	CO, NM	3089 [c]	4.0 [c]	22.7 [c]	0.18	Na-HCO_3-Cl	5.2-9.2	410-171,000	24-9964
Uinta	UT	558 [c]	34.2 [c]	17.7 [c]	1.93	Na-HCO_3-Cl	7.0-8.2	6,350-42,700	21963-147690

Sources:
[a] (Alabama State Oil and Gas Board (AOGB), 2003).
[b] (Nelson, 2005)
[c] (PTTC, 2000); (GRI (Gas Research Institute), 2000); (US Environmental Protection Agency and Advanced Resources International, 2002); CO, NM, WY, MT Oil and Gas Commissions; (Williams. B, 2001). These sources are quoted in ALL-Consulting and Montana Board of Oil and Gas Conservation (2004).
[d] (Rice and Bartos, 2001).
[e] (The Seacreast Group, 2003)
TCM = Thousand cubic metres of gas

limit (10meq/l) for methane production in wells drilled directly into coal seams (Van Voast, 2003). Figure 2.11 also shows varying degrees of chloride concentrations amongst the different basins. This is even more noticeable in basins presenting strong marine associations (Black Warrior, San Juan, Piceance, and Uinta).

Differences within basins can be attributed to well depth and their distance to recharge areas, as well as water age. As water flows through a coal seam gas basin, it dissolves and mixes with minerals along its path of flow. This process has been explained in detail throughout this chapter, but it is important to underscore that the closer a well is to the recharge area, the less mineralised the resulting water will be. The same holds inversely true for deeper parts of the basin: the closer a well is to the deepest part of the basin, the more mineralised the resulting CSG water will be. In the Powder River basin, for instance, CSG water produced on the basin margins has a low TDS suitable for human consumption (<500 mg/l); however, in inner parts of the basin this water has TDS values as high as 3010mg/l (Table 2.2) rendering it unsuitable for most beneficial applications.

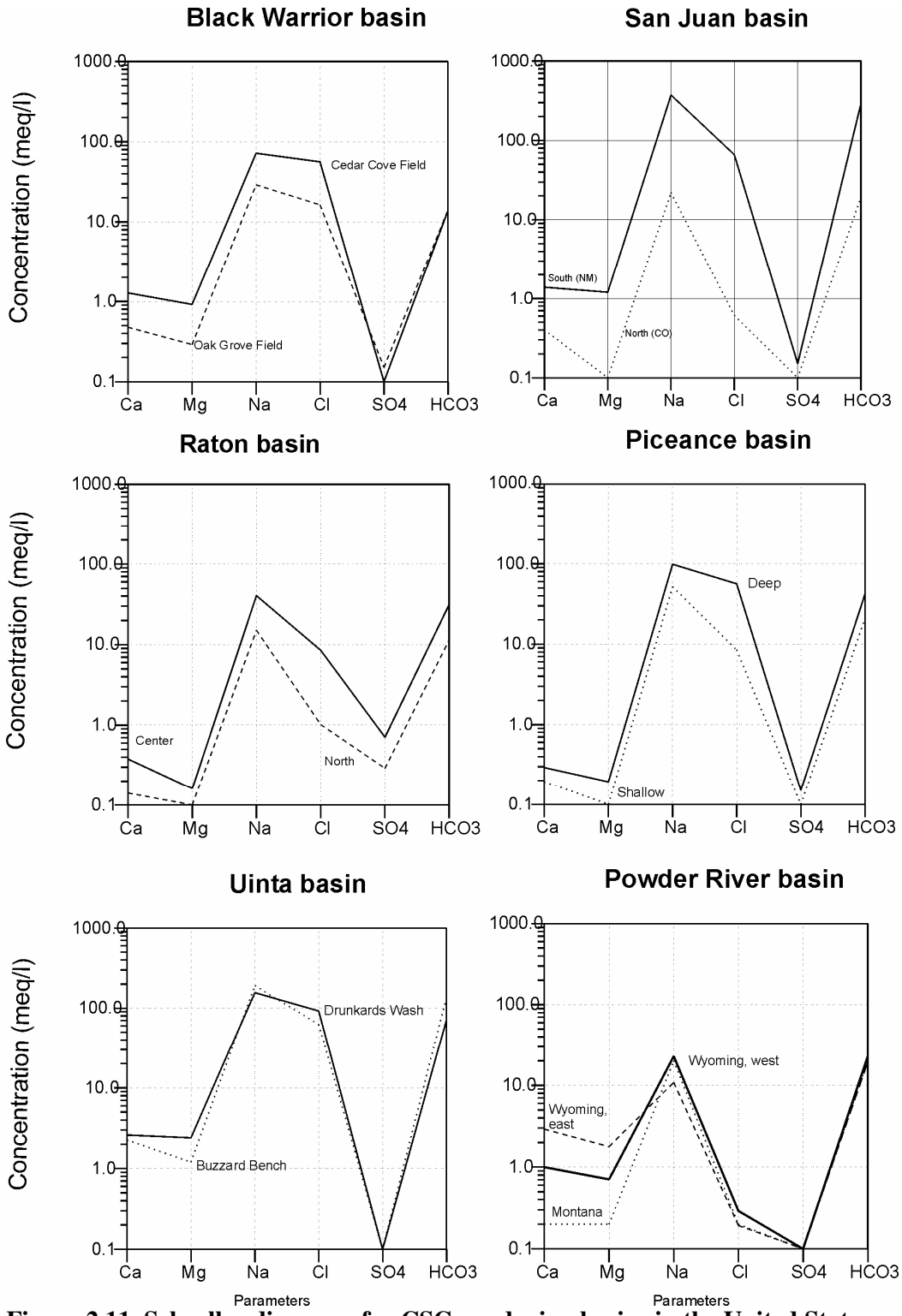

Figure 2.11. Schoeller diagrams for CSG producing basins in the United States (Van Voast, 2003).

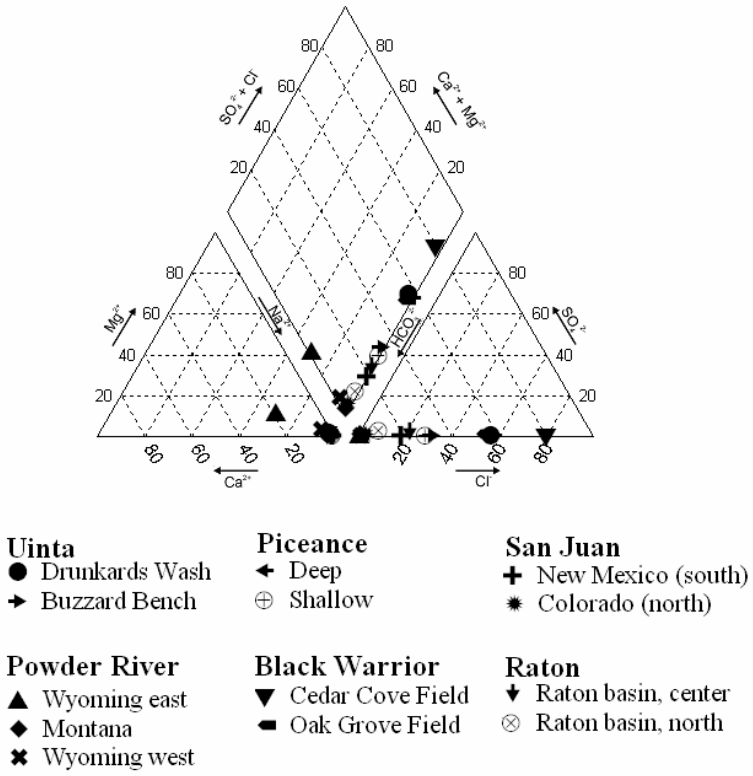

Figure 2.12. Piper diagram for six major basins in the United States. Data taken from Van Voast (2003).

The data presented in Figure 2.11 can also be plotted in a Piper diagram (Figure 2.12) to visually group all of the samples for the selected basins and to identify major trends. In this way, all of the samples have sodium as a major ion, followed by bicarbonate or chloride. Samples for Uinta (Buzzard Bench), Piceance (shallow), and Raton (centre) basins are of the Na^+-HCO_3^--Cl^- type, while samples for Uinta (Drunkards Wash), Piceance (deep), and Black Warrior (Oak Grove Field) basins are of the Na^+-Cl^--HCO^-_3 type. In the cases of Uinta and Piceance, the second major ion (Cl^- or HCO_3^-) can vary depending on the location of wells within the basin from which samples are extracted. In general, Cl^- concentrations near recharge areas are lower than in deeper parts of the basin (Van Voast, 2003), and this could explain why Cl^- is the second major ion in Piceance (deep) but the third major one in shallow parts of this basin (Piceance, shallow in Figure 2.11). The water quality for San Juan, Powder River, and Raton (north) basins is of the Na^+- HCO_3^- type. These waters have little or no chloride, which is believed to be due to the proximity to recharge areas (San Juan and Raton, North) or to their non marine nature in the case of the PRB (Van Voast, 2003). In all of these cases, however, the major cation is sodium.

CSG water quality from potential New Zealand basins

New Zealand has been following the developments of coalbed methane (coal seam gas) in the US with keen interest. The first ones to explore this technology in New Zealand were R C Macdonald and Partners Ltd who established Southgas Ltd in 1984. Southgas explored the CSG potential of the Ohai Coalfields. They obtained good gas results, however their project was incompatible with the coal mining project established at the site, so Southgas had to abandon this operation (Johnson, 2004). In the mid 1990's they changed their name to Westgas Ltd, and they devoted themselves to the Greymouth Coalfield. Here, Westgas has tapped into significant amounts of gas from sandstone-coal reservoirs, but exploration and production issues still need to be resolved before commercialisation (Cave, 2002).

Up to 1990 there was a generalised belief that CSG could only be minable if it was a consequence of the thermogenic processes in bituminous (high-rank) coals (Johnson, 2004). However, in the 1990's developments in the Powder River Basin (US) proved that commercially quantities of coal seam gas could be recovered from low-rank coals (Johnson, 2004). New Zealand coals present some of the same characteristics as those found in the Powder River Basin (Moore, 2002). Therefore, New Zealand coals hold significant potential for CSG development and extraction. Many companies seized this opportunity, and since the 1990's have obtained different exploration licences. Kenham Holdings, for example, has acquired CSG exploration licenses covering the lignite deposits of Central Otago and Eastern Southland, and a licence to explore the sub-bituminous coal seams of the Maramarua Coalfield. In addition, Kenham has an exploration licence for the bituminous resource in the Buller and Reefton coalfields, located in the New Zealand South Island. Other companies that have joined the CSG play include Resource Development Technologies (Waikato coal region), Solid Energy (Taranaki and the South Island West Coast), and Bridge Petroleum (Southern Waikato Coal Region and King Country).

Methods

Since 2000 Kenham Holdings, with the aid of CRL Energy Ltd and L&M Mining Ltd, has been exploring and developing the CSG resource in New Zealand. As part of their work these companies determine which coal fields hold better potential for CSG extraction, characterise the gas held in those coal seams, and produce estimates on the quantity of gas that could eventually be extracted. The licenses under exploration are for lignites and sub-bituminous coals, therefore these would only involve biogenic methane. The exceptions are Buller and Reefton which would hold bituminous coal reserves. The CSG water disposal issue was acknowledged by these companies for the successful development of CSG projects in New Zealand.

In 2003, CRL Energy Ltd collected water samples from their drilling operations. These samples were often collected by field operators only when the opportunity presented itself – that is, when artesian conditions were encountered or when water was air-lifted to clear the boreholes in order to carry out basic falling head tests. In a few instances, samples were collected personally, but in the majority of these cases, samples were collected without following any sampling protocols (i.e. no prior purging); samples were analysed anyway to prove that a proper sampling programme was indeed necessary to produce high quality data.

It should be noted that the methods used for much of this research are non-ideal; however, they were necessary given the business and political pressures on the partners in the research, CRL Energy Ltd and L&M Mining Ltd. This matter and the methods used by on-site personnel for collecting these samples are discussed in some detail in section A.3 (Appendix 3). Figure 2.13 shows the exploration sites from which water samples were collected and analysed. In some cases samples were sent to certified laboratories for full analysis, but in other cases samples were analysed just for major ions and basic chemical properties at the Environmental Engineering Laboratory (EEL, University of Canterbury).

Hill Laboratories and the CRL Energy laboratory are certified labs in New Zealand. These labs operate following guidelines from the APHA (American Public Health Association. et al., 1999) with very low detection limits. Therefore, when possible, the same standard was used at the EEL (University of Canterbury). When

this was not possible, HACH methods or analytical procedures were used to complement the sample analysis.

In sum, because of business and political decisions the choice of sample collection and analyses were in many cases non-ideal methods. To remediate the situation and validate the data collected, a higher analytical treatment and interpretation of the data was later carried out throughout this work (i.e. Chapters 3-5 and Appendix B.2). Sample analyses (TDS, alkalinity, hardness, and calcium) at the EEL (University of Canterbury) were carried out using the Standard Methods from the APHA (American Public Health Association. et al., 1999). In addition, sulphate and chloride were analysed using HACH methods (Hach Company., 2003), and pH and Specific Conductance were measured using calibrated metres. Once these analyses were carried out, it was straight forward to compute the bicarbonate content (from carbonate equilibrium) and magnesium concentrations (from hardness and calcium concentrations). It was then possible to estimate sodium concentrations by assuming zero electro neutrality in the water samples. A summary of these methods is presented in Appendix A, section A.1.

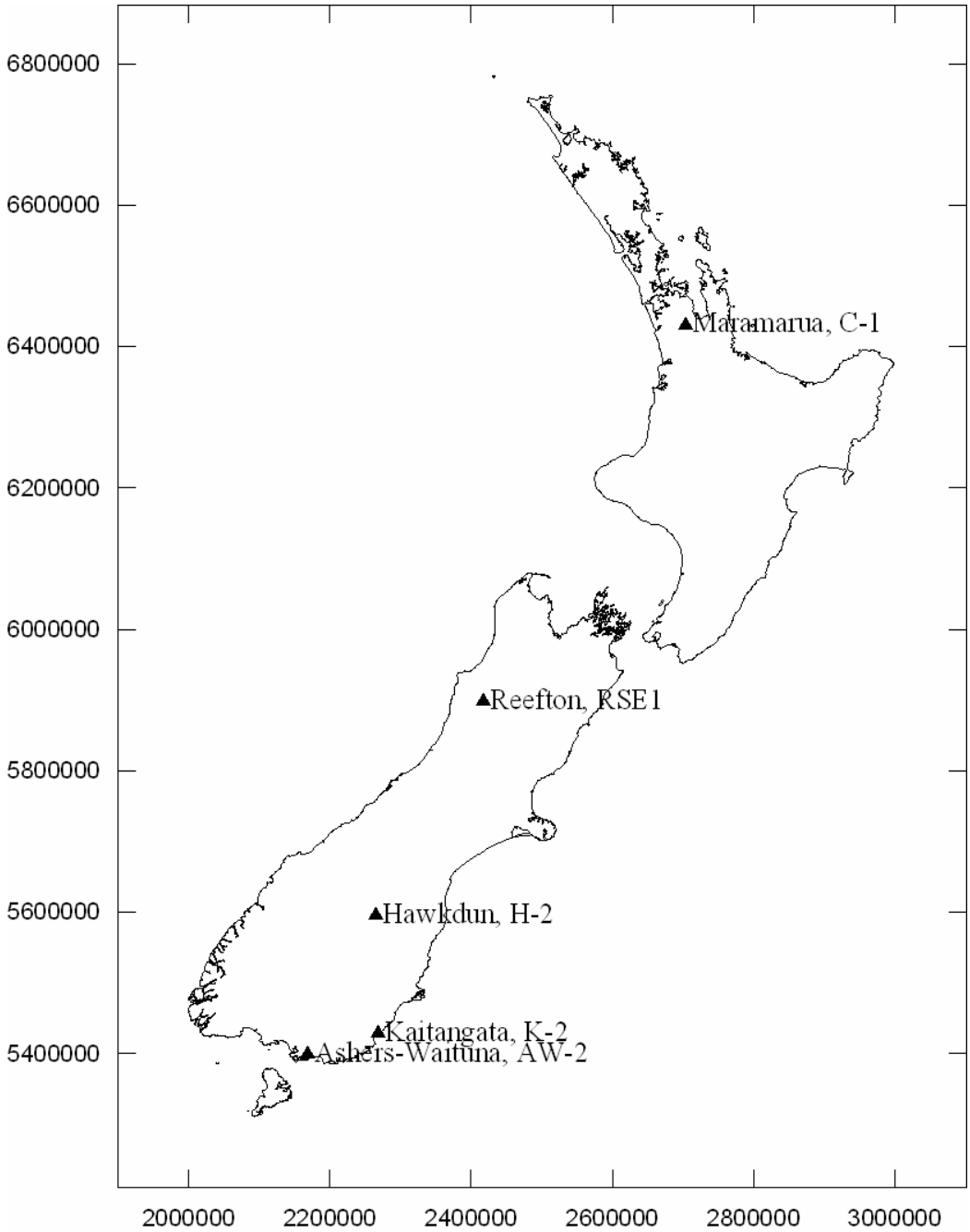

Figure 2.13. Kenham Holdings sites from which water samples have been collected.

CSG exploration in New Zealand

Water samples from the locations in Figure 2.13 indicate that the sampled water is not CSG water. This is mainly because the boreholes at those locations were not cased down to coal, and the techniques used for sampling the boreholes were not adequate for sampling CSG waters (i.e. not enough purging). Notwithstanding, sample results and analyses for Ashers-Waituna, Reefton, Kaitangata, and Hawkdun are presented in Appendix A (A.2). These results do not follow the geochemical signature of CSG waters, and therefore are not what could be expected from real CSG dewatering operations. In 2004-2005, however, good CSG water samples were obtained for a location in Maramarua. Consequently, results from Maramarua exploration and sampling are presented in the following paragraphs.

Maramarua. The Maramarua coalfield (Figure 2.14) has good potential for CSG development because its Kupakupa Seam contains substantial amounts of sub-bituminous coal (Pope and Trumm, 2004). The 20m thickness of the Kupakupa Seam would facilitate CSG production because wells targeting that seam would cover a large vertical surface area within the seam itself. Coal from this field generally has low ash and sulphur contents and is of the sub-bituminous C-B type. The Eocene Kupakupa Seam has impermeable claystone cap rocks which prevents water (and gas) from escaping the seam; this seam has been identified as an aquifer with sufficient hydrostatic head capable of preventing natural CSG desorption (Pope and Trumm, 2004).

In August 2003, borehole C1 was drilled in the Clifton sector of the Maramarua Coalfield (Figure 2.14). The drill penetrated through different layers of clay, and mudstone before reaching an 11.55 m layer of coal (Kupakupa Seam). It then went through two thin layers of mudstone and coal and then stopped at a depth of 207m (Table 2.3). This well had sub artesian pressure, and the well had to be sampled using a pump capable of purging the well and collecting a sufficient volume of water for analysis. This was carried out by a subcontractor (D. J. Phelps & Co Ltd) who used a Grundfos submersible pump (MP1) to purge the well until pH, temperature, and conductivity became stable. This pump was small enough (ϕ=50mm) to fit down the borehole (≈100mm), but was quite effective in extracting at least 380 litres of

water before collecting the actual sample. The sample was collected in this fashion on the 18/9/2003 and subsequently analysed at Hill Laboratories. The results of this analysis are presented in Table 2.4. As with the Hawkdun samples, the borehole was not cased all the way down to coal level, therefore this sample does not exclusively represent coal seam waters. In this way, water from other units (i.e. mudstones, sandstones and siltstones) had the possibility of entering the hole and mixing with coal seam waters. The 18/9/2003 sample has the chemical signature of CSG waters: high pH, low calcium and magnesium concentrations, and high sodium and bicarbonate. The sulphate concentration for this sample is reasonably low (27.6 mg/l) and below the concentration for the limit of methane production (500 mg/l) in wells presented by Van Voast (2003). The major ions for this sample are sodium and bicarbonate, therefore this water is classified as of the Na-HCO_3^- type. It is also worth noting the relatively high chloride and iron concentrations (49.3 mg/l and 55.9 mg/l), the high DOC (130 mg/l), and the high value for total hydrocarbons (mostly C10-C14).

Some key measurements were taken on site while carrying out the sampling. For example, the on site measurement for pH is 7.5 and the specific conductance 1200 µS/cm. These values differ significantly to the ones taken by Hill laboratories which suggest the possibility of a mistake in the laboratory data. This was further corroborated when the TDS value was calculated manually from the data presented in Table 2.4 and using Eq 2.13. In this way, the calculated TDS value is 696 mg/l which is 65% of the value reported by Hill Laboratories (1160 mg/l). TDS and Specific Conductance are related through common approximations, and can be expressed in terms of each other using Eq 2.14 and Eq 2.15 ($0.54 < A < 0.96$). The TDS value reported by Hill Laboratories exceeds by far the reported value for Specific Conductance (718 µS/cm) reported along with TDS, and thus contradicts Eq 2.15. Furthermore, the Specific Conductance calculated using Eq 2.14 and the data in Table 2.4 (980 µS/cm) is higher than the one reported by Hill Laboratories (718 µS/cm) and closer to the value measured on site (1200 µS/cm). A conservative approach for these two values would be to adopt the on site measurement for Specific Conductance (1200 µS/cm) and the calculated TDS value (696 mg/l).

$$TDS\ (mg/l) = \sum ions\ (mg/l) + SiO2\ (mg/l) - [HCO_3^-\ (mg/l) \cdot 0.5082]$$

Eq 2.13. (Hounslow, 1995)

$$Specific\ Conductance\ (\mu S/cm) = SUM\ of\ cations\ (meq/l)\ *100$$

Eq 2.14 (Hounslow, 1995)

$$TDS\ (mg/l) = A \cdot Specific\ Conductance\ (\mu S/cm)$$

Eq 2.15

The value of *A* ranges from 0.54 to 0.96, but usually assumes values between 0.55 and 0.76 depending on the water being analysed (Hounslow, 1995). For the particular case of the Maramarua CSG samples, *A* ranged from 0.51 to 0.62

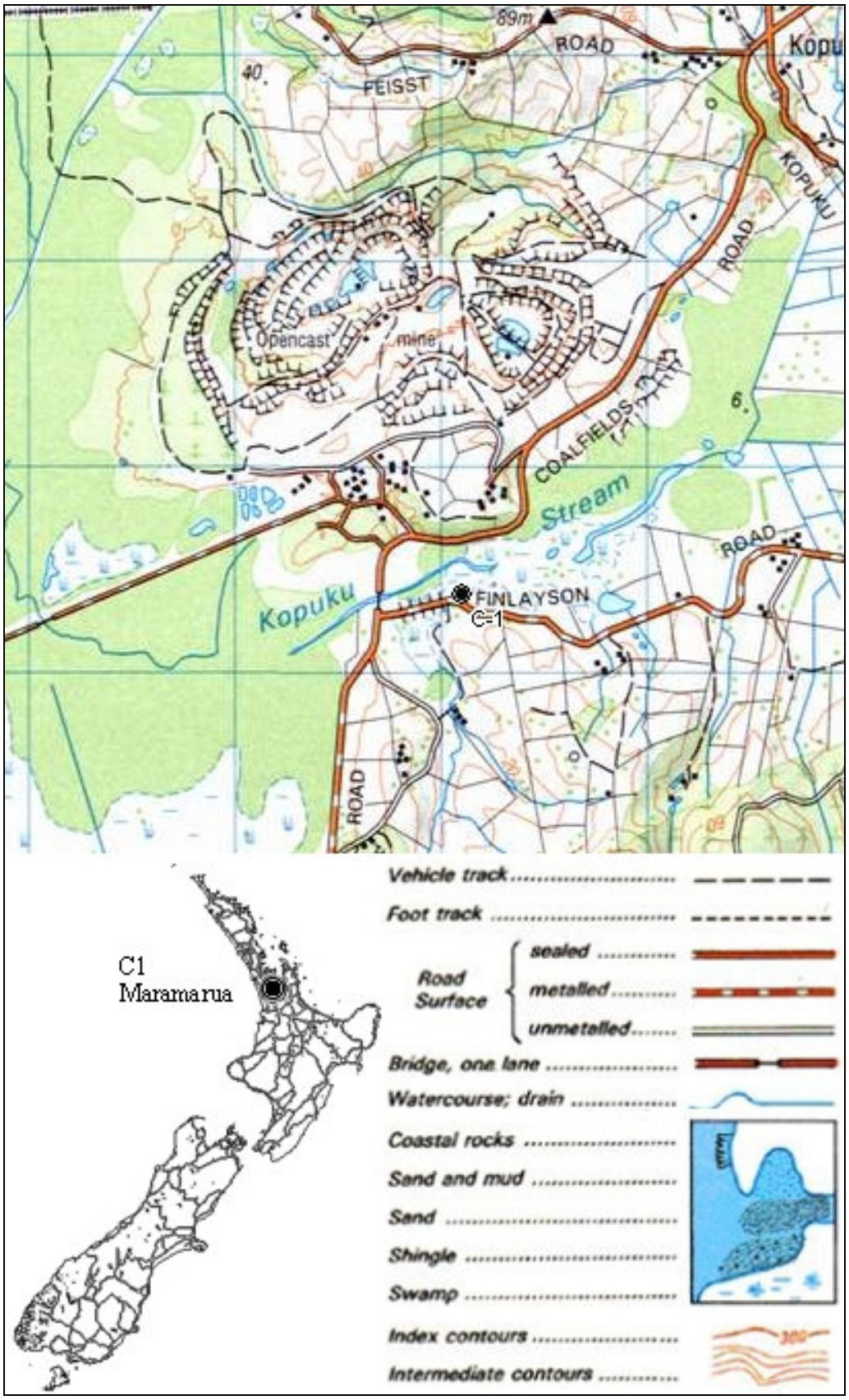

Figure 2.14. Location of borehole C1

Table 2.3. Drill hole summary for borehole C1

From (m)	To (m)	Thickness (m)	Formation	Member	Lithology
0.00	4.00	4.00			Recent, yellow brown CLAY
4.00	13.00	9.00			Grey-brown, firm grey MUDSTONE
13.00	73.20	60.20	Whaingaroa Siltstone		Grey-green, firm, moderately to very calcareous, glauconitic SILTSTONE
73.20	114.24	41.04	Mangakotuku	Mangakotuku Siltstone	Grey, slightly olive green, firm slightly calcareous and glauconitic SILTSTONE. Some fossil fragments.
114.24	123.00	8.76		Pukemiro Sandstone.	Green-grey, firm, very glauconitic, muddy very fine SANDSTONE.
123.00	139.50	16.50		Glen Afton Claystone.	Grey brown, firm slightly glauconitic CLAYSTONE
139.50	191.75	52.25	Waikato Coal Measures		Brown, firm, very slightly carbonaceous MUDSTONE. Occasional hard bars up to 0.30m thick.
191.75	203.30	11.55			COAL: Hard, black, highly fractured, clean with resinous zones.
203.30	204.60	1.30			Dark grey, firm, fractured, moderately carbonaceous MUDSTONE.
204.60	204.82	0.22			COAL; Black, very shaly.
204.82	206.00	1.18			Dark grey, CARBONACEOUS MUDSTONE
206.00	207.00	1.00			Light grey-white, slightly sandy CLAYSTONE. Weathered basement.

From Pope and Trumm (Pope and Trumm, 2004) and Edbrooke et al. (Edbrooke et al., 1994)

Table 2.4. Maramarua C1 samples

		Sample date	
		18/09/2003 [1], [3]	19/08/2004 [2], [4]
pH	pH units	8.5	7.8
Specific Conductance (T=25ºC)	µS/cm	1200 [6]	1310
TDS	mg/l	696 [7]	782
Hardness	mg/l as $CaCO_3$	76.7 [7]	18
Alkalinity	mg/l as $CaCO_3$	340	360
Bicarbonate (HCO_3^-)	mg/l	402	435 [5]
Carbonate (CO_3^{2-})	mg/l	8.8 [5]	<2
Carbon dioxide ($CO_{2\,(aq)}$)	mg/l	4.2 [5]	25
Calcium (Ca^{2+})	mg/l	20	6 [3]
Magnesium (Mg^{2+})	mg/l	6.5	0.9 [3]
Sodium (Na^+)	mg/l	184	334 [3]
Potassium (K)	mg/l	9.5	3 [3]
Chloride (Cl^-)	mg/l	49.3	146
Sulphate (SO_4^{2-})	mg/l	27.6	0.7
Fluoride (F)	mg/l	0.32	0.79 [3]
Boron (B)	mg/l	1.95	2.5 [3]
Silica (SiO_2)	mg/l	3.5	10.7 [3]
DOC	mg/l	130	11 [3]
Total Iron (Fe)	mg/l	55.9	0.4 [3]
Manganese (Mn)	mg/l	0.242	<0.01 [3]
Arsenic (As)	mg/l	<0.01	<0.02 [3]
Barium (Ba^{2+})	mg/l	0.154	0.024 [3]
Chromium (Cr^{2+})	mg/l	0.031	<0.01 [3]
Mercury (Hg)	mg/l	0.0009	<0.002 [3]
Selenium (Se)	mg/l	<0.01	<0.02 [3]
Zinc (Zn^{2+})	mg/l	0.17	1.28 [3]
Hydrocarbons C7-C9	mg/l	<0.3	<0.03 [3]
Hydrocarbons C10-C14	mg/l	117	<0.05 [3]
Hydrocarbons C15-C36	mg/l	4	<0.1 [3]
Hydrocarbons Total	mg/l	121	<0.2 [3]

[1] This sample was collected from the borehole prior to casing installation (to isolate the coal seam from other units).
[2] This sample was collected after borehole C-1 had been re-drilled and cased down to coal thus effectively isolating the coal seam.
[3] Sample was analysed by Hill Laboratories, Hamilton, and NZ.
[4] Sample was analysed by the CRL Energy Ltd Laboratory, Wellington, NZ.
[5] Calculated from carbonate equilibrium.
[6] On site measurement
[7] Calculated from measured ion concentrations

Exploration hole Maramarua C-1 was redrilled in June 2004 for the purpose of conducting a gas flow test. The well was completed with steel casing (100 mm) all the way down to the coal seam, effectively isolating it from nearby units, and thus preventing the mixing of coal seam waters with waters alien to the coal formation. This enabled the efficient pumping of water from the coal seam thereby reducing hydrostatic pressure and promoting desorption and gas flow. Once the gas flow test started, it was possible to collect samples for analysis.

On 19/8/2004 one sample was collected and sent to CRL Energy Ltd in Wellington where a detailed analysis was carried out. Results for this analysis are presented in Table 2.4 alongside the results from the sample taken from the uncased borehole on the 18/09/2003. The 19/8/2004 sample fits more closely the geochemical signature for coal seam gas waters than the 18/09/2003 sample. For example, calcium and magnesium concentrations are even lower in the 2004 sample than in the 2003 sample (70% and 86% less respectively), and bicarbonate and sodium concentrations are higher (8.2% and 81.5% higher respectively). In this case, chloride concentrations are higher than before, reaching a value of 146 mg/l (196% higher than the original value). Of significance is the fact that sodium levels have increased by almost 82%. Also, DOC values have decreased to 11 mg/l while iron levels have decreased significantly (0.4 mg/l). In general, most trace elements decreased in concentration except for zinc which increased moderately in 2004 (from 0.17 to 1.28 mg/l).

The Total Hydrocarbons for this sample are almost non-detectable (<0.2 mg/l) and the sulphate concentration is very low (0.7 mg/l which constitutes a 97.4% decrease in the 2003 value). The most likely reason behind these differences lies in the fact that for the second round of sampling (August 2004) the well was cased down to coal. Thus, when the well was sampled, one would expect that only water from the coal seam would enter the well, whereas in the previous sampling round (September 2003) one would expect that the sampled water was a mixture of coal seam water and water from other units (sandstones, siltstones, and mudstones). The 2004 values for Specific Conductance and TDS compare better to the on-site measurements taken during sampling in 2003 than to the subsequent lab results. This confirms the hypothesis that the 2003 laboratory results were erroneous (most likely a typographic error in writing down these values or swapping them by mistake). A noticeable difference is the high chloride composition in the August 2004 sample which classifies these CSG waters as Na-HCO_3^--Cl. This is possible because the 2004

sample is not expected to contain water from units other than coal and thus, the high chloride content in the pure CSG water would not be expected to have been diluted out as in the previous case.

Differences between the 18/09/2003 sample and the 19/8/2004 sample can be observed graphically by the use of Piper (Figure 2.15) and Schoeller (Figure 2.16) diagrams. The 18/9/2003 sample has a different ion composition than the 19/8/2004 sample. This can be observed graphically by inspecting the Piper diagram on Figure 2.15; on this diagram both samples plot at a different location.

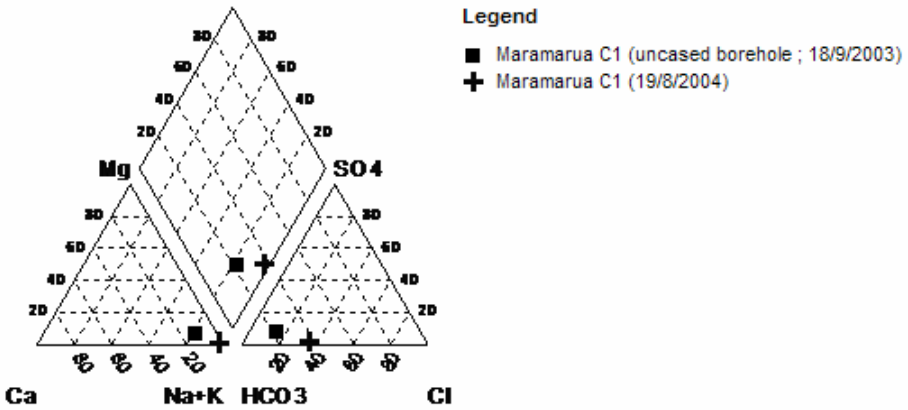

Figure 2.15. Piper diagram for Maramarua C-1 samples

The Schoeller diagram (Figure 2.16) shows that calcium, magnesium, and sulphate concentrations are higher in the 2003 sample than in the one taken in 2004. Sodium and Chloride, however, tend to be lower. In both of these samples sulphate levels are below the limit of 500 mg/l (≈10meq/l) for methane producing wells in the United States (Van Voast, 2003). This value is lower in the 2004 sample than in the 2003 sample, which is promising in terms of methane production. Because of the steel casing installation, one would expect that the Schoeller diagram for the 2004 sample presented in Figure 2.16 represents the true geochemical signature for CSG waters in Maramarua. At this stage it is interesting to note that desorption results from coal canisters taken from this borehole indicate that this coal seam holds significant amounts of methane (Pope and Trumm, 2004). Since the coal type is sub-bituminous, it is not likely for this methane to have been generated by thermogenesis; therefore

this methane must have been generated by biogenic processes, which in turn produce CSG water with the previously defined geochemical signature.

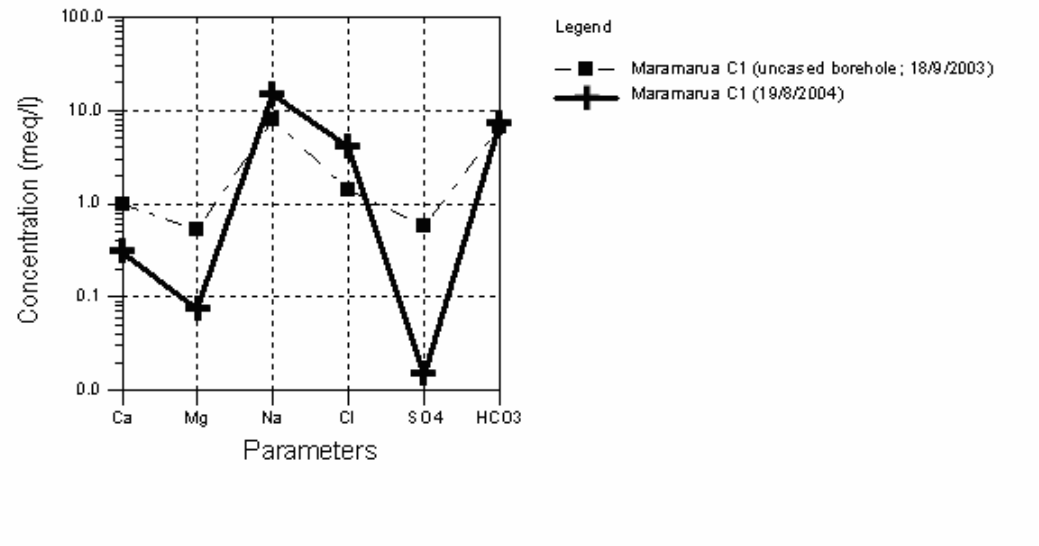

Figure 2.16. Schoeller diagram for Maramarua C-1 samples.

Very low tritium concentrations (-0.003 ± 0.016 TU) in samples collected on the 20th and 21st of October, 2004, suggest there is no recent recharge in the Maramarua coal aquifer. A qualitative interpretation of this value (<0.8 TU) classifies this water as sub-modern or pre-1952 (Clark and Fritz, 1997). Since tritium concentrations are basically nil, then the aquifer is either confined or so deep that recharge takes a long time. Log bore data (Table 2.3) taken while the well was being drilled suggests the aquifer is confined by a 16.5 m claystone cap (Pope and Trumm, 2004). Therefore, if no dispersion is assumed within the aquifer, then it is possible to apply a piston flow model (PFM) for a quantitative estimate of residence time. A PFM is a model that assumes little or no dispersion; it has been compared to a train moving people on a single path as opposed to people travelling in cars on a highway (Clark and Fritz, 1997). Consequently, the PFM assumes tritium concentrations change only due to isotopic decay (Maloszewski and Zuber, 1982). According to this, water from the Maramarua C-1 well would be at least older than 86 years.

A high transit time in the coal aquifer means CSG waters are subjected to geochemical processes as they flow through the seam. This leads to a more quantitative interpretation of the Maramarua CSG water samples using the *source-rock deduction* method described by (Hounslow, 1995). In this method, different ratios of chemical constituents give insight into the origin of the water being analysed. The attention values used in this method are derived from a mass balance approach using collections of water quality data (Hounslow, 1995), therefore this method can give a good estimate on the origins of a particular water. The calculated ratios for the 19/8/2004 sample, their attention values, and conclusions are presented in Table 2.5. The first ratio, which has to do with the proportion of sodium and chloride ions in halite (NaCl), indicates there is extra sodium (not accounted by halite dissolution) which could have resulted from the dissolution of albite (sodium feldspars) or an ion exchange process. However, the second ratio which tests for nonhalite sodium indicates that the extra sodium is not likely to originate from plagioclase (albite) weathering. Therefore, the main process responsible for enhancing sodium concentrations would have to be ion exchange. This is confirmed by comparing silica concentrations with nonhalite sodium using the third ratio on Table 2.5. Because silica concentrations are low in comparison to nonhalite sodium, then the majority of the sodium is likely to have taken place through a cation exchange process.

The fourth ratio indicates that there is more calcium than sulphate in the water and this would indicate carbonate weathering. The same conclusion is reached when analysing the ratio of bicarbonate and silica. A high TDS value and the magnesium concentrations relative to calcium (sixth and seventh ratios) point towards carbonate, limestone and dolomite weathering. However, high bicarbonate concentrations can also result from methane generation processes, which also account for the low sulphate concentrations in the CSG water. Therefore, it is possible that some carbonate weathering did occur, but bicarbonate concentrations were enhanced and sulphate concentrations were reduced through the methanation process. According to the last ratio in Table 2.5, the low chloride concentrations in the water sample are due to rock weathering. This is possible if there is some halite dissolution processes taking place. Lastly, the calculated Langelier Index for this sample is -0.48 which indicates that the sample is undersaturated with respect to calcite. However, this value can change once the sample is exposed to local atmospheric conditions. Sparging experiments conducted at the EEL have yielded positive Langelier Indexes for the

same type of water. This means that, once these CSG waters reach equilibrium with the atmosphere, they become oversaturated with calcite so they precipitate calcium carbonate.

Table 2.5. Rock-source deduction based on elemental rations (Hounslow, 1995).

Parameter	value	attention value	conclusion
$[Na^+] / [Na^+ + Cl^-]$	0.8	>0.5	Sodium source other than halite: albite or ion exchange
$[Na^+ + K^+ - Cl^-] / [Na^+ + K^+ - Cl^- + Ca^{2+}]$	0.001	<0.2	Plagioclase weathering is unlikely
$[SiO_2] / [Na^+ + K^+ - Cl^-]$	0.02	<1	Cation exchange
$[Ca^{2+}] / [Ca^{2+} + SO_4^{2-}]$	0.95	> 0.5	Calcium source other than gypsum: carbonates or silicates
$[HCO_3^-] / [SiO_2]$	40	> 10	Carbonate weathering*
$[Mg^{2+}] / [Ca^{2+} + Mg^{2+}]$	0.2	<0.5 and *	Limestone-dolomite weathering
TDS (mg/l)	782	>500	Carbonate weathering or brine or seawater
$[Cl^-]$ / Sum [Anions]	0.3	<0.8	Rock weathering
Langelier Index	-0.48	<0	Undersaturated with respect to calcite

Notes:
Ratios were calculated with concentrations in meq/l.
This source-rock deduction was carried out on the sample collected on the 19/8/2004. This sample was sent to Hill Laboratories (certified lab) for a full ion concentration analysis yielding very good results (electroneutrality = 4%).

Summarising, the majority of the sodium would originate from ion exchange processes in the aquifer. Some halite dissolution would be responsible for some sodium and the majority of the chloride. High bicarbonate concentrations would be due to carbonate weathering and biogenic (methanogenic) processes which are also responsible for low sulphate concentrations. Carbonate and dolomite weathering would also be responsible for calcium and magnesium concentrations. However, because of the high bicarbonate content, these cations would rapidly precipitate out of solution in the aquifer. In addition, the same ion exchange process responsible for sodium enhancement aids in the depletion of calcium and magnesium concentrations.

Discussion

Coal seam gas exploration in New Zealand has enabled the possibility of a new energy source with promising economic prospects. However, this technology will co-produce CSG water which, if not dealt with properly, can cause environmental problems due to its quality and quantity.

Based on the limited data able to be presented here, CSG waters in New Zealand do not differ much to CBM waters in the United States. This has been determined by analysing Maramarua water samples, which have been the best samples so far in terms of obtaining true CSG waters. Other samples, like the first Maramarua sample and samples from other locations, have helped to assess the correct sampling procedure which would go hand in hand with CSG mining operations. For example, in normal CSG mining operations each well would be continuously pumped to lower the coal aquifer pressure and to desorb and mine the coal seam gas. Constant pumping would flush the well of drilling fluids and stagnant water, and would produce large amounts of water referred to as CSG waters. Samples taken from exploration boreholes without adequate pumping (Reefton, Kaitangata, and Ashers Waituna; see Appendix A) are non indicative of CSG waters. These holes could have contained a large proportion of stagnant water and drilling fluids. Another issue to consider is casing. Casing in production wells is important because it effectively isolates the coal seam from other units above or below it. This ensures that only the coal seam is effectively being dewatered while increasing efficiency and decreasing the amount of co-produced water. This is particularly important if the adjacent formations have a high concentration of ions that could increase the chemical loading of CSG waters. More so, having a lower amount of better-quality water to dispose of is always better than the alternative. Consequently, the Maramarua C-1 well was cased in 2004 to carry out a gas flow test, which involved the pumping of large amounts of water. Therefore, samples from this well truly reflect the nature of coal aquifer waters (CSG waters).

The Maramarua CSG samples have a geochemical signature that is consistent with the signature for CSG waters defined by Van Voast (2003). This signature validates the model for the genesis and evolution of CSG waters flowing through the coal aquifer. As follows, Maramarua CSG waters have low calcium and magnesium concentrations in comparison to sodium and bicarbonate. Chloride concentrations are

also high, and constitutes the third major ion dissolved in these waters. Sulphate levels are very low (<2mg/l); lower than the 500 mg/l limit set by Van Voast (2003) for methane producing wells in the US.

Chemical analysis (*rock source deduction*) of Maramarua CSG water samples provides insight into the origins and processes involved in shaping this particular water quality. This method is a simple approach but is a good way of verifying an actual sample's origins especially if specific biogeological processes are suspected to have taken part in its formation. In the case of Maramarua, these processes are a combination of weathering of rocks (carbonates, dolomite, and halite), cation exchange, and biogenic processes. Nil tritium concentrations suggest aquifer recharge is taking place at a very slow rate, which would allow enough time for the CSG water generation processes to take place.

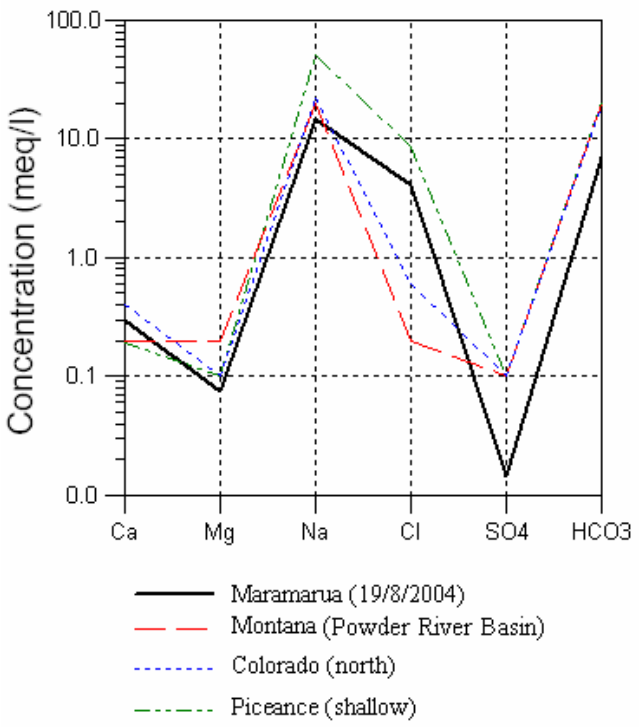

Figure 2.17. Maramarua CSG water compared against CBM samples from US basins. Sources: CRL Energy and Van Voast (2003). Sulphate concentrations for US sites may be lower than 0.1 meq/l.

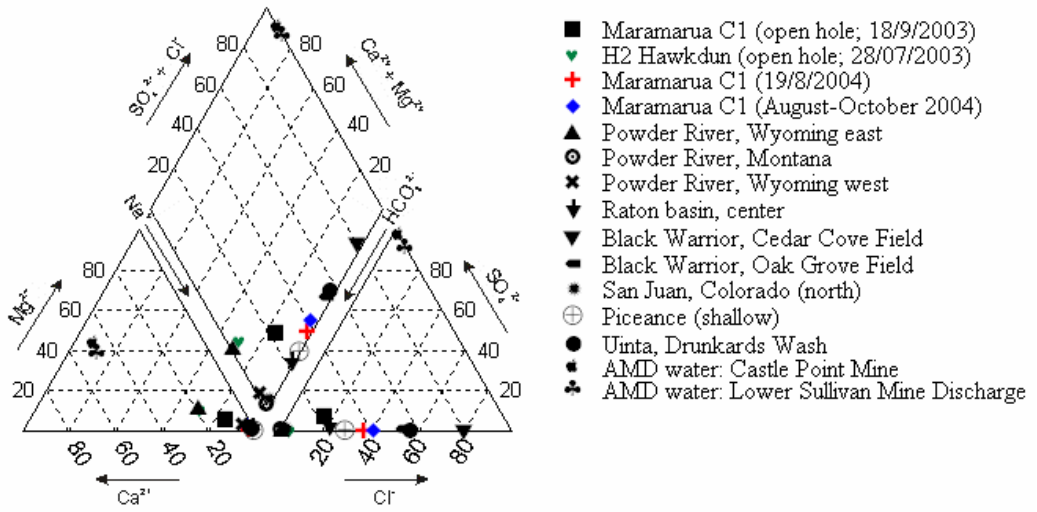

Figure 2.18. Piper diagram for NZ CSG water samples compared against US CBM and NZ AMD samples.

The major ion concentration of the Maramarua C-1 samples is similar to the chemistry of selected basins in the United States. Figure 2.17 compares major ion concentrations between Maramarua CSG water and typical CBM water from Montana (Powder River Basin), Colorado (Raton Basin, north), and Piceance (Figure 2.10). In Figure 2.17, Maramarua CSG water looks very similar (in terms of concentration) to the Montana CBM water: similar calcium and sodium concentrations, less magnesium and bicarbonate, and more chloride. Magnesium concentrations for Maramarua are similar to the ones from Colorado and Piceance, but chloride is significantly higher. The overall chemical signature for Maramarua CSG waters is similar in shape and order of magnitude to Piceance CBM waters, but shifted downwards due to less sodium, chloride, and bicarbonate concentrations. Sulphate concentrations for Maramarua are also lower, but individual samples from these US basins could have even lower sulphate concentrations than the values reported in Figure 2.17 depending on how deep within the basin the sampled wells are located. Nevertheless, this comparison places Maramarua CSG waters along the same category as US CBM waters. This can be extended further by grouping the data according to their major anion/cation percentages using the Piper diagram on Figure 2.18. This figure shows how sodium is the major cation in CSG water samples in both NZ and the US. In the NZ AMD samples, however, sodium is the minor cation. Hence, these data are plotted at a different place in the diagram. Because AMD chemistry is so different in terms of anion/cation composition, it might be better to plot these data in a modified Piper diagram to adequately represent these samples (Haefner, 2002). However, for

comparison sake, AMD waters are plotted in the standard Piper diagram along with CSG waters. Most CSG samples plot at the bottom right hand corner of the cation triangle; the exceptions are the Maramarua sample taken when the borehole had no casing installed and the Wyoming east (Powder River) data. The bottom right-hand triangle in the Piper diagram of Figure 2.18 represents the major anion composition. In all of the CSG samples bicarbonate is the major anion followed by chloride; in some of these samples chloride concentrations are greater than bicarbonate concentrations (Black Warrior and Uinta for example). However, AMD samples have sulphate as the major anion, followed by some chloride, and little or no bicarbonate. AMD waters have a completely different anion/cation chemistry. The piper diagram on Figure 2.18 (middle rhombus shaped section) shows that CSG waters have a very low hardness content, but varying degrees of chloride in contrast to the high concentrations of sulphate, chloride, calcium, and magnesium of AMD waters.

Coal seam gas waters in New Zealand, from this initial assessment, are indeed similar to CBM waters in the United States. Therefore, the problems (and solutions) related to management and disposal of CBM waters in the United States will be the same in New Zealand once production is underway. Large quantities of alkaline water with significant loading of dissolved salts will have to be managed as the CSG extraction process takes place. These problems will become more complicated with varying topographic, climatic, and recharge conditions. These conditions (physical parameters) will come into play with local industries (including the agricultural sector) to define the problem and its solutions within the bounds of local environmental regulations. However, to solve the problem, it is first necessary to define it. This involves determining the actual quality of CSG waters in selected basins and modelling (forecasting) produced quantities; clearly, more research is needed on both these topics prior to any definitive general statements can be made on CSG water in New Zealand. On these lines, it is necessary to anticipate the potential variations on both quality and quantity, and to understand how these changes can affect local systems. Once this is understood, the next stage is to analyse the range of disposal and treatment options available, and to determine the most suitable option for a particular CSG basin.

References

Alabama State Oil and Gas Board (AOGB), 2003, Coalbed Methane Resources of Alabama. http://www.ogb.state.al.us/, Volume 2005.

ALL-Consulting, 2003, Handbook on Coal Bed Methane Produced Water: Management and Beneficial Use Alternatives.: Tulsa, Oklahoma, Ground Water Protection Research Foundation, US Department of Energy, National Petroleum Technology Office, Bureau of Land Management.

ALL-Consulting, and Montana Board of Oil and Gas Conservation, 2004, Coal Bed Methane primer. New Source of Natural Gas–Environmental Implications. Background and Development in the Rocky Mountain West: Tulsa, Oklahoma, US Department of Energy, National Petroleum Technology Office.

American Public Health Association., American Water Works Association., and Water Environment Federation., 1999, Standard methods for the examination of water and wastewater: [Washington, D.C.], American Public Health Association, 1 computer optical disc p.

ASTM, D 388-05, Standard Classification of Coals by Rank, ASTM International.

Bartos, T.T., Ogle, K.M., Wyoming. State Engineer's Office., United States. Bureau of Land Management., and Geological Survey (US), 2002, Water quality and environmental isotopic analyses of ground-water samples collected from the Wasatch and Fort Union formations in areas of coalbead methane development : implications to recharge and ground-water flow, eastern Powder River Basin, Wyoming: Cheyenne, Wyo.

Denver, CO, US Dept. of the Interior US Geological Survey :

Branch of Information Services distributor, vi, 88 , (4 folded) p.

Cave, M., 2002, Turning a coalbed methane project into a co-producing hydrocarbon project, 2002 New Zealand Petroleum Conference proceedings: Wellington, N.Z., New Zealand Crown Minerals, p. 13.

Chapelle, F., 2001, Ground-water microbiology and geochemistry: New York, N.Y., Wiley, 477 p.

Clark, I.D., and Fritz, P., 1997, Environmental isotopes in hydrogeology: Boca Raton, FL, CRC Press/Lewis Publishers, 328 p. p.

Claypool, G.E., and Kaplan, I.R., 1974, The origin and distribution of methane in marine sediments: Journal of Marine Science, v. 3, p. 99-139.

Decker, A.D., Klusman, R., Horner, D.M., and Anonymous, 1987, Geochemical techniques applied to the identification and disposal of connate coal water: Proceedings - International Coalbed Methane Symposium, v. 1987, p. 229-242.

Edbrooke, S.W., Sykes, R., and Pocknall, D.T., 1994, Geology of the Waikato Coal Measures, Waikato Coal Region, New Zealand., Institute of Geological & Nuclear Sciences Monograph, p. 236.

Energy Information Administration, 2004, Advance Summary: US Crude Oil, Natural Gas, and Natural Gas Liquids Reserves 2003 Annual Report: Washington, DC 20585, Office of Oil and Gas, US Department of Energy, p. 18.

Freeze, R.A., and Cherry, J.A., 1979, Groundwater: Englewood Cliffs, N.J., Prentice-Hall, xvi, 604 p.

Gamson, P.D., Beamish, B.B., and Johnson, D.P., 1996, Coal Microstructure and Micropermeability and Their Effects on Natural-Gas Recovery, *in* Gayer, R.A., and Harris, I.H., eds., Coalbed methane and coal geology: London, Geological Society, p. 165-179.

GRI (Gas Research Institute), 2000, Coalbed Methane Potential of the US Rocky Mountain Region, p. 3pp.

Hach Company., 2003, Water analysis handbook : drinking water, wastewater, seawater, boiler/cooling water, ultrapure water: Loveland, Colo., Hach, 1268 p.

Haefner Ralph J, and US Geological Survey, 2002, Water Quality at an Abandoned Coal Mine Reclaimed with PFBC By-Products: Columbus, Ohio, U.S. Geological Survey, p. 37.

Hagmaier, J.L., 1971, Groundwater flow, hydrogeochemistry, and uranium deposition in the Powder River Basin, Wyoming [Ph.D thesis]: Grand Forks, University of North Dakota, Department of Geology.

Hamilton, T.M., 1970, Groundwater flow in part of the Little Missouri River Basin, North Dakota [Ph.D thesis]: Grand Forks, University of North Dakota, Department of Geology.

Hem, J.D., 1985, Study and interpretation of the chemical characteristics of natural water, U. S. Geological Survey Water-Supply Paper, p. 263.

Hounslow, A., 1995, Water quality data : analysis and interpretation: Boca Raton, Lewis Publishers, 397 p.

Jenden, P.D., and Kaplan, I.R., 1986, Comparison of microbial gases from the Middle America Trench and Scripps Submarine Canyon: implications for the origin of natural gas: Applied Geochemistry, v. 1, p. 631-646.

Johnson, K.C., 2004, The New Zealand coal seam gas scene, 2004 New Zealand Petroleum Conference proceedings: Wellington, N.Z., New Zealand Crown Minerals, p. 7.

Kjeldsen, P., Barlaz, M.A., Rooker, A.P., Baun, A., Ledin, A. and Christensen, T.H., 2002: Present and Long-Term Composition of MSW Landfill Leachate: A Review. Critical Reviews in Environmental Science and Technology, 32(4): 297-336..

Krevelen, D.W.v., 1961, Coal: typology, chemistry, physics, constitution: Amsterdam, New York,, Elsevier Pub. Co., xviii, 514 p.

Lee, R.W., 1981, Geochemistry of water in the Fort Union Formation of the northern Powder River Basin, southeastern Montana, U. S. Geological Survey Water-Supply Paper.

Maloszewski, P., and Zuber, A., 1982, Determining the Turnover Time of Groundwater Systems with the Aid of Environmental Tracers .1. Models and Their Applicability: Journal of Hydrology, v. 57, p. 207-231.

Moore, T.A., Manhire D.A., Flores R.M., 2002, Coalbed Methane opportunities in New Zealand: Similarities with the Powder River Basin coalbed methane paradigm, AusIMM Conference: Auckland, New Zealand.

Nelson, C.R., 2005, Geologic assessment of the natural gas resources in the Powder River Basin Fort Union Formation coal seams, Proceedings - International Coalbed Methane Symposium, Volume 2005, p. 14.

Nuccio, V.F., 2002, Coalbed Methane- What is it? Where is it? And why all the fuss?, Coalbed methane of North America, II Rocky Mountain Association of Geologists, 2002: Denver, Colo., The Rocky Mountain Association of Geologists, p. 6.

Oremland, R.S., Marsh, L.M., and Polcin, S., 1982, Methane Production and Simultaneous Sulfate Reduction in Anoxic, Salt-Marsh Sediments: Nature, v. 296, p. 143-145.

Pope, S., and Trumm, D., 2004, Coal Seam Gas Desorption Results: Drill Holes C1, K1 and K3, Maramarua Coalfield, Waikato, 2003.: Christchurch, CRL Energy Ltd, p. 27.

PTTC, 2000, Coal bed methane strategraphic traps in the ferron coals of east-central Utah, PTTC Rocky Mountain Newsletter, Volume September.

Rice, C.A., and Bartos, T.T., 2001, Nature and Characteristics of Water Co-Produced with Coalbed Methane with emphasis on the Powder River Basin, USGS Coalbed Methane Field conference May 9-10, 2001., Volume Open File Report 01-235: Casper, Wyoming., USGS.

Rice, D.D., 1992, Controls, habitat, and resource potential of ancient bacterial gas, *in* Vially, R., ed., Bacterial gas : proceedings of the conference held in Milan, September 25-26, 1989: Paris, Editions Technip, p. 91-118.

—, 1993, Composition and origin of coalbed gas, *in* Law, B.E., and Rice, D.D., eds., Hydrocarbons from coal, Volume AAPG Studies in Geology, American Association of Petroleum Geologists, p. 159-184.

Rice, D.D., and Claypool, G.E., 1981, Generation, accumulation, and resource potential of biogenic gas: AAPG Bulletin, v. 65, p. 5-25.

Rosen, M.R., White, P.A., and New Zealand Hydrological Society., 2001, Groundwaters of New Zealand: Wellington, N.Z., The Society, xiii, 498 p.

Schoell, M., 1980: The hydrogen and carbon isotopic composition of methane from natural gases of various origins. Geochimica et Cosmochimica Acta, 44(5): 649-661.

Scott, A.R., 2000, Coalbed Methane Potential in Texas, Gulf Coast Association of Geological Societies Transactions, Volume L.

Stumm, W., and Morgan, J.J., 1996, Aquatic chemistry : chemical equilibria and rates in natural waters: New York, Wiley, xvi, 1022 p.

The Seacreast Group, 2003, Water quality data collected from water wells in the Raton basin, Colorado: Denver, Colorado, Colorado Oil and Gas State Conservation Comission.

US Environmental Protection Agency, 2004, Evaluation of Impacts to Underground Sources of Drinking Water by Hydraulic Fracturing of Coalbed Methane Reservoirs, US Environmental Protection Agency.

US Environmental Protection Agency, and Advanced Resources International, 2002, Enhanced CBM Recovery, US Environmental Protection Agency.

Van Voast, W.A., 2003, Geochemical signature of formation waters associated with coalbed methane: Aapg Bulletin, v. 87, p. 667-676.

Van Voast, W.A., and Hedges, R.B., 1975, Hydrogeologic aspects of existing and proposed strip coal mines near Decker, Southeastern Montana.: Bulletin - Montana Bureau of Mines and Geology, v. 97, p. 31.

Whiticar, M.J., Faber, E., and Schoell, M., 1986, Biogenic methane formation in marine and freshwater environments: CO2 reduction vs. acetate fermentation--Isotope evidence: Geochimica et Cosmochimica Acta, v. 50, p. 693-709.

Williams. B, 2001, Personal communication between Mr. Williams/ V.P., Redstone and Dr. Langhus/ALL-LLC. March 23, 2001.

Woltemate, I., Whiticar, M.J., and Schoell, M., 1984, Carbon and hydrogen isotopic composition of bacterial methane in a shallow freshwater lake: Limnology and Oceanography, v. 29, p. 985-992.

Wyoming State Engineers Office, and Wyoming State Geological Survey, 2005, The Coal Section.

"You could not step twice into the same river;
for other waters are ever flowing on to you. "
Heraclitus, On the Universe.
Greek philosopher (540 BC - 480 BC)

Chapter 3

Coal Seam Gas Water Quality Variability

Introduction

Coal Seam Gas water samples collected from borehole C-1 in Maramarua (2004 and 2005) provide valuable information about the nature of these waters and the aquifer through which they flow. Twenty two water samples were collected from this borehole between August and October, 2004, and eleven more samples were collected between April and June, 2005. These samples are very similar in chemical composition, but are not identical and present some variations in ion concentrations. After these observations, some questions naturally arise: are these variations expected within a coal seam aquifer along with CSG extraction? What are the underlying reasons for these variations? Are greater variations expected with time as dewatering continues? To answer these questions it is necessary to understand which variables play an important part in water quality variations. This chapter aims at defining these key variables in order to understand variations and their cause in water quality from CSG producing wells.

Preliminary analysis of Maramarua data

Between August and October 2004 dewatering of the Maramarua C-1 borehole produced 22 samples that were analysed at the EEL (Environmental Engineering Laboratory, University of Canterbury). Pumping took place at continuous intervals that were interrupted whenever the pump broke down. Pump problems are common in CSG dewatering operations at the start of the project as equipment (i.e. pump) is being tested and operators learn how to work with it. In this particular

operation, a “sucker rod” pump was used to dewater the well. Sucker rod pumps consist of a rod that is able to move in a vertical motion thanks to the constant movement of a walking beam connected to a flywheel trough a crank and Pittman arm (Figure 3.1). The flywheel is powered by a motor that makes it turn, thus driving the whole system into motion. As the rod moves vertically, a plunger attached at the end of the rod pushes the liquid up with the aid of a travelling valve (a ball in a cage). The size of the pump (crank arm, pitman arm, and walking beam) determines its capacity. Big pumps, for example, can pump liquid from wells deeper than 3000m (Karassik, 1986).

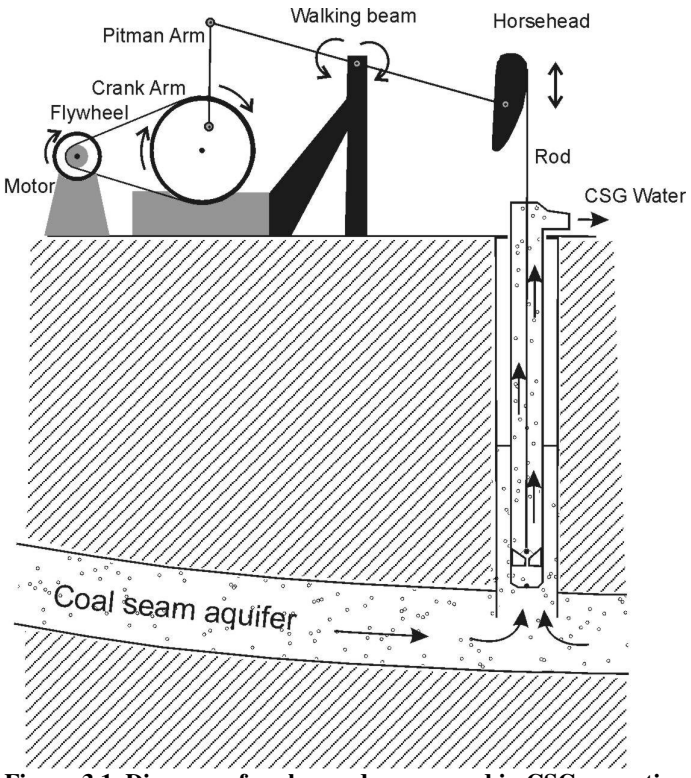

Figure 3.1. Diagram of sucker rod pump used in CSG operations. Adapted from Hoffman (2004).

Figure 3.2. Sucker rod pump used in Maramarua, 2004.

The sucker rod pump used in Maramarua was a second hand Anderson pump that had been used before in petroleum exploration (**Figure 3.2**). The on-site operator experienced a few problems with this pump; it was suspected the pump was too small for this particular application. To achieve the desired drawdown, the pump had to be manually lowered as dewatering went on. However, the lower the water level, the harder it was for the pump to lift water up to the surface. This is because water pressure is directly proportional to the distance from the surface. As a result, the pump being used at Maramarua broke down often after the water level (distance from the surface) reached approximately 100 m. The pump would break down either by the walking beam snapping into two, the rod or rod connector breaking, or the Pitman arm snapping. However, water samples were collected whenever pumping was resumed and had been ongoing for at least two hours. As a result, these samples represent the water inside the well with the water level fluctuating between 25 m and 150 m (Table 3.1). The water column inside the well sometimes would sit in the well for several days when the pump was not working. When this took place, the water level would slowly rise inside the well (due to artesian pressure), but it would start to decrease as soon as the pump was fixed and dewatering resumed.

Figure 3.3 shows these cycles plotted against elapsed time in days. When pumping takes place continuously (days 5-16; 42-44; 47-51; 63-64; 78-80), there is a progressive decrease of water column height. Pump break-up marks the end of each of

these cycles, increasing the height of the water column, and thereby generating a high water column measurement at the start of the next pumping round (when the pump has been repaired). However, as the operator fixes the pump and learns from his mistakes, efficiency of the overall pumping procedure is improved. As a result, each cycle gets shorter with time, and it is possible to achieve a lower water column inside the well.

Table 3.1. Water levels for samples collected from Maramarua C-1, 2004.

Sample N°	Sample date	Sample time	Water level [a]	Water column [b,c,d]
1	1/08/2004	16:45	25	175
2	6/08/2004	18:45	40	160
3	7/08/2004	17:30	60	140
4	8/08/2004	17:40	65	135
5	9/08/2004	16:50	70	130
6	10/08/2004	17:10	80	120
7	16/08/2004	17:40	126	74
8	20/08/2004	18:10	55	146
9	12/09/2004	17:22	66	134
10	13/09/2004	14:00	91	109
11	14/09/2004	9:30	100	100
12	17/09/2004	15:30	46	154
13	18/09/2004	9:35	62	139
14	18/09/2004	12:45	64	136
15	18/09/2004	18:15	70	130
16	19/09/2004	15:00	100	100
17	20/09/2004	8:30	105	95
18	21/09/2004	15:30	120	80
19	4/10/2004	17:10	140	60
20	5/10/2004	10:15	150	50
21	20/10/2004	18:00	130	70
22	21/10/2004	18:00	144	56

a. Distance from surface in metres
b. Height of water column inside the well in metres
c. Well depth: 200 m
d. Twelve-metre coal seam at 192 m

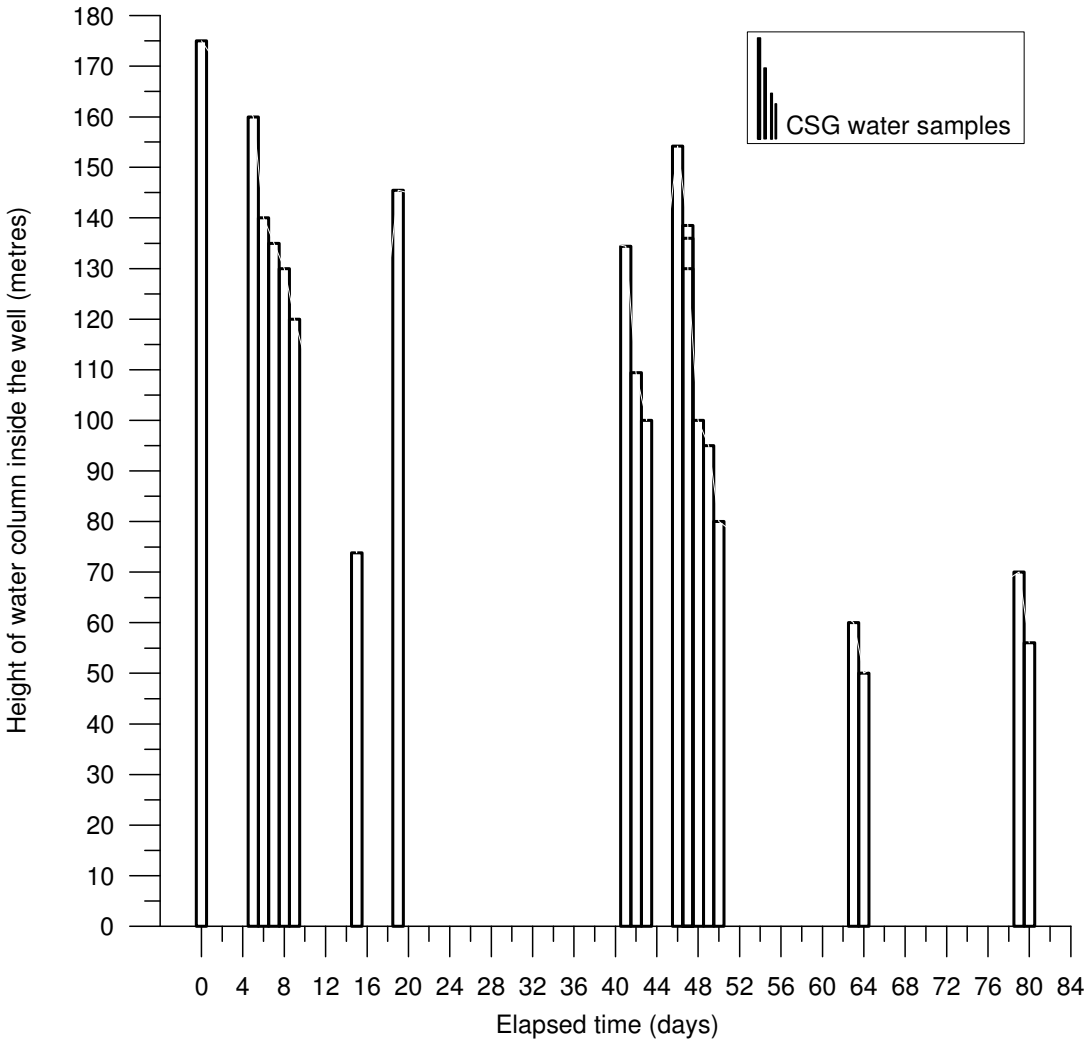

Figure 3.3. Well purging and sample collection at Maramarua (C-1) using a sucker rod pump. Start date was on the 1/08/2004 (day 0) and finish date was 21/10/2004 (80 days later).

The dewatering programme was suspended in November 2004 due to ongoing pump problems. However, the test was resumed in April, 2005 when a Progressive Cavity (PC) pump was installed. This pump operates under a different principle than the former sucker rod pump, so it is able to pump water to the surface without breaking down. Progressive cavity pumps consist of a single-helix shaped rotor which revolves inside a double-helix shaped stator (Figure 3.4). The rotor is powered by a vertical well head drive on the surface, and the output pressure will be directly proportional to the number of stages (length) of the rotor. Consequently, the pump can be designed for a particular application, resulting in a continuous fluid flow.

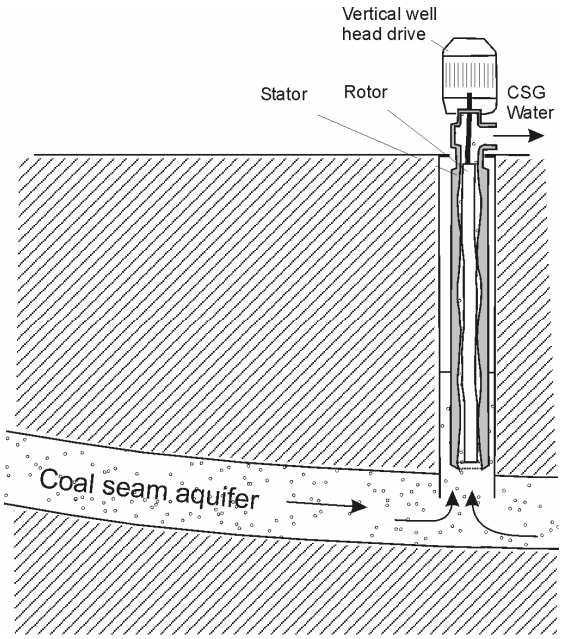

Figure 3.4. Diagram of a progressive cavity pump

Table 3.2. Water levels for samples collected from Maramarua C-1, 2005.

Sample N°	Sample date	Sample time	Water level [(a)]	Water column [(b,c,d)]
1	22/04/2005	17:45	40	160
2	23/04/2005	18:55	50	150
3	25/04/2005	18:15	70	130
4	27/04/2005	17:30	90	110
5	29/04/2005	NA	110	90
6	3/05/2005	11:00	130	70
7	10/05/2005	17:15	145	55
8	23/05/2005	08:00	180	20
9	24/05/2005	17:30	60	140
10	10/06/2005	20:15	170	30
11	11/06/2005	NA	180	20

[(a)] Distance from surface in metres
[(b)] Height of water column inside the well in metres
[(c)] Well depth: 200 m
[(d)] Twelve-metre coal seam at 192 m

Eleven more samples were collected using the progressive cavity pump between April and June, 2005. Each time a sample was taken, the water level depth was recorded (Table 3.2) and the sample was sent to the EEL for its chemical analysis. With this pump, it was possible to lower the piezometric surface more rapidly and without major breakdowns (Figure 3.5). There was still an instance in which the pump had to be turned off (day 32) for minor repairs, but 9 samples were taken before this took place. Once the repairs were completed, the dewatering process continued and 2 more samples were taken once the water level inside the well was sufficiently low.

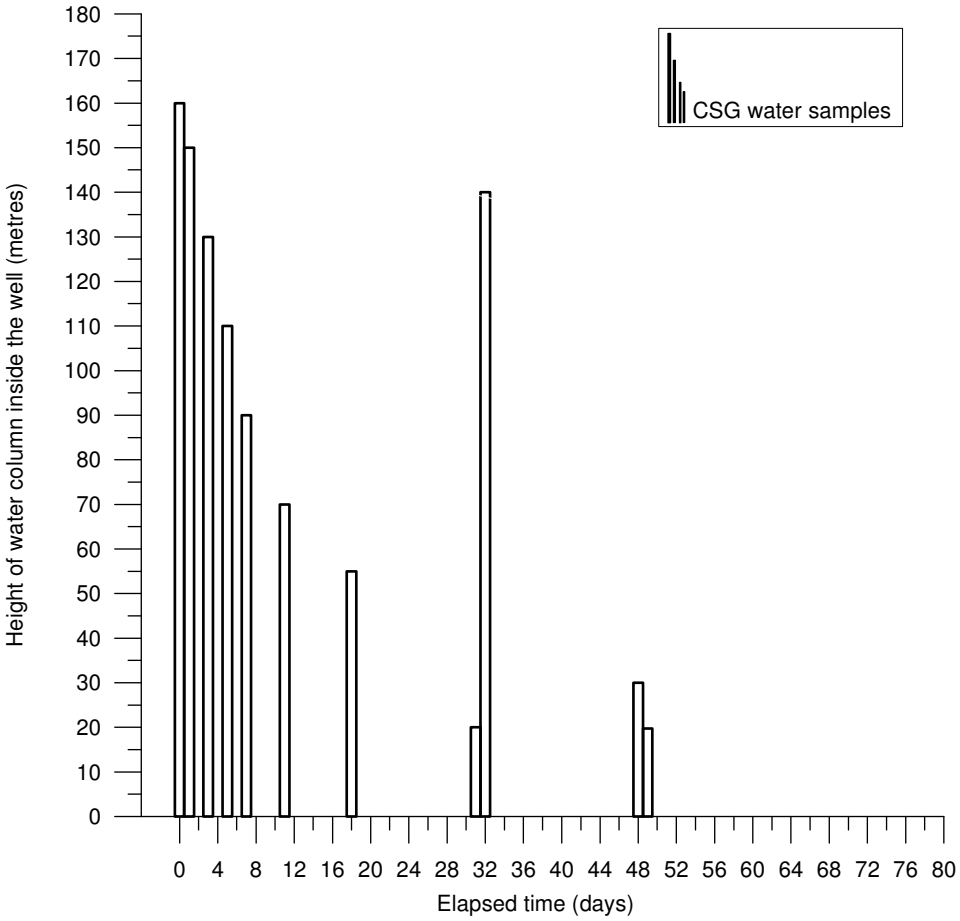

Figure 3.5. Well purging and sample collection at Maramarua (C-1) using a progressive cavity pump. Start date was on the 22/04/2005 (day 0) and finish date was 11/06/2005 (49 days later)

These two dewatering rounds produced two similar sets of water samples for well C-1. The first set of samples was subjected to at least five dewatering cycles while the second set was subjected to only two; lower water levels were achieved during the second round of sampling. Potential problems associated with sampling include pump problems (i.e. not enough purging prior to sample collection) and inaccuracies in sample analysis at the EEL. However, this methodology was chosen after discussions with the mining companies funding this research (see section A.3 in Appendix A). This means that all the data are likely to have higher uncertainty than in more standard hydrogeological research.

Common standards for sampling wells usually involve purging the well and taking the sample after removing 3-5 well volumes or until pH, specific conductance, and temperature remain constant (Nielsen, 1990). Therefore, stagnant water is effectively purged from the well prior to taking the sample. In this case, the well was

purged continuously, sometimes beyond the volume specified by the standard because the aim of the test was to lower the water level to just above the coal seam rather than just pumping water out of the coal aquifer. However, water level fluctuations inside the well could have had an impact in the samples' water quality. Also, it is necessary to discriminate between variations due to the sampling methodology and variations due to the inherent characteristics of this particular aquifer. This suggests carrying out an analysis focusing on the variations of the water quality parameters to uncover underlying characteristics.

The 33 samples collected during sampling rounds 1 and 2 were analysed at the EEL. The analytical methods used at the EEL were the same APHA and HACH methods used in the various locations described in Chapter 2, which are presented in Appendix A (section A.1). In addition, a sample collected on 19/8/2004 (see Table 2.4, Chapter 2) was sent to a certified laboratory for full analysis. The samples analysed at the EEL (University of Canterbury) provided an invaluable insight into the variability of the Maramarua CSG waters because these samples were taken in a consecutive fashion over a period of 3 months in August-October (2004) and 3 months in April-June (2005). The results from these analyses are presented in Table 3.3, and a discussion relating to their accuracy and precision is presented in Appendix B (section B.2). These samples exhibit low concentrations of calcium and magnesium accompanied by high concentrations of bicarbonate and chloride. Also, the calculated sodium concentrations for these samples is consistently high (average = 313 mg/l). Sulphate levels are generally very low (< 2 mg/l) and below the detection limit imposed by the measuring method being used (HACH). The low sulphate levels, along with the previously stipulated chemical signature, is enough to confirm this well's potential as a likely producer of methane gas (Van Voast, 2003). Specific conductance (1284-1424 μS/cm) values are consistent with the specific conductance of brackish waters; the 19/08/2004 sample (see Table 2.4, Chapter 2) falls within this range. TDS values are in the range of 702-814 mg/l which covers the TDS value for the sample taken on the 19/8/2004. The major ions are sodium, bicarbonate and chloride thus classifying this water as of the Na-HCO_3^- -Cl^- type (Figure 3.6).

The sample taken on the 19/8/2004 was analysed at the CRL Energy laboratory and Hill Laboratories, which are certified labs. Therefore, the systematic and random errors that could have been committed by these labs should be lower than the ones that could have been made at the EEL. Therefore, the 19/8/2004 sample

could better represent the true chemical concentrations than the samples analysed at the EEL (University of Canterbury) from August-October, 2004 and April-June, 2005. In any case, these latter samples are extremely valuable in determining the potential variations in CSG quality through time. Figure 3.7 shows the magnified cation triangle corresponding to the Piper diagram (Figure 3.6) for these samples. On this diagram, however, samples appear clustered together so small variations are hard to interpret. Therefore, Figure 3.7 shows these samples plotted on a magnified portion of the cation triangle. On this diagram, the samples appear clustered together along the bottom right hand corner. However, the samples collected on the 22/04/05 and 23/04/05 appear to be outside the main cluster of points. These two samples were the first samples to be taken at the beginning of the second sampling round where the well had a high water level. Therefore these samples could have been contaminated with stagnant water or residues from the PC pump installation, and should not be considered in a final analysis. Also, the sample collected on the 19/8/2004 has the highest sodium and lowest magnesium concentrations, and this also results in this point being outside the main cluster (Figure 3.7). This could be due to this sample being analysed at a different laboratory than the rest of the samples, which translates into different accuracies and systematic errors. Therefore, sample 19/8/2004 should not be compared against the rest of the samples analysed at the EEL.

Table 3.3. Samples analysed at the Environmental Engineering Laboratory, University of Canterbury

#	Date	Time	pH	Sp Cond µS/cm T=25°C	TDS mg/l	Alkalinity mg/l as $CaCO_3$	Hardness mg/l as $CaCO_3$	Ca^{2+} mg/l	Mg^{2+} [(a)] mg/l	Cl^- mg/l	SO_4^{2-} mg/l	HCO_3^- [(b)] $\cdot 10^2$mg/l	CO_3^{2-} [(b)] mg/l	$CO_{2\,(aq)}$ [(b)] mg/l	Na^+ mg/l
1	01/08/2004	16:45	7.9	1424	798	428	27.3	7.39	2.13	140	< 2	5.1	2.9	21	326[(c)]
2	06/08/2004	18:45	7.9	1390	814	425	29.0	4.48	4.34	142	< 2	5.1	2.9	22	327[(c)]
3	07/08/2004	17:30	7.8	1354	786	416	25.0	4.80	3.16	142	< 2	5.0	2.3	26	325[(c)]
4	08/08/2004	17:40	7.8	1389	772	413	23.0	4.90	2.62	145	< 2	5.0	2.3	26	317[(d)]
5	09/08/2004	16:50	7.8	1386	774	421	25.3	5.32	2.91	142	< 2	5.1	2.2	29	316[(e)]
6	10/08/2004	17:10	7.8	1390	702	410	24.8	4.56	3.25	142	< 2	5.0	2.0	29	317[(d)]
7	16/08/2004	NA	7.8	1391	800	394	23.3	5.79	2.13	142	< 2	4.8	2.0	28	311[(d)]
8	20/08/2004	18:10	7.9	1357	740	394	32.0	7.79	3.05	143	< 2	4.7	2.6	20	308[(d)]
9	12/09/2004	17:22	7.7	1325	742	391	32.7	5.40	4.67	143	< 2	4.7	1.7	32	313[(d)]
10	13/09/2004	14:00	7.7	1358	768	388	32.0	5.20	4.63	141	< 2	4.7	1.7	31	308[(c)]
11	14/09/2004	09:30	7.7	1380	766	385	30.5	5.20	4.26	141	< 2	4.7	1.7	31	305[(d)]
12	17/09/2004	15:30	7.7	1410	786	390	30.5	5.60	4.02	140	< 2	4.7	1.7	31	314[(d)]
13	18/09/2004	09:35	7.8	1396	734	390	32.5	4.80	5.00	144	< 2	4.7	2.0	27	311[(d)]
14	18/09/2004	12:45	7.8	1418	746	390	31.0	5.00	4.51	142	< 2	4.7	2.1	25	320[(d)]
15	18/09/2004	18:15	7.7	1325	772	390	25.0	4.40	3.41	146	< 2	4.7	1.7	32	306[(d)]
16	19/09/2004	15:00	7.6	1338	770	388	26.5	4.40	3.78	142	< 2	4.7	1.3	40	309[(d)]
17	20/09/2004	08:30	7.6	1361	786	390	26.5	6.39	2.56	146	< 2	4.7	1.3	40	317[(d)]
18	21/09/2004	15:30	7.6	1284	792	395	31.5	7.19	3.29	144	< 2	4.8	1.4	40	320[(e)]
19	04/10/2004	17:10	7.9	1326	766	390	30.0	6.39	3.41	141	< 2	4.7	2.7	20	318[(e)]
20	05/10/2004	10:15	7.9	1380	784	393	28.0	5.99	3.17	148	< 2	4.7	2.7	20	317[(c)]
21	20/10/2004	18:00	7.6	1390	746	390	28.0	5.99	3.17	145	< 2	4.7	1.4	40	317[(d)]
22	21/10/2004	18:00	7.7	1385	743	390	27.0	5.60	3.17	151	< 2	4.7	1.7	32	318[(c)]
23	22/04/2005	17:45	7.3	1253	834	345	52.0	12.00	5.40	148	38	4.2	0.6	71	289[(e)]
24	23/04/2005	18:55	7.4	1280	652	363	40.0	8.40	4.60	145	14	4.4	0.8	59	297[(e)]
25	25/04/2005	18:15	7.2	1270	828	365	28.0	6.40	2.90	145	< 2	4.4	0.5	94	313[(e)]
26	27/04/2005	17:30	7.4	1309	812	375	23.0	6.70	1.50	144	< 2	4.6	0.8	61	313[(e)]
27	29/04/2005	NA	7.4	1296	826	378	24.0	5.60	2.40	148	< 2	4.6	0.8	61	308[(e)]
28	3/05/2005	11:00	7.5	1309	782	383	19.0	5.20	1.50	143	< 2	4.6	1.0	49	307[(e)]
29	10/05/2005	17:15	7.5	1305	784	375	20.0	4.80	1.90	148	< 2	4.5	1.0	48	314[(e)]
30	23/05/2005	8:00	7.7	1318	780	383	18.0	4.80	1.50	143	< 2	4.6	1.7	31	312[(e)]
31	24/05/2005	17:30	7.4	1296	822	380	29.0	7.90	2.40	143	< 2	4.6	0.8	62	306[(e)]
32	10/06/2005	20:15	7.7	1317	844	380	24.0	4.00	3.40	145	< 2	4.6	1.6	31	313[(e)]
33	11/06/2005	10:30	7.4	1314	792	380	22.3	4.80	2.50	NA	< 2	4.6	0.8	62	NA

[(a)] Calculated from hardness and calcium concentrations

[(b)] Calculated from carbonate equilibrium; the calculated average relative standard deviation was 20 % for HCO_3^- , 18 % for CO_3^{2-}, and 26% for $CO_{2\,(aq)}$ (Appendix B, section B.2).

[(c)] Calculated assuming zero electro neutrality and mean differences in electro neutrality from samples of known sodium concentrations (Appendix B, section B.1).

[(d)] Calculated using sodium probe

[(e)] Determined using Atomic Absorption

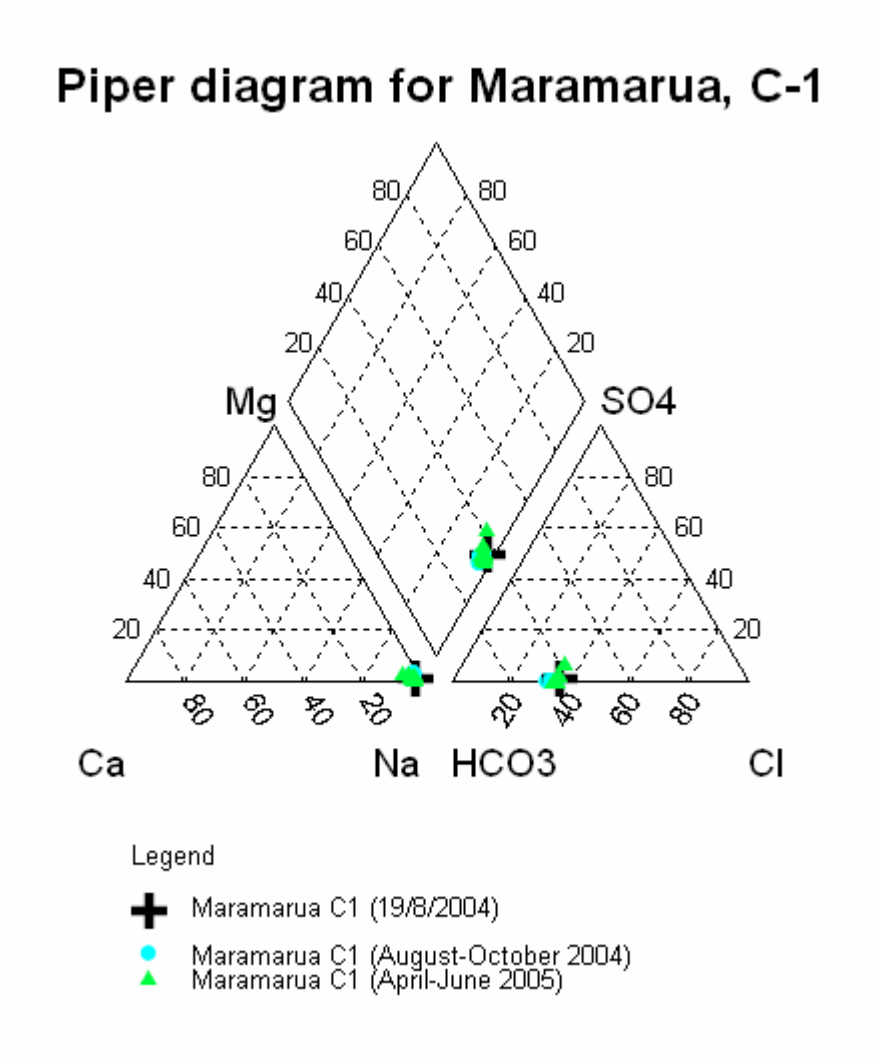

Figure 3.6. Piper diagram for Maramarua, C-1

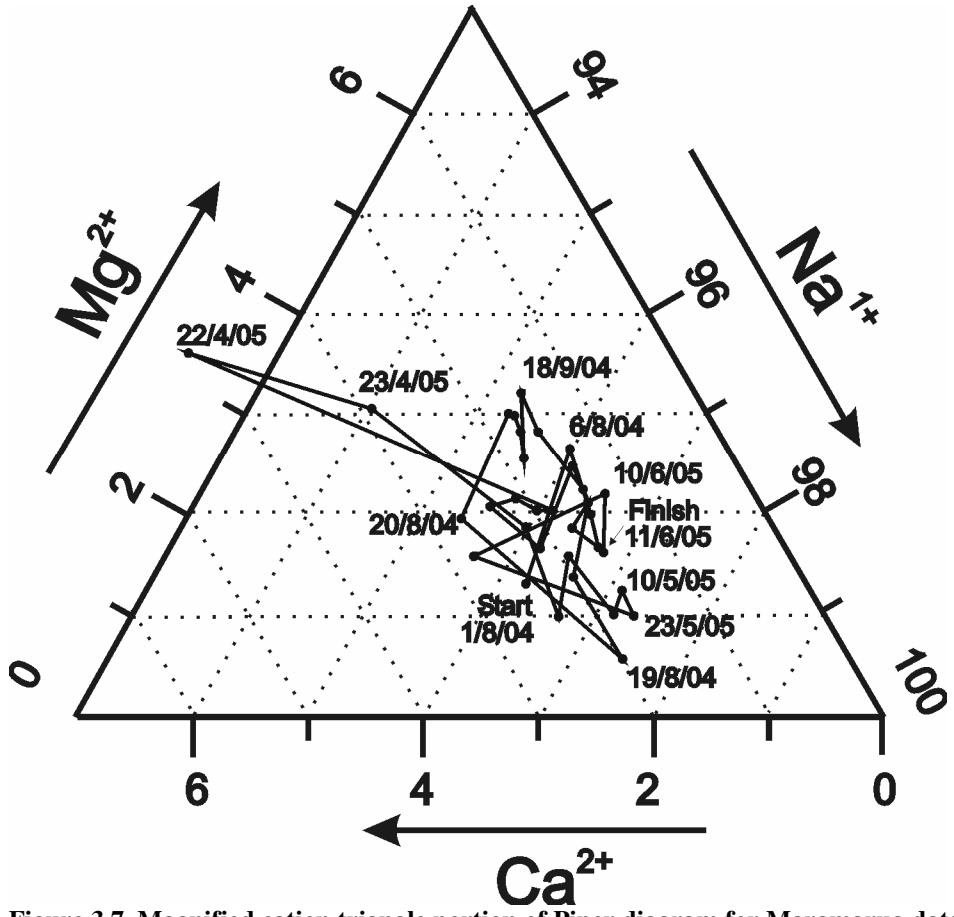

Figure 3.7. Magnified cation triangle portion of Piper diagram for Maramarua data.

Another way of analysing water quality variations in the collected samples is by inspecting their Schoeller diagram (Figure 3.8). On this diagram, the variations in magnesium are quite noticeable and, as previously mentioned, the lowest magnesium concentration corresponds to the sample collected on the 19/8/2004; this sample is also responsible for the highest sodium concentration. This diagram also shows two points having sulphate concentrations that are above the limit detected for most of the samples. These points correspond to samples collected on the 22 and 23/04/2005 which are suspected to be contaminated with stagnant water. The higher sulphate concentrations confirm these suspicions. Therefore, samples taken on the 22 and 23/04/2005 are disregarded from future analyses.

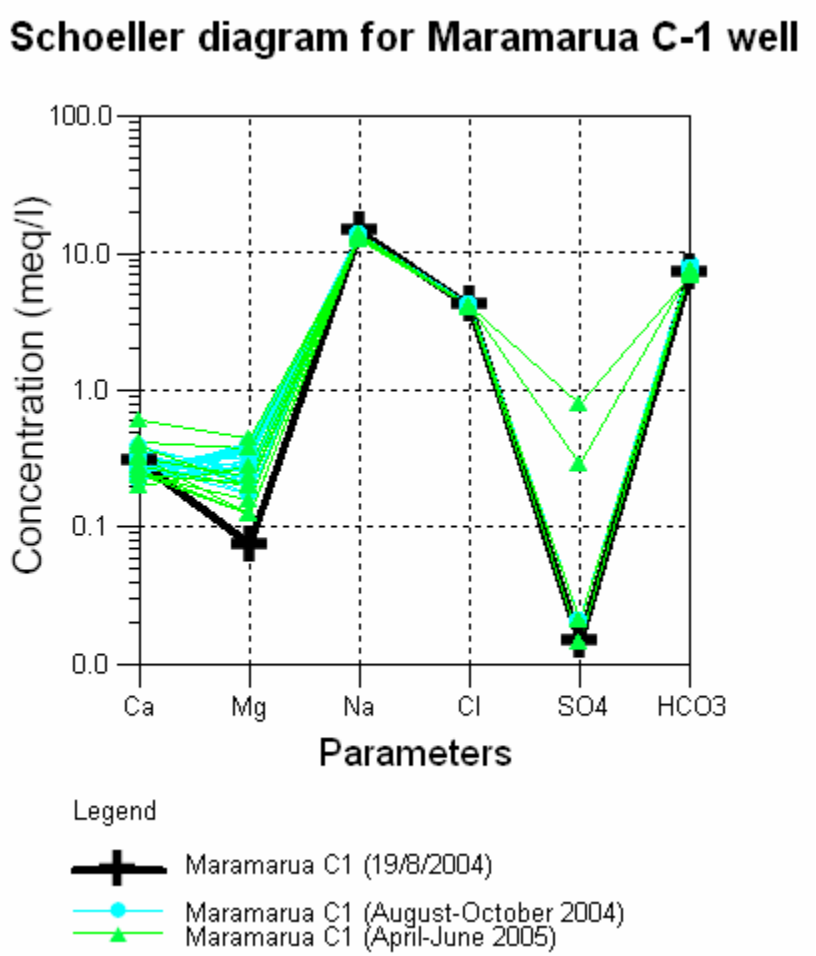

Figure 3.8. Schoeller diagram for Maramarua, C-1

Time series analysis of Maramarua data

The Maramarua data presented in Table 3.3 constitute discrete observations of changes in water quality parameters due to the dewatering process. These data, however, are not equally spaced; therefore it is not possible to carry out a classic time series analysis. For example, trend analysis (curve fitting) becomes complicated, and the computation of autocorrelation coefficients is impaired (Chatfield, 1996). Nevertheless, it is possible to plot the data on a time plot to show underlying trends. Figure 3.9 shows the bicarbonate, calcium, sodium, and chloride concentrations in water samples with ongoing dewatering. During the first sampling round, bicarbonate concentrations start at $5.1 \cdot 10^2$ mg/l but, during the first month, concentrations decrease drastically. The trend is almost logarithmic (1/ln(x)) with bicarbonate concentrations stabilising at around $4.7 \cdot 10^2$ mg/l. During the second sampling round, bicarbonate concentrations start at a much lower

value than before ($4.4 \cdot 10^2$ mg/l) but soon stabilise around $4.6 \cdot 10^2$ mg/l. During the first sampling round, calcium concentrations seem to follow a cyclic trend (going from 4.40 to 7.79 mg/l) reaching an average value of 5.57 mg/l. However, during the second sampling round, calcium levels seem to decrease in a logarithmic fashion (1/ln(x)) starting at 6.40 mg/l and finishing at 4.80 mg/l (with one exception at 7.90 mg/l). An even more erratic trend is shown for sodium concentrations. For sodium, during the first round of sampling concentrations seem to decrease drastically from 326 mg/l to 308 mg/l during the first month. However, after the first month, sodium concentrations start to rise and to stabilise at around 318 mg/l. During the second round of sampling, sodium concentrations follow a cycle at around an average value of 314 mg/l. In the case of chloride, concentrations do not follow a particular pattern and seem to fluctuate between 140.2 mg/l and 151 mg/l with an average value of 143.7 mg/l. Chloride concentrations seem fairly constant during the first sampling round except for a couple of samples at the end of the round; during the second sampling round, chloride concentrations do not present major variations.

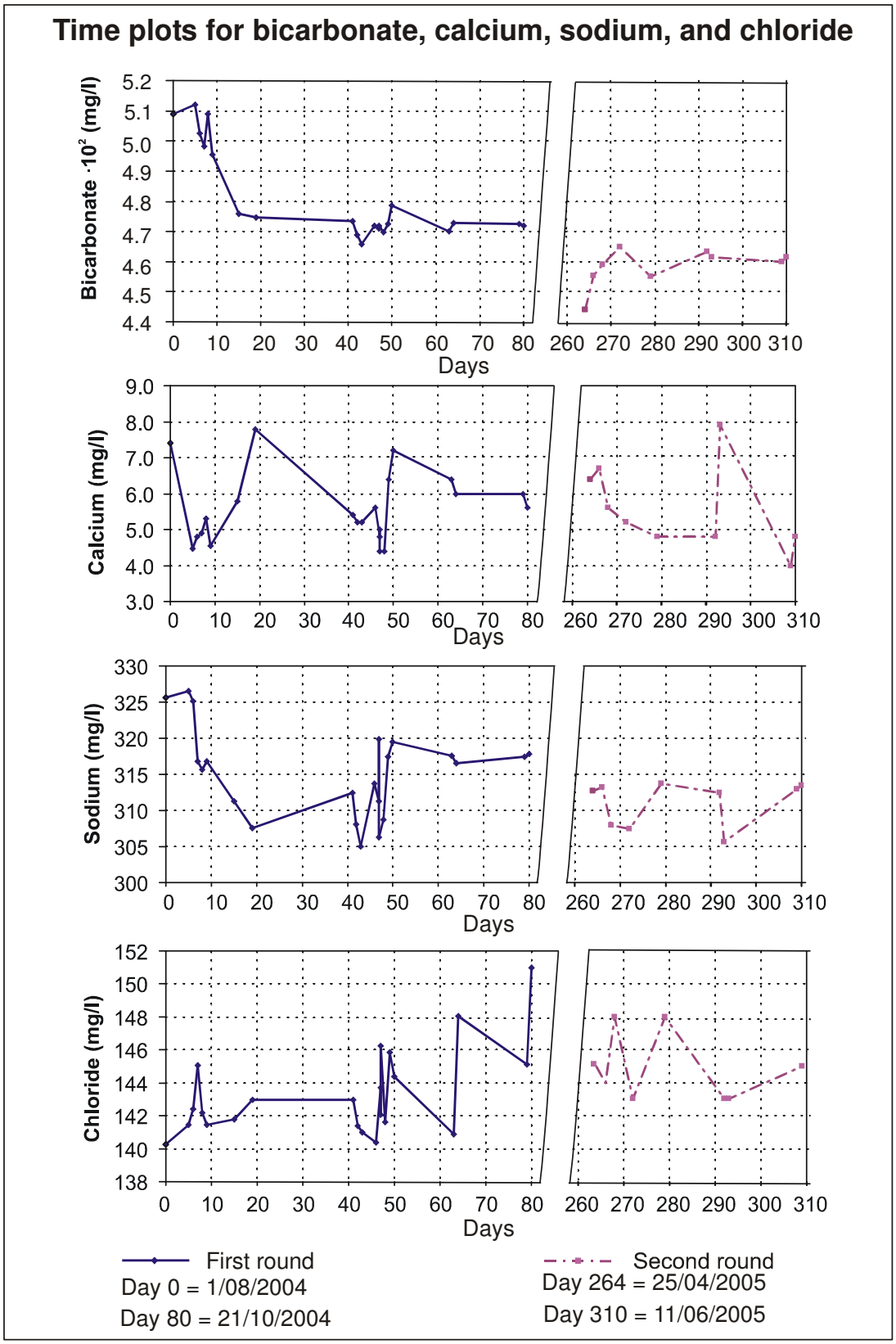
Time plots for bicarbonate, calcium, sodium, and chloride
Bicarbonate ·10² (mg/l)
Calcium (mg/l)
Sodium (mg/l)
Chloride (mg/l)
Days
First round
Day 0 = 1/08/2004
Day 80 = 21/10/2004
Second round
Day 264 = 25/04/2005
Day 310 = 11/06/2005

Figure 3.9

More plots like the ones in Figure 3.9 are presented in Appendix B (section B.3). All of these plots show the same erratic variations as the previous plots. At times, some of these plots even seem to follow a trend like the logarithmic trend for bicarbonate concentrations in the first sampling round (Figure 3.9). However, as in the case of bicarbonate, the trend seems to disappear during the second round of sampling. An analytical trend analysis of the data is not straight forward because samples were not collected at equally spaced intervals - if some sampling points are taken consecutively they appear clustered together, whereas if the sampling interval between points is large then important features or events could be missing. Nevertheless, these data hold important information about the nature of CSG waters, the dewatering process, and the sources of variation. This is specially so because each sample has 12 parameters (pH, TDS, calcium, alkalinity, etc) that describe the water quality at a given point in time. This suggests the use of a multivariate analysis to extract useful information.

Multivariate analysis of Maramarua data

There are various techniques that can be used in multivariate analysis. Each of these techniques, however, produces different outcomes depending on the desired objective. For example, multiple regression is concerned with the variance of only one variable without considering the behaviour of independent variables, cluster analysis allows the classification of observations according to their characteristics, and factor analysis helps uncover the underlying structure existing within multiple observations (Davis, 2002). Factor analysis is a powerful tool capable of uncovering the nature of CSG waters from the Maramarua C-1 well. Principal component analysis (PCA), which is a basic form of factor analysis, can also be used for this purpose, but factor analysis is more effective because it allows for further simplification of the problem. A description of the PCA and factor analysis techniques is presented in Appendix B (sections B.4 - B.5).

Maramarua CSG water quality data review for factor analysis

The Maramarua CSG water quality data presented in Table 3.3 were considered for a factor analysis. However, before carrying out the actual analysis it was necessary to discard outliers and deal with missing values while at the same time checking for normality. Samples # 23 and # 24 were discarded because, as previously stated, these samples appear to have been contaminated with residues from the second pump installation. The missing chloride and sodium values for sample #33 were replaced by their averages (disregarding samples # 23 and # 24). Since sulphate levels were below detection limits for the filtered data set, sulphate was not considered in the subsequent analysis. Because the number of observations is low (31), additional checks are necessary before carrying out the factor analysis.

An underlying assumption of factor analysis is that the multivariate data are normally distributed (Davis, 2002). This is so that it is possible to apply the normal procedure for calculating the variance/covariance matrix (i.e. the mean approximated by the average). Also, this helps when dealing with a reduced number of observations, which is the case here. Therefore, the Maramarua water quality in Table 3.3 was tested for normality. When the data did not fulfil the requirements of a normal distribution, a transformation was applied to force the data into a normal distribution. A description of this procedure and the selected transformations is presented in Appendix B (section B.7).

Maramarua CSG water quality data consist of 31 observations containing 12 variables each. These variables are the chemical properties and constituents listed in Table 3.3 but excluding sulphate and including the water levels (water column) listed in tables 1 and 2. However, some of these variables are either not independent variables or are strongly related towards each other. For example, in a closed system with pH values between 4.3 and 8.3, bicarbonate is the major species contributing to alkalinity (Snoeyink and Jenkins, 1980); since the Maramarua CSG water samples have pH values between 7.2 and 7.9 their bicarbonate concentrations and alkalinity are practically identical. Therefore the factor analysis should be carried out either with alkalinity or with bicarbonate, but the uncertainty associated with alkalinity titrations (3.17% max) is lower than the one for bicarbonate (23.8% max), so the factor analysis is carried out just with alkalinity. A similar issue arises with hardness, calcium, and magnesium concentrations.

Hardness is the sum of calcium and magnesium ions, and since calcium and hardness are known values, magnesium is calculated by taking their difference. However, this procedure makes either magnesium or hardness redundant, and since magnesium is a calculated value, it has a higher uncertainty associated with it. Therefore, magnesium is not considered in the factor analysis of Maramarua data. Specific conductance and TDS are strongly correlated having a linear relationship (Snoeyink and Jenkins, 1980), therefore only one of these variables should be considered. Since specific conductance values were already used in determining the ionic strength for carbonate and carbon dioxide calculations, the TDS value was used when carrying out the final factor analysis. Summarising, to carry out the factor analysis of Maramarua data there are 31 observations available with 10 variables which can be either transformed or not transformed depending on their normality (Appendix B, section B.7).

Before the analysis was carried out, the data were normalised and the eigenvalues were calculated to decide how many factors to extract. This preliminary analysis and the subsequent factor analysis were carried out on the correlation matrix [R]. Table 3.4 presents the calculated eigenvalues and their contribution to the total variance. Because, these values have been calculated using the correlation matrix [R], the total variance is 10 ([R] is a 10x10 matrix with "1" on its diagonal and the total variance corresponds to their sum). The eigenvalues are ranked according to their contribution to the total variance which is noticeably significant for the first 5 eigenvalues accounting for 90.9% of the total variance. This can be seen graphically by inspecting the eigenvalue (scree) plot on Figure 3.10. In this plot, eigenvalue n°5 represents an elbow or a point where each subsequent eigenvalue's contribution becomes negligible in comparison to the previous ones. Therefore, in the final factor analysis only 5 factors were extracted. The final analysis was carried out using varimax rotation to further rotate the remaining 5 factors once the last 5 eigenvalues had been removed. Once this was carried out, the resulting factor score coefficients were either close to the factor axes or far from them, which facilitates the interpretation of results. Later, different factor analyses were carried out extracting 2, 3, 4, 6, 7, and 8 factors. It was found that with fewer than 5 factors the analysis became complicated because the factors became too cluttered by having too many factor score coefficients with high values. On the other hand, when extracting more

than 5 factors the analysis became restricted because there were fewer factor score coefficients with high values present after the second factor.

Table 3.4. Eigenvalues (CSG water samples) calculated from correlation matrix

N°	Eigenvalue (λ)	Contribution	Cumulative
1	4.5	44.9%	44.9%
2	1.7	17.4%	62.3%
3	1.3	12.5%	74.8%
4	0.9	8.8%	83.5%
5	0.7	7.4%	90.9%
6	0.5	4.7%	95.6%
7	0.3	2.8%	98.4%
8	0.1	1.4%	99.8%
9	0.02	0.2%	99.99%
10	0.001	0.0%	100.0%
Total	10.00	100%	

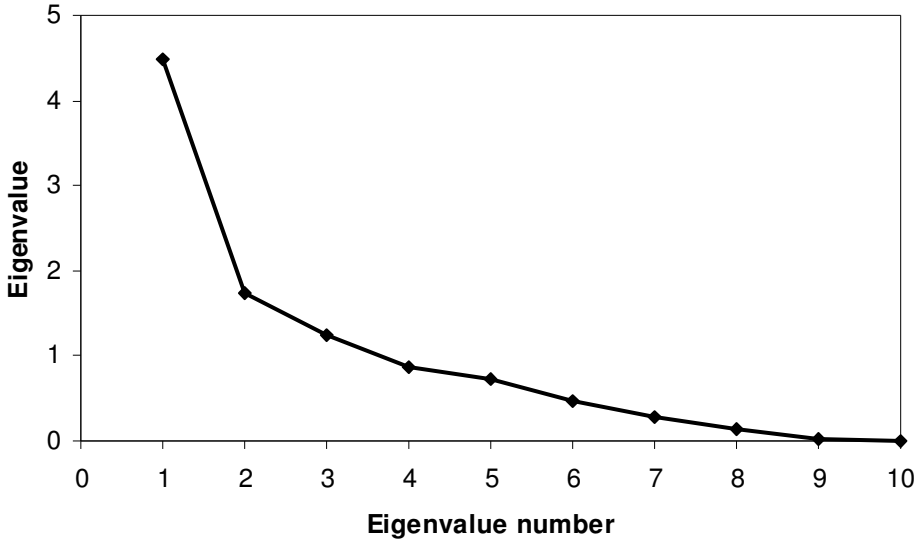

Figure 3.10. Eigenvalue plot for Maramarua CSG water quality data

Factor analysis results

Maramarua factor analysis results are presented on Tables 3.5 and 3.6. These are true factors in the sense that the effect of the unique factors, resulting from the factor extraction process, has been taken into account. Also, these factors have been varimax rotated to further enhance factor axes differences. To simplify the notation, future mention of these calculated factor score coefficients and factor scores is done without stating each time that these are "true" and rotated. Also, the factor score coefficients sometimes are simply referred to as "factors".

The calculated communalities resulting from the factor extraction process are presented in Table 3.5. No single communality is unusually low, which is a good indication of the efficiency of the factor extraction process (no additional factors are needed). Also, this suggests that the analysis is valid even though a limited number of observations (31) were used. The sum of the communalities is equal to the sum of the first five eigenvalues (9.09) because this is the total variance after the five factors have been extracted and rotated; hence these factors account for 90.9% of the total variance.

Table 3.5. Factor score coefficients ([*B*]) for Maramarua CSG waters

Variable	B_1	B_2	B_3	B_4	B_5	h_i [3]
pH	0.3589	0.1417	0.0631	0.0422	-0.0246	0.979
Water column	-0.3459	-0.4394	-0.4511	-0.0719	-0.2575	0.901
TDS	0.0578	0.0726	-0.1154	-0.1144	0.8218	0.891
Alkalinity	-0.0558	-0.4556	-0.1068	0.0928	-0.0141	0.913
Hardness	0.0824	0.1791	-0.1266	-0.3637	-0.2364	0.788
Calcium	0.0364	-0.0306	0.2098	-0.7901	0.1794	0.891
Chloride	-0.0713	-0.3162	0.7003	-0.2143	-0.2832	0.875
Carbonate	0.3200	0.0425	0.0625	-0.0491	0.0571	0.985
CO_2	-0.3979	-0.1769	-0.1032	0.0629	-0.0551	0.977
Sodium	-0.0532	-0.6077	0.2250	-0.0530	0.0343	0.888
						Total
λ_I [1]	3.283	1.653	1.596	1.332	1.226	9.09
% [2]	32.8%	16.5%	16.0%	13.3%	12.3%	90.9%

[1] Eigenvalue calculated after factor extraction and varimax rotation
[2] Eigenvalue contribution to total variance in percentage units
[3] Communalities are calculated by adding the squares of the factor loading coefficients

Table 3.6. Factor scores, [*S*], for Maramarua CSG waters

Date	S_1	S_2	S_3	S_4	S_5
01/08/2004	1.0806	-1.7242	-1.4594	-1.2706	1.4743
06/08/2004	1.0657	-1.8485	-1.1296	0.4842	1.1597
07/08/2004	0.3166	-1.9188	-0.3941	0.6977	0.3844
08/08/2004	0.1694	-2.3146	0.5543	0.6392	-0.2024
09/08/2004	0.2315	-1.0327	-0.6657	0.5322	0.0388
10/08/2004	0.0297	-1.2713	-0.3515	1.4514	-2.2934
16/08/2004	0.8232	0.4930	0.0042	0.1760	1.5518
20/08/2004	1.3011	0.3876	0.1638	-2.1763	-1.1710
12/09/2004	-0.1423	0.2897	-0.6171	-0.2459	-1.6422
13/09/2004	0.2054	1.2577	-1.1473	0.0655	-0.3737
14/09/2004	0.2979	1.5735	-1.2144	0.2735	-0.2056
17/09/2004	-0.0593	0.9772	-2.2516	-0.0604	0.4237
18/09/2004	0.3029	0.4858	-0.4220	0.1514	-2.0792
18/09/2004	0.5775	0.2204	-0.6046	0.1506	-1.2525
18/09/2004	-0.2903	-0.1319	0.1042	0.8259	-0.6136
19/09/2004	-0.5049	0.5646	-0.9678	1.1654	-0.1399
20/09/2004	-0.5109	-0.3700	0.7347	-0.8306	0.3452
21/09/2004	-0.2960	-0.5482	0.6583	-1.7892	0.6267
04/10/2004	2.0715	1.2728	0.0992	-0.7119	0.5049
05/10/2004	1.9526	0.4578	1.9767	-0.8545	0.4333
20/10/2004	-0.3499	0.1147	0.8386	-0.3643	-0.9738
21/10/2004	0.1837	-0.5129	2.3056	-0.3320	-1.3518
22/04/2005	-2.3685	-0.1422	-0.1854	-1.0811	0.2993
23/04/2005	-1.5631	-0.2401	0.1610	-0.6533	0.5398
25/04/2005	-1.4207	0.2828	0.6393	-0.1136	0.4688
27/04/2005	-0.8739	0.6717	-0.0426	1.1058	0.7770
29/04/2005	-0.8854	-0.0103	1.3702	0.9270	0.2904
03/05/2005	0.5521	0.9800	0.9301	1.5307	0.7749
10/05/2005	-1.5771	0.4486	-0.6590	-1.9631	0.0700
23/05/2005	0.5995	1.1126	0.8673	1.2654	1.0537
24/05/2005	-0.9186	0.4751	0.7044	1.0051	1.0823

To aid in the interpretation of results, it is possible to plot the factor score coefficients in a bar chart to compare each variable (factor components) within a given factor. The five factor score coefficients are presented in this way in Figures 3.11-3.15.

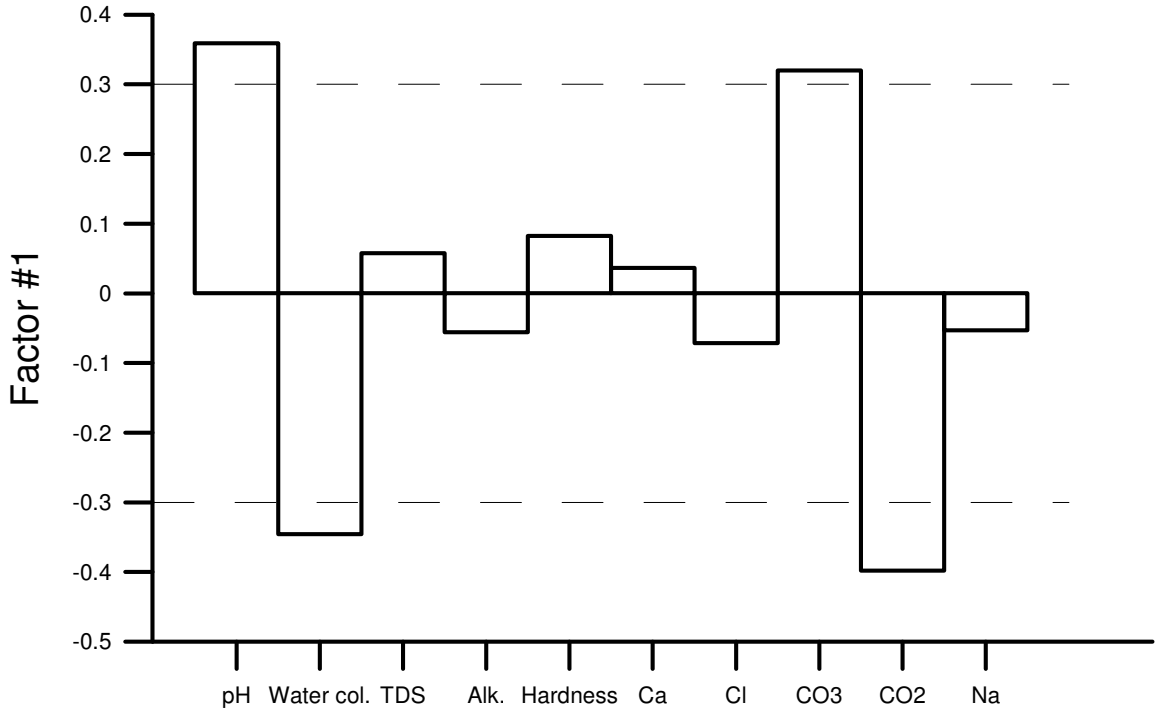

Figure 3.11. Plot of components for factor score coefficient #1

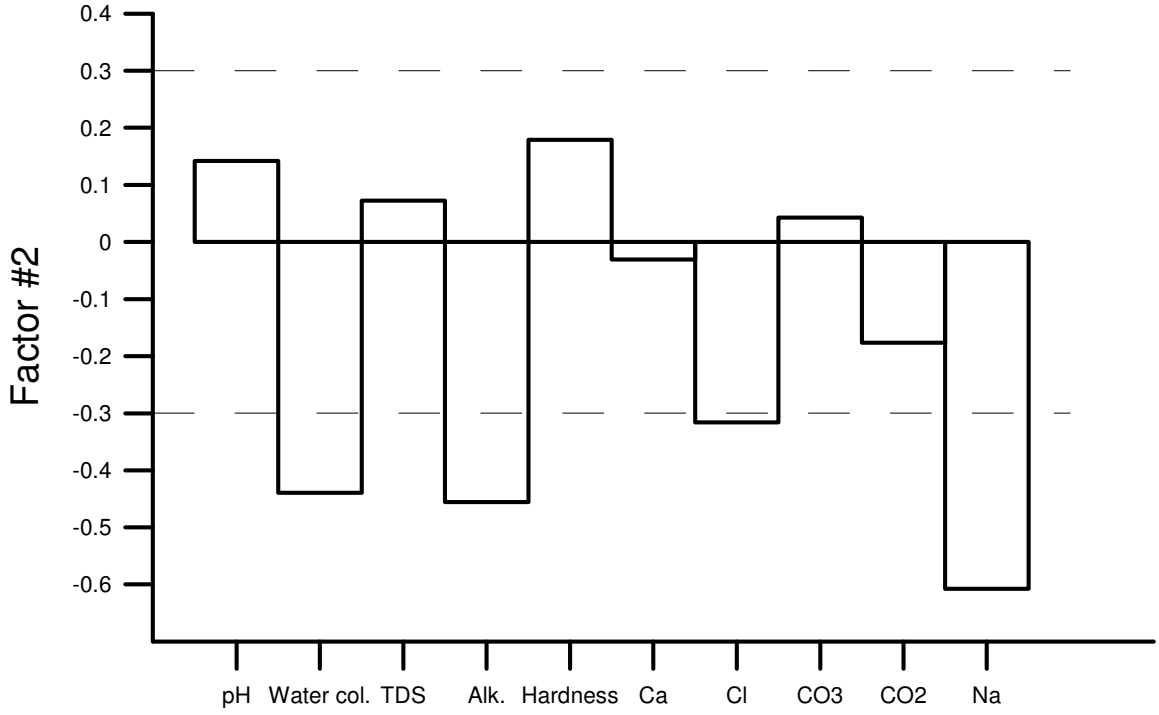

Figure 3.12. Plot of components for factor score coefficient #2

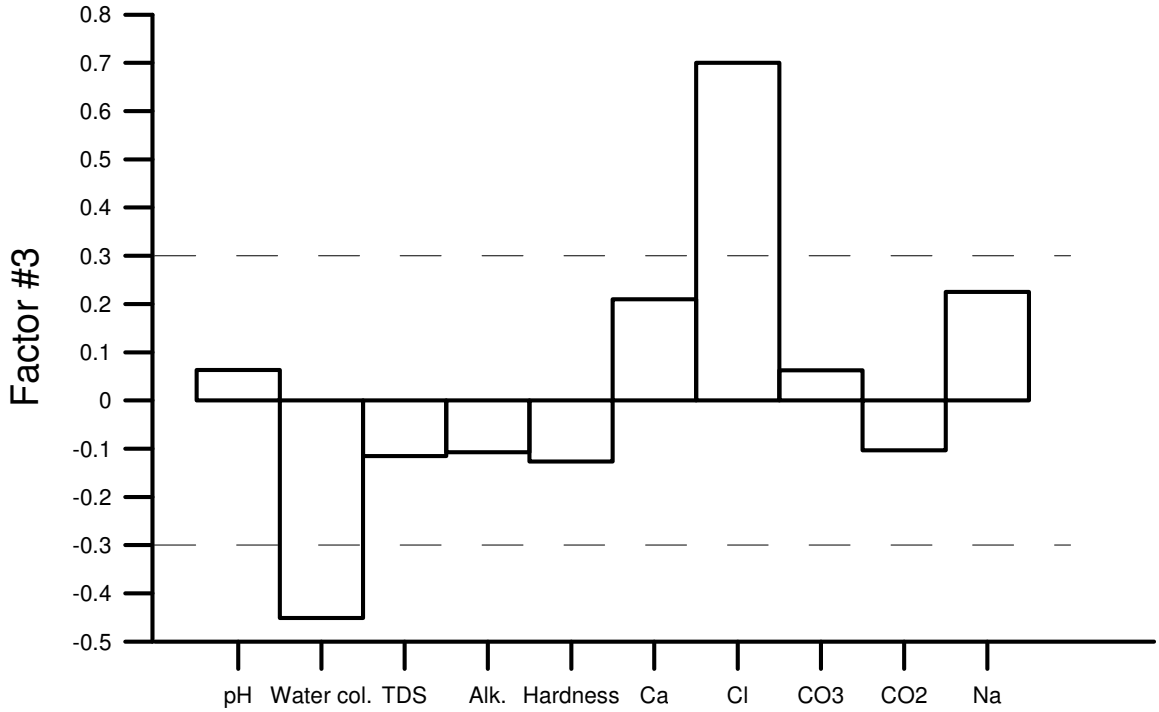

Figure 3.13. Plot of components for factor score coefficient #3.

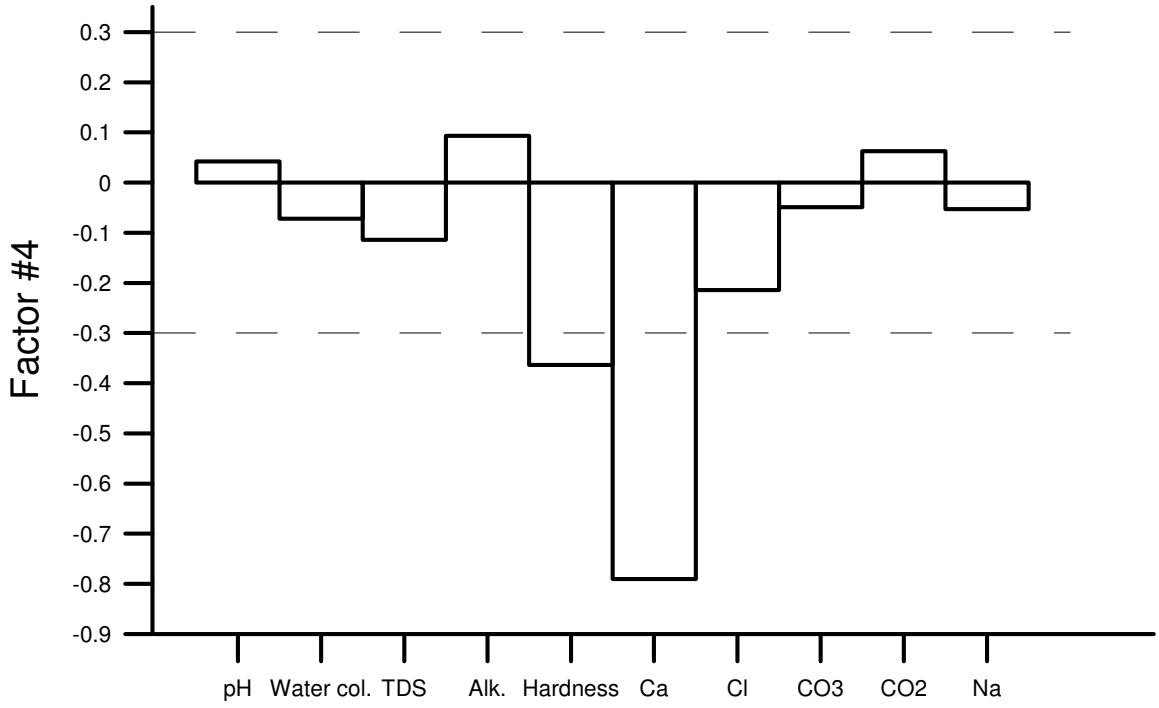

Figure 3.14. Plot of components for factor score coefficient #4.

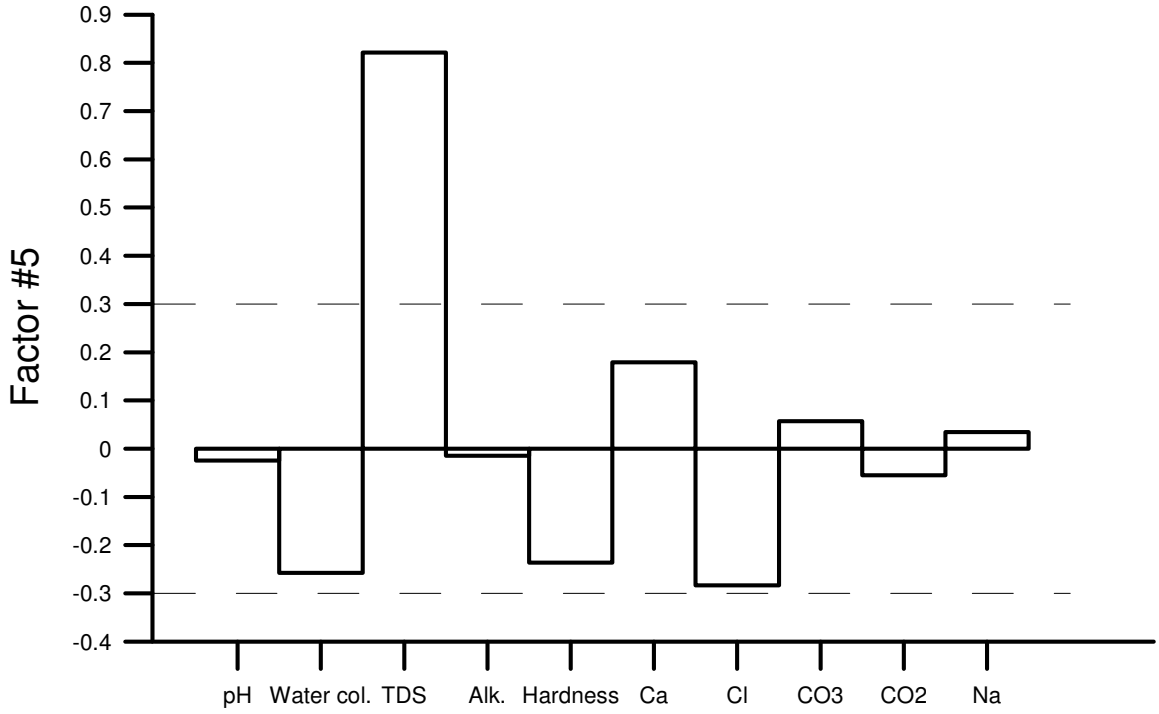

Figure 3.15. Plot of components for factor score coefficient #5.

Discussion of factor analysis results

Eigenvalue analysis of Maramarua CSG water quality data indicates that about 45% of the total variance (Table 3.4) is due to the first eigenvalue. However, the eigenvector associated with this eigenvalue is unrotated, and some of its components are high, some are low, and some are of considerable magnitude somewhere in the midrange. These last components are also contributing to the variance associated with this first eigenvector, but do not necessarily reflect the effect posed by high value components. In a way, these can be regarded as noise, which also contributes to the variance, within the first factor. Once five factors are extracted and rotated this noise is minimised (the midrange values disappear), but the variance associated with the first factor changes because the variance for the extracted factors is redistributed among the rest of the extracted factors. Therefore, the new variance associated with the first factor is about 33% (Table 3.5). The same analysis holds true for the remaining 4 extracted factors. In this way, the second factor accounts for about 17% of the total variance; the third factor now closely follows the second one with about 16%, and the fourth and fifth factors account for 13.3% and 12.3% of the variance respectively. Altogether, these first five

factors still account for 90.9% of the total variance. The analysis of the factor score coefficients is carried out by examining the significant factor components within each factor. Even though factor rotation minimises midrange values, a value of 0.3 has been chosen as a cutting value for determining which components are significant within each factor.

Factor #1

The components of the factor score coefficients for the first factor are distributed in such a way that only the components for carbon dioxide, pH, water column, and carbonate (in order of importance) are significant (i.e. > + 0.3 or < - 0,3; Figure 3.11). This figure indicates that a strong decrease in carbon dioxide tends to be associated with a significant decrease in water column together with a considerable increase in pH and carbonate concentrations. This description fits the carbonate speciation model described by solving the carbonate equilibrium equations as stated in Snoeyink (1980) and Freeze (1979). If the carbonate equilibrium equations (Figure 3.16) are solved for different pH values assuming a total inorganic carbon content of 1M, then the resulting carbonate speciation plot will be the one presented in Figure 3.17. This plot shows that, for pH values greater than 7, carbonate concentrations tend to increase with increasing pH values while carbon dioxide concentrations tend to decrease. Therefore, the first factor score coefficient represents changes in pH values resulting from the carbon dioxide degassing process.

$$H_2CO_3^* \Leftrightarrow H^+ + HCO_3^- \qquad K = 10^{-6.3}$$

$$HCO_3^- \Leftrightarrow H^+ + CO_3^{2-} \qquad K = 10^{-10.3}$$

$$C_{T,CO_3} = [CO_3^{2-}] + [HCO_3^-] + [H_2CO_3^*]$$

$$Alkalinity = [HCO_3^-] + 2[CO_3^{2-}] + [OH^-] - [H^+]$$

Where,

$$H_2O + CO_{2\,(aq)} \Leftrightarrow H_2CO_3 \qquad K = 10^{-2.8}$$

$$[H_2CO_3^*] = [H_2CO_3] + [CO_{2\,(aq)}]$$

Figure 3.16. Carbonate equilibrium equations at standard conditions (Snoeyink and Jenkins, 1980).

Solving the carbonate system of equations (Figure 3.16) can help describe the degassing process. This system was solved using activity coefficients calculated from ionic strength effects estimated by taking into account specific conductance values (Appendix A). The lowest pH value detected in the Maramarua CSG water samples was 7.2 (25/04/2005), so pH values in the aquifer have to be less than or equal to this value because as carbon dioxide concentrations increase (due to higher CO_2 pressure in the aquifer) pH values decrease (Figure 3.17). If the carbonate equilibrium equations are solved with a pH of 7.2 then the calculated aquifer CO_2 pressure is 0.026 atm. Once this water is exposed to the surface, the pressure drops to normal levels ($10^{-3.5}$ atm at standard conditions) and the calculated pH is 9.1. However, these changes do not occur instantaneously as revealed by the different pH values in the Maramarua CSG water quality data. As the well is dewatered, different samples are collected under different degassing and agitation conditions. This water may remain inside the well for a certain amount of time before it is collected (different water levels), and this also induces degassing and different qualities of water. On the other hand, degassing can be caused by water agitation inside the well which occurs when the pump is operating, hence the negative value for the water column component. Even when the sample is in a bottle, CO_2 degassing, carbonate precipitation, and a rise in pH may still take place if there is a gap and enough time for the carbon dioxide to escape. Consequently, the first factor shows that about 33% of the variations are due to this degassing process either during sampling or subsequently during sampling storage and handling.

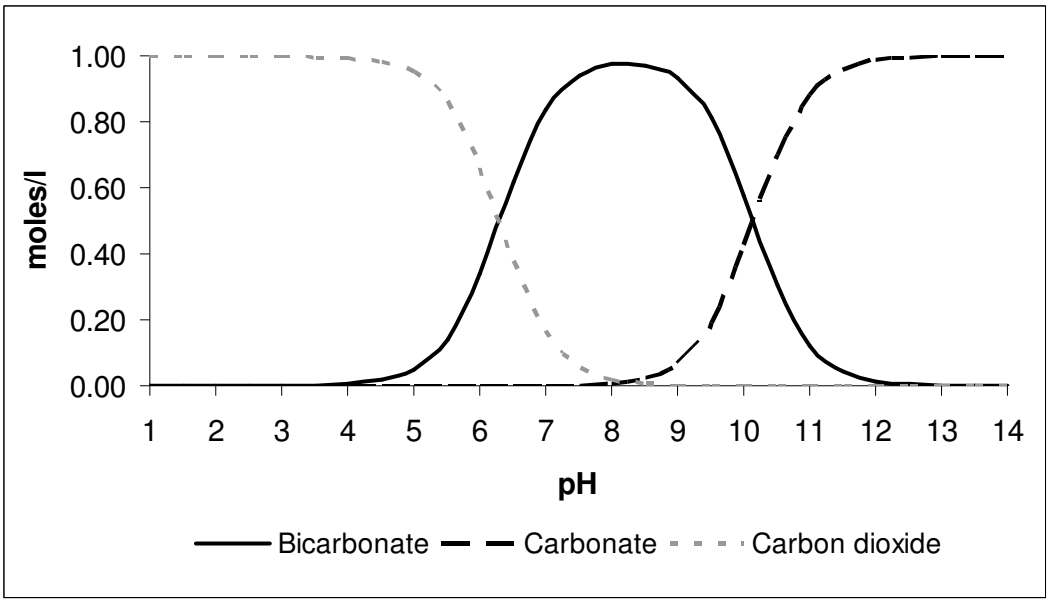

Figure 3.17. Distribution of major species of dissolved inorganic carbon

Factor #2

The major components in the second factor, which accounts for 16.5% of the variance, are sodium, alkalinity (equivalent to bicarbonate for the studied pH range), water column, and chloride (Figure 3.12). These ions happen to be the major ions in the samples (water of the Na-HCO_3-Cl type as illustrated in Figure 3.6), so this factor is showing the correlation between the ionic strength of the samples (due to its major ions) and the water column inside the well. A low water column would indicate that the pumping process is continuous and there is a low retention time in the vicinity of the well (this area would be susceptible to erosion/dilution). As a result, the CSG water pumped out of the aquifer would be less mineralised than the water pumped out of the well after a long period of exposure in the vicinity of the well; this situation would originate with discontinuous pumping, low pumping rate, or after a long standby period (high water column). As dewatering progresses with time, the loose formations around the vicinity of the well become less prone to dilution (because they have already been exhausted), and the end result is a slightly less mineralised water. This can be observed with sodium and bicarbonate concentrations during the first pumping round (Figure 3.9) as concentrations decrease in a logarithmic (1/ln(x)) fashion. It is not possible to observe this with chloride because its concentrations stay fairly constant with fluctuations through out time independently of pumping (Figure 3.9).

On the contrary, a high water column inside the well would mean that the pumping rate is not high enough or that it has stopped at some point. In this situation the contact time between the CSG water and the loose formations in the vicinity of the well would be higher than when the water level was low. This would increase the ionic strength of the sample (due to enhanced dissolution), but it would also lead to CO_2 degassing and carbonate precipitation inside the well. Therefore, the overall ionic strength of the CSG water would not necessarily increase when the water column is high (and so TDS does not have a high weighting in this factor), but there would be less dissolved bicarbonate although the major ions would still be Na- HCO_3-Cl. In addition, when measuring TDS in laboratories, normal random errors are always being committed. For example, APHA(1999) reports an error of 7.2 % in the standard deviation of standardised TDS samples (appendix 2, section 2.2). These differences could mask TDS variations to some extent, which also explains why TDS does not show in this factor.

Figure 3.18 shows the factor scores for the first two factors (S_1 and S_2 from Table 3.6) plotted on a Cartesian system. The symbols represent pH and are labelled according to their Na-HCO_3-Cl concentrations, divided in 4 groups. This figure shows how the first factor is strongly linked to pH (from degassing, see analysis Factor #1) as pH increases with increasing values for the first factor scores. The second factor, on the other hand, has a strong connection to the Na-HCO_3-Cl strength of the samples. Here, factor scores linked to samples with lower Na-HCO_3-Cl concentrations are plotted on top of the graph, while factor score values with low Na-HCO_3-Cl concentrations tend to plot at the bottom of the graph. This shows the strong correlation between the second factor and the Na-HCO_3-Cl strength of the samples.

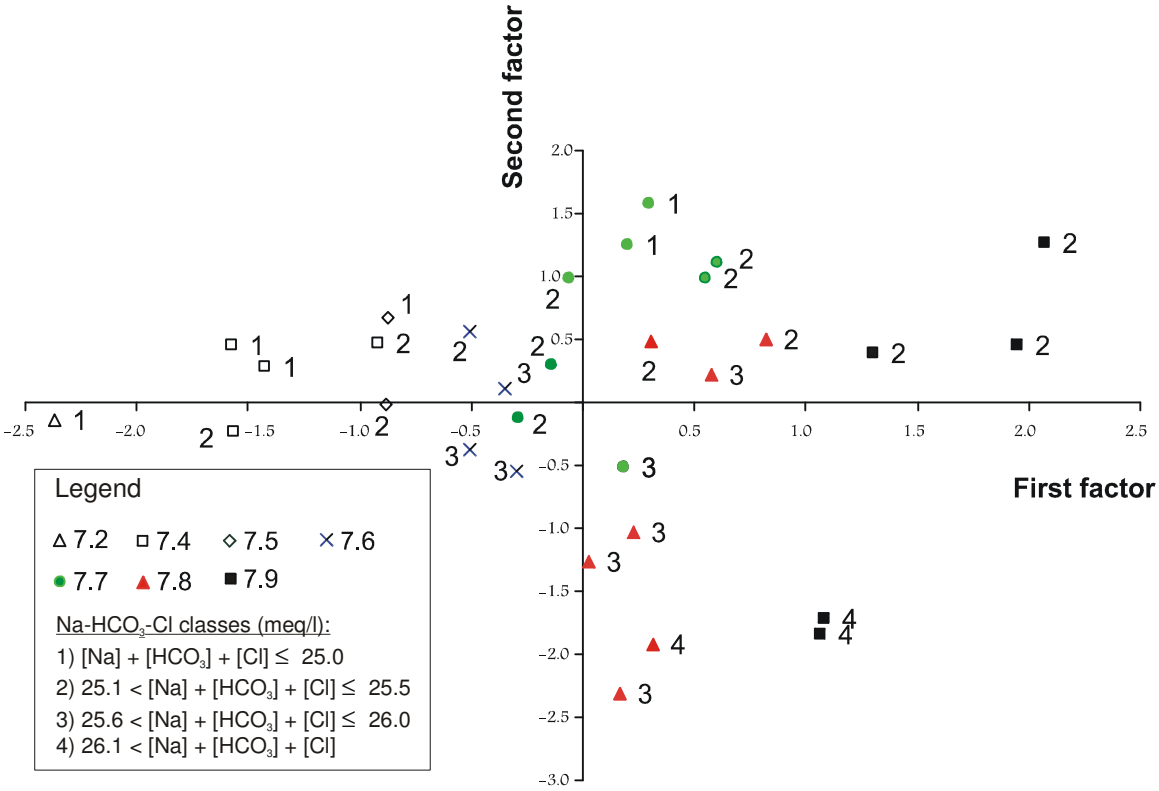

Figure 3.18. Plot of factor scores for the first two factors.

Factor #3

The third factor has a similar variance contribution than the second one because it amounts to 16.0% of the variance (just 0.5% less than the second factor). This factor shows a negative correlation between chloride and water column. This complements the interpretation of the second factor which showed a positive correlation between chloride and water column indicating that chloride is the third major ion present in CSG samples. However, in the case of the third factor, the negative correlation between chloride and water column would indicate that chloride concentrations are high with water column decline. Therefore, the second and third factors indicate that chloride concentrations are fairly independent of water levels inside the well - where factor #2 shows a positive correlation with water levels, factor #3 shows a negative one. In this way, chloride concentrations tend to remain constant throughout dewatering (the relative standard deviation of the 31 samples is 1.8%).

Factor #4

Factor #4 shows a strong correlation between calcium and hardness. This is not unexpected as the value for hardness includes the value for calcium plus the value for magnesium. Therefore, a strong change in calcium concentrations would cause a change in hardness. The calcium coefficient for this factor is more heavily weighted than the hardness one (which also includes magnesium), so calcium is the main source of variation associated with this component. Calcium concentrations could vary significantly with calcium carbonate precipitation, which occurs with CSG water degassing. However, factor #4 does not include heavily weighted coefficients for any of the components associated with calcium carbonate precipitation (pH, water column, carbonate, and carbon dioxide). Since there are no other high-value coefficients for this factor, the calcium variation could be attributed to the analytical determination of calcium. APHA reports a RSD of 9.2% associated with this technique, but laboratory titrations conducted at the EEL could have been as high as 17.3% (Appendix B, section B.2).

Factor #5

In factor #5 the only significant component is TDS. Therefore, this factor represents an independent source of variation associated with the TDS content of the Maramarua CSG water samples. This variation would be linked to the analytical technique used to measure TDS rather than to an actual process in the aquifer or in the well. This is because one would expect a strong correspondence between TDS and the coefficients for the major ions present in the samples (Na-HCO_3-Cl), but these coefficients are too low for factor #5. In the analytical determination of TDS sometimes there are significant differences in results because the reaction which dissociates bicarbonate into carbonate, carbon dioxide, and water may not always reach completion (Appendix B, section B.2). As mentioned in factor #2, the relative error of this technique could be as high as 7.2%, so there is a high uncertainty surrounding TDS determinations. Consequently, factor #5, which represents 12.3% of the variance, most likely represents the uncertainty associated with this measuring procedure.

Table 3.7. Summary of factor score coefficients reification

Factor #	Total variance contribution (%)	Processes or analytes responsible for this contribution
1	32.8%	○ Carbon dioxide degassing process
2	16.5%	○ Relationship between major ion composition (Na-HCO_3-Cl) and water column decline
3	16.0%	○ Chloride variation in the well independent of water level
4	13.3%	○ Calcium variations due to errors in analytical determination
5	12.3%	○ Variations attributed to analytical method for determining TDS

Table 3.7 summarises the reification of the Maramarua C-1 CSG water factors. Water abstracted from this well exhibits basically the same chemical characteristics and concentrations throughout different samples, but with minor variations. Factor analysis of these data has revealed that the majority of these variations (about 33%) are due to carbon dioxide coming out of solution and escaping into the atmosphere. This takes place either inside the well or later with sample handling. The second source of variation (16.5%) is linked to an increase in ionic strength due to changes in pumping rate which may affect dissolution in the vicinity of the well. The third factor (16%) shows that chloride concentrations are independent of water level inside the well. Lastly, factors 4 (13.3%) and 5 (12.3%) both relate to a systematic form of variation associated with the analytical determination of calcium and TDS respectively. Since the main source of variation is due to CSG water degassing, it would help to verify this conclusion with a laboratory experiment.

Degassing investigation analysis

The aim of this degassing investigation work was to verify the factor analysis results- carbon dioxide degassing and carbonate speciation (factor #1), which were responsible for about one third of the total variance (32.8%). For this purpose both a practical and theoretical investigation were carried out. The practical experiment used actual CSG water, while the theoretical one used a chemical speciation model, Visual MINTEQ, and sample analysis results.

Methods

Practical experiment

A practical experiment was set up with actual Maramarua CSG water. The experiment consisted of selecting a recently collected sample (11/06/2005) and very carefully (avoiding unnecessary agitation) measuring its key chemical properties – specific conductance, alkalinity, pH, hardness, and calcium. Special provisions were made to measure calcium and hardness – samples were centrifuged and filtered (using 0.22 μm filters) to ensure that only diluted ions were measured. A certain volume (1.5 L) of water was placed in a 2 L Erlenmeyer flask. The flask and the water were weighed and the measurement recorded. A porous hollow coil was then introduced inside the flask, and air was continuously pumped through it, generating bubbles in the water. A picture of this experimental setup is presented in Figure 3.19. The principle in this experiment is to generate air bubbles in order to cause agitation and accelerate the carbon dioxide degassing process. While this was carried out, a "cold finger", which was basically an open glass column with an inner glass coil with circulating cold water, was introduced into the system to a level just above the water mark. This cold finger acted as a trap for water vapour leaving the system. Water particles leaving the system would condense on the cold finger and would slowly drip back into the sample. The opening on top of the flask was wrapped with plastic around the cold finger to avoid losses. This sparging experiment was run for 6 hours at a temperature of about 20°C. After this time, the flask was weighed again and the water specific conductance was recorded. Any discrepancies due mainly to water vapour escaping the system were corrected by adding deionised water until the original weight and specific conductance were achieved (there was a loss of 5.57 ml of water). It was assumed that the effects of carbon dioxide degassing on weight and specific conductance were negligible, and this was later confirmed with calculations indicating carbon dioxide differences posing no effects in relation to these variables (Table 3.10). Once the sample had been corrected, the sparged CSG water was analysed to obtain the same key chemical properties measured before sparging.

Figure 3.19. Sparging of CSG water

Theoretical experiment

The theoretical experiment consisted of modelling the practical experiment using a chemical speciation model, Visual MINTEQ. This model is a Visual Basic version of the EPA MINTEQA2 v. 4.0 model, which is a chemical speciation model designed to calculate the equilibrium composition of aqueous solutions (US Environmental Protection Agency, 2005). A complete Maramarua CSG water sample analysis taken on 19/8/2004 was used as input for the model both with its original pH, and with the final pH at the end of the sparging experiment. The equilibrated mass distribution resulting from running the model was noted and its results were compared against the sparging results.

Experimental results

Results for the practical experiment are presented in Table 3.8. Once the sparging was over, the water was left undisturbed for about 8 hours on a closed container. After this period of time large light grey fragments were observed at the bottom of the bottle.

The sample was corrected by adding deionised water to account for water losses through evaporation (0.26%). Initial and final conditions after sparging differ mainly in pH, hardness, and calcium.

Table 3.8. Results of sparging experiment

Parameters	Units	initial conditions	after sparging
pH	pH units	7.4	8.6
Specific Conductance	µS/cm	1314	1315
Alkalinity	As mg/l $CaCO_3$	380	380
Hardness	As mg/l $CaCO_3$	22.3	14.7
Calcium	mg/l	4.8	2.9
Magnesium	mg/l	2.5[(1)]	1.9[(1)]
Weight (water+flask)	grams	2136.88	2136.84[(2)]

[(1)] Calculated from hardness and calcium concentrations
[(2)] Value corrected with deionised water. Original value was 2131.31g (0.26% loss)
Sample was sparged for 6 hours at a temperature of 19.5°C

Results from the theoretical experiment using the Visual MINTEQ model are presented in Table 3.9. The original sample had a pH of 7.8 and, according to MINTEQ, presented some carbonate and zinc precipitation in the form of smithsonite. However, zinc precipitation for this pH value could be virtually nonexistent because the saturation index for zinc (calculated with MINTEQ) is zero for smithsonite ($ZnCO_3$), and the rest of the minerals are undersaturated. On the other hand, smithsonite and calcite precipitation are significant when running the model with a pH of 8.6, which corresponds to the pH of the 11/06/2005 sample after the sparging experiment. Under these conditions, the calculated saturation index for smithsonite continues to be zero, but could have had a larger value before zinc precipitation took place. The calcite saturation index is 0.003, which means the solution is oversaturated with respect to calcite and will tend to precipitate this mineral.

Table 3.9. MINTEQ modelling results

Modelling of 19/8/2004 sample with original pH (7.8) γ = 0.9989 kg/l				
Parameter	**total dissolved moles/kg**	**%dissolved**	**total precipitated moles/kg**	**% precipitated**
Barium	$1.4562 \cdot 10^{-7}$	100	0	0
Calcium	$1.4970 \cdot 10^{-4}$	100	0	0
Chloride	$4.1181 \cdot 10^{-3}$	100	0	0
Carbonate	$7.4015 \cdot 10^{-3}$	99.766	$1.74 \cdot 10^{-5}$	0.234(1)
Fluoride	$4.1582 \cdot 10^{-5}$	100	0	0
Potassium	$7.6722 \cdot 10^{-5}$	100	0	0
Magnesium	$3.7019 \cdot 10^{-5}$	100	0	0
Sodium	$1.4528 \cdot 10^{-2}$	100	0	0
Sulphate	$7.2870 \cdot 10^{-6}$	100	0	0
Zinc	$2.1972 \cdot 10^{-6}$	11.221	$1.74 \cdot 10^{-5}$	88.779(1)
Modelling of 19/8/2004 sample with sparging experiment pH (8.6) γ = 0.9973 kg/l				
Parameter	**total dissolved moles/kg**	**%dissolved**	**total precipitated moles/kg**	**% precipitated**
Barium	$1.4562 \cdot 10^{-7}$	100	0	0
Calcium	$6.5374 \cdot 10^{-5}$	43.67	$8.43 \cdot 10^{-5}$	56.33(2)
Chloride	$4.1181 \cdot 10^{-3}$	100	0	0
Carbonate	$7.0936 \cdot 10^{-3}$	98.58	$1.03 \cdot 10^{-4}$	1.425(1,2)
Fluoride	$4.1582 \cdot 10^{-5}$	100	0	0
Potassium	$7.6722 \cdot 10^{-5}$	100	0	0
Magnesium	$3.7019 \cdot 10^{-5}$	100	0	0
Sodium	$1.4528 \cdot 10^{-2}$	100	0	0
Sulphate	$7.2870 \cdot 10^{-6}$	100	0	0
Zinc	$1.3288 \cdot 10^{-6}$	6.79	$1.83 \cdot 10^{-5}$	93.214(1)

(1)Precipitates as smithsonite ($ZnCO_3$)
(2)Precipitates as calcite ($CaCO_3$)
Note: Liquid density changes as minerals precipitate from solution. Therfore,
C (moles/l) = C(moles/kg) * γ (kg/l)

In addition, MINTEQ was run a few more times but with pH values of 8.9 and 6.6 to predict what minerals could precipitate out under these conditions. When running the model with a pH of 8.9, the saturation index for calcite remained at 0.003, but this time dolomite ($Mg\ CO_3$) and hydrozincite reached equilibrium with a saturation index of zero. Consequently, calcium, magnesium, carbonate and zinc precipitated out of solution. Finally, successive model executions using decreasing pH values revealed that at a pH of 6.6, smithsonite became undersaturated with respect to carbonate and no precipitation took place.

Discussion of experimental results

The immediate results from the sparging experiment using sample collected on 11/06/2005 indicate a rise in pH from 7.4 to 8.6, and calcium precipitation in the order of 40%. Hardness is reduced by 34% after sparging, and this is mainly a consequence of calcium precipitation. Magnesium precipitation could have also taken place (25% at the most), but it is not possible to determine this with certainty because the measuring procedure is not sufficiently accurate at such low concentrations. However, modelling work with Visual MINTEQ on the 19/8/2004 sample has verified these results - MINTEQ predicted 56.3% of calcium precipitation when the sample pH was set to 8.6. In addition, MINTEQ predicted zinc precipitation at pH 8.6, and possible magnesium precipitation at pH 8.9. Also, Visual MINTEQ shows that CSG waters are undersaturated with respect to calcite at the wellhead (pH =7.8), which suggests these waters do not tend to precipitate calcium carbonate minerals in the aquifer (and at the wellhead). However, once CSG waters reach equilibrium with the atmosphere (pH =8.6), the saturation index for calcite increases, and CSG waters tend to precipitate calcium carbonate minerals.

These experimental results are in accordance with the carbonate equilibrium model described by Figure 3.16, and the calcium carbonate equilibrium equations presented in Eq 3.1. In these set of equations, the equilibrium constants are defined at standard conditions, and activity coefficients are not considered (these can be easily calculated). This system of equations can be solved graphically or analytically, and the MINTEQ model uses a similar but more extensive set of equations taking into account activity coefficients. Nevertheless, these equations work well as a simplified model for understanding the processes involved in carbonate chemistry equilibrium. Solving these equations reveals the relationship between pH, alkalinity, and the different carbonate species (bicarbonate, carbonate, carbon dioxide, and carbonic acid). This relationship was explained in the factor analysis results discussion, but a more detailed explanation relating to the sparging experiment is warranted.

$$CaCO_{3(s)} + H^+ \Leftrightarrow Ca^{2+} + HCO_3^- \qquad K = \frac{10^{-8.3}}{10^{-10.3}}$$

$$S.I. = pH - pH_{water\ in\ equilibrium\ with\ CaCO_{3(s)}}$$

Eq 3.1

When CSG waters are in the aquifer, the partial pressure of carbon dioxide can be up to two orders of magnitude greater than at the surface. In this case, the carbonate system behaves as a closed system with a constant elevated partial pressure of carbon dioxide. At this pressure, some carbon dioxide will remain dissolved in the water, and the only other carbonate species present will be bicarbonate. Furthermore, CSG waters will be completely undersaturated - according to MINTEQ modelling, this could occur at pH 6.6 because at this pH value smithsonite ($ZnCO_3$) remains completely dissolved in the aquifer. However, once CSG waters are pumped to the surface, these waters are exposed to a much lower atmospheric pressure; carbon dioxide gas will come out of solution and their carbonate equilibrium will start to change. Unless special provisions are taken (like the use of micropurge sampling and cell flows) it is practically impossible to avoid the degassing process.

The sample collected on 11/06/2005 from the Maramarua C-1 well had already lost some carbon dioxide, and its pH (7.4) was already higher than aquifer pH. However, because this sample was stored in a closed plastic bottle which had been completely filled with CSG water (leaving no air gaps), the degassing effect was somehow controlled. The carbonate species and properties for this sample are presented in Table 3.10. Before sparging, the major ion of the carbonate species was bicarbonate (462 mg/l) followed by dissolved carbon dioxide (62 mg/l). The calculated saturation index for this sample is negative (-0.95) which means this sample is not precipitating calcium carbonate. Once the sample was sparged, the carbon dioxide degassing process was accelerated because the sample was exposed to the open atmosphere and to a lower atmospheric pressure. As a consequence, the pH rose from 7.4 to 8.6, and the carbonate equilibrium changed (Table 3.10). This time, dissolved carbon dioxide concentrations were very low (3.7 mg/l), and carbonate concentrations increased to 12 mg/l; the major carbonate ion continued to be bicarbonate, but its concentration decreased to 438 mg/l. In general, these

results can be interpreted graphically using Figure 3.17. This figure shows how carbon dioxide decreases while carbonate increases as pH values increase. Bicarbonate may reach a maximum at pH 8.3, but it then starts to decrease with increasing pH values. The sparged Maramarua 11/06/2005 sample has a pH of 8.6, therefore bicarbonate concentrations for this sample must have increased to a maximum at pH 8.3 (starting at pH 7.4), and then decreased to 438 mg/l with a final pH of 8.6.

Another significant consequence resulting from sample sparging is the saturation index, which in this case resulted in a positive value (0.29). This value is close to zero because most of the calcite has precipitated (it must have been higher at some point but then decreased as calcite precipitated). This was verified by measuring calcium concentrations before and after sparging with differences of 40%. In addition, MINTEQ modelling with the full 19/8/2004 sample analysis results has resulted in a positive saturation index (0.003), which also helps to corroborate the calculated value for the 11/06/2005 sample (0.29).

Table 3.10. Carbonate species and properties for 11/06/2005 sample

Carbonate species or property	units	before sparging	after sparging
pH	pH units	7.4	8.6
HCO_3^-	mg/l	461.5	437.7
CO_3^{2-}	mg/l	0.8	12.4
$CO_{2\,(aq)}$	mg/l	61.7	3.7
H_2CO_3	mg/l	0.098	0.006
$H_2CO_3^*$	mg/l	61.8	3.7
Saturation Index	pH units	-0.95	0.26

Notes:
The different carbonate species were calculated using Figure 3.16 with activity coefficients, and an alkalinity of 380 as mg/l $CaCO_3$
The Saturation Index (or Langelier Index) was calculated by the difference between the actual water pH and the pH of water in equilibrium with $CaCO_3$ (Eq 3.1).

In the factor analysis, it was possible to correlate the carbonate precipitation process to water levels fluctuations. Higher levels would imply that the water has been in the well for a longer time. Therefore, higher water levels would expose CSG water to a lower atmospheric pressure, and the degassing/precipitation process would be promoted. Aquifer pH could be as low as 6.6 because at this pH value, MINTEQ predicts no solid precipitation. However, when CSG water is abstracted, its pH inside the well immediately begins to rise because of the pressure difference. When the sample is

collected pH could rise further with agitation and sample handling. For example, the full sample collected on the 19/08/2004 had a pH of 7.8. The difference between this pH value and the pH of the water in the aquifer (6.6) is high (1.2 units), and it represents the amount of degassing that has taken place.

Alkalinity before and after sparging did not change (Table 3.8). Once again, this result is entirely expected according to carbonate equilibrium (Figure 3.16); in this system of equations, the concentration of the different carbonate species can be calculated if pH and alkalinity are known. By using Figure 3.16, it is possible to verify that the addition or removal of carbon dioxide does not influence the final alkalinity value, and this confirms the experimental result in Table 3.8. This result has further implications for sampling CSG waters – when sampling, it would be ideal to measure pH at the wellhead because this value changes with degassing. Samples can be analysed for alkalinity at a later stage in the lab since this value will not change as carbon dioxide is lost.

MINTEQ modelling revealed that degassing is likely to cause calcium precipitation as calcium carbonate ($CaCO_3$) and zinc precipitation as smithsonite ($ZnCO_3$). Most likely, the grey coloured precipitate, formed after sparging the 11/06/2005 sample, could have included both calcium carbonate and smithsonite. According to MINTEQ, zinc precipitation could be as high as 93% and, in the case of the 19/8/2004 sample which had a zinc concentration of 1.28 mg/l this could represent a significant reduction (0.09 mg/l) if the CSG water is exposed to the open atmosphere for some period of time. For example, it could be desired to precipitate zinc in a pond prior to discharge; this would effectively reduce zinc concentrations in the CSG water, but would result in a sludge with high zinc concentrations which would have to be properly handled.

Conclusion

A CSG dewatering operation in Maramarua has produced a set of water samples with some minor variations in chemical composition. The setup was ideal for this purpose, because the samples were abstracted as the well was subjected to intermittent and continuous dewatering with two different pumps. Consequently, the resulting data set permitted studying the causes of variation in water quality while considering obvious changes throughout the dewatering process (water level fluctuations).

A factor analysis has unveiled calcium carbonate precipitation with carbon dioxide degassing as the number one cause of variation (32.8%). This is significant because all CSG aquifers have high bicarbonate concentrations, and are located at depths associated with high aquifer pressure. Therefore, all CSG waters are highly sensitive to variations due to internal changes in their carbonate equilibrium arising from changes in the pressure to which they are subjected. These variations can be minimised if samples are collected with minimum disturbance, and if provisions are taken to prevent carbon dioxide gas from coming out of solution once the sample is collected. Higher variations are expected if the sample is exposed to the open atmosphere for a prolonged period of time or has undergone violent agitation. This was verified experimentally with a sparging experiment and subsequent modelling work. A recommendation from these findings is to sample CSG waters on site by measuring pH and avoiding degassing as much as possible. It is not necessary to measure alkalinity on site since this value will not change with degassing.

The second source of variation is related to the major ion composition (Na-HCO_3-Cl) of CSG waters. Factor analysis results indicated that about 16.5% of the variance is due to the relationship between sample mineralization and water column. This could reflect the influence pumping has on the dissolution of minerals present in formations near the well. The third factor (16% of variation) shows the negative correlation between chloride and water level, which complements the positive correlation found in the second factor, and suggests chloride concentrations are fairly independent of water level. The fourth (13.3% of variation) and fifth (12.3% of variation) factors are linked to measuring errors that could have been committed when determining calcium and TDS

concentrations respectively. It was possible to verify the interpretation of the first factor (which is the most important one) using an experimental setup and further theoretical modelling - it was not possible to verify the interpretation of the rest of the factors, but these factors are not as relevant as factor #1.

CSG waters from Maramarua C-1 have a high bicarbonate concentration, which plays an important role in shaping their quality once abstracted; this makes these waters extremely unstable once pumped to the surface. An initial inspection might give the impression of these waters being chemically stagnant, however a closer examination reveals that, once exposed to surface atmospheric pressure, these waters have the potential to precipitate calcium, zinc, and magnesium in carbonate form. In addition, pH rises considerably, but bicarbonate concentrations decrease slightly while small amounts of carbon dioxide gas are vented. Consequently, different pumping rates, along with changes in pressure, will produce a continuously changing water quality. Indeed, as Heraclitus put it, the nature of water flow is constant change - this applies to all sorts of water bodies, even the ones taking place underground (aquifers). Although factor analysis results, sparging experiments, and MINTEQ modelling are in accordance with each other and yield similar inferences, this research would have benefited from replicates and tests on other water samples to give confidence to these conclusions.

References

American Public Health Association., American Water Works Association., and Water Environment Federation., 1999, Standard methods for the examination of water and wastewater: [Washington, D.C.], American Public Health Association, 1 computer optical disc p.

Chatfield, C., 1996, The analysis of time series : an introduction: London, Chapman & Hall, xii, 283 p.

Davis, J.C., 2002, Statistics and data analysis in geology: New York, J. Wiley, xvi, 638 p. p.

Freeze, R.A., and Cherry, J.A., 1979, Groundwater: Englewood Cliffs, N.J., Prentice-Hall, xvi, 604 p.

Hoffman, R.D., and Animated Software Company., 2004, Internet glossary of pumps: [California], Animated Software Co.

Karassik, I.J., 1986, Pump handbook: New York, McGraw-Hill, 1 v. (various pagings) p.

Nielsen, D., 1990, Practical handbook of ground-water monitoring: Chelsea, MI, Lewis Publishers, x, 717 p.

Snoeyink, V.L., and Jenkins, D., 1980, Water chemistry: New York, Wiley, xiii, 463 p.

US Environmental Protection Agency, 2005, Exposure Assessment Models, US Environmental Protection Agency, p. web page.

Van Voast, W.A., 2003, Geochemical signature of formation waters associated with coalbed methane: Aapg Bulletin, v. 87, p. 667-676.

Chapter 4

Potential environmental impacts associated with coal seam gas water management in New Zealand

Introduction

The environmental impacts that could arise from CSG water extraction depend on the quantity and quality of produced water, and on the method of treatment and disposal being used. For example, if CSG waters are disposed of on the land, the main impacts would be on plant development and soil stability, whereas if these waters are disposed of on rivers, the impacts would be on aquatic life. Understanding these impacts is necessary to adequately manage CSG waters so that environmental effects are minimised; if properly managed, CSG waters can be used for beneficial applications and can become a valuable resource.

In the United States, impacts associated with CSG water discharge have been noted in the Powder River Basin (PRB) and have been reported by Bauder (2001), Wheaton and Donato (2004), McBeth et al. (2003), and Davis et al. (2006b). However, in other CSG producing basins in the US (San Juan, Raton, Uinta) impacts have been minimal because the lower volumes of water being produced have allowed injection into receiving aquifers as the main method of disposal (ALL-Consulting and Montana Board of Oil and Gas Conservation, 2004). Similarly, producers in the Black Warrior Basin in Alabama have successfully treated their low-volume CSG water by directing it through a sequence of treatment/storage ponds in order to discharge it into surface streams (Davis et al., 1993). All of these disposal methods have had to comply with US regulations (National Pollutant Discharge Elimination Permits) to minimise potential impacts at a reasonable price.

Although CSG water tends to have the same major ion composition throughout different basins (Van Voast, 2003), the magnitude of potential environmental impacts change across basins due to differences in local climate, receiving soils, surface waters, and quantities of CSG water being abstracted. This chapter outlines the potential environmental problems associated with CSG waters in New Zealand while considering overseas experience. In this context, the New Zealand regulatory framework is explained, and management options are outlined. This chapter explains the potential environmental impacts associated with CSG water disposal in New Zealand. Other impacts not directly related to CSG water (i.e. noise, land or scenery disturbance, and air pollution) are not the focus of this study, but would need adequate characterisation for a complete assessment of environmental effects from the regulatory point of view. Such an assessment, for example, would depend on the specific details for each particular operation including location, dewatering method, and proximity to populated centres. The chapter finishes with a New Zealand case study of the Maramarua basin.

Assessing environmental impacts related to CSG water management and disposal

CSG waters, as described in Chapter 2, can be detrimental to receiving environments mainly because of the high sodium, chloride, and bicarbonate concentrations associated with their geochemical signature. Other issues to consider are water pH, salinity (specific conductance), and boron (when present). Trace elements detected in PRB CSG water include barium, arsenic, aluminium, iron, selenium, fluoride, copper, molybdenum, manganese, chromium, and zinc (McBeth et al., 2003). In addition, well stimulation techniques could include the injection of sand and fluids to open cleats and promote gas desorption and transport; these fluids can range from water based to biodegradable compounds, and the latter could result in CSG water having high BOD during the first months of dewatering (Davis et al., 1993). The problem ceases to become a pure CSG project if the CSG has been exposed to secondary processes such as, for example, the mixing with heavier hydrocarbons from conventional natural gas linked to oil production (Rice, 1993). In these situations trace elements like iron, manganese, and organics could be present in higher concentrations (Davis et al., 1993).

The impacts associated with CSG water disposal depend on the method of disposal being implemented. The major disposal options are discharge to land and surface waters; the impacts for each of these receiving environments will be different and need to be assessed before disposal is implemented. In general the longer the path from the discharge point, the larger the potential for environmental damage. The situation becomes complicated when valuable resources are compromised (fertile soils, pristine aquifers, rivers, and wetlands), and when there are unpredictable links between receiving environments (i.e. aquifer interconnection or runoff to recharge areas). Therefore, each disposal option and its impacts needs to be properly assessed before it can be implemented.

In New Zealand, the Resource Management Act (RMA) is the main legistation controlling contaminant discharges into the environment. It is the role of regional councils to implement the RMA by issuing regional policy statements and implementing regional plans. Proposed activities have to undergo a thorough consent process and, to aid in their decisions, regional councils may rely on various New Zealand guidelines. If no local guidelines are available, overseas guidelines may be employed or site-specific guideline values may be developed (Cavanagh and Coakley, 2005). Full-scale CSG production has not yet taken place in New Zealand, and the effects associated with CSG water discharge are generally unknown. Therefore, regional councils have not yet had to assess resource consents for large CSG mining activities, which involve CSG water disposal.

Land disposal of CSG waters

Land disposal of CSG waters can have different impacts depending on whether these waters are being disposed directly on to the land or used for irrigation of fertile soils. The major issues with CSG water are its salinity (specific conductance) and its major ions (sodium and chloride) which can be toxic to plants and may damage the permeability of soils (i.e. high Exchangeable Sodium Percentage or ESP levels). Salinity is generally measured in dS/m units, however in previous chapters it has been reported as µS/cm to show all significant figures (1 dS/m = 1000 µS/cm). In this chapter, salinity will be reported as dS/m to allow for a direct comparison between selected samples and salinity

values in various irrigation water quality guidelines, which are used in assessing salinity problems associated with land disposal of CSG waters.

High salinity can have a detrimental effect on vegetation because plants need to exert extra osmotic force to extract water from the soil-water interface (Ayers et al., 1985). With increasing salinity levels, plant growth is suppressed and, at critical levels, plants can die (Jensen, 1983). Some plants are more tolerant to salinity than others. For example, barley has a 100% tolerance to salinity levels of 5.3 dS/m, while carrots have a 100% tolerance at salinities of 0.7 dS/m. In contrast, halophytes, which grow on wetland environments, can tolerate extremely high saline levels (up to 90 dS/m) (Settle et al., 1998). For agricultural applications, salinity levels greater than 3 dS/m have been identified as "severe" by Ayers et al. (1985).

On the other hand, salinity can play an important role in keeping soil particles flocculated and maintaining good permeability. Oster and Schroer (1979) observed a correlation between infiltration rates and total ion concentration (salinity). This occurrence is explained because, at high salt concentrations, pH values are lower than 8.5 and soil particles tend to remain flocculated (US Salinity Laboratory Staff, 1954). At lower salinity levels, the soil-water solution may have pH values above 8.5 and the sodium ions, which were originally part of the soil, can hydrolyze and rearrange clay particles causing overall soil dispersion and the loss of permeability (US Salinity Laboratory Staff, 1954).

The high sodium together with low calcium and magnesium concentrations in CSG waters have the potential to cause soil dispersion and loss of infiltration. The problem of irrigating soils with saline/sodic water has been studied by US Salinity Laboratory Staff (1954), Oster and Schroer (1979), and Ayers et al. (1985) among others. These researchers have developed guidelines to prevent infiltration problems based on the Sodium Adsorption Ratio (SAR) and salinity of irrigation waters while considering the ESP of the soil. Using various saline/sodic water combinations on non-saline/non-sodic loams, Oster and Schroer (1979) showed that infiltration rates decreased as SAR values increased and salinity decreased. From the soil point of view, an ESP value of 15 has been selected in the US as the limit for soils containing clay minerals to become degraded (Shainberg and Letey, 1984; US Salinity Laboratory Staff, 1954). A

relationship between ESP and SAR has been established relating the ESP value of 15 to a SAR value of 12.8 for soils in Western States in the US (US Salinity Laboratory Staff, 1954). Research by Robinson (2003) has revealed that continuous cycles of irrigation with deionised water and synthesized CSG water from the PRB, produces soil salinisation and potential infiltration problems in PRB soils.

Salinity and infiltration problems due to sodium are complex and need to be studied within the context of each individual basin. For example, the guidelines by Ayers et al. (1985) were developed for semi-arid to arid climates on soils with sandy-loam to clay-loam textural range. Therefore, it is not simple to apply these principles and guidelines to soils in humid regions, like most of the soils in New Zealand.

New Zealand regions exhibit a wide variation of climates ranging from very dry climates with poorly leached soils (Alexandra) to humid climates with extremely leached soils (Hokitika), and New Zealand soils are a consequence of the water balance throughout these different regions (McLaren and Cameron, 1990). Most of the climates in New Zealand are humid, and saline soils are practically non existent in humid climates because salts originally present in soils are leached into the groundwater and are eventually flushed into the ocean (US Salinity Laboratory Staff, 1954), therefore salinisation is not a major concern in New Zealand (ANZECC and ARMCANZ, 2000). Most of the soils in New Zealand are well drained and have moderate (medium) cation exchange capacities (Figure 4.1), however saline and alkaline soils do exist in some areas of Central Otago at about 200-600m elevation (Allen et al., 1998).

New Zealand soils tend to have considerable amounts of organic matter ("Medium" category in Figure 4.2), and Bresler et al. (1982) have suggested that soils having substantial amounts of organic matter have good water retention ability, are relatively stable, and not prone to swelling or dispersion. Nevertheless, there is apprehension in New Zealand about the long term effects of discharging high-SAR/ saline water on to the land. For example, an ESP value of 6 is generally being used in Resource Consent Applications for approving land treatment of dairy farm effluent which is high in sodium (Cameron et al., 2003). From the regulatory point of view, regional councils in New Zealand may use the *Australian and New Zealand Guidelines for Fresh and Marine Water Quality* (ANZECC and ARMCANZ, 2000) or other relevant

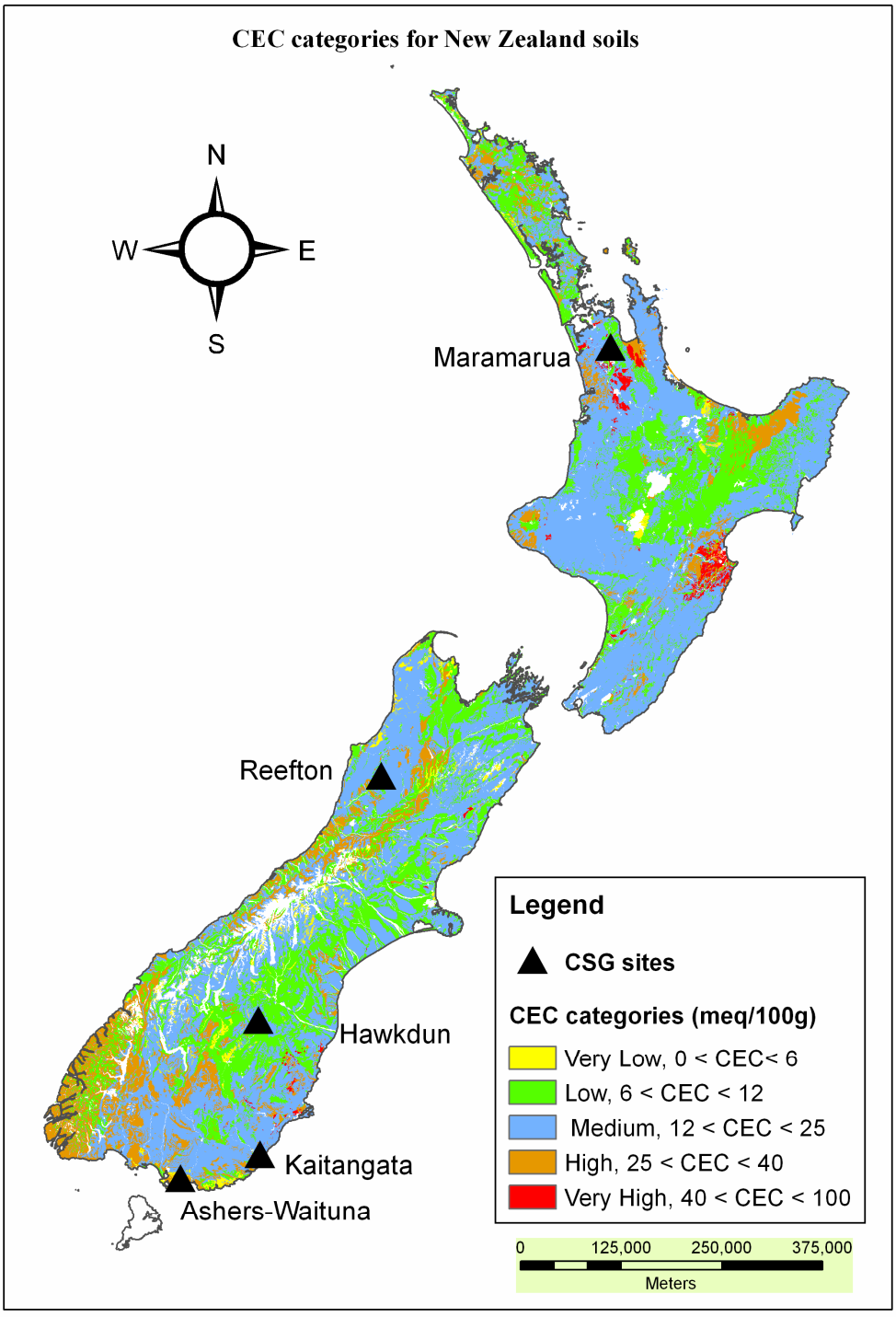

Figure 4.1. Cation exchange capacities for New Zealand soils. Map compiled from Landcare Research New Zealand Ltd (2000b).

guidelines (including international guidelines) to assess salinity and infiltration problems caused by high SAR water discharges. These guidelines do not state specific trigger values because salinity and sodicity problems need to be assessed for each particular situation while considering parameters like water quality, soil properties, climate, type of irrigation, and water management practices (ANZECC and ARMCANZ, 2000).

In New Zealand, sodium-loaded liquid wastes from processing and cleaning are generally being disposed on farmland as the preferred alternative to surface water disposal (Menneer et al., 2001). These wastewaters can have high SAR levels, which could generate infiltration problems, effluent runoff, and ponding (Cameron et al., 2003).

Research by Menneer et al. (2001) and Cameron et al. (2003) has focused on studying the effects of land disposal of dairy farm effluent on New Zealand soils. Using repacked soil cores in a laboratory study, Menneer et al. (2001) noticed a decrease in hydraulic conductivity after irrigating with high-SAR solutions followed by leaching with deionised water. This reduction occurred at SAR values of 3.5 for Waitoa soils and 8.5 for Te Puninga soils (silt loams with 27% and 21% clay respectively); during SAR application the infiltration rate was enhanced due to the elevated salinity of the applied solutions.

Cameron et al. (2003) studied the effects of dairy farm effluent (SAR ~ 8.6) application on a Lismore soil (stony silt loam) with 0, 4, and 10 years of treatment (0 was the control). Although the soils that had previously been irrigated with dairy farm effluent had larger ESP values than the control, these soils showed better wet aggregate stability and permeability upon continuous treatment with high-SAR solutions. This was attributed to the high carbon content (lactose) of dairy farm effluent which improved soil structure by providing bonding agents (Cameron et al., 2003). In addition, it was suggested that an ESP value of 6 may not be appropriate for these situations because, even though there might not be infiltration problems during applications (due to high salinity), a soil with a high ESP value could undergo a loss in permeability upon leaching with rainfall water.

These findings have great implications for land disposal applications of CSG waters in New Zealand. Firstly, the control water in the experiment by Cameron et al. (2003) has a chemistry similar to CSG waters for infiltration analysis purposes, and this

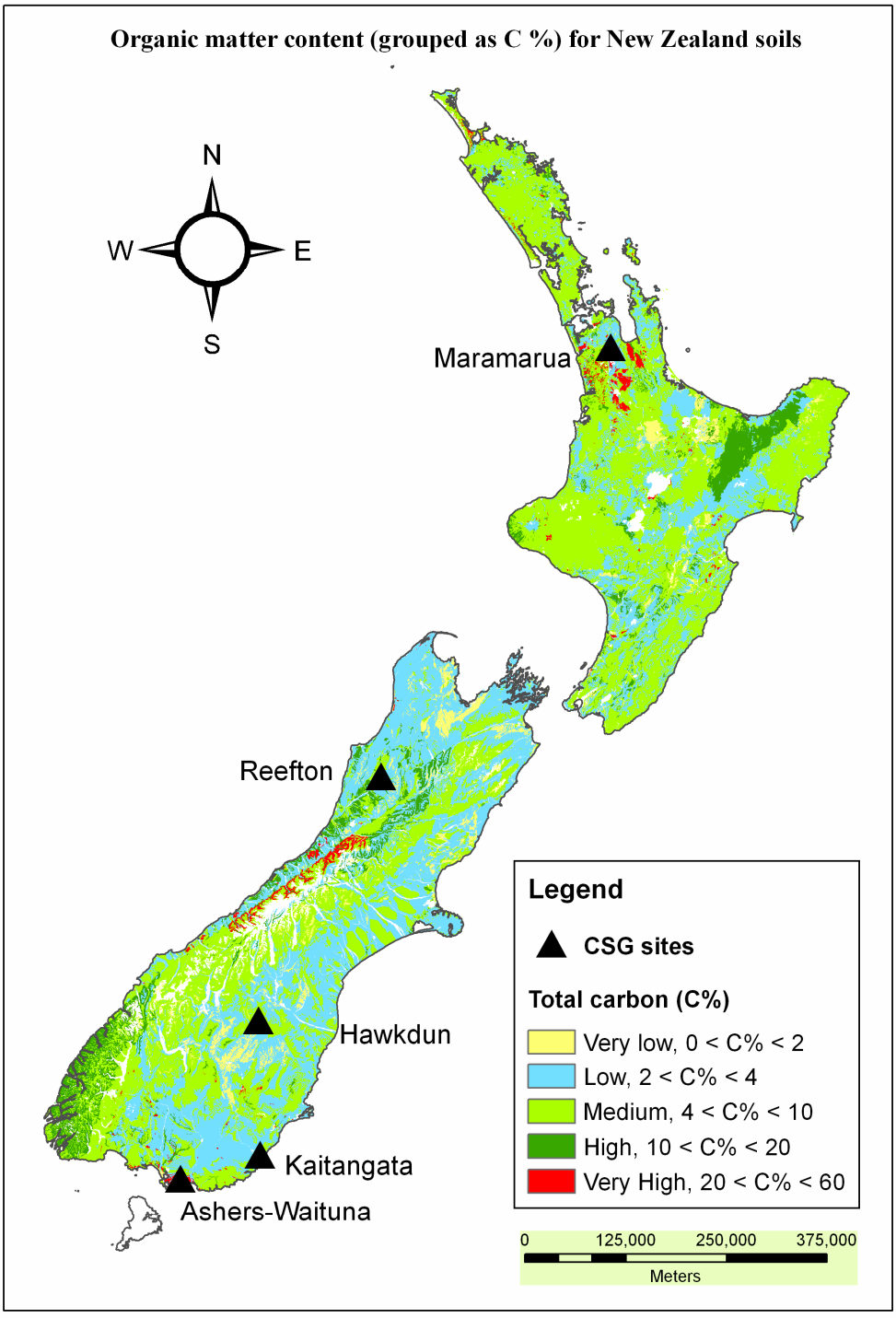

Figure 4.2. Organic matter content (as carbon percentage) for New Zealand soils. Map compiled using Landcare Research New Zealand Ltd (2000b)

sample showed significant reduction in hydraulic conductivity and wet aggregate stability. Secondly, CSG waters have low organic carbon concentrations (see Chapter 2) (Taulis et al., 2005) so their land disposal would not condition soils, as in the case of dairy farm effluent. Consequently continuous disposal of high-SAR CSG water could produce more infiltration problems than dairy farm effluent, and these effects would be even more noticeable after long periods of precipitation.

Figure 4.3 shows the potential infiltration problems that could arise due to the disposal of high-SAR CSG waters on New Zealand soils. A detailed explanation of the procedure used to create and calibrate the model for Figure 4.3 is presented in Appendix C (section C.1.2).

In general, the risks are low to moderate, but some high-risk areas do exist in coastal areas (South of Thames and Napier) and south mountainous areas (Central Otago). CSG sites presently under exploration are indicated on the map; in the North Island, Maramarua is located in an area of moderate risk surrounded by patches of low and high risk. In the South Island, Ashers-Waituna and Kaitangata are close to the ocean, but Reefton and Hawkdun are located further inland. Ashers-Waituna is located in an area of low risk, while Kaitangata is located in an area with patches of low, moderate, and high risk of dispersion. Reefton is surrounded by low and moderate risk patches, while Hawkdun is located in an area of moderate risk with low to high risk areas downstream from its location. In general, Figure 4.3 gives a good indication of the infiltration problems on soils that could arise due to high-SAR water disposal. However, this model is useful only for general assessments, and more detailed studies should rely on actual field sample analyses.

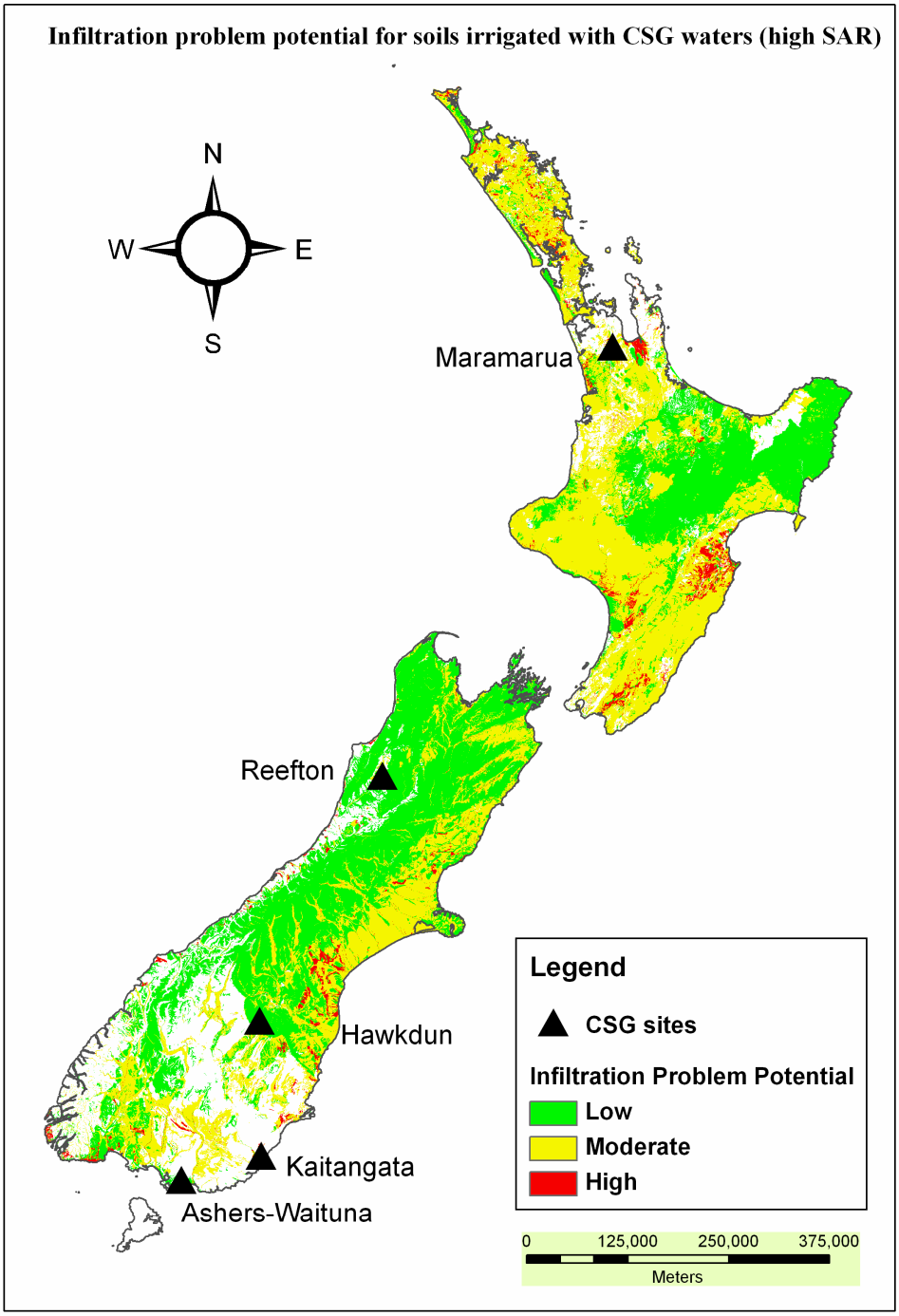

Figure 4.3. Infiltration problem potential for New Zealand soils exposed to high-SAR water for prolonged periods of time. Model produced using the FSDL (Landcare Research New Zealand Ltd, 2000b) and assumptions in Appendix C.

In addition to salinity and infiltration problems, CSG waters can generate other problems when carrying out land disposal applications. CSG waters generally contain high sodium and chloride concentrations which pose specific ion toxicity issues when used for crop irrigation. Toxicity effects from sodium and chloride include leaf burn, scorch and dying of leaf tissue, and in time these effects may significantly reduce crop yield (Ayers et al., 1985). In some instances, CSG waters may also contain appreciable quantities of boron (Taulis et al., 2005), which may cause a toxicity hazard (Ayers et al., 1985). Another trace element to consider is zinc, which has the potential to accumulate in soils thus becoming present in plant tissue and causing significant growth reduction. However, zinc poses a reduced toxicity risk for plants (Ayers et al., 1985) because of the high pH (> 6) of CSG waters which constraints zinc accumulation on soils,. In addition to zinc, CSG waters from other basins in New Zealand could have other trace elements depending on specific aquifer characteristics, therefore sample collection and water characterisation at each site is important to determine the range of trace elements that could be present.

If sprinkler irrigation is used, the toxicity is aggravated because toxic ions are absorbed through leaves hit by sprinkler water (Ayers et al., 1985). Toxicity guidelines which would apply to CSG waters when used in irrigation applications are presented in Table 4.1. Less stringent but more crop-specific toxicity trigger values are presented in the *Australian and New Zealand Guidelines for Fresh and Marine Water Quality* (ANZECC and ARMCANZ, 2000). In addition, with land application of CSG water there could be indirect toxicity problems arising from the mobilisation of certain trace elements in the soil. For example, McBeth et al (2003) have suggested that arsenic, selenium, and fluorine could become soluble and mobile in soils irrigated with CSG water. This can take place because these ions form anionic species with soil particles, and can become soluble when soils are irrigated with alkaline waters (McBeth et al., 2003). However, New Zealand soils are generally low in selenium, which is a dietary supplement in New Zealand, so increased selenium mobility could prove beneficial in some instances.

Table 4.1. Toxicity guidelines for managing water quality issues relating to irrigation applications[1]

Specific ion toxicity	Units	Degree of restriction on use		
		None	Slight to moderate	Severe
Sodium (Na^+)				
Surface irrigation	SAR units	< 3	3 - 9	> 9
Sprinkler irrigation	meq/l	< 3	> 3	
Chloride (Cl^-)				
Surface irrigation	meq/l	< 4	4 – 10	> 10
Sprinkler irrigation	meq/l	< 3	> 3	
Boron (B)	mg/l	< 0.7	0.7 – 3.0	> 3.0

[1](Ayers et al., 1985)

Coal seam gas basins in the United States can present different concentrations of toxicity inducing ions in their co-produced waters, thus various restrictions levels rule their reutilisation (Table 4.1). For example, on the basis of sodium toxicity, every single one of the US basins presented in Chapter 2 (Black Warrior, Piceance, Uinta, San Juan, Raton, and Powder River) produce CSG waters with SAR values greater than 20, which poses severe restrictions. On the other hand, only the Black Warrior, Piceance, Uinta, and San Juan (New Mexico) have CSG waters with chloride concentrations greater than 10 meq/l, which would result in severe restrictions on their utilisation. Also, since the majority of the sodium is generated from ion exchange processes with only some halite dissolution (if any), chloride concentrations are always lower than sodium in CSG waters. In this way, the US CSG water quality data presented in Chapter 2, indicates that chloride concentrations can range from 1% to 78% of the sodium concentrations (meq/l). New Zealand CSG waters are subject to the same relationship between sodium and chloride. For example, the Maramarua CSG water presented in Chapter 2 exhibits a ratio of about 3.5 sodium cations to 1 chloride anion (or chloride concentrations corresponding to 28% sodium in meq/l). This shows that the main specific ion toxicity issue with CSG waters resides in their sodium concentrations.

Surface water disposal of CSG water

Disposal of CSG water into existing streams, main rivers, and wetlands has the potential to alter local conditions and change the distribution of plant and fish population. In addition, seepage from land disposal of CSG water can result in additional discharges which would likely be into surface water bodies. Riparian vegetation on wetlands and rivers are exposed to the same toxicity problems found on plants when CSG waters are disposed on the land. The saline and sodic nature of CSG waters may modify riparian and wetland plant communities by giving way to more saline tolerant species (Kristin et al., 2006). For example, in the Powder River Basin (MT), die-off of plants on an ephemeral channel was detected after only weeks of CSG discharges, and encroachment of halophytic weed species was detected on the same channel within one season (Montana State University, 2006b). A similar issue may arise in fish communities with changes in assemblage composition with increasing CSG discharges (Davis et al., 2006a).

In the United States, there is a lack of information related to the effects of CSG water on aquatic life mainly because of the absence of baseline information prior to discharge operations; in some cases, there has been no clear distinction between CSG water discharges and related water discharges from the petroleum industry. Therefore, it has not been easy to pinpoint the environmental impacts of discharging CSG water to surface waters.

As salinity levels increase, low salinity tolerant species die while high salinity tolerant species flourish (Williams, 2001, as cited in Davis et al., 2006b). An example of this occurred in the Black Warrior Basin in Alabama, where the population of gulf darters (*Etheostoma swaini*) decreased in streams receiving CSG waters, while rough shinners multiplied in areas downstream from the discharge (O'Neil et al., 1991, as cited in Davis et al. 2006b). In the Powder River Basin, oil field brines caused a significant salinity increase in the Powder River (from 4170-4840µS/cm to 6000-6740 µS/cm) downstream from the discharge point (Boelter et al., 1992, as cited in Davis et al., 2006b). Water samples collected from these sections of the Powder River (PR) were used in laboratory tests using water fleas – their survival and reproduction was significantly affected by an increase in water salinity, which was mainly due to high bicarbonate, chloride, sodium, and potassium ions in solution (Boelter et al., 1992, as cited in Davis et al., 2006b).

Studies carried out in Cedar Cove field in Alabama suggested little or no chronic impacts at chloride concentrations of 593 mg/l (O'Neil et al., 1989). However, some CSG producers in the Black Warrior Basin experienced problems passing chronic toxicity tests on water fleas at chloride concentrations of 230 mg/l (Davis et al., 1993). Unfortunately, when producers have failed passing toxicity tests, it has been difficult to identify the underlying cause for the failure because these tests are not able to pinpoint the specific ions causing the toxicity. For example, chronic toxicity tests on water fleas have had negative outcomes at chloride concentrations in the 550-600 mg/l range (Mount et al., 1993a, as cited in Davis et al., 1993), but at chloride concentrations of 230 mg/l, bicarbonate concentrations of 730mg/l may become chronically toxic (Davis et al., 1993).

Research by Skaar (Skaar et al., 2004, as cited in Davis et al. 2006b) has focused on assessing acute toxicity effects of $NaHCO_3$ on fathead minnows and pallid sturgeon using synthetic CSG water from both the Powder River and the Tongue River. This

research showed that $NaHCO_3$ was lethal to 50% of pallid surgeons at concentrations of 1158 mg NaHCO3/l in PR water and 1828 mg $NaHCO_3$/l in Tongue River water after 96 hours of exposure. In addition, $NaHCO_3$ concentrations of 1643 mg $NaHCO_3$/l were lethal to 50% of fathead minnows in PR water after 96 hours of exposure, but only 23% of fathead minnows perished at $NaHCO_3$ concentrations of 4000 mg $NaHCO_3$/l in Tongue River water (Skaar et al., 2004, as cited in Davis et al. 2006b). CSG waters described in Chapters 2 and 3 can have similar $NaHCO_3$ concentrations. For example, CSG waters from the PRB (Montana side, Figure 2.10 in Chapter 2) would have sodium and bicarbonate concentrations equivalent to about 1500 mg $NaHCO_3$/l, while Maramarua CSG waters would have sodium and bicarbonate concentrations close to 1000 mg $NaHCO_3$/l.

Research by Mount (1993b, as cited in Davis et al. 2006b) has suggested 50% mortality of fathead minnows after 96 hours of exposure to potassium concentrations of about 500 mg/l, bicarbonate of about 2000 mg/l, and chloride of about 4500 mg/l. Below lethal concentrations of $NaHCO_3$, the effects of chronic exposure has been studied by Skaar (Skaar et al., 2004, as cited in Davis et al. 2006b). Fathead minnow eggs were hatched at $NaHCO_3$ concentrations of 1400 mg/l with only 8.1% survival rate after 96 hours (94.3% in the control). After 37 days, the survival rate was only 2.4%, in comparison to an 89% survival rate in the control (Skaar et al., 2004, as cited in Davis et al. 2006b).

The Dissolved oxygen concentration is a critical parameter affecting fish water quality (Davis et al., 2006b). “Dissolved oxygen levels below 5.0 mg/l can stress aquatic life and prolonged periods of low DO can result in fish kills” (Ji, 2005, as cited in Davis et al. 2006b, p.17). Coal seam gas waters typically contain low quantities of dissolved oxygen because these are generated under extreme anaerobic conditions (ALL-Consulting, 2003). Notwithstanding, dissolved oxygen levels may increase considerably due to agitation while water is transported on channels or if aerated on purpose for some beneficial application. In some areas of Wyoming, for example, CSG water quality has been good enough to sustain fishponds with rainbow trout, blue gill, and small-mouth (ALL-Consulting and Montana Board of Oil and Gas Conservation, 2004).

Other CSG water parameters like pH, turbidity, and trace metal concentration could pose some effects depending on the quality of the water. CSG waters tend to have alkaline pH, and some fish species are susceptible to high pH values (Eisler, 1991, as cited in ALL-Consulting, 2003). Uncontrolled CSG water discharges could disturb sediments deposited on the banks of streams and increase local turbidity, which would also increase due to CSG water salinity. This could give a competitive advantage to non-sight feeding fish and, in the long run, could affect natural fish distributions. CSG waters may contain heavy metals like barium, arsenic, selenium, copper, molybdenum, chromium, and zinc, which can accumulate in fish negatively affecting their reproduction, development, and survival (Eisler, 1991, as cited in ALL-Consulting, 2003).

In New Zealand, no research has been carried out about the effects of CSG water discharges on aquatic life. However, research by Main (1988), Collier et al. (1990), and West et al. (1997) has focused on studying the response of aquatic fauna to acidity and pH changes. Using field trials, Main (1988) discovered that kokopu whitebait (*Galaxias argentus*, *Galaxias fasicatus*, and *Galaxias postvectis*) showed no pH preference, while koaro (*Galaxias brevipinnis*) preferred circum-neutral pH over acidic pH values. Main (1988) also suggested that adult kokopu can be found in acidic streams as a result of competition with brown trout (*Salmo trutta*), which is an introduced species intolerant of low pH values (<5.0). High alkalinity in CSG water discharges could buffer acidic streams and raise pH values. This could become a problem if brown trout find their way to these now neutral streams and start competing with kokopu whitebait. Also, the mixing of CSG waters with acidic streams could shift the carbonate equilibrium of CSG waters generating dissolved carbon dioxide, which can be toxic to fish at elevated concentrations (Alabaster et al., 1980, as cited in Main 1988). West et al. (1997) carried out laboratory trials using New Zealand native fish, and they discovered that some species (*Galaxias fasicatus*, *Galaxias brevipinnis*, and *Anguilla australis*) exhibited a preference for water with below neutral pH values. In particular, West et al. (1997) noted that juvenile banded kokopu (*Galaxias fasicatus*) preferred pH values between 5.8 and 7.1, and that this could pose problems for the ability of these fish to inhabit or migrate through lowland habitats with above neutral pH values. CSG water discharges could impact lowland habitats by raising their pH considerably, and this could restrict the habitat and migration habits of

young banded kokopu. West et al. (1997) also noted that native shrimp (*Paratya curvirostris*) were unable to detect pH changes and died under high pH conditions.

About half of native New Zealand fishes are diadromous (McIntosh and McDowall, 2004), which means these fishes could have no problems adapting to increased salinity due to CSG water discharges. However, this could result in changes in fish assemblages and biodiversity as less salinity resistant fish die giving way to diadromous species. Having a tolerance to salinity does not necessarily mean diadromous fish could be impervious to CSG water discharges. For example, the New Zealand common smelt (*Retropina retropina*) can be both diadromous and non-diadromous (if land-locked), and these fish are considered to be the most sensitive to pollutants in New Zealand (NIWA, 2006a).

In New Zealand, discharges to surface waters are managed by regional councils which may use the *Australian and New Zealand Guidelines for Fresh and Marine Water Quality* (ANZECC and ARMCANZ, 2000) for assessing resource consent applications. For example, these guidelines provide default trigger values for pH, dissolved oxygen, clarity, turbidity, boron, and zinc to provide different levels of protection in rivers and streams. However, councils may develop their own trigger values customized to their local conditions, and for particular discharge scenarios. In the case of Maramarua, CSG water from C-1 had a pH ranging from 7.2 to 8.6 (see Chapter 3), but the ANZECC water quality guidelines state an upper limit of 8.0 for upland rivers (>150 m altitude) and 7.8 for lowland rivers in slightly disturbed ecosystems. Another example with this water is boron, which had a concentration of 2.5 mg/l in the 19/8/2004 Maramarua CSG water sample, but the trigger value for slightly to moderately disturbed systems in the ANZECC water quality guidelines is 0.37 mg/l.

Disposal alternatives and management options

Alternatives for CSG water disposal include aquifer injection, treatment prior to disposal, and resource utilisation. In addition, if CSG basins are close to the sea, it is possible to discharge them directly into the ocean. Injection consists of pumping CSG co-produced water into other aquifers in order to safely dispose of them. These aquifers need to be able to accommodate the produced water quantities without compromising other resources. For example, aquifers being abstracted for irrigation are not suitable for deep well injection because the injected CSG water could contaminate these aquifers if the CSG water is highly mineralised. Also, it is not possible to re-inject CSG waters back into the original coal aquifer from which they were abstracted as this would raise the hydrostatic pressure and stop the gas desorption process. In New Zealand, groundwater is a very important resource as it represents about 30% of the total water allocation (Robb, 2000, as cited in Rosen et al. 2001). In addition, some aquifers in New Zealand are of significant ecological importance because they contain a variety of groundwater invertebrates (Scarsbrook and National Institute of Water and Atmospheric Research (N.Z.), 2003) that could be jeopardised by CSG water injection. Nevertheless, in the United States aquifer injection is considered to be an environmentally safe method for CSG water disposal (ALL-Consulting, 2003). However, the cost associated with deep well injection is considered to be the upper limit cost for acceptable management of CSG waters (Lee-Ryan et al., 1991).

Resource utilisation options include using CSG waters for livestock and wildlife watering, fish culture, and human drinking. Water with a salinity value below 1.5 dS/m is considered “excellent” for stock watering, and water with salinity values between 1.5 and 5.0 dS/m is considered “very satisfactory” (Ayers et al., 1985). In addition, typical solutes present in CSG water do not pose any toxicity issues to livestock or poultry – the only issue would be boron which, when present, may cause problems at concentrations above 5 mg/l (Ayers et al., 1985). In the US, wildlife watering is important in semi-arid to arid regions in the western United States (Montana and Wyoming). In these regions, CSG water can be used to provide water to deer, coyotes, bobcats, and badgers (ALL-Consulting, 2003). The main limitation for using CSG water to provide wildlife watering

is that this water source would only be temporary and would decline in time as the CSG is being extracted. On the other hand, using CSG waters in livestock applications is less constrained, as there is a fair degree of control over how to water livestock, and other alternatives can be sought after as CSG waters become unavailable. In New Zealand the weather is generally humid and there are no native mammals with special water requirements, therefore wildlife watering is not necessary. CSG waters could be used in New Zealand to water livestock during drought periods, or in remote areas away from direct drinking water sources.

Using CSG waters to build commercial fisheries is an interesting opportunity, but requires fully assessing CSG water quality and a compatible fish species to live in that specific environment. In addition, CSG waters are formed in an anaerobic environment thus having low dissolved oxygen concentrations, which is necessary for fish survival (ALL-Consulting, 2003). Once abstracted, CSG waters can be aerated or sparged, as part of the treatment process, increasing dissolved oxygen levels. In the US, not-so-mineralised CSG water has been successfully used in privately owned fishponds in Wyoming to support populations of rainbow trout, blue gill, and small-mouth bass (ALL-Consulting, 2003). In New Zealand, similar commercial fisheries can be established depending on the water quality of the water being co-produced with CSG operations.

Water being co-produced with CSG extraction can be of acceptable quality for human drinking if it comes from wells located near recharge areas or shallow basins. This is because under such circumstances CSG water tends to be less mineralised than water abstracted from deep CSG aquifers. In Wyoming, CSG water near the Powder River basin margins is suitable for human consumption because this water has not entered deep into the coal aquifer. However, as CSG water travels through the aquifer deep into the basin, it becomes more mineralised and becomes less suitable for human drinking. In New Zealand, drinking water is generally abundant and there is no need to look for alternative forms of supply. Therefore, CSG water is not likely to be used for human drinking applications in New Zealand.

Whether land disposal or surface water disposal is implemented, storage ponds need to be implemented to store CSG waters when conditions are not ideal for their disposal. For example, during periods of high rainfall, irrigation of agricultural soils (i.e.

land disposal) is not necessary so CSG waters need to be stored for future use/disposal. Conversely, during periods of low rainfall, rivers typically have low flows, and this limits the dilution of CSG waters into these rivers so, again, CSG waters need to be stored for future disposal when flows are high again. Ideally, a combination of surface and land disposal can help minimise the size of these storage ponds, but some situations do not allow implementation of either land or surface disposal.

Treating CSG waters before disposal enables the removal of ions so that these waters can be used in beneficial applications or safely disposed into a fresh water body or to land. Options for treatment include evaporation, electrodialysis reversal, reverse osmosis, aeration/sedimentation, wetland systems, and ion exchange technology. Evaporation (or distillation) involves boiling water into steam to segregate water impurities, thus requiring a significant input of energy. In electrodialysis reversal, anion and cation selective membranes are used to separate charged ions from CSG waters, whereas with reverse osmosis CSG water is filtrated by pumping it through a semipermeable membrane. This latter system requires a pump to continuously pump water through, and regular membrane maintenance. Typically, each treatment technology has a given ion removal capacity at a certain operational constraint and associated cost. This is a critical issue because, in some instances in the US, CSG water treatment and disposal costs have been so elevated that some CSG operators have been forced to abandon certain projects without ever producing any gas (Burkett et al., 1991). Research by Lee-Ryan et al. (1991) has indicated that evaporation is the most expensive treatment option followed by on-site deep well injection, electrodialysis, reverse osmosis, and aeration/sedimentation (Figure 4.4). Evaporation can remove 100% of the dissolved solids in CSG waters, but this system requires high energy input to be able to evaporate the water (Lee-Ryan et al., 1991). According to the Gas Technology Institute (GTI) (2002, as cited in ALL-Consulting, 2003) electrodialysis can lower the dissolved solids content of CSG waters to acceptable levels. However, to effectively lower the SAR of the water, this system needs to use additional chemical treatment (ALL-Consulting, 2003). Reverse Osmosis can remove TDS (including sodium) concentrations from CSG waters with efficiencies of up to 94% (Lee-Ryan et al., 1991). On the other hand, this system requires high maintenance and pre-filtering to avoid membrane fouling, and it is necessary to

dispose of concentrated brines resulting from this treatment process. Simple aeration/sedimentation is the cheapest option for treating CSG waters, but this treatment system only reduces iron and zinc by allowing their precipitation. Using this system, iron concentrations have been reduced to values lower than 3 mg/l (Lee-Ryan et al., 1991). In addition, this system can increase the DO of CSG waters, to improve their quality for river disposal. Aeration would also promote degassing (pH increase and carbon dioxide release), which would take place with rapid calcium carbonate precipitation (see Chapter 3) thus increasing SAR values to levels expected under atmospheric conditions, which would allow for accurate assessment of potential infiltration problems associated with CSG water discharge to land.

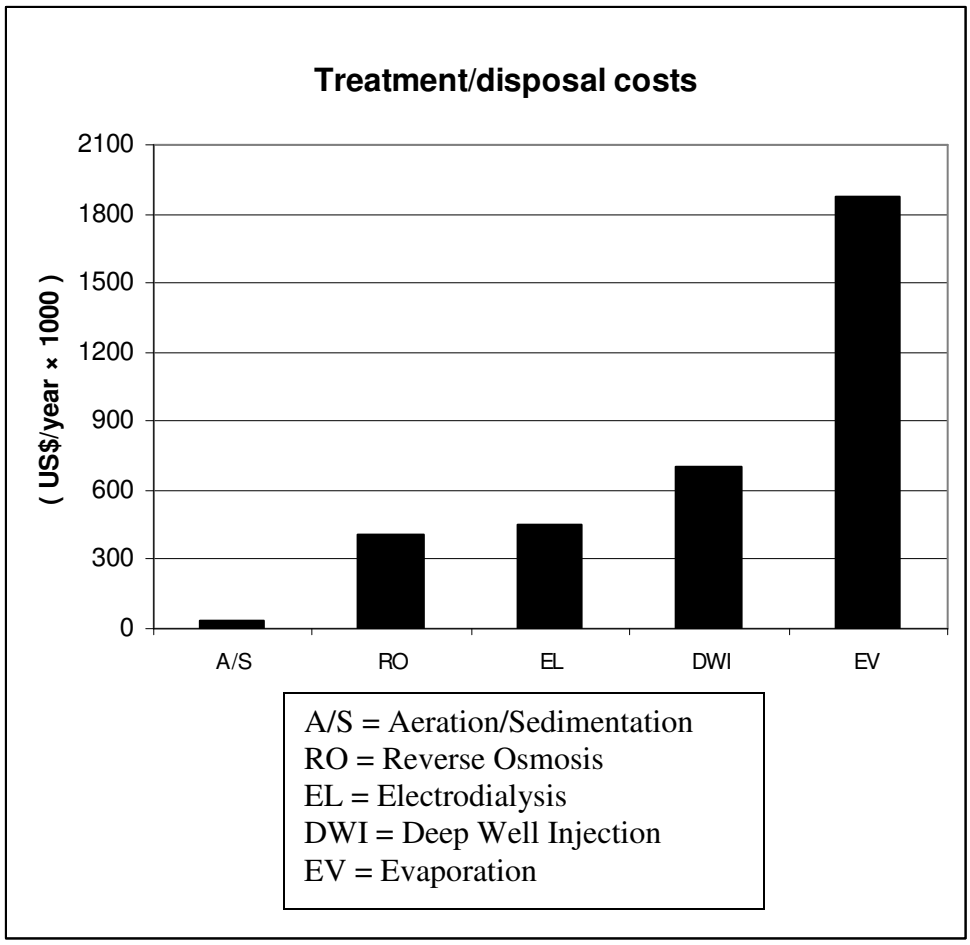

Figure 4.4. Annual costs associated with different treatment/disposal technologies (Lee-Ryan et al., 1991). Assuming each technology is able to treat a CSG water volume of 138,500 m^3 per year (on average).

Wetland treatment systems offer a low-cost treatment option for the long-term treatment of CSG waters, but at lower removal rates than when using chemical treatments

(Kirkpatrick, 2005). Field trials using wetlands to treat CSG waters in the US have indicated that wetlands have the capacity to remove iron and barium from CSG water, but they fail to reduce SAR (Sanders et al., 2001, as cited in ALL-Consulting 2003). Research by Kirkpatrick (2005) corroborated the 2001 studies indicating that the use of native plant species in wetlands for the treatment of CSG waters, resulted in an overall increase in salinity, SAR, and pH. However, the main problem with CSG treatment using wetland systems is that CSG projects have a limited life span, and they experience a marked decrease in water production over time. If the influx of water into the wetland is stopped, then its waters would start to evaporate and salinity levels around the wetland would increase. Increased salinity would have a negative effects on plants and animals that have been established there and, in the long run, this would result in a dead environment, which would have to be restored.

CSG water can also be treated using ion exchange technology. Trials carried out by Drake Engineering Inc (DEI) using synthetic resins have indicated that this technology makes it possible to remove sodium ions, while lowering salinity and pH; this CSG water treatment system allows for multiple modules, each one having treatment rates of up to 0.8 m^3/min (87.5% sodium removal) and at fairly low costs (Montana State University, 2006a). Figure 4.5 shows a schematic of the DEI CSG water treatment system. A similar system by RIMCON LLC uses pits filled with synthetic zeolites which operate in columnar mode and in series to treat CSG water by removing sodium ions at approximately 1.5 m^3/min at 0.1US$/barrel (Detmer, 2005). However this system requires the construction of lined ponds for storage and operation as well as the zeolite pits. Both the RIMCON and the DEI treatment systems result in concentrated brines for disposal or management. Both the zeolites and the resins need to be regenerated either with acid or concentrated salt solutions for reuse before treatment.

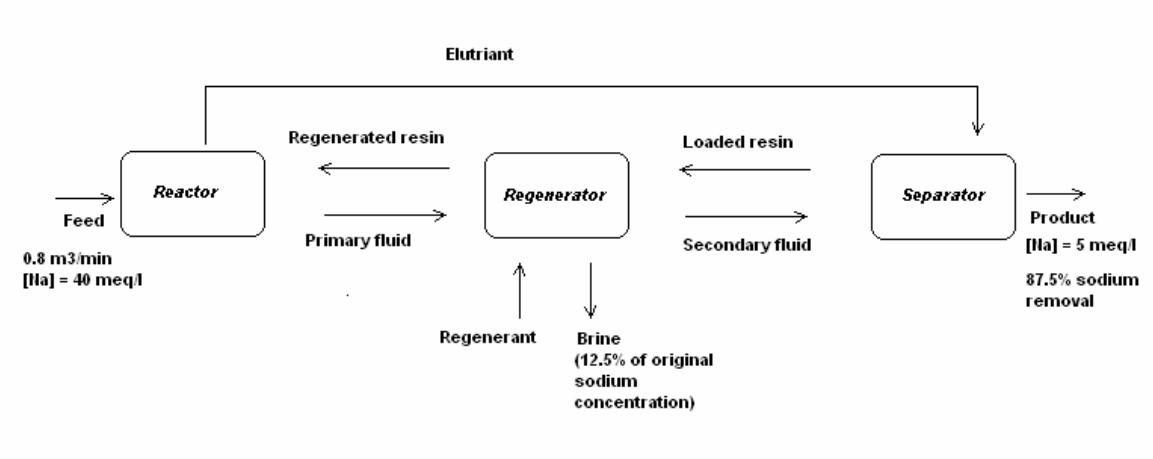

Figure 4.5. Drake Engineering Inc. CSG water treatment system.

In addition to treatment systems, it is possible to condition CSG waters or the soil itself by the addition of chemical products. For example, it is possible to reduce CSG water pH by adding sulphuric acid to the water, and it is possible to reduce the SAR by dissolving calcium-bearing minerals (ALL-Consulting, 2003). It is also possible to add gypsum ($CaSO_4$) to receiving soils, which can lower the SAR and raise the salinity of the soils, thus reducing infiltration problems. However, these techniques are not very effective because calcium dissolution is constrained in high salinity water (Ayers et al., 1985), and the high bicarbonate concentrations and elevated pH in CSG waters causes calcium precipitation (as $CaCO_3$) under normal atmospheric conditions. This was observed in Chapter 3 where calcium precipitation took place after the CSG water reached equilibrium with the atmosphere - in this case a decrease in 40% of calcium (due to calcium carbonate precipitation) was responsible for an increase of 23% in SAR values. Consequently, larger quantities of gypsum would be required which, apart from being expensive, can also increase the salinity hazard.

Other disposal options for CSG waters include using it for dust control or water blending for disposal through beneficial application. For example, if not too mineralised, CSG waters can be used for irrigation of agricultural soils, and blending them with fresh water can lower sodium and chloride concentrations, thus minimising their sodicity, salinity, and toxicity effects. Research by Bodger (2005) showed that CSG waters can be used to neutralise Acid Mine Drainage (AMD) waters in areas where CSG and AMD occurrences are in close proximity. In laboratory experiments, AMD waters were blended

with CSG waters resulting in a final water solution with reduced AMD acidity (higher pH) and the precipitation of aluminium, iron, and sulphate, which were originally present in the AMD. Other applications include the use of CSG waters for dust control or watering stock. Water with a salinity value below 1.5 dS/m is considered “excellent” for stock watering, and water with salinity values between 1.5 and 5.0 dS/m is considered “very satisfactory” (Ayers et al., 1985). In addition, typical solutes present in CSG water do not pose any toxicity issues to livestock or poultry – the only issue would be boron which, when present, may cause problems at concentrations above 5 mg/l (Ayers et al., 1985).

Case Study: Assessing the environmental effects of CSG water disposal in Maramarua

In this section, a case study of the potential environmental impacts associated with CSG water disposal in the Maramarua area will be described. This assessment will consider both land and surface water disposal of CSG water while considering potential solutions. The analysis will be done in accordance with Waikato Regional Council (WRC) regulations as outlined in the Proposed Waikato Regional Plan (PWRP). Also, supporting documents such as the ANZECC water quality guidelines and relevant international guidelines will be used in conjunction with the PWRP.

Site description

The potential CSG-producing area being studied covers a large section of agricultural lowland with sparse residential development less than a kilometre west of Maramarua town (Figure 4.6). To the south, there are a series of low forested hills and to the west there are inland wetlands. In the centre of the area there is an existing open cast coal mine covering a 3 km^2 area. The area is dissected by Kopuku and Coalfields roads.

The drainage area is characterised by a complex system of small creeks and agricultural drains. These feed the main water courses in the area – the Kopuku stream to the south and the Koterauto Stream in the East, which flow mainly to the west into the Whangamarino wetland. In addition, the Department of Conservation (DOC) indicates two inland wetland areas (Kopuku and Whangamarino) which are designated as conservation units, and may be sensitive to water discharge operations (Figure 4.7). The Kopuku Wetland water was sampled for basic analytes on a site visit in September 2004. Results from this sampling are presented in Table C.2 (Appendix C). Other conservation areas include the Ruaotehuia Stream located towards the north east of the permit area, and part of the Maramarua forest located at the most eastern bound vertex of the permit area. In addition, there are patches of indigenous forests in close proximity to the wetlands (Figure 4.7).

The area towards the north and west of the mine is mainly agricultural (rural) with low rolling hills (New Zealand. Mines Division. et al., 1983). A study carried out in 1983 (New Zealand. Mines Division. et al., 1983) suggested these soils have good agricultural value since they were used for intensive grazing and cropping. In addition, data from the NZLRI database indicates that, besides being used for pasture, this area is covered with patches of native vegetation and non-arable land (Landcare Research New Zealand Ltd, 2000a).

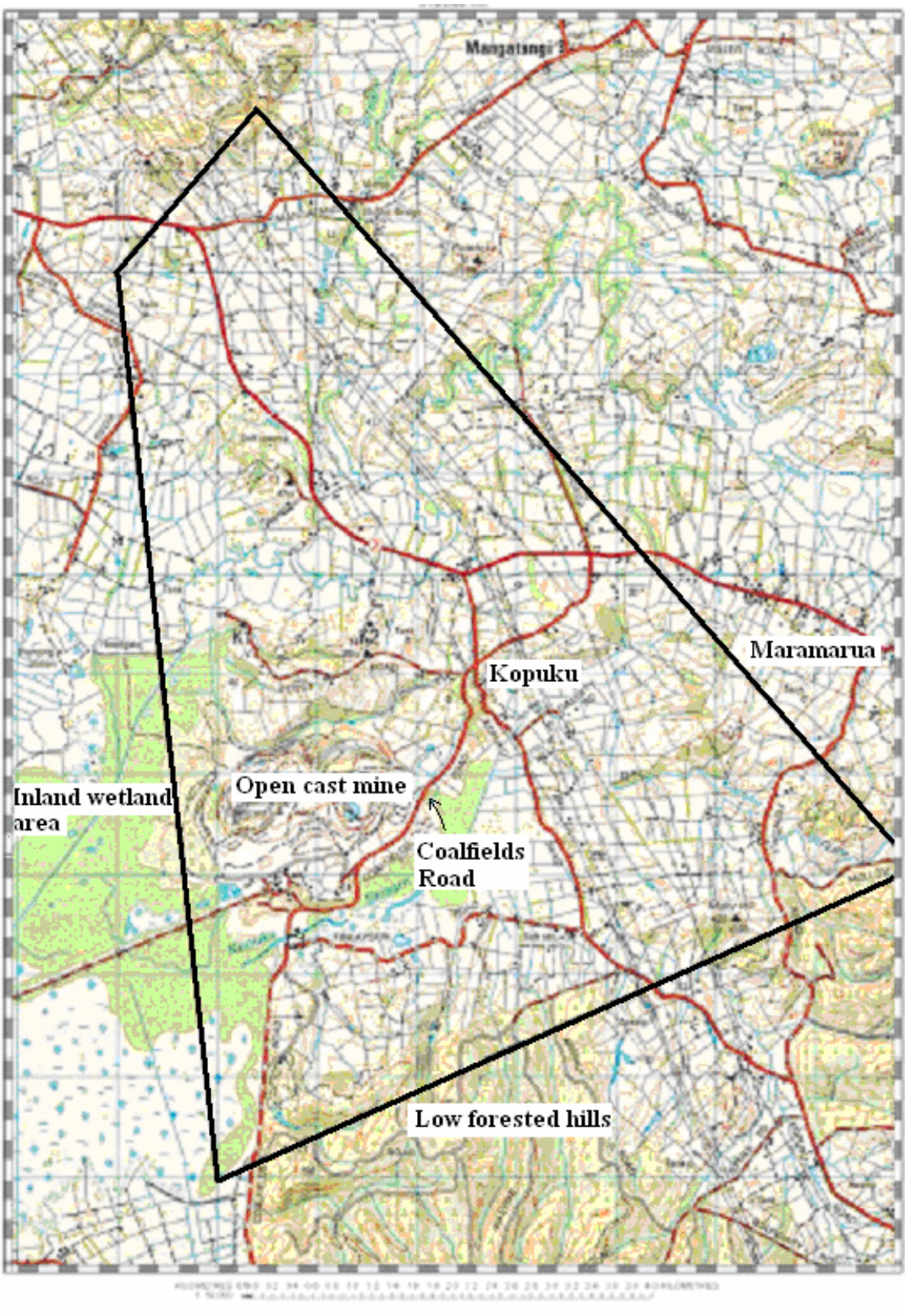

Figure 4.6. CSG extraction area under exploration (Pope and Trumm, 2004).

The area has a humid climate with peak rainfall occurring between May and July, and the driest months taking place between October and February (New Zealand. Mines Division. et al., 1983). The closest weather station to the CSG exploration well (C-1) is the Maramarua Forest weather station, which is about 7 km from the site and it registered an annual average rainfall of 1263 mm/year between 1947 and 1980 (New Zealand. Mines Division. et al., 1983).

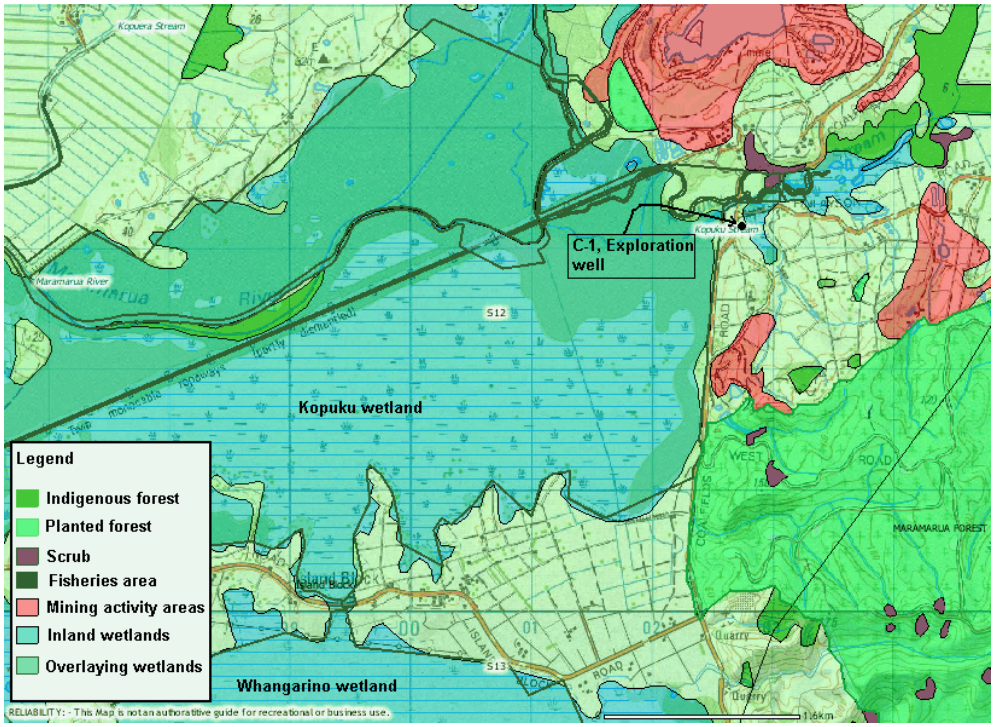

Figure 4.7. Protected wetland areas. Adapted from DOC GIS database (Department of Conservation, 2006a).

Maramarua CSG water

Gas flow testing from well C-1 has produced water quality samples of the Na-HCO_3-Cl^- type (Chapters 2 and 3). It will be assumed that the water that might need to be disposed of in future large-scale operations is of similar water quality to previous samples because previous sampling rounds (Chapter 3) have suggested there is little or no chemical variation over time. Nevertheless, different areas of the basin could produce different water qualities depending on the depth of the coal seams within the basin or proximity of extraction wells to recharge areas. However, since no samples from other locations are available within this area, it will be assumed that the C-1 water quality will be the one prevailing. Because full-scale production is not currently taking place, it will be assumed that the water abstraction rate corresponds to the rate used for the gas flow testing, which was about 40 m^3/day per well (similar to the Raton or Powder River basins; see Table 2.2, Chapter 2).

Soil Sampling

During the first part of the gas flow testing, CSG water was discharged directly into a receiving wetland. For the second part, however, CSG water was discharged onto adjacent land. Right after the discharge had commenced, 6 soil samples were taken from 3 locations which had not been exposed to CSG water. These samples were collected from the 0-15 cm and the 15-45cm intervals, and their location in relation to C-1 is presented in Figure 4.8. These pits were located approximately 100 metres from C-1 and at 55 (Pit 1-Pit 2), 40 (Pit 1- Pit 3), and 23 (Pit 2- Pit 3) metres apart from each other.

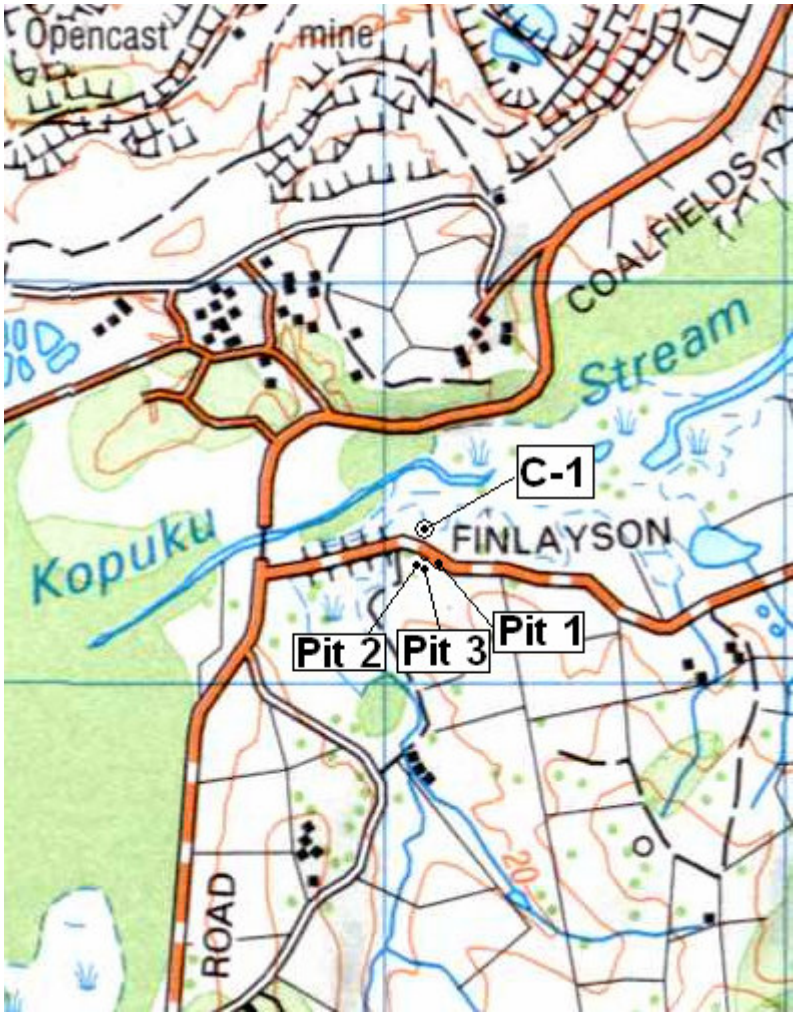

Figure 4.8. Location of soil sampling pits in relation to C-1

The material excavated from these pits was sent to The University of Canterbury where the samples were split into two batches. The first batch was analysed at the Geomechanics Laboratory (University of Canterbury) where sieving and sedimentation analyses were carried out in accordance to NZS 4402:1986 Test 2.8.2 (dry sieving) and Test 2.8.4 (Hydrometer). The particle size distribution resulting from these analyses is presented in Figure 4.9. These results show that the soil samples collected consisted mainly of loams with about 13-32% clay. The second batch was sent to Hill Laboratories where a chemical analysis was carried out. In general, these soils had below neutral pH (5.1-6.1), some calcium (26-164 mg/l), low magnesium (<18 mg/l), low sodium (<5 mg/l), low salinity (<143µS/cm), and low CEC (<14 meq/100g). These data were useful in determining the salinity, sodicity, and toxicity hazards outlined in the next sections.

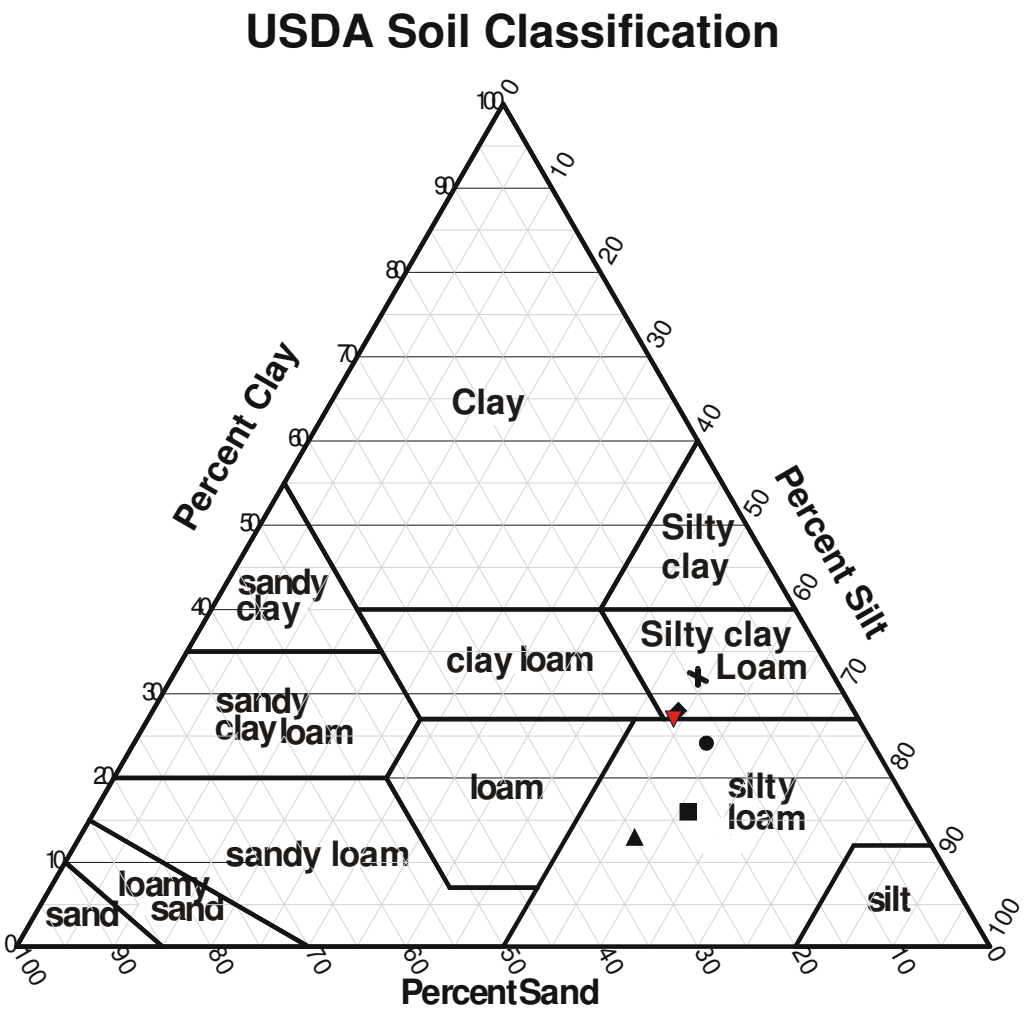

SOIL DATA						
	Sample No.	Elevation	Percentages of material			Classification
			Sand	Silt	Clay	
■	Pit 1 0-150	15 masl	23	61	16	Silt loam
●	Pit 1 150-450	15 masl	17	59	24	Silt loam
▲	Pit 2 0-150	8 masl	30	57	13	Silt loam
◆	Pit 2 150-450	8 masl	18	54	28	Silty clay loam
▼	Pit 3 0-150	16 masl	19	54	27	Silty clay loam
✚	Pit 3 150-450	16 masl	14	54	32	Silty clay loam

Figure 4.9. Textural properties of soil samples collected from Maramarua

Effects arising from land disposal of CSG waters

Once full-scale CSG production begins in Maramarua, large quantities of CSG water will have to be disposed of in this area. The trend in the Waikato Region is to dispose wastewaters onto the land instead of directly to water (Environment Waikato, 2002), therefore Maramarua CSG water will probably end up being disposed on adjacent land. It is assumed that the discharge will not be on protected land (native forests or land draining into protected wetlands), but CSG water could find its way through these areas and agricultural areas in the form of runoff and subsurface flow.

As agriculture and irrigation demand increases, CSG water itself can be used to irrigate agricultural soils. This is a particularly important application because in New Zealand irrigation water doubles every 10 years, and about 80% of all water allocations goes towards irrigation (ANZECC and ARMCANZ, 2000). Although Maramarua receives plenty of rainfall throughout the year and does not rely solely on irrigation, future water demand due to increased agricultural activity or diary farming could result in increasing water demand. Under these circumstances, CSG waters from this area can become a valuable resource. For this purpose, it is necessary to adequately manage the use of CSG waters to minimize problems like salinity, loss of permeability, and specific ion toxicity issues.

Assessment of salinity hazard

Methods

According to the FSDL, soils in the Maramarua area, where extraction well C-1 is located, have a low salinity class (<143µS/cm). This was corroborated with the soil samples taken from Pits 1, 2, and 3 which presented low salinity values (< 80µS/cm; Table C.3, Appendix C). This does not necessarily mean that saline soils will never become a problem- if these soils are continually irrigated with saline CSG water, salts will start to accumulate in the soil profile. Rainfall can leach these salts from the soils, but it will not be possible to leach sodium as this ion is chemically adsorbed by the clay particles forming the soil. Thus, with time, the ESP of the soil will increase and, if

leaching is not sufficient, the overall salinity of the soil will increase. In addition, the salinity of the CSG water itself can become a problem to plants when this water is used for irrigation even if the soils are non-saline. Therefore, the soil salinity model presented in the ANZECC water quality guidelines (ANZECC and ARMCANZ, 2000) was utilized to assess soil performance under continuous CSG water discharge. In this model, long term effects of irrigating with high-salinity/sodic waters are quantified by estimating the leaching fraction based on steady-state salinity conditions. Therefore, over time, salt equilibrium takes place between the inputs (irrigation and rainfall water) and the outputs (evapotranspiration, evaporation, and leaching fraction). However the EC of the evaporation and evapotranspiration fraction (PET) is nil because salts stay in the soil as water leaves the system. Under this situation, the leaching fraction (LF) is estimated by considering the ratio of inputs (EC of irrigation and rainfall) to outputs (EC of soil saturation extract) (ANZECC and ARMCANZ, 2000). In addition, the FAO guidelines (Ayers et al., 1985) were used to support this model when studying the effects of the water itself. The final model and its raw results are presented in Eqs C.2-C.9 and Tables C.3-C.11 presented in Appendix C. This model starts by determining the leaching fraction under rain fed conditions and then it assesses soil irrigation with CSG waters.

Before carrying out salinity calculations, the SAR of the CSG water to be discharged was adjusted for calcium carbonate precipitation. For these calculations the SAR adjustment procedure developed by Suarez (1981, as cited in Ayers et al., 1985) produced a value of 36.5 (Table C.2, Appendix C). Yearly precipitation was assumed to be 1263 mm/year (Maramarua Forest) having a low specific conductance (0.03 dS/m). The calculations were carried out for three situations: irrigation with 100% CSG water, irrigation with 70% CSG water and 30% rainfall, and irrigation with 50% CSG water and 50% rainfall water. This model was specifically used for determining the effects of water quality on soils, and did not attempt to model water demand – it merely assumed that a given volume of CSG water would have to be disposed on the land, with the option of blending with rainfall water. The changes in ESP, leaching fraction, and soil electrical conductivity were calculated for the six soil samples even though some of these samples were taken from below the top soil boundary (15-45 cm). Also, ESP was corrected as recommended in the ANZECC guidelines, by using a relationship between SAR and ESP

(Appendix C Eq. C.6) based on 59 soil samples from 9 states in the Western United States (USSL, 1954, as cited in ANZECC and ARMCANZ 2000).

Results

Results from the salinity assessment are presented in Table 4.2, which shows changes in soil salinity with and without ESP correction to show the complete range of values that could be obtained as ESP values increase. Average leaching fractions (LF_{av}) decrease when ESP values increase due to continuous CSG water discharge (moving horizontally across Table 4.2), and this causes an overall increase in soil salinity (EC_{SE}). For example, if ESP values are not corrected, soil salinity (EC_{SE}) is low (<0.95 dS/m). However, once ESP corrections are put in place, soil salinity values increase considerably often exceeding the limits for sensitive crops (0.95 dS/m) and moderately sensitive crops (1.9 dS/m) stated in the ANZECC water quality guidelines. This may cause a yield loss in moderately sensitive and sensitive crops (<100% yield) especially when using 100% CSG water (Table 4.2). However, if the CSG water is blended with rainfall water (EC=0.03 dS/m), the increase in ESP values and decrease in leaching fractions are reduced. In sample 3, the leaching fraction seems to decrease with increased blending, however this is so because this sample has the lowest clay percentage (13%), and this produces a leaching fraction of high magnitude which in turn generates lower soil salinity values and better yields (100%).

Table 4.2. Summary of salinity hazard assessment results.

Irrigation water composition	ID	Pit	Clay %	No ESP correction: ESP %	No ESP correction: LF_{av} %	No ESP correction: EC_{SE} dS/m	With ESP correction: ESP %	With ESP correction: LF_{av} %	With ESP correction: EC_{SE} dS/m	Sensitive crops Yield (%)	Moderately sensitive crops Yield (%)	NZ White clover Yield (%)
100% CSG water and no rainfall water	1	1	16	1.20	99.9	0.60	34.5	24.8	2.4	<100	<100	86
	2	1	24	1.40	99.9	0.60	34.5	28.1	2.1	<100	<100	89
	3	2	13	1.31	99.9	0.60	34.5	87.4	0.7	100	100	100
	4	2	28	1.91	99.9	0.60	34.5	25.6	2.3	<100	<100	87
	5	3	27	0.57	99.9	0.60	34.5	25.6	2.3	<100	<100	87
	6	3	32	0.36	99.9	0.60	34.5	34.9	1.7	<100	100	93
70% CSG water and 30% rainfall water	1	1	16	1.20	100	0.42	26.7	25.4	1.7	<100	100	93
	2	1	24	1.40	100	0.42	26.7	28.5	1.5	<100	100	95
	3	2	13	1.31	89.0	0.47	26.7	78.7	0.5	100	100	100
	4	2	28	1.91	100	0.42	26.7	26.3	1.6	<100	100	94
	5	3	27	0.57	100	0.42	26.7	26.3	1.6	<100	100	94
	6	3	32	0.36	100	0.42	26.7	34.5	1.2	<100	100	98
50% CSG water and 50% rainfall water	1	1	16	1.20	99.9	0.30	20.4	26.3	1.2	<100	100	98
	2	1	24	1.40	99.9	0.30	20.4	29.3	1.0	<100	100	100
	3	2	13	1.31	79.8	0.38	20.4	71.4	0.4	100	100	100
	4	2	28	1.91	98.0	0.31	20.4	27.3	1.1	<100	100	99
	5	3	27	0.57	99.9	0.30	20.4	27.3	1.1	<100	100	99
	6	3	32	0.36	99.9	0.30	20.4	34.6	0.9	100	100	100

Notes:

1) Results for Moderately tolerant crops, tolerant crops, and very tolerant crops indicated a 100% yield in all of the cases being analysed (Appendix C tables C.5, C.7, and C.9).
2) Barley (forage) was used as an example of a very tolerant crop, but results indicated a 100% yield in every instance (Appendix C tables C.5, C.7, and C.9).
3) Refer to tables C.4-C.11 in Appendix C for raw results.
4) Samples are arranged in order. For example, sample 1 (ID=1) from Pit 1 corresponds to the sample taken from the 0-15cm interval, while sample 2 (ID=2) from Pit 1 corresponds to the sample taken from the 15-45 cm section.
5) New Zealand white clover (Trifolium reperis) is an example of a sensitive crop
6) Assuming long-term irrigation and steady-state conditions these changes could take place in 5 to 10 years (US Salinity Laboratory Staff, 1954)

An example with an actual crop used for grazing in New Zealand (white clover or *Trifolium reperis*) shows how the yield of a sensitive crop can become affected by CSG water (Table 4.2). In this example, when using solely 100% CSG water, this crops's yield is often less than 90% especially in those soil samples with the largest clay percentage (Table 4.2). However, if this water is blended with 30% rainfall water, the yield improves so this time it is above 90%. If the CSG water is blended with 50% rainfall water, yield improves significantly (above 98 %).

In addition, CSG water itself can be used to analyse the salinity hazard affecting the water availability to crops just by analysing the specific conductance of the water. Doing so can provide independent support to the results of applying the salinity model (Table 4.2). In this case, Maramarua CSG water has a specific conductance of 1.31 dS/m so this water is classified as having a "slight to moderate" restriction on its use for irrigation (Ayers et al., 1985).

Discussion

The salinity model described in the preceding section shows how, with increasing CSG discharge, soil salinity problems become evident. The model has to be used with care because it has been developed mainly for arid and semi-arid conditions, and some of its assumptions might not be relevant to New Zealand. For example, the relationship linking soil ESP to SAR (Appendix C Eq. C.6) has been established for Western United States soils which exist under completely different weather conditions than the ones for New Zealand. Thus soil response to high-SAR water might not be as drastic as the one depicted by this relationship, and long-term ESP values might be lower than anticipated but no lower than the results obtained without ESP correction (Table 4.2). Also, salinity effects will vary with depth and this would also have to be considered. For example, the ANZECC guidelines state that changes in salinity could be noticed in a matter of months for surface soils (1-10cm), while changes in ESP and CEC in deeper soil sections could take up to several years to take effect (ANZECC and ARMCANZ, 2000). In any case, this soil salinity model has shown how irrigation with CSG water can have an impact on soil salinity and crop yield for sensitive and moderately sensitive crops.

Salinity in itself can improve the permeability of soils, and this can be observed with the increase in leaching fraction when comparing solely rain-fed conditions against the condition where soils are irrigated with CSG water (LF_{av} values in Table 4.2). However, when the soil ESP increases due to continuous CSG water irrigation, the leaching fraction gets reduced. This is because some of the sodium will hydrolyze (due to the presence of OH^-) or tend to associate with bicarbonate ions (HCO_3^-) with decreasing salinity (US Salinity Laboratory Staff, 1954); if the clay fraction is significant, the soil will become dispersed by the sodium ions now in solution, and a loss in permeability will have taken place. This was observed in Table 4.2 where samples with the higher clay percentage (samples 1, 2, 4, 5, and 6) tended to experience the highest loss in leaching fraction. This is more evident when the change in leaching fraction under rain-fed conditions is compared against the leaching fraction under CSG water irrigation with and without ESP correction (Appendix C, Table C.11). Thus, continuous CSG water irrigation will increase soil ESP, and this in the long run will decrease the leaching fraction. As less water is leached from the soil profile, more salts are retained after evaporation, and the soil increases its overall salinity. This was observed in Table 4.2 as the specific conductance of the soil (EC_{SE}) increased as ESP values increased with increasing CSG water irrigation.

For this particular location and CSG water quality, salinity appears not to pose a serious risk. However, the FAO guidelines (Ayers et al., 1985) may indicate a more significant hazard potential (slight to moderate). The boundary between “slight” and “moderate” is not clear with these guidelines, and this might lead to an overestimation of the effects of CSG water discharge.

Assessment of soil infiltration problems

In the previous section, modelling results indicated that an increase in soil sodium content (ESP) generates lower leaching fractions, which translates into a loss of permeability. In this case, the decrease in leaching was not significant enough to cause significant losses in yield. However, with higher clay contents and higher sodium concentrations the problem could become aggravated. This problem is particularly important right after rainfall because salts will be leached from the soil, but sodium will

be retained attached to clay particles. As a consequence, ESP value will be maintained while soil salinity will decrease, and soil dispersion will take place (ANZECC and ARMCANZ, 2000). Therefore it is necessary to assess the loss of structural stability (infiltration loss) due to continuous CSG water discharge.

Figure 4.10, is a magnification of Figure 4.3 showing the risk of infiltration loss associated with soils in the Maramarua (C-1) area. This figure shows that soils in the vicinity of C-1 can have either a low, moderate, or high infiltration problem. The soils towards the southwest of C-1 are at high risk because, according to the FSDL, these soils are classified as clays, which puts them at high risk of dispersing when irrigated with CSG water. However, soil samples collected from approximately 100 m south of C-1 had a low clay content, and are classified as loams (Figure 4.9).

To evaluate potential infiltration problems, the ANZECC guidelines recommend an assessment using the specific conductance (in logarithmic form) and SAR of irrigation waters (ANZECC and ARMCANZ, 2000). The FAO guidelines recommend a similar procedure, but with specific conductance in linear form while applying a calcium carbonate precipitation correction to the calculated SAR values. These guidelines assume well-drained loams (sand loams to clay loams) in semi-arid or arid climates, so they have to be used carefully in humid climates. Nevertheless, it is still possible to use them in humid climates in conjunction with other analyses (like the calculation of leaching fractions and IPP index). A plot showing the SAR values vs. the logarithm of the specific conductance (EC) for Maramarua CSG water, according to the ANZECC guidelines, is presented in Figure 4.11 (a similar graph showing the same results but using the FAO guidelines is presented in Figure C.4, Appendix C). In addition to presenting pure CSG water, different combinations resulting from blending CSG water with rain water and wetland water (adjacent Kopuku swamp) are shown in the same figure. Rain water is assumed to have a specific conductance value of 0.03 dS/m, whereas wetland water is assumed to have a specific conductance value of 0.273 dS/m (measured on site). Both blending waters are assumed to have nil sodium concentrations, and results from these blendings have not been corrected for calcium carbonate precipitation, so actual SAR values could be higher than the ones shown in the graph.

Figure 4.11 shows that irrigation with pure CSG water will produce soil infiltration problems (loss of water and air permeability), and no blending combination will be able to correct this problem. Even blendings with higher rain-water or wetland-water volumes will produce a water quality within the hazardous zone; blending with 90% wetland water almost reduces the problem to acceptable levels, but this water blending is highly inefficient as a method of CSG water disposal (only 10% reduction).

Soils in Maramarua could experience soil infiltration problems if exposed to CSG water. An initial look at the distribution of the IPP index in the area (Figure 4.10) shows that there are some soils in the vicinity of C-1 with a high potential for infiltration reduction if exposed to high-SAR water. This was verified by calculating the leaching fraction and soil salinity resulting from Maramarua CSG water disposal on these soils over a prolongued period of time (5-10 years according to USSL, 1954). Results indicated a significant reduction in leaching fraction, which would result in an important loss in soil permeability. This is verified by the SAR/Salinity diagram in Figure 4.11, which indicates that soils' structural problems are likely to occur if CSG water is disposed on these soils.

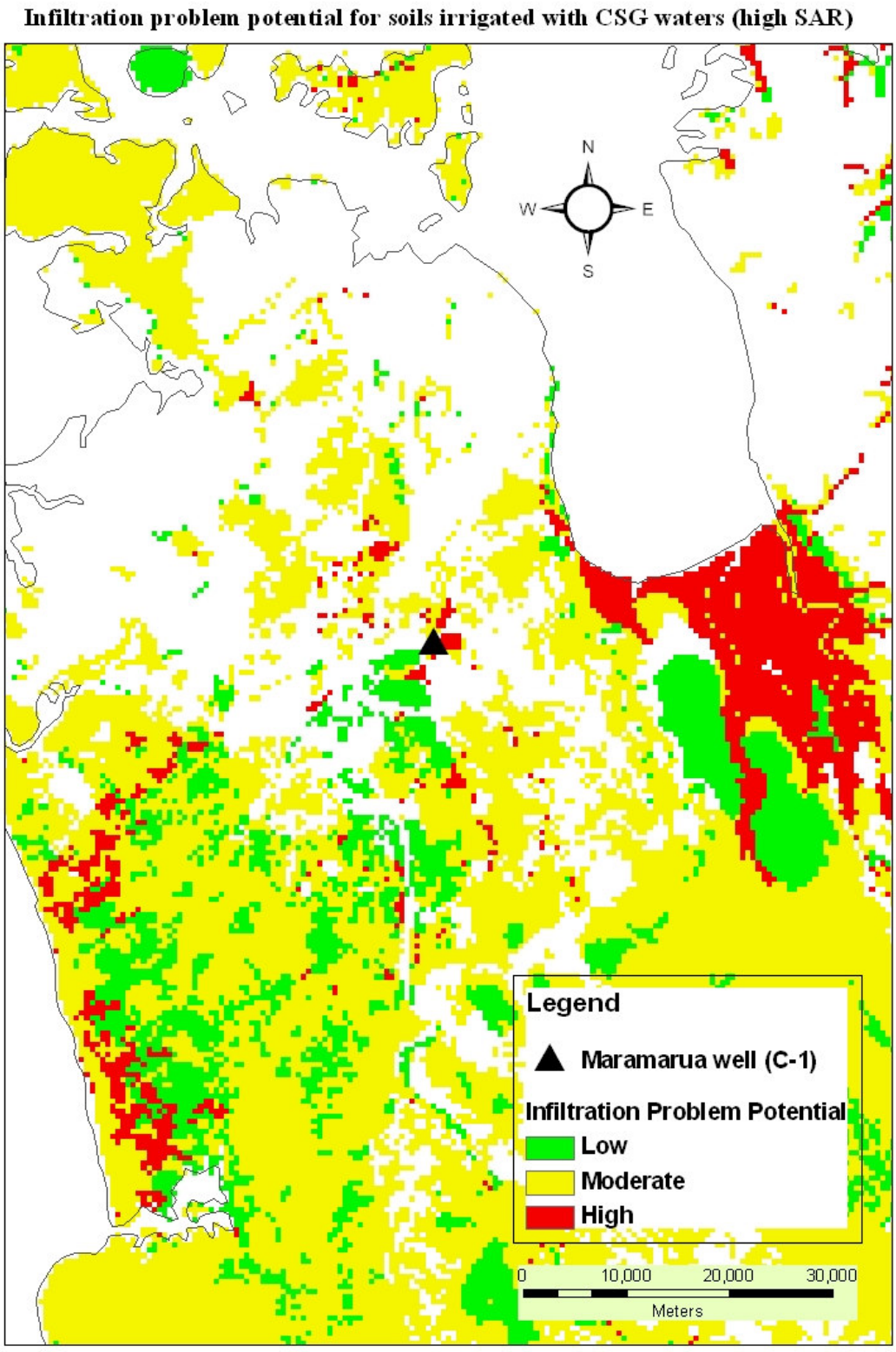

Figure 4.10. Infiltration problem potential at Maramarua due to high-SAR water discharges

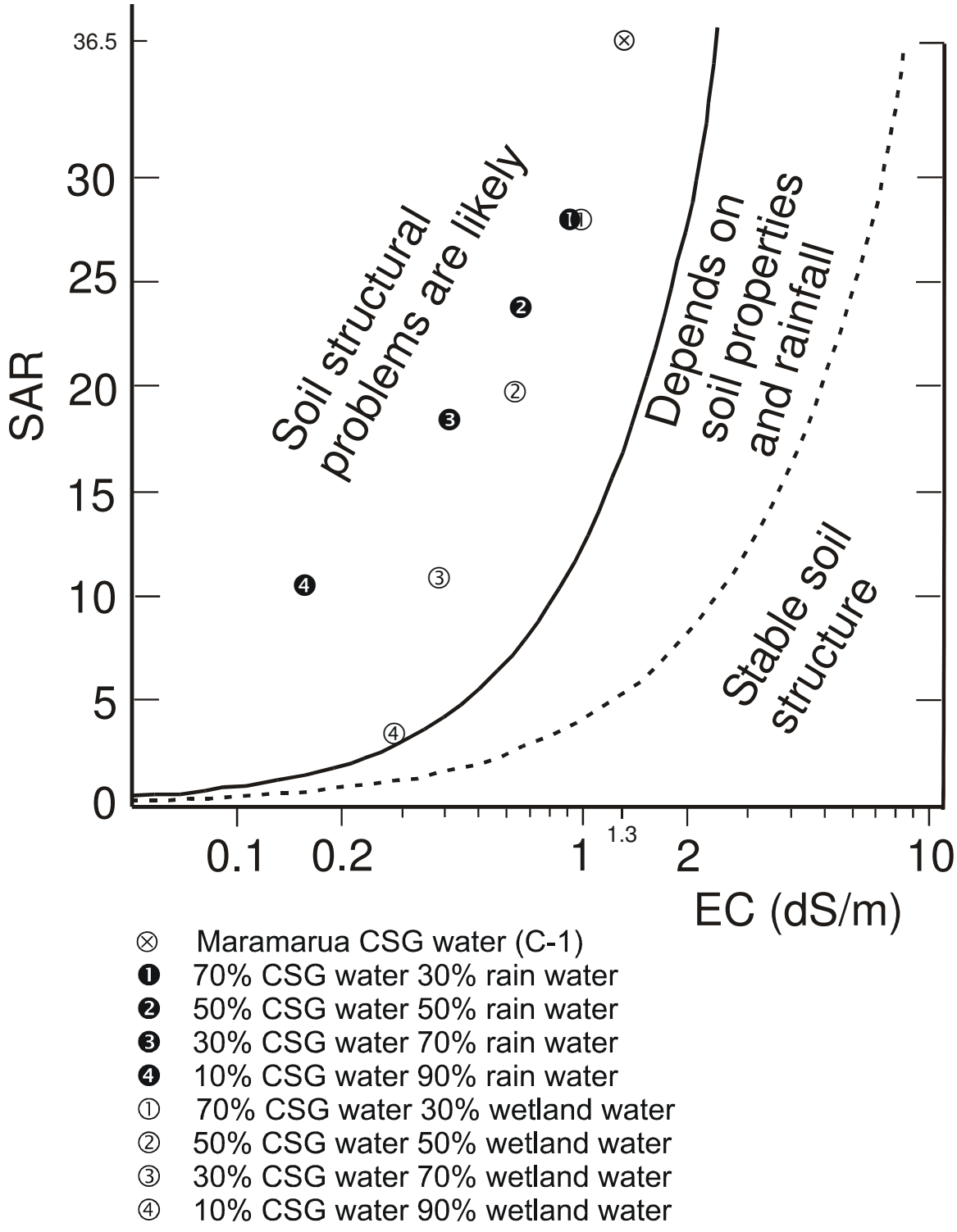

Figure 4.11. Assessment of soil degradation using SAR and EC of irrigation water. Adapted from ANZECC (2000).

Assessment of specific ion toxicity

When applying the FAO toxicity guidelines presented in Table 4.1, the effects of irrigating with Maramarua CSG water range from “slight” to “severe”. For example, the SAR of CSG water from C-1 is 36.5, and the lower limit for the “severe” restriction category (to assess sodium toxicity) in the FAO guidelines is 9. Similarly, chloride and boron concentrations produce effects which range from “slight” to “moderate”.

The ANZECC guidelines provide a description of the crops that can be grown under specific ion concentrations. Under these guidelines, the use of Maramarua CSG water for irrigation does not generate any restrictions in relation to chloride, but its sodium concentrations may pose a problem for “sensitive”, “moderately sensitive”, and some “moderately tolerant” crops (Table 4.3). In addition, the high-SAR of this CSG water (36.5) can generate leaf scorch and leaf tip burn in crops like avocado, deciduous fruits, nuts, and citrus, and it can have a stunted growth effect in beans. These effects along with sodium toxicity and possible calcium or magnesium deficiency may also extend to crops like clover, oats, tall fescue, rice, and dallis grass (ANZECC and ARMCANZ, 2000). Boron concentrations may also pose a problem when irrigating with CSG water from Maramarua. In this case, short-term effects could be noticed in very sensitive crops (blackberry and lemon), sensitive crops (onion, garlic, sweet potato, wheat, and barley), moderately sensitive crops, (pea, carrot, and potato), and in some moderately tolerant crops (lettuce, clover, oat, and corn) (Ayers et al., 1985, as cited in ANZECC and ARMCANZ 2000).

Table 4.3. Crop tolerance to sodium and chloride toxicity associated with Maramarua CSG water

Ion	CSG Water mg/l	Sensitive	Moderately sensitive	Moderately tolerant	Tolerant
Chloride	146	OK	OK	OK	OK
Sodium	334	Not OK	Not OK	May be OK	OK

Notes:

CSG water from Maramarua C-1 (19/8/2004 sample, see Chapter 2)

Sensitive crops: almond, apricot, citrus, plum, grape
Moderately sensitive: pepper, potato, tomato
Moderately tolerant: barley, maize, cucumber, lucerne, safflower, sesame, sorghum
Tolerant: cauliflower, cotton, sugar beet, sunflower

Blending CSG water with rain water or surface water could lower the concentration of specific ions like sodium or boron so that guidelines limits are met. However, the water used for blending needs to have a significantly lower concentration value for the specific ion under consideration. For example, a blending of 50% CSG water and 50% rain water would generate a final sodium concentration of 168 mg/l which would enable irrigation on “moderately tolerant crops” and on some “moderately sensitive crops”. Using more rain water (70%) and less CSG water (30%) would yield a final concentration of 101mg/l which would clear any sodium toxicity problems (even in sensitive crops), however this method does not allow the disposal of large amounts of CSG water. In addition, blending would require large ponds and mixing equipment, which would increase costs and project footprint.

Effects arising from surface water disposal of CSG waters

The Maramarua basin under exploration is administered by Environment Waikato. This council has a regional policy statement which will be implemented by a proposed regional plan. At the time of the writing of this thesis, the Waikato Regional Plan was being revised by the Environment Court. However, it is foreseen that the final plan will not include major changes, so the policies and methods included in the Proposed Waikato Regional Plan (PWRP), can be used to assess the effects of disposing CSG waters on surface waters in the Maramarua area. In addition, the methodology outlined in the plan can be complemented by using the ANZECC water quality guidelines.

Because full-scale production is not yet underway in Maramarua, the total amount of water to be disposed of is unknown. This value will depend on the number of production wells and the rate at which these will be producing CSG water. For example, if 20 wells are drilled in this basin, and each well produces $40m^3$ of CSG water per day, then the total amount to be disposed of will be $800m^3$/day. This quantity of water would have an impact on low lying areas around the region. For example, the Whangamarino wetland has a "wet/dry" seasonal cycle (Department of Conservation, 2006b), and its water level rarely surpasses the 5 metre mark (Environment Waikato, 2006).

Under the discharge-to-water scenario, analytes of concern would have to be monitored only after reasonable mixing of CSG water with the receiving surface water body (Environment Waikato, 2002). Different standards would apply depending on the use of the water body, and monitoring would have to be enforced. For example, specific ions or properties to monitor would be changes in pH, dissolved oxygen, and temperature.

The ANZECC guidelines recommend a trigger value of 7.8 for pH values in lowland river areas. The nearest stream to C-1 is Kopuku stream, which flows through Kopuku Wetland. Since this stream is located in a lowland area, the 7.8 pH trigger value would apply. Maramarua CSG water has an initial pH of 7.4 once pumped to the surface; however, as this water reaches equilibrium with the atmosphere, its pH can rise up to 8.6 (see chapter 2), therefore monitoring of pH values after mixing would have to be carried out. Dissolved oxygen readings were carried out on-site with a meter in September 2004. The minimum DO saturation (%) reading detected at the wellhead was 22.5%, but this

value is significantly higher than the one for Kopuku Wetland (3.9%). In addition, the temperature at the wellhead was 18.3°C which is 5.6°C higher than the temperature measured on that same day for the wetland (12.7°C). The PWRP states that, as a result of permitted activities, the water temperature of the receiving body must not change in more than 3°C, so temperature would also have to be monitored. Since the PWRP states that permitted discharges into surface water bodies must not make the surface water unsuitable for irrigation, specific ions and properties like sodium, chloride, boron, and salinity would also have to be monitored.

It is unlikely that a resource consent to discharge Maramarua CSG water into the Kopuku and Whangamarino wetlands would be granted because the Whangamarino wetland is listed under the 1996 Waikato Conservancy Conservation Management Strategy as an area requiring protection (Environment Waikato, 2002). The Kopuku Wetland and stream are connected to Whangamarino wetland, and any discharge would affect the latter. However, it is important to study the effects of potential CSG water discharge into the Kopuku Wetland because, if land disposal is implemented, CSG water disposed on the land could find its way to this wetland (or Whangamarino) in the form of surface runoff or subsurface flow.

Potential effects on aquatic life

The freshwater fish database (managed by NIWA) has data on the different species of fish in the Kopuku area between 1983 and 1988. The species of native fish recorded were Black mudfish (*Neochanna diversus*), Koaroa (*Galaxias brevipinnis*), Longfin eel (*Anguilla dieffenbachii*), Crans bully (*Gobiomorphus basalis*), Common bully (*Gobiomorphus cotidianus*), Shortfin eel (*Anguilla australis*), and Banded kokopu (*Galaxias fasciatus*); while the exotic fish registered at the site were Goldfish (*Carassius Auratus*), Catfish (*Ameiurus nebulosus*), and Gambusia (*Gambusia affinis*) (NIWA, 2006b).

From the list, two native species of interest are Banded kokopu and Shortfin eels because, as previously mentioned, these species are noted for preferring less-than-neutral pH values; since the pH measured at Kopuku is 6.59, these fishes can live in this environment. However, if Kopuku Wetland starts receiving CSG water, its pH could

increase above neutral levels. As a result, Shortfin eels and Banded kokopu could end up abandoning these wetland areas to live in environments with lower pH values.

Gambusia is an introduced species in New Zealand and is considered undesirable for their extremely aggressive nature and propensity to attack native fish (NIWA, 2006b). In particular, Gambusia are known to attack young Black mudfish, which is listed as "indeterminate" in the threatened species list (LFTB Study Group., 1986). However Black mudfish are able to co-exist with Gambusia because of their ability to survive in environments that dry up periodically, whereas Gambusia do not (NIWA, 2006b). This is significant in the Whangamarino wetland, as this area has a hydrological regime exhibiting a "wet/dry" seasonal cycle (Department of Conservation, 2006b). CSG water discharges could alter this equilibrium by supplying extra quantities of water to zones that normally would dry up. This could put Black mudfish at the mercy of Gambusia, and their numbers could decrease.

Increasing salinity, as a result of CSG water discharges, could also endanger some species. Most of the native species listed are diadromous and would be able to survive in saline environments. However, Crans bullies do not have a marine phase and are non-diadromous (NIWA, 2006b); their ability to survive in a wetland receiving CSG water discharge would be limited.

Potential effects on vegetation

The vegetation found near C-1 corresponds to the vegetation of Kopuku and Whangamarino wetlands. These consists of sedges (Baumea), Manuka (*Leptospermum scoparium*), and Wire rush (*Empodisma minus*). In addition, various threatened plants have been registered in the wetland including Club moss (*Lycopodium serpentinum*), Orchid (*Corybas carseii*), and Water milfoil (*Myriophyllum robustum*) (Department of Conservation, 2006b). In addition, marginal vegetation like Carex secta, Coprosma tenuicaulis, Juncus, Flax, and Cabbage trees along with Kahikatea (*Podocarpus dacrydiodes*) and Climbing fuchsia (*Fuchsia perscandens*) can be found at the northern end of Kopuku Wetland (LFTB Study Group., 1986). Also, most of the Whangamarino wetland is covered with introduced willows (*Salix cinerea and S. fragilia*).

CSG water discharges into these wetland areas could generate negative impacts on native vegetation from increased water levels and salinity. For example, studies carried out by Eser (2000) suggested that increasing Lake Taupo's water levels would most likely decrease native plant communities, while promoting the spread of Salix cinerea in the Stump Bay wetland (adjacent to Lake Taupo). The same effect could take place in the Whangamarino and Kopuku wetlands if CSG water discharges produce a significant increase in water levels. In addition, the salinity of CSG waters could alter the salinity of the receiving wetlands negatively affecting plant communities. Sedges, for example, have very low tolerance to salinity (<0.5 ppt) (Knight, 1997) so their ability to grow would become impaired as salinity increases due to CSG discharges (C-1 salinity = 0.65 ppt).

These effects are unlikely to be detected at once, however as more wells are completed and these wetlands receive CSG water, effects would start to take place depending on the quantity and quality of the water being discharged. In particular, effects would be most noticeable at margins and in zones experiencing natural dry periods. Once more information becomes available, it will be important to carry out mixing and dilution studies to determine the extent of these effects.

Conclusions

The effects arising from CSG water disposal are tangible, and can be identified according to the selected method of disposal. If CSG waters are disposed on land, this could result in increased soil salinity, degradation of soil structure, and plant toxicity effects. On the other hand, if CSG waters are disposed on surface waters, the potential effects include the loss of riparian vegetation and fish communities. Sometimes, this loss can have significant implications on biodiversity as resilient species flourish while more sensitive species disappear. Also, the extent of these effects depends on the specific conditions at each basin where CSG water is being disposed.

The effects of CSG water disposal clearly depend on the ultimate fate of CSG water. Some methods of disposal could produce significant effects (surface water disposal to small streams or wetlands for example), while others would generate negligible effects (i.e. aquifer injection). However, if there are links between receiving environments the problem becomes complicated. For example, if CSG waters are disposed on a river, its aquatic fish and plant communities become affected, but if water is abstracted for irrigation downstream from the discharge point, the effects could extend to crops on the receiving soils.

When CSG waters are disposed on land, its dissolved ions (mainly sodium, bicarbonate, and chloride) become part of the soil-water solution and tend to remain within the soil structure. Soil salinity will promote permeability by keeping particles flocculated, and this has been observed by Oster and Schroer (1979) and US Salinity Laboratory Staff (1954) among others. Although increased soil salinity does not damage soils, it has negative effects on plants as these need to exert an extra effort in extracting water from the soil-water solution. During rainfall events most of these ions are leached from the soil thus reducing soil salinity levels. However, sodium cannot be removed by this method because this ion remains adsorbed to the soil clay particles. In this chapter, the same effects were noted when analysing data from Maramarua. In this case, CSG water discharges would cause an increase in ESP values, which in turn would increase soil salinity values. Long term salinity effects for this location would impair these soils for the cultivation of sensitive crops and moderately sensitive crops. Likewise, the FAO

water quality irrigation guidelines recommend care when irrigating with water quality like the one for Maramarua CSG water.

The more clay particles a soil has, the more sodium will remain adsorbed to its clay component. Once a soil starts to accumulate sodium, it becomes prone to dispersion. That is, its clay particles will become attracted to each other (due to the sodium ion) and will become rearranged. This will cause loss of aggregation which results in overall loss of permeability. This problem has been observed with high-SAR irrigation water by US Salinity Laboratory Staff (1954), Ayers and Westcot (1985), and Oster and Schroer (1979). Most recently Robinson (2003) verified these effects experimentally using CSG water and soils from the PRB. Maramarua CSG water could generate the same infiltration problems with soils from the area. Various CSG water and freshwater blendings would generate water solutions having SAR/salinity combinations which could produce soil infiltration problems in the long-run. These problems are mainly due to the high-SAR content of CSG waters from Maramarua, and the moderate clay content in some of the soils in the area.

The SAR component of CSG waters can easily be underestimated. This is because CSG waters have a high bicarbonate content and are generated in underground environments exposed to high hydrostatic pressures. However, once these waters are pumped to the surface they become exposed to normal atmospheric pressure, and calcium is precipitated in the form of calcium carbonate. This effect was measured experimentally in Chapter 3, and it was responsible for a 23% increase of the original SAR values. In this chapter, this effect was taken into account by correcting CSG water quality from Maramarua (19/8/2004) using the procedure described by Suarez (1981). As a result, SAR values increased from 33.6 to 36.5 (8.6%). Therefore, SAR values from CSG water samples need to be adjusted to account for calcium carbonate precipitation. The procedure proposed by Suarez (1981) is an effective approximation, but an exact value can be calculated if sparging experiments (like the one carried out in Chapter 3) are carried out.

Other effects associated with CSG water discharge, which have been noted in the Maramarua case study include specific toxicity issues related to some of its ions. In particular, sodium and boron toxicity problems could become a problem in sensitive

crops. The effects of sodium could extend even to moderately tolerant crops, but its effects could be mitigated if CSG waters are blended with waters having low sodium concentrations. In addition, chloride concentrations could pose “slight” to “moderate” effects depending on the type of crop being grown.

Effects of CSG water discharges into surface waters are more difficult to quantify because these depend on the nature of plant and fish communities present in the receiving bodies. In the US, effects have been noted in riparian vegetation of the PRB and some fish communities in the Black Warrior Basin. In Maramarua, the effects have not been noticed at this stage because full-scale water production has not yet begun. However, native fish species like Banded kokopu and Shortfin eels could become affected by an increase in pH due to CSG water discharges. In addition, other native fishes could end up being displaced by introduced species (like Gambusia) if CSG waters improve the habitats of the introduced species. However, most native New Zealand fishes spend some time living in the sea, so they would have some ability to adapt to increased salinity and pH arising from CSG water discharges. Riparian plant communities would be affected in a similar way as the vegetation growing on soils exposed to CSG water discharges. These plants would mainly be exposed to high ion toxicity resulting from sodium, chloride, and boron. In this way, sensitive species could disappear while more resilient species could invade areas formerly inhabited by these sensitive species. For example, in the Kopuku and Whangamarino wetlands the noxious Salix cinerea could end up spreading as a result of CSG discharges, while more sensitive native species like Sedges could end up disappearing.

In this chapter, the effects associated with CSG water discharges have been studied using background literature studies supported by a case study of the Maramarua area. This case study has provided an assessment based on the ANZECC water quality guidelines (2000). Throughout this chapter, a new methodology for assessing potential environmental effects associated with CSG water management has been developed using pre-existing concepts and environmental guidelines. This includes assessment of CSG water quality, soils, surface waters, plant and aquatic life in relation to disposal operations. Much of the analysis in this chapter is based on conjecture because of the current lack of data; still, it is hoped that this work will help future investigators by

identifiying key issues and appropriate approaches to environmental impact assessment. Similar studies to this one could be carried out for other CSG sites around New Zealand once CSG water quality data for these sites becomes available. While some regions (i.e. Ashers-Waituna) are located in areas of low risk, other regions like Hawkdun would be prone to problems arising from CSG water disposal. For purposes of issuing resource consents, similar analyses like the one performed on Maramarua could be carried out on each site where CSG development will take place.

References

ALL-Consulting, 2003, Handbook on Coal Bed Methane Produced Water: Management and Beneficial Use Alternatives.: Tulsa, Oklahoma, Ground Water Protection Research Foundation, US Department of Energy, National Petroleum Technology Office, Bureau of Land Management.

ALL-Consulting, and Montana Board of Oil and Gas Conservation, 2004, Coal Bed Methane primer. New Source of Natural Gas–Environmental Implications. Background and Development in the Rocky Mountain West: Tulsa, Oklahoma, US Department of Energy, National Petroleum Technology Office.

Allen, R.B., McIntosh, P.D., and Wilson, J.B., 1998, The distribution of plants in relation to pH and salinity on inland saline/alkaline soils in Central Otago, New Zealand. (vol 35, pg 517, 1997): New Zealand Journal of Botany, v. 36, p. 153-153.

ANZECC, and ARMCANZ, 2000, Australian and New Zealand Guidelines for Fresh and Marine Water Quality, ACT: Australian and New Zealand Environmental and Conservation Council (ANZECC), Agricultural and Resource Management Council of Australia and New Zealand (ARMCANZ): Canberra.

Ayers, R.S., Westcot, D.W., and Food and Agriculture Organization of the United Nations., 1985, Water quality for agriculture: Rome, Food and Agriculture Organization of the United Nations, xii, 174 p.

Bauder, J., 2001, Quality and Characteristics of Saline and Sodic Water Affect Irrigation Suitability: MSU, Bozeman, MT, p. http://waterquality.montana.edu.

Bodger, F., 2005, The use of coal seam gas waters in New Zealand to treat acid mine drainage, Civil Engineering: Christchurch, University of Canterbury, p. 44.

Bresler, E., McLean, B.L., and Carter, D.L., 1982, Saline and sodic soils: Principles-dynamics-modeling., Advanced series in agricultural sciences., Volume 10: New York, NY, Springer-Verlag.

Burkett, W.C., McDaniel, R., and Hall, W.L., 1991, The Evaluation and Implementation of a Comprehensive Production Water Management Plan, Coalbed Methane Symposium: Tuscaloosa, Alabama.

Cameron, K.C., Di, H.J., Anwar, M.R., Russell, J.M., and Barnett, J.W., 2003, The "critical" ESP value: does it change with land application of dairy factory effluent?: New Zealand Journal of Agricultural Research, v. 46, p. 147-154.

Cavanagh, J., and Coakley, J., 2005, An introduction to policy on metal contaminants, *in* Moore, T.A., Black, A., Centeno, J.A., Harding, J.S., and Trumm, D.A., eds., Metal Contaminants in New Zealand, Volume In Press, Corrected Proof: Christchurch, resolutionz press, p. 5-23.

Collier, K.J., Ball, O.J., Graesser, A.K., Main, M.R., and Winterbourn, M.J., 1990, Do organic and anthropogenic acidity have similar effects on aquatic fauna?: Oikos, v. 59, p. 33-38.

Davis, H.A., Simpson, T.E., Lawrence, A.W., Miller, J.A., and Anonymous, 1993, Coalbed methane produced water management strategies in the Black Warrior Basin of Alabama: Proceedings - International Coalbed Methane Symposium, v. 1993, p. 317-338.

Davis, W.N., Bramblett, R.G., and Zale, A.V., 2006a, Effects of coalbed natural gas activities on fish assemblages in the Powder River Basin, 2005, *in* Montana Cooperative Fishery Research Unit, ed.: Bozeman, Montana State University, p. 3.

—, 2006b, The effects of coalbed natural gas activities on fish assemblages: a review of the literature: Bozeman, Montana State University, p. 48.

Department of Conservation, 2006a, New Zealand map service, DOCgis GeoSpatial Information Platform, p. http://extranet.doc.govt.nz/bip/.

—, 2006b, New Zealand's Wetlands of International Significance: Whangamarino, http://www.doc.govt.nz/Conservation/Wetlands/.

Detmer, E., 2005, Zeolite water conditioning system: Sheridan, p. Personal conversation.

Environment Waikato, 2002, Waikato Regional Plan - Proposed plan and maps on CD-ROM as amended by decisions (appeals version), *in* Waikato Regional Council, ed.: Hamilton, Waikato Regional Council,.

—, 2006, River Levels and Rainfall. Whangamarino Wetland. Levels at Ropeway on Island Block Road, Meremere, Volume 2006: Hamilton, Environment Waikato, p. web page and online database system.

Eser, P., and Rosen, M.R., 2000, Effects of artificially controlling levels of Lake Taupo, North Island, New Zealand, on the Stump Bay wetland: New Zealand Journal of Marine and Freshwater Research, v. 34, p. 217-230.

Jensen, M.E., 1983, Design and operation of farm irrigation systems: St. Joseph, Mich., American Society of Agricultural Engineers, xi, 829 p. p.

Kirkpatrick, A.D., 2005, Assessing constructed wetlands for beneficial use of saline-sodic water: Bozeman, Montana State University,.

Knight, R.L., 1997, Wildlife habitat and public use benefits of treatment wetlands: Water Science and Technology, v. 35, p. 35-43.

Kristin, K., Bauder, J., and Wheaton, J.R., 2006, http://waterquality.montana.edu/docs/methane/cbmfaq.shtml, Water quality and Irrigation Management, Volume 2006: Bozeman, Montana State University.

Landcare Research New Zealand Ltd, 2000a, New Zealand Land Resource Inventory (NZLRI): Lincoln, Landcare Research New Zealand Ltd.

—, 2000b, The New Zealand National Soils Database Spatial Extension, Soil Fundamental Data Layers: Lincoln, Landcare Research New Zealand Ltd.

Lee-Ryan, P.B., Fillo, J.P., Tallon, J.T., and Evans, J.M., 1991, Evaluation of management options for coalbed methane produced water, Coalbed methane symposium: Tuscaloosa, Alabama, The University of Alabama,, p. 31-41.

LFTB Study Group., 1986, South Island Phase II Lignite Site Selection Studies Programme. Resource definition, geotechnical, hydrology, and mine planning studies. Hawkdun deposit.: Wellington, N.Z., Liquid Fuels Trust Board.

Main, M.R., 1988, Factors influencing the distribution of kokopu and koaro (Pisces: Galaxiidae) : a thesis submitted in partial fulfilment of the requirements for the degree of Master of Science in Zoology in the University of Canterbury, 127 leaves, [36] leaves of plates p.

McBeth, I., Reddy, K.J., and Skinner, Q.D., 2003, Chemistry of trace elements in coalbed methane product water: Water Research, v. 37, p. 884-890.

McIntosh, A., and McDowall, R., 2004, Fish Communities in rivers and streams, *in* Harding, J.S., New Zealand Hydrological Society., and New Zealand Limnological Society., eds., Freshwaters of New Zealand: [Wellington, N.Z.],

New Zealand Hydrological Society ; New Zealand Limnological Society, p. 17.1-17.9.

McLaren, R.G., and Cameron, K.C., 1990, Soil science : an introduction to the properties and management of New Zealand soils: Auckland, N.Z., Oxford University Press, viii, 294 , 8 of plates p.

Menneer, J.C., McLay, C.D.A., and Lee, R., 2001, Effects of sodium-contaminated wastewater on soil permeability of two New Zealand soils: Australian Journal of Soil Research, v. 39, p. 877-891.

Montana State University, 2006a, Coal Bed Methane Water Treatment System, http://waterquality.montana.edu/docs/methane/cbm-wts.shtml, Montana State University., p. Drake Engineering Inc. Water Treatment System.

—, 2006b, Frequently Asked Questions Coal Bed Methane (CBM), Volume 2006: Bozeman, Montana State University, p. Web page http://waterquality.montana.edu/docs/methane/cbmfaq.shtml.

New Zealand. Mines Division., Longworth McKenzie Cole., and Worley Consultants Ltd., 1983, New Zealand coal resources survey : preliminary mining and environmental constraints assessment pilot study : Maramarua coalfield: [Wellington, N.Z.], Mines Division Ministry of Energy, 2 v. p.

NIWA, 2006a, NIWA Atlas of New Zealand Freshwater Fishes, Common smelt (Retropinna retropinna), http://www.niwascience.co.nz/rc/freshwater/fishatlas/species/common_smelt, Volume 2006, NIWA.

—, 2006b, NZFFD, New Zealand Freshwater Fish Database, NIWA, p. http://www.niwascience.co.nz/services/nzffd/.

O'Neil, P.E., Harris, S.C., and Mettee, M.F., 1989, Stream Monitoring of Coalbed Methane Produced Water from the Cedar Cove Degasification Field, Alabama, The 1989 Coalbed Methane Symposium: Tuscaloosa, Alabama, The University of Alabama,.

Oster, J.D., and Schroer, F.W., 1979, Infiltration as Influenced by Irrigation Water-Quality: Soil Science Society of America Journal, v. 43, p. 444-447.

Pope, S., and Trumm, D., 2004, Coal Seam Gas Desorption Results: Drill Holes C1, K1 and K3, Maramarua Coalfield, Waikato, 2003.: Christchurch, CRL Energy Ltd, p. 27.

Rice, D.D., 1993, Composition and origin of coalbed gas, *in* Law, B.E., and Rice, D.D., eds., Hydrocarbons from coal, Volume AAPG Studies in Geology, American Association of Petroleum Geologists, p. 159-184.

Robinson, K.M., 2003, Effects of saline-sodic water on EC, SAR, and water retention: Bozeman, Montana State University.

Scarsbrook, M.R., and National Institute of Water and Atmospheric Research (N.Z.), 2003, A guide to the groundwater invertebrates of New Zealand: Wellington [N.Z.], Niwa, 59 p.

Settle, T., Mollock, G.N., Hinchman, R.R., and Negri, M.C., 1998, Engineering the use of green plants to reduce produced water disposal volume., Society of Petroleum Engineers: Inc. Devon Energy Corporation, Oklahoma City, OK. Argonne National Laboratory, Argonne IL.

Shainberg, I., and Letey, J., 1984, Response of Soils to Sodic and Saline Conditions: Hilgardia, v. 52, p. 1-57.

Suarez, D.L., 1981, Relationship between pHc and sodium adsorption ratio (SAR) and an alternative method of estimating SAR of soil or drainage waters: Soil Science Society of America Journal, v. 45, p. 469-475.

Taulis, M., Milke, M., Trumm, D., O'Sullivan, A., Nobes, D., and Manhire, D., 2005, Characterisation of Coal Seam Gas waters in New Zealand, 2005 New Zealand Minerals Conference: Auckland, New Zealand.

US Salinity Laboratory Staff, 1954, Diagnosis and improvement of saline and alkali soils: [Washington,, US Govt. Print. Off.], vii, 160 p. p.

Van Voast, W.A., 2003, Geochemical signature of formation waters associated with coalbed methane: Aapg Bulletin, v. 87, p. 667-676.

West, D.W., Boubée, J.A.T., and Barrier, R.F.G., 1997, Responses to pH of nine fishes and one shrimp native to New Zealand freshwaters: New Zealand Journal of Marine and Freshwater Research, v. 31, p. 461-468.

Wheaton, J.R., and Donato, T.A., 2004, COALBED-METHANE BASICS: Powder River Basin, Montana: Butte, Montana Bureau of Mines and Geology, p. 20.

Chapter 5

Sodium removal from Maramarua coal seam gas waters using Ngakuru zeolites

Introduction

Zeolites are minerals having a porous structure, crystalline characteristics, and an alumino-silicate configuration resulting in an overall negative charge which is balanced by loosely held cations like Na^+, K^+, Ca^{2+}, and Mg^{2+} (Christie et al., 2002). This makes zeolites excellent materials to be used in cation exchange applications. In addition, zeolites can also function as ionic sieves capable of absorbing certain ions and not others, depending on the size of the cavities forming the porous structure and on the size of the ions entering the zeolite structure (Coombs, 1959). Other properties of importance include a high degree of hydration/dehydration, low density, good crystal stability when dehydrated, and their ability to adsorb ions in gaseous form (Christie et al., 2002). Common zeolite applications include their use as pet litter, oil/chemical and odour absorbents, wastewater treatment, and their use as slow release fertilisers (NZ Natural Zeolite, 2006).

Zeolites in New Zealand occur mainly in the Taupo Volcanic Zone, Northland , Auckland, and Southland (Christie et al., 2002). Ngakuru zeolites are located in the Taupo Volcanic Zone about 20 km south of Rotorua. These zeolites are hydrothermally altered and occur in lake sediment beds of Quaternary age up to 45 m deep (Mowatt, 2000). The main type of zeolites in Ngakuru is mordenite (40-80%) followed by clinoptilolite (20-60%), and cristobalite (0-10%) (Mowatt, 2000). Bolan and Mowatt (2000) have successfully used these zeolites in trials to remove ammonium cations in wastewaters from tannery operations. In these experiments, wastewaters with ammonium concentrations of 300 mg/l and 720 mg/l, were passed through columns containing 100 g of zeolites at a flow rate ranging from 2.5 to 4.5 ml/min/kg zeolite. The zeolites were capable of removing up to 77% of the ammonium cations in the wastewater. Previous

New Zealand studies by Nguyen and Tanner (1998) also focused on removing ammonium cations but this time from dairy farm effluent and piggeries, and by using clinoptilolite and mordenite obtained from different sites. Their studies concluded that the ammonium removal capacity of these zeolites decreased when sodium ions were present in the waste stream. This generated ammonium removal capacities of up to 15 % with the mordenite, and 30% with the clinoptilolite.

Coal seam gas (CSG) waters are a new type of wastewater which could become fairly common on the New Zealand landscape and waterways. These groundwaters are a by-product of natural gas extraction from underground coal seams. Their production rate sometimes can be as high as $40m^3$/day per well with as many as 13000 wells in areas like the Powder River Basin, in the United States (Nelson, 2005). CSG waters tend to exhibit similar quality in terms of salinity and major ion composition. Their specific conductance varies depending on their travel time within the coal aquifer which accounts for different degrees of mineralization, and their major ions are sodium, bicarbonate, and sometimes chloride. Overall, these waters tend to be fairly alkaline with low calcium, magnesium, and sulphate concentrations (Van Voast, 2003). The main issue with these waters is their elevated sodium content, which in conjunction with their low calcium and magnesium concentrations, can generate soil infiltration problems in the long run, as well as short term toxicity effects in plants due to the sodium ion itself (see Chapter 4). Other toxicity effects can arise due to their chloride content and to small amounts of boron (if present).

Coal seam gas is still under exploration in New Zealand, but its development is imminent within the next few years. CSG water samples taken from CSG pilot scale operations have produced CSG waters with high sodium and low calcium and magnesium concentrations (Taulis et al., 2005), and their extraction rate has been as high as those rates experienced in US basins. In New Zealand, the disposal of CSG waters is regulated by Regional Councils, which promote land disposal of wastewaters over surface water disposal (ANZECC and ARMCANZ, 2000). However, the environmental effects due to CSG water disposal could extend to receiving environments both on the land and on surface waters. In some instances, CSG waters could damage valuable agricultural soils or riperian vegetation on protected ecosystems so restrictions on their disposal will be stringent. On the other hand, CSG water quality could be good enough to ensure little or

no environmental damage, or the receiving environment could have a good capacity for assimilating CSG water discharges. Therefore, treatment of CSG waters prior to disposal will need careful consideration in many NZ CSG locations. One way of reducing sodium concentrations of CSG waters might be by using New Zealand natural zeolites as exchange materials. Treating CSG waters in this way could not only make CSG waters comply with local regulations, but it could also *transform* CSG waters into a useable water resource. There is a direct economic benefit from using Ngakuru zeolites instead of commercial ion exchange resins. Ngakuru zeolites are easy to mine and readily available – their price ranges from about NZ $75/tonne to $350/tonne depending on their quality whereas the price of synthetic zeolites can be as high as NZ $ 69/kg (Christie et al., 2002). Hence, the objective of this research is to study the feasibility of New Zealand natural zeolites for CSG water treatment.

Materials and Methods

Materials

Ngakuru zeolite samples were obtained from NZ Natural Zeolite, a subsidiary of Resource Refineries Ltd. Samples were provided in three sets; all of these were from a quarry containing zeolites having a high cation exchange capacity (CEC) and good resistance to mechanical breakdown. An additional zeolite sample (marketed as kitty litter) with a lower CEC was obtained for comparison purposes when carrying out batch experiments. These samples were sieved and grouped into 0.15-0.3 mm, 0.3-0.6mm, and 0.6-1.180mm particle size ranges. The moisture content for these samples ranged between 3.4% and 4.5% with a specific density of about 1.5 g/cm^3. X-ray diffraction analyses were carried out on the high CEC samples at the Geological Sciences Department (University of Canterbury) using an X-ray diffractometer for mineral identification (see Appendix E). These analyses revealed that the main crystalline materials present in these zeolites were 70-75% mordenite ([Ca, Na_2, K_2] $Al_2Si_{10}O_{24}$ – $7H_2O$, hydrated calcium sodium potassium) and 25-30% sanidine ($KAlSi_3O_8$, Potassium Aluminum Silicate). Previous studies by Mowatt (2000) had revealed that their CEC ranged from 40 to 110 meq/100 g, while their surface area ranged from 34 to 138 m^2/g.

Synthetic solutions of NaCl, NaOH, HCl, $CaCl_2$, and KCl in various concentrations (ranging from 0.01M to 1 M) were prepared for batch testing and preliminary flow-through testing. These solutions were characterised by measuring their pH and specific conductance according to APHA (1999) methods. For the final flow-through study, actual Maramarua CSG water samples were used to assess the sodium removal capacity of Ngakuru zeolites. These samples had been collected between August and October, 2004, and April and June, 2005. The sample volumes remaining after carrying out chemical analyses, had been stored at a temperature below 4°C. The samples were combined and then filtered through a 1.2 µm glass filter, making up about 4.5 litres of CSG water. The chemical analyses results for this composite sample are presented in Table 5.1.

Table 5.1. Chemical analyses results for composite CSG samples

	Unit	Composite sample analysis 23/03/2006	CSG sample 19/08/2004
pH	pH units	8.57 (1)	7.8 (4)
Specific conductance	µS/cm	1264 (1)	1310 (2)
Total alkalinity	mg/l as $CaCO_3$	488 (2)	360 (4)
SAR		29.6	33.6
Bicarbonate	mg/l	564 (3)	435 (3)
Sodium	mg/l	304 (2)	334 (2)
Chloride	mg/l	147 (2)	146 (4)
Total Organic Carbon	mg/l	29.2 (2)	NA
DOC	mg/l	NA	11(2)
Carbonate	mg/l	14.8 (3)	<2 (3)
Dis. carbon dioxide	mg/l	5 (3)	25 (4)
Reactive silica	mg/l	10.4 (2)	10.7 (2)
Total calcium	mg/l	6 (2)	6 (2)
Total potassium	mg/l	4 (2)	3 (2)
Total magnesium	mg/l	1.2 (2)	0.9 (2)
Sulphate	mg/l	2.9 (2)	0.7 (4)
Total boron	mg/l	2.5 (2)	2.5 (2)
Fluoride	mg/l	1.10 (2)	0.79 (2)
Dissolved iron	mg/l	0.09 (2)	NA
Total iron	mg/l	<0.4 (2)	0.4 (2)
Dissolved manganese	mg/l	0.03 (2)	NA
Total manganese	mg/l	0.04 (2)	<0.01(2)
Total aluminium	mg/l	<0.06 (2)	NA
Total cobalt	mg/l	<0.004 (2)	NA
Total chromium	mg/l	<0.01 (2)	<0.01(2)
Total nitrogen	mg/l NH_4-N	0.07	NA
Total nickel	mg/l	<0.01 (2)	NA
Total zinc	mg/l	0.12 (2)	1.28 (2)

(1) Measured at the Environmental Engineering Laboratory, University of Canterbury
(2) Sample analysed through Hill Laboratories, Hamilton, New Zealand
(3) Calculated using from carbonate chemistry using alkalinity and pH values
(4) Sample analysed by CRL Energy Ltd Laboratory, Wellington, NZ
(5) NA = not available

Although some of these samples had been stored for as long as 19 months before mixing to produce the composite sample, the overall geochemical signature for the final sample still resembled the original CSG water. One of the original samples corresponding

to the one collected on the 19/08/2004 is presented along with the composite sample in Table 5.1. Differences between these two samples are attributed to variations in original sample concentrations, carbon dioxide degassing, and biodegradation of dissolved organic matter. For example, some of the original samples presented some variation in sodium concentrations: the maximum sodium concentration was 334 mg/l for the 19/08/2004, while the minimum was 289 mg/l for 02/04/2005 (see Chapter 3). As a result of mixing different volumes of water with varying concentrations, the final composite sample exhibited a sodium concentration of 304 mg/l. This value, along with calcium and magnesium concentrations, produced a SAR value of 29.6 which was not corrected to account for carbonate precipitation because this process would have taken place during mixing and throughout the long storage period. Evidence of this is the high pH value obtained after mixing the stored samples to form the composite sample (Table 5.1). The final composite sample had an alkalinity of 488 mg/l as $CaCO_3$, whereas the maximum recorded alkalinity in the original samples was 425 mg/l as $CaCO_3$ and the alkalinity for the 19/08/2004 sample was 360 mg/l as $CaCO_3$. This overall increase in alkalinity is possibly due to anaerobic degradation of dissolved organic carbon within the sample bottles. In any case, the major chemistry of the composite sample is similar to the one for the original CSG water samples, and this can be observed with the corresponding Schoeller diagrams (Figure 5.1) which are almost identical.

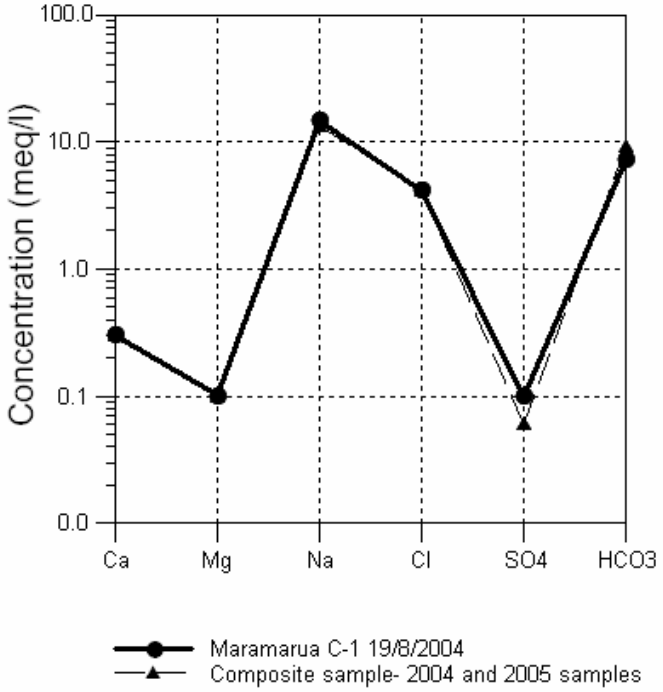

Figure 5.1. Schoeller diagrams for the 19/8/2004 sample and the composite sample (2004-2005) for Maramarua CSG water

Methods

The Ngakuru zeolites capacity to remove sodium ions in solution was assessed with a preliminary batch study, followed by flow-through tests using an ion exchange column.

Batch tests

Four types of batch tests were carried out as preliminary experiments to determine the feasibility of using Ngakuru zeolites for the removal of sodium cations from solution, and for initial sizing calculations. The following tests were carried out in four phases.

Phase I. The first batch tests focused on assessing the sodium removal capacity of Ngakuru zeolites while evaluating the effects of particle size using 1 M NaCl solutions. For this purpose, the first set of zeolites was rinsed with deionised water and then dried in an oven at 100ºC. Samples were then sieved through 150, 300, 600, 1180, and 2360 µm sieves, and about 1 gram of each of these was placed in conical flasks along with about 50 ml of 1 M NaCl solution. In addition, about 1 gram of pet litter zeolite (unwashed, air-

dried, unsieved) was placed in a conical flask with about 50ml of 1M NaCl. The flasks were then shut closed with a plastic stopper and placed in a flask shaker (Figure 5.2), which was activated for 1 hour 45 min (Batch test n°1) and 8 hours (Batch test n°2). Once the shaking had finished, the zeolite solution was filtered through a 1.2 µm glass filter and analysed for calcium, hardness, pH, and specific conductance according to APHA (1999) methods.

Figure 5.2. Flask shaker used in batch testing of Ngakuru zeolites and NaCl solutions

Phase II. A second type of batch-testing experiment was carried out to determine whether there was any dissolution taking place along with the sorption. This experiment consisted of washing a 1180µm-sized particles sample (from first set) with deionised water, and then drying it at a temperature of 100ºC. About 2 grams of this sample were placed in a conical flask along with about 100 ml of 0.005 M NaCl solution. In addition, a 1 gram sample was placed in a conical flask but this time containing about 50 ml of deionised water. Both flasks were closed with a plastic stopper and shaken for about 9.5 hours. Following the shaking, the zeolitic solution was filtered through 1.2 µm glass filters, and the final solutions were analysed for calcium, hardness, pH, and specific conductance according to APHA(1999) methods.

Phase III. Another type of batch testing experiment was carried out to determine the effect of different concentrations on zeolite ion exchange reactions. For this purpose, 600 µm zeolites (from first set) were washed with deionised water and dried in a convection

oven at around 100ºC. Four samples of about 2 grams each, were placed in conical flasks with about 120 ml of concentrated sodium solutions. The solutions used were 1 M, 0.1 M, and 0.01 M of NaCl plus a 0.01 M solution of NaOH. These flasks were shaken for approximately 4 hours and, subsequently, the zeolitic solution was filtered through 1.2 µm glass filters. The final solutions were analysed for calcium, hardness, pH, and specific conductance according to APHA(1999) methods, and also for sodium using a calibrated Cole-Parmer sodium ion electrode (see Appendix A.1 for a summary of these procedures and calibration method for the sodium ion electrode).

Phase IV. The objective of the last type of batch testing was to determine whether it was possible to regenerate Ngakuru zeolites after they had absorbed sodium cations. This also helped assess how rigid or prone to mechanical breakdown were the zeolites, and to determine a maximum sodium exchange capacity (useful for preliminary sizing calculations in the flow-through experiments). To do this, different service/regeneration cycles were carried out using concentrated sodium solutions for service, and various calcium, potassium, and acid solutions for regeneration. For example, the first of these experiments used 1180 µm zeolites which had been previously washed with deionised water and dried in a convection oven at approximately 100ºC. A 13.4 gram sample was placed in a conical flask along with 220 ml of a 0.01M NaOH solution, and it was then shaken continuously for 5 hours. After this period of time, the sample was filtered using a 1.2 µm glass filter, and the final solution was analysed for calcium, hardness, pH, and specific conductance according to APHA(1999) methods. In addition, sodium concentration was determined using a calibrated Cole-Parmer sodium ion electrode. The zeolite sample remaining after filtering was then washed with deionised water, dried in a 100ºC convection oven, and sieved through a 1180 µm sieve. The zeolitic material was then weighed and placed in a conical flask along with 150ml of 0.1 M HCl solution. Subsequently, the conical flask was shaken for approximately 5 hours, and at the end of this period, the sample was filtered using a 1.2 µm glass filter. The final solution was analysed for calcium, hardness, pH, specific conductance, and sodium. This cycle was repeated five times with different dissolved salts of varying concentrations, while analysing the final solutions resulting from each shaking period. In addition, some of

these samples were analysed for potassium at the Department of Chemistry (University of Canterbury) using atomic absorbtion and in accordance to APHA(1999) methods; two of the samples were analysed for chloride and sulphate using HACH methods 8225 and 8051 (Hach Company, 2003). Similar experiments like the one just mentioned were carried out, but with different solutions and with both 1180 and 600 µm particle sizes. Table 5.2 summarises these batch test experiments and their corresponding service/regeneration cycles.

Table 5.2. Summary of batch tests to assess zeolite regeneration potential in Phase IV

Experiment number	Cycle phase	Particle size (µm)	Zeolite weight (g)	Dissolved salt	Concentration M	Volume ml	Analyses after shaking
1	Service	1180	13.4	NaOH	0.01	220	Typical
	Regeneration	1180	8.5	HCl	0.1	150	Typical
	Service	1180	7.1	NaOH	0.01	130	Typical
	Regeneration	1180	4.6	HCl	1	125	Typ. $+Cl^-$ $+SO_4^{2-}$
	Service	1180	3.8	NaOH	0.01	125	Typ. $+Cl^-$ $+SO_4^{2-}$
	Regeneration	1180	3.4	$CaCl_2$	0.09	125	Typical + K^+
	Service	1180	3.0	NaCl	0.01	125	Typical + K^+
	Regeneration	1180	2.7	$CaCl_2$	0.01	125	Typical + K^+
	Service	1180	2.5	NaCl	0.01	125	Typical + K^+
	Regeneration	1180	2.2	KCl	0.1	125	Typical
	Service	1180	2.1	NaCl	0.01	125	Typical + K^+
2	Service	600	4.0	NaCl	0.01	225	Typical + K^+
	Regeneration	600	2.7	HCl	1	125	Typical
	Service	600	2.1	NaCl	0.01	125	Typical
	Regeneration	600	1.9	$CaCl_2$	0.09	125	Typical + K^+
	Service	600	1.8	NaCl	0.01	125	Typical + K^+
	Regeneration	600	1.7	$CaCl_2$	0.01	125	Typical
	Service	600	1.6	NaCl	0.01	125	Typical
	Regeneration	600	1.5	KCl	0.1	125	Typical
	Service	600	1.4	NaCl	0.01	125	Typical + K^+
3	Service	1180	2.0	NaCl	0.01	125	Typical + K^+
	Regeneration	1180	1.2	$CaCl_2$	0.09	125	Typical
	Service	1180	1.0	NaCl	0.01	125	Typical + K^+
	Regeneration	1180	0.8	$CaCl_2$	0.01	125	Typical
	Service	1180	0.7	NaCl	0.01	125	Typical
	Regeneration	1180	0.6	KCl	0.1	125	Typical
4	Service	1180	2.0	NaCl	0.01	125	Typical + K^+
	Regeneration	1180	1.0	$CaCl_2$	0.01	125	Typical + K^+
	Service	1180	0.8	NaCl	0.01	125	Typical + K^+
	Regeneration	1180	0.7	KCl	0.1	125	Typical
5	Service	1180	2.1	NaCl	0.01	125	Typical + K^+
	Regeneration	1180	1.2	KCl	0.1	125	Typical

Notes:
1. After each cycle phase samples were dried in a convection oven at around 100ºC, and sieved prior to starting the next phase
2. Zeolite samples correspond to the ones from set 1
3. Typical analyses are: pH, Specific conductance, calcium, hardness, and sodium

Flow-through tests

The objective of column tests, or flow-through tests, was to determine the sodium exchange capacity of Ngakuru zeolites in laboratory experiments resembling field-operating conditions. This also helped to determine the efficiency of the process and the optimal operating mode.

Flow-through tests involved the use of a zeolite-packed column with feed solution running through it. The column used in these experiments was especially designed and manufactured at the University of Canterbury, and it consisted of a 3 mm glass tube of about 75 cm in length, with a funnel attached to one of its openings. In addition, this column had a sintered glass filter at the funnel, and two taps for controlling flow in and out of the column (Figure 5.3). Most of the experiments with the ion exchanged column used about 240 g of zeolite material, but about 180 g were used in Experiment N°7.

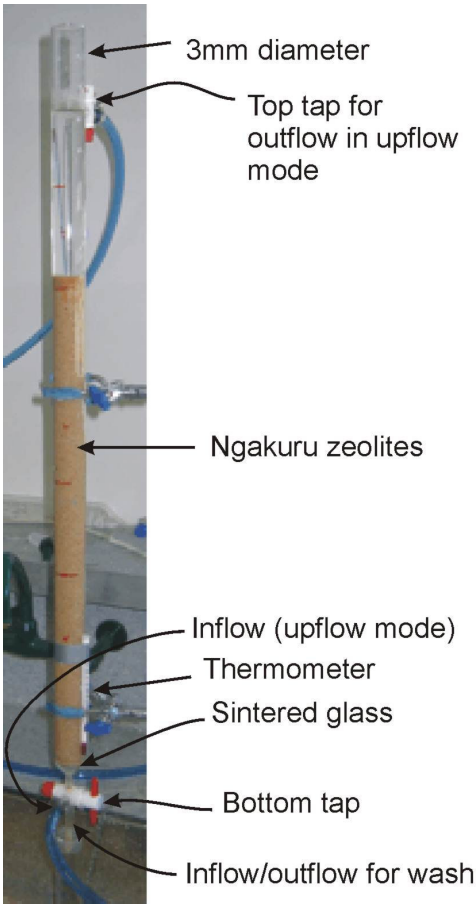

Figure 5.3. Glass column used in flow-through experiments

The first flow-through experiments were carried out in downflow mode, but this led to channelling and preferential flow so, to avoid these problems, it was decided to run the column in upflow mode for most of the experiments. In downflow mode, the feed solution was supplied through gravity dripping by a reservoir located over the glass column. This reservoir had an adjustable tap which enabled the selection of desired flow rates. In upflow mode, the feed solution was supplied through a 10mm plastic tube attached to the bottom tap. The other end of the tube fed directly into a container holding the feed solution, which was fed into the column with the aid of a peristaltic pump. This pump had a control dial allowing it to regulate flow rate, which was useful throughout the different modes of operation (the average retention time was about 14 minutes).

Typical operation mode included service, backwash, regeneration, and rinse. Service was carried out either in upflow or downflow mode at a specified flow rate, while backwash was carried out with deionised water at a high flow rate (as high as 180 cm^3/min) and always in upflow mode. Regeneration was carried out in the same direction of flow and same rate as in service mode using 1 litre KCl (1 M) and $CaCl_2$ (0.044 M) solutions. The next step was the rinsing step, which was necessary to remove any excess regenerant prior to service. This step was carried out with deionised water in upflow mode and at two different flow rates – a slow rate (as slow as the regeneration rate) to displace excess regenerant from the zeolite bed, and a fast rate (about twice as fast) to remove any residual solution from the zeolites. After rinsing, the bottom tap of the column was opened to drain any remaining liquid from the column. The complete cycle was carried out only when using regeneration - when solely carrying out service tests, the cycle was interrupted and used zeolites were discarded. In addition, one of these experiments was carried out with a warmed feed solution (~40°C) to determine if efficiency improved significantly with higher temperatures. Table 5.3 summarises the different experiments and provides relevant details.

Table 5.3. Summary of flow-through experiments

N°	Experiment type	Feed Solution	Direction of flow	Flow Rate cm^3/min	Feed volume litres	Zeolites particle size (µm)	Zeolites Mass grams	Retention Time min
1	No prior regeneration	0.01 M NaCl	downflow	21-26	10.1	1180	269.7	13.2
2	No prior regeneration	0.1 M NaCl	downflow	33	1.8	600	240.0	8.4
3	Prior regeneration with 1M KCl (1litre) and zeolites from experiment n° 2	0.1 M NaCl	upflow	13-19	1.83	600	240.0	17.4
4	No regeneration but feed solution was heated to ~40°C	0.1M NaCl	upflow	13-19	1.5	300	240.1	17.1
5	No prior regeneration	0.044M NaCl	upflow	12-21	2.7	600	240.1	16.1
6	Prior regeneration with 0.044M $CaCl_2$ (1 litre) and zeolites from experiment n° 5	0.044 M NaCl	upflow	14-20	2.7	600	240.1	15.6
7	No prior regeneration	Maramarua CSG water Equivalent to 0.013 M NaCl (1)	upflow	15-17	4.53	600	180.0	11.3

(1) Equivalent concentration was calculated using the composite sample (Table 5.1) with sodium concentrations of 304 mg/l. Differences in specific conductance and chloride concentrations are assumed negligible in this conversion.

During experiment n°4, the feed solution was heated to 100°C, but it cooled down while being pumped into the column, entering it at a temperature of approximately 40°C. The original NaCl concentration was 0.1M, but this could have increased because of water evaporation from the heated beaker. In addition, the zeolites were washed with deionised water inside the column before the experiment started. This was done to keep the zeolite bed moist in order to promote saturated flow at the start of the test.

In experiments n° 1, 2, 4, and 5 (Table 5.3) zeolites were prewashed with deionised water before each service run. Experiments n° 3, 5, and 6 tested regenerated zeolites that had previously been used in experiments n° 2, 4, and 5 respectively, so no pre-washing was carried out (except for the rinsing after the regeneration cycle).

Experiment n°7 was carried out without any pre-washing and with no previous regeneration.

In each of these experiments, 100 ml aliquots were collected during service runs either from the top tap (upflow mode) or bottom tap (downflow mode). These aliquots were stored in sample bottles and analysed after the service run had finalised. Before analysis, samples were filtered using 1.2 µm glass filters. Basic analyses carried out at the Environmental Engineering Laboratory (EEL, University of Canterbury) included pH, specific conductance, calcium, and hardness, which were carried out according to the methods outlined in APHA (1999). Also, sodium concentrations were determined using a calibrated Cole-Parmer sodium ion electrode. For experiments n° 6 and 7 (Table 5.3) samples were analysed for pH and specific conductance at the EEL, and then sent to Hill Laboratories for a complete analysis.

Data from flow-through experiments allowed for the construction of breakthrough curves showing the sodium absorption capacity of Ngakuru zeolites. This allowed for the calculation of the total number of exchanged sodium cations for a given mass of zeolites, while taking into account the interaction of other ions (Ca^{2+}, Mg^{2+}, H^{+}). Further interpretation of data included calculating and plotting absorption isotherms, and comparing these to other isotherms from known equilibrium relationships. In addition, it is possible to calculate the separation factor, *r*, for the whole isotherm (or *R* for a section of the isotherm) to determine the type of reaction taking place in relation to absorption kinetics. A description of the assumptions and calculation procedures used in these calculations is presented in Appendix D (section D.1).

Results

Batch test results

Phase I. Results for this experiment are presented in Appendix D (Tables D.1 and D.2). Different particle sizes produced zeolitic solutions having approximately the same hardness and calcium concentrations. However, a minor trend was noticed where exchanged cations seemed to increase slightly with fine particle size (passing 150 µm and retained on the 150 µm sieve) and with coarser sizes (1180 µm and 2360 µm). This can be observed by analysing the plots of calcium concentrations vs. particle size in Figure

5.4. In theory, smaller particle sizes have more surface area and would offer best ion exchange results, but this was not noticeable in these experiments. Small particles tend to become buoyant during experiments, and this produces operational problems; larger particles do not have as much buoyancy as smaller ones, but the same amount of material, consisting of larger particles, has less surface area available for the exchange. In these experiments, particle size did not pose a major influence in ion exchange processes. Figure 5.4 also shows that shaking time does have an influence on reaction kinetics as the zeolitic solutions that were shaken for 8 hours have more calcium ions than the solutions that had been shaken for just 1.75 hours. Hardness analyses (Table D.1, Appendix D) also showed that zeolitic solutions that had been shaken for 8 hours released more calcium and magnesium (hardness) than the ones shaken for just 1.75 hours. In addition, the pet litter zeolite sample that was shaken for 1.75 hours produced significantly lower concentrations of calcium ions in solution (46 mg/l/g) than the zeolitic solutions shaken for the same period of time but containing zeolites from set n°1 (78-99 mg/l/g zeolites). There was no pattern in pH changes for the different shaking times and particle sizes being tested (pH 4.5-5.7). This analysis also helps to make initial “go” or “no go” decisions when working with a new material. In this case pet litter exchanged less calcium than high-grade zeolites, and this suggests pet litter contains less ion exchange minerals (i.e. mordenite) than high grade zeolites. Since calcium determination is simple, accurate, and fast, this can save time and money during the initial assessment of an ion exchange material. Based on these results it was decided to work with high-grade zeolites with a medium ranged particle size (300 or 600 μm).

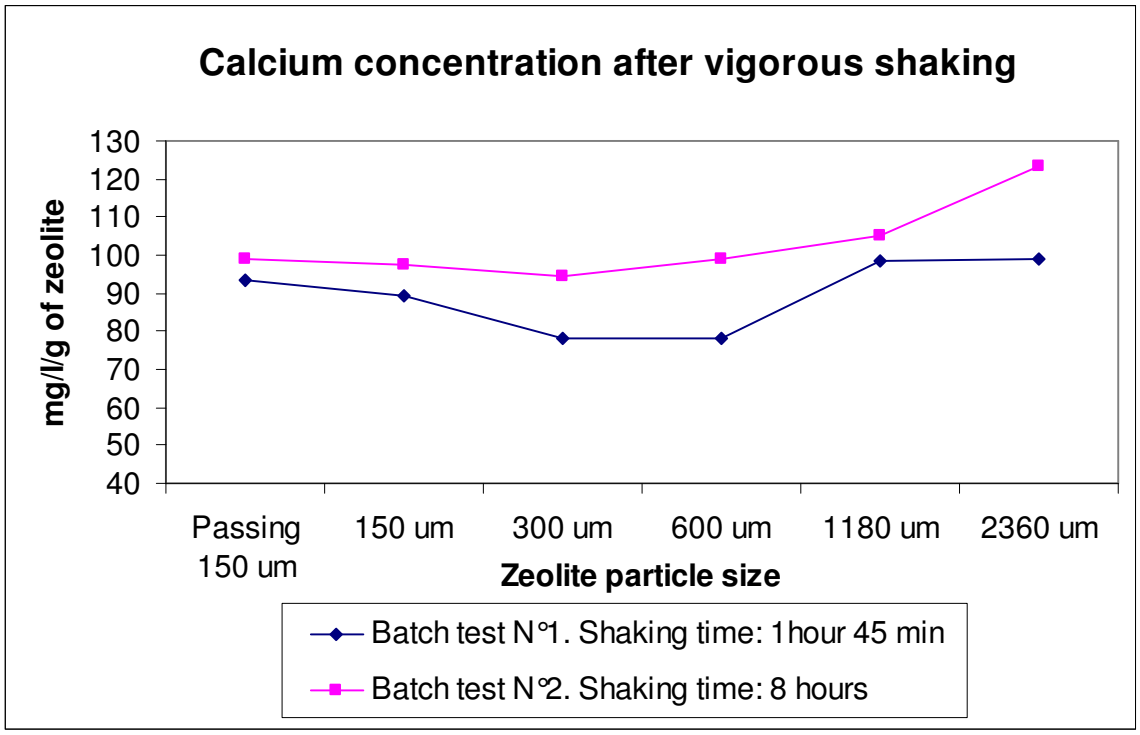

Figure 5.4

Phase II. Results for this experiment are presented in Table D.3 (Appendix D). Shaking for 9.5 hours with low concentration NaCl solution (0.005 M) revealed that there was little or no change in specific conductance (from 538 to 546 µS/cm), and some calcium (8 mg/l) and hardness (32 mg/l as $CaCO_3$) were detected at the end of the shaking time. In addition, pH decreased from 6.2 to 5.5, which suggests that hydrogen ions were being exchanged for sodium. When using deionised water, results indicated very small amounts of calcium (3.2 mg/l) and hardness (4.2 mg/l as $CaCO_3$) being released, and a slight increase in specific conductance (from 1.9 to 41.8 µS/cm). The pH of this sample was 6.4 indicating little or no difference from the original pH of deionised water (pH 7). These results suggest that some dissolution could be taking place, but at this stage it was not possible to measure the magnitude of this (albeit low) dissolution. If the reaction taking place had been solely an ion exchange reaction, specific conductance would have remained the same, and few cations would have been detected in the deionised water with the zeolites.

Phase III. The results of batch testing Ngakuru zeolites using different types of concentrated solutions are presented in Appendix D (Table D.4) and plotted in Figure 5.5. These results show that more sodium cations are absorbed while more hardness cations (calcium & magnesium) are released from the zeolites at higher NaCl concentrations. In addition, the type of solution itself can play an important role in the exchange process. For example, Table D.4 (Appendix D) shows that the 0.01 M NaOH absorbs almost as much sodium as the more-concentrated-0.1 M NaCl solution, but with practically no calcium and magnesium being released. In all of these experiments the pH decreased by about 1 pH unit after shaking, which shows that hydrogen ions are being released as part of the exchange/dissolution process.

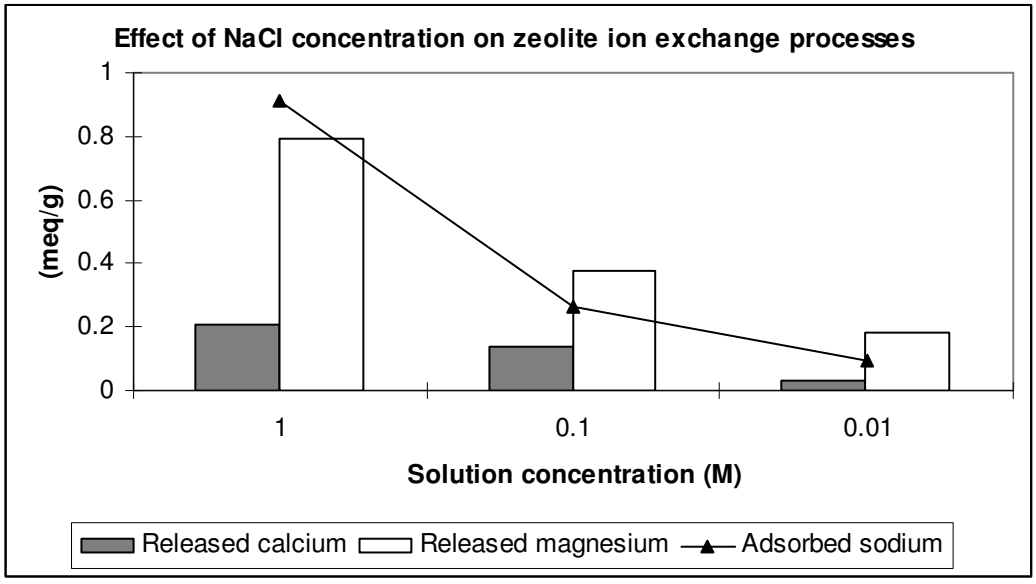

Figure 5.5

Phase IV.

Experiment n°1

Table 5.4 shows the results from service/regeneration cycles using the same batch of 1180 µm zeolites and different solutions. After 5 service/regenerations cycles the zeolites were still adsorbing sodium ions (16.6 meq/100g on the 6th service run [n°11]); there was a significant decrease in mass (83.3%) mainly due to mechanical wear and tear (due to the violent shaking), but this could also have been due to some dissolution. The

last column in Table 5.4 shows the exchange that has taken place between the zeolite and the main cations originally in solution (Na^+, Ca^{2+}, K^+, or H^+).

Chemical analyses of sample solutions revealed the nature of the ion exchange processes taking place during shaking. The first batch service run (n°1) showed that the original zeolite material contains calcium (0.07 meq/l) and magnesium (0.04 meq/l) as occluded salts. These results are consistent with the calcium and magnesium (hardness) concentration obtained during the first phases. After the first regeneration (with HCl in n°2) a maximum magnesium concentration of 2.85 meq/l was detected in the solution after the exchange. It was possible to verify that magnesium remained within the zeolite even after a few service/regeneration runs (n° 3, 5, 6, 7, and 8); when regenerating with a higher valence regenerant (Ca^{2+} in n°6), magnesium concentrations in solution increased to 2.01 meq/l even though the previous service run had yielded a low magnesium concentration value (0.08 meq/l). Similar results were obtained with calcium - these cations were released during the first service run and during the two following service/regeneration cycles (n° 1-5). The maximum calcium concentration was detected during the first regeneration run (n°2, 5.9 meq/l) and after regenerating with a strong acid (n°4, 2.0 meq/l). Thereafter more calcium cations were released but these were mainly a product of regenerating with $CaCl_2$ in regeneration run n°6 (172 meq/l). In sum, during each service run sodium cations were adsorbed by the zeolites, while calcium, magnesium, potassium, and some hydrogen ions were released; during regeneration, the opposite exchange is taking place – hydrogen, calcium, or potassium ions are being exchanged for sodium ions in the zeolite.

Throughout all of the service runs in Table 5.4, pH values decreased considerably after each run. This indicated that hydrogen ions were being released from the zeolites as part of the exchange process. For example, after the first service run, pH values decreased from 11.23 to 9.91, and after the last service run these values decreased from 6.34 to 4.64. A pH decrease of almost 7-fold was detected after service runs n° 3 and n°5 (from 11.23 down to 4.77 and 4.01), but this is due to HCl being used in the previous regeneration runs.

Unfortunately, it was not possible to measure potassium during the first service run and the following 2 service/regeneration runs, but it was possible to measure

potassium cations in some of the subsequent samples. Results indicated that there is some potassium originally present in the zeolite material, and that this is slowly being released with each service/regeneration run. The fourth service run (n°7 in Table 5.4) produced a solution with 0.2 meq/l of K^+ cations, while the fifth service run (n°9 in Table 5.1) produced 0.1 meq/l of K^+. The last service run produced more potassium (3.1 meq/1), but this is a product of previous KCl regeneration.

Chloride and sulphate were measured after runs n° 4 and 5 to determine whether dissolution of these anions was taking place. In both instances, sulphate concentrations were nil. A difference of 8.6% was detected in chloride concentrations after regenerating with 1M HCl in run n°4.

Table 5.4. Experiment n°1. Batch sorption experiments with 1180µm zeolites

n°	Reaction type	zeolite weight g	sample volume litres	Sol. type	initial pH	final pH	final Na^+ meq/l	final Ca^{2+} meq/l	final Mg^{2+} meq/l	final K^+ meq/l	trapped cations[2] meq/l	released cations[3] meq/l	charge balance[4] meq/l	main cation exchange[5] meq/100g
1	Service	13.36	0.220	0.01M NaOH	11.23	9.91	3.4	0.07	0.04	NA	6.6	6.6	0.0	10.8
2	Regeneration	8.54	0.150	0.1M HCl	1.12	1.33	15.9	5.9	2.85	NA	38	24.6	13.7	27.9
3	Service	7.13	0.130	0.01M NaOH	11.23	4.77	2.8	0.32	0.12	NA	7.2	7.2	0.0	13.1
4	Regeneration	4.57	0.125	1M HCl	0.25	0.26	9.5	2.0	0.00	NA	11.5	11.5	0.0	26.1
5	Service	3.81	0.125	0.01M NaOH	11.23	4.01	3.5	0.24	0.08	NA	6.5	6.5	0.0	21.2
6	Regeneration	3.35	0.125	0.09M $CaCl_2$	5.32	4.06	1.0	172	2.01	0.0	4.0	3.2	0.8	3.9
7	Service	3.03	0.125	0.01M NaCl	6.34	3.21	8.8	0.36	0.04	0.2	1.2	1.3	0.1	5.0
8	Regeneration	2.72	0.125	0.01M $CaCl_2$	6.62	4.7	0.5	18	0.60	0.0	2.3	1.1	1.2	2.2
9	Service	2.46	0.125	0.01M NaCl	6.34	3.49	8.4	0.4	0.00	0.1	1.6	0.9	0.7	8.0
10	Regeneration	2.23	0.125	0.1M KCl	6.76	3.13	5.4	0.8	0.00	0.0	NA	7.1	NA	30.2
11	Service	2.06	0.125	0.01M NaCl	6.34	4.64	7.3	0.4	0.00	3.1	2.7	3.5	0.7	16.6

Notes:

1) NA = not available
2) Trapped cations for each run:
   a. Na^+ : n°1, 3, 5, 7, 9, 11
   b. H^+ : n°2, 4
   c. Ca^{2+} : n°6, 8
   d. K^+ : n°10
3) Released cations for each run
   a. n°1, 3, 5, 7, 9, 11: $Mg^{2+} + Ca^{2+} + K^+ + H^+$
   b. n°2: $Mg^{2+} + Ca^{2+} + Na^+$
   c. n°4: $Mg^{2+} + Ca^{2+} + K^+ + Na^+$
   d. n°6, 8: $Mg^{2+} + H^+ + K^+ + Na^+$
   e. n°10: $Mg^{2+} + Ca^{2+} + Na^+ + H^+$
4) Charge balance = released cations – trapped cations
5) Main cation exchange (MCE) = meq of main cation intervening in the exchange reaction per 100g of zeolites

$$MCE = \frac{100 \cdot Exchanged\ ion\ (meq/l) \cdot Sample\ volume\ (l)}{Zeolite\ weight\ (grams)}$$

Experiment n°2

This experiment was very similar to experiment n°1 except in this case 600 µm zeolites were used instead of 1180 µm, and the only type of solution used during service was NaCl. Likewise, results from this experiment were similar to the results obtained in the previous experiment. Experiment n°2 results and observations are presented in Appendix D.

Experiment n°3-n°5

Experiments n°3-n°5 aimed at reproducing the results obtained in experiment n°1. The results from these experiments are presented in Tables D.6-D.8 in Appendix D. In these experiments, 1-3 service/regeneration cycles were done with 1180 µm zeolites. The decrease in zeolite mass (due to shaking) was 73%, 65%, and 46% for 3, 2, and 1 cycles respectively.

On average, there was a concentration of calcium of about 0.62 meq/l being released from the zeolites during the first service run in each of these experiments. Similarly, average concentrations of magnesium (0.23 meq/l) and potassium (0.50 meq/l) showed that these zeolites were releasing the same number of cations when exposed to the same volume of NaCl concentrated solution (0.01M).

Throughout these experiments, pH tended to decrease after each service or regeneration run, which shows that hydrogen ions are being released as part of the exchange. However, pH tended to increase slightly after the first service run in each of these experiments, which indicates that hydrogen ions might have been absorbed by the zeolites but only during the first run (Tables D.6-D.8 in Appendix D).

Since it was not possible to measure potassium concentrations in most of these experiments, charge balance results are not always available. However, charge balance for those samples with known potassium concentrations, indicate an average charge excess of 1.06 meq/l.

Flow-through tests

Experiments n°1 and n°2

The first two flow-through experiments (n°1 and n°2 in Table 5.3) produced good results, but these were carried out in downflow mode which generated preferential flow as the feed solution entered the packed zeolite column. It was suspected this led to inefficiencies in zeolite utilisation, therefore these experiments were regarded as preliminary, and analyses of the 100 ml aliquots were done on a limited number of samples. Nevertheless, these experiments provided important information and operational experience to be used through out the rest of the experimental work. Results from experiments n°1 and n°2 are presented in Appendix D (Tables D.9 & D.10 and Figures D.2 & D.3).

Experiment n°3

This experiment was carried out in upflow mode with KCl-regenerated zeolites from experiment n°2. In this experiment, 1780 ml of 0.1 M NaCl were run through the column, producing 18 100 ml-sample aliquots. Chemical analyses for these samples are presented in Appendix D (Table D.11), and a plot of sodium concentration vs. volume flowing through the column is presented in Figure D.4 (Appendix D). The total sodium exchange taking place throughout this experiment was at least 40.9 meq/100g. This value was calculated by adding the milliequivalences of sodium adsorbed by the zeolites throughout the duration of the experiment - the remaining sodium concentration was determined with a calibrated sodium electrode in each aliquot after it had percolated through the column, since the original concentration and volume of the feed solution are known then it is possible to calculate the adsorbed sodium (simple subtraction). This process was carried out for each of the sample aliquots, and these values were then added together resulting in the total sodium adsorbtion for this experiment (in meq). Since the zeolite's weight is known, then this value can be expressed in meq/100g.

Experiment n°4

Results for this experiment (no regeneration, feed at 40°C) are presented in Appendix D (Table D.12). Calcium and magnesium concentrations were calculated for samples n°1, 3, 10, and 15. Calcium and magnesium concentrations for sample n°3 contained the highest concentrations measured for this experiment, and these concentrations decreased in samples n°10 (by 46% and 16% respectively) and 15 (35% and 14% respectively).

A plot of the sodium sorption results is presented in Appendix D (Figure D.4). Sodium concentrations in the collected samples increased in logarithmic form (R^2=0.99) until reaching the original sodium concentration after 1400 ml of feed solution had gone through the column. The total sodium absorption was calculated by subtracting the residual sodium concentration in collected samples from the original sodium concentration in the feed solution, and by adding these values throughout the duration of the experiments. At the end of this experiment, the total sodium sorption by Ngakuru zeolites was 19.3 meq/100g.

Samples in experiment n°4 had pH values in the 4.07-5.38 range consistently lower than the original pH value of 5.85 (Table D.12 in Appendix D). The pH values for sample n°2 was the highest pH value recorded, followed by the pH value for sample n°3; pH values in the following samples stayed fairly constant at an average of 4.14.

Experiment n°5

Experiment n°5 showed that it is possible to absorb sodium ions from a 0.044M (1000 mg/l) NaCl solution using Ngakuru zeolites. In addition, calcium, magnesium, and hydrogen ions were released from the zeolites during the exchange process. Results from this experiment are presented in Table D.13 (Appendix D), and a plot of the sodium sorption and cation release is presented in Figure D.5 (Appendix D).

The total sodium sorption that took place throughout this experiment was 15.9 meq/100g. The maximum sodium sorption took place at the beginning of the experiment - sample n°1 had the lowest sodium concentration (14.5 meq/l), but sodium concentrations in succeeding aliquots increased almost linearly (Figure D.5, Appendix D) until about 700 ml of feed solution had flowed through the column. From then onwards,

sodium concentrations increased logarithmically (Figure D.5, Appendix D) until reaching a final value of 38.4 meq/l (sample n°27). The relationship between sodium and flow-through volume can be approximated by a linear trendline with an R^2 value of 0.95 (Eq 2, Appendix D). The total sodium sorption that took place during this experiment was 15.9 meq/100g.

Calcium concentrations in aliquots tended to increase linearly for the first 5 samples (Figure D.5, Appendix D) starting at 10.7 meq/l (sample n°1) and finishing at 12.8 meq/l (sample n°5). However, from then onwards calcium concentrations decreased in inverse logarithmic form until reaching a final value of 4.8 meq/l in sample n°25.

Similarly, magnesium concentrations were the highest at the beginning of the experiment, with sample n°1 having a concentration of 14.3 meq/l. However, throughout this experiment, magnesium concentrations decreased in an inverse logarithmic fashion (Figure D.5, Appendix D) until reaching a value of 1.1 meq/l (sample n°25).

Throughout this experiment, pH values stayed fairly low and within the 4.45-4.79 pH range. This is almost 2 pH units below the original pH (6.35), and it shows that hydrogen ions are also taking part of the cation exchange. However, there was no identifiable trend in pH values as the experiment was being conducted.

Specific conductance of the outflow remained fairly constant throughout this experiment. The conductance of the untreated feed solution was 5.1 dS/m, and the conductance of the outflow was very similar and remained fairly unchanged throughout the different samples measured in this experiment (average = 5.05, $\sigma = 0.06$).

Experiment n°6

Experiment n°6 was carried out with regenerated zeolites (using $CaCl_2$) from experiment n°5. Results for this experiment are presented in Table 5.5, and plots of the cation exchange process are presented in Figures 5.6 and 5.7.

Table 5.5. Results for experiment n°6

Sample n°	vol. through ml	pH pH units	Na^+ meq/l	Ca^{2+} meq/l	Mg^{2+} meq/l	K^+ meq/l
1	100	5.25	11.1	27.2	0.58	1.74
2	200	4.81	15.6	NA	NA	NA
3	300	4.7	17.0	24.1	0.26	2.38
4	400	4.65	19.1	NA	NA	NA
5	500	4.67	21.1	20.3	0.17	2.74
6	600	4.93	NA	NA	NA	NA
7	700	4.55	22.7	16.8	0.14	2.79
8	800	4.55	NA	NA	NA	NA
9	900	4.56	26.8	14.0	0.12	3.04
10	1000	4.55	NA	NA	NA	NA
11	1100	4.56	28.7	11.9	0.12	3.10
12	1200	4.56	NA	NA	NA	NA
13	1300	4.57	31.1	10.0	0.10	3.04
14	1400	4.57	NA	NA	NA	NA
15	1500	4.57	31.3	8.5	0.10	2.97
16	1600	4.59	NA	NA	NA	NA
17	1700	4.59	33.3	7.6	0.10	3.02
18	1800	4.61	NA	NA	NA	NA
19	1900	4.62	34.3	6.8	0.11	3.02
20	2000	4.63	NA	NA	NA	NA
21	2100	4.62	35.1	6.2	0.11	2.92
22	2200	4.64	NA	NA	NA	NA
23	2300	4.63	34.8	5.9	0.11	2.86
24	2400	4.63	34.7	NA	NA	NA
25	2500	4.67	34.5	5.2	0.11	2.76
26	2600	4.84	NA	NA	NA	NA
27	2700	4.84	35.8	4.9	0.12	2.81

Notes:

1) Feed solution is a 0.044 M NaCl solution with pH= 5.85
2) Original Na^+ concentration is 0.044 M (1000 mg/l = 43.5 meq/l)
3) Na^+, Ca^{2+}, Mg^{2+}, and K^+ concentrations were measured through Hill Laboratories
4) Ca^{2+}: 1 meq/l = 20.04 mg/l; Mg^{2+}: 1 meq/l = 12.15 mg/l; K^+:1 meq/l = 39.1 mg/l
5) Aliquot volume is 100 ml
6) For further information about experiment setup refer to Table 5.3
7) NA = no data available

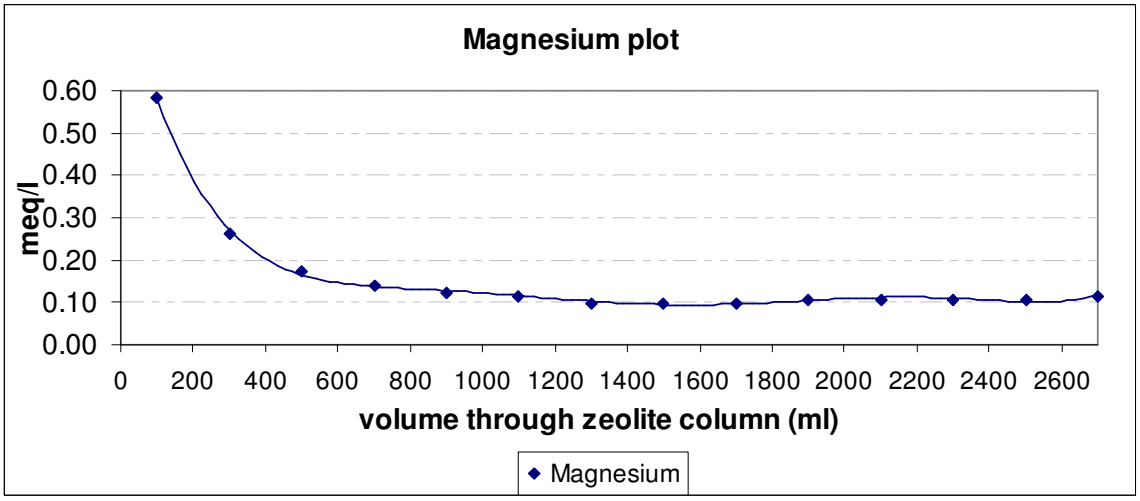

Figure 5.6

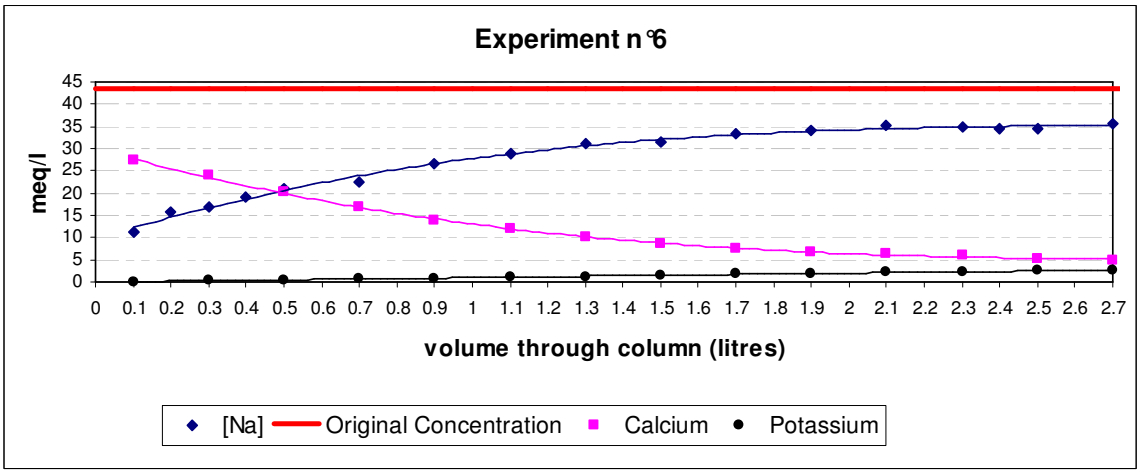

Figure 5.7

The total sodium sorption that took place throughout this experiment was approximately 16.7 meq/100g. The maximum sodium sorption was registered in sample n°1 which had 75% less sodium than the original feed solution (11.1 meq/l vs. 43.5 meq/l). The sodium sorption process took place in an almost linear fashion during approximately the first 700 ml of treated feed solution, however from then onwards the sodium sorption process increased logarithmically until samples reach a steady sodium concentration of 35.8 meq/l (sample n°27). In these experiments, breakthrough is defined as the point at which the concentration of a target ion matches a predetermined concentration (Wachinski, 1997). Therefore, if in this case sodium is the target ion then

sample n°21 corresponds to the breakthrough point (35.1 meq/l). The best fit for these data is given by a logarithmic equation with an R^2 value of 0.98 (Eq 5.1).

$$[Na] = 8.1 \times \ln(v) + 27.9$$

where,
$[Na]$ = sodium concentration in sample aliquot (meq/l)
v = volume through column in litres
Eq 5.1

Calcium concentrations decreased logarithmically throughout this experiment (Figures 5.6 and 5.7), but the best fit is given by a third order polynomial equation (R^2=0.999). Calcium concentrations at the start of the experiment are as high as 27.2 meq/l (sample n°1), but at the end of this experiment calcium concentrations reached a low value of 4.9 meq/l (sample n°27).

On the other hand, magnesium concentrations are very low in comparison to calcium concentrations throughout this experiment (Table 5.5 and Figure 5.6). Magnesium concentrations at the start of the experiment were about 29.1 mg/l as $CaCO_3$ (0.58 meq/l), from then onwards magnesium concentrations decreased logarithmically and, after about 1000ml of feed solution had flowed through the column, magnesium concentrations stabilised at value of around 0.11 meq/l.

Potassium concentrations in aliquots were fairly constant throughout this experiment averaging 2.8 meq/l. The minimum potassium concentration was 1.74 meq/l and it occurred at the start of the experiment (sample n°1).

Throughout this experiment, pH values stayed below the original pH value of 5.85. The first sample had the highest pH value (5.25), and subsequent pH values stayed below the 5.0 mark. After 600 ml of treated feed solution, pH values remained constant at around 4.6, however the last two samples of this experiment showed a slight pH increase (4.84).

Specific conductance remained constant throughout this experiment. The conductance of the untreated feed solution was 5.0 dS/m, and this value remained fairly unchanged throughout the different outflow samples measured in this experiment (average = 5.11 dS/m, σ = 0.13).

The breakthrough curve in this experiment can be standardised by calculating its adimensional isotherm, which represents the relative change in concentration of the outflow solution in relation to the relative change in sodium content within the zeolite. The isotherm for experiment n°6 is presented in Figure 5.8, and it shows the sodium exchange process until the experiment reaches breakthrough (35.1 meq/l in this case); the liquid phase is the change in sodium concentration in the outflow solution divided by the maximum outflow concentration minus the initial outflow concentration. Similarly, the solid phase is the relative change in sodium absorbance, within the zeolites, as the experiment approaches breakthrough. The resulting isotherm is linear (Figure 5.9), with an R^2 value of 0.99. In addition, the separation factor (R) was calculated for each step of this experiment, and this value ranged from 0.92 to 1.51 with and average of 1.2 ($\sigma = 0.2$; see Table D.14 in Appendix D).

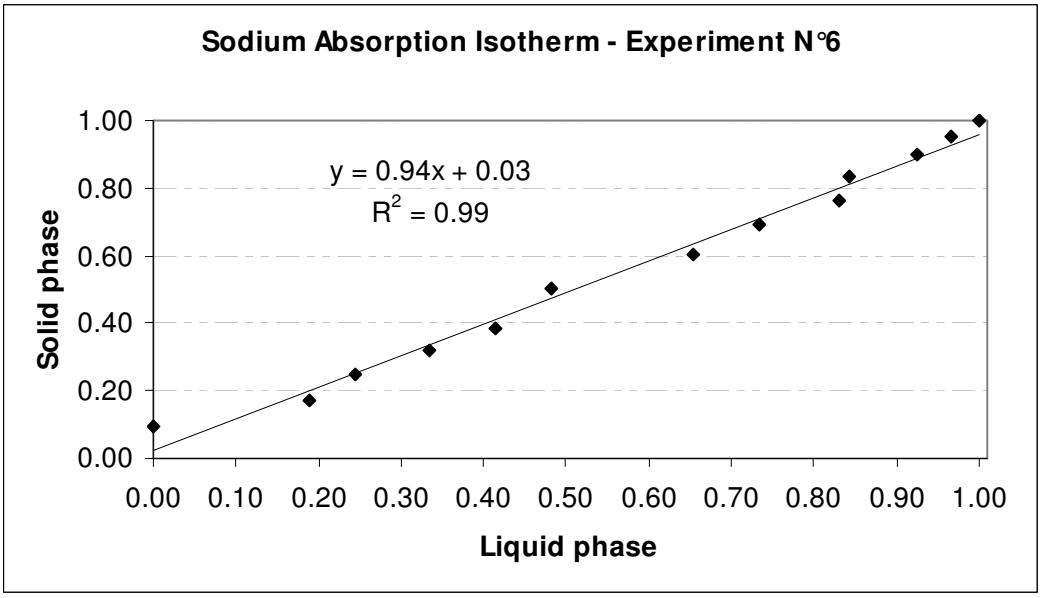

Figure 5.8. Fractional solid-concentration isotherm for experiment n°6.

$$Q = 0.94 \times C + 0.03$$

Where,

$$C = \frac{c - c'}{c'' - c'}$$

$$Q = \frac{q - q'}{q'' - q'}$$

c = outflow concentration
c'= minimum outflow concentration (first sample, 11.1 meq/l)
c'' = maximum outflow concentration (breakthrough, 35.1 meq/l)

q = sodium ion in zeolite
q' = initial zeolite sodium absorption (3.2 meq)
q'' = total zeolite absorption (at breakthrough, 35.0 meq)

Figure 5.9

Experiment n°7

Experiment n°7 was carried out with actual CSG water from Maramarua (Table 5.1). The same cations analysed in the previous experiments, were also analysed in experiment n°7, but in this case a more thorough analysis was carried out in 4 of the samples to compare these against the original feed solution (Table 5.1). Major cation exchange results and properties for aliquots throughout this experiment are presented in Table 5.6, and detailed analyses for selected samples are presented in Table 5.7.

Table 5.6. Column test results for experiment n°7

Sample n°	vol. through ml	pH pH units	Sp. Conductance dS/m	Na^+ meq/l	Ca^{2+} meq/l	Mg^{2+} meq/l	K^+ meq/l
1	103	6.45	2.11	5.4	3.5	12.51	0.7
2	207	7.03	1.42	4.5	2.4	7.91	0.6
3	309	7.09	1.20	4.4	1.9	5.78	0.6
4	409	7.26	1.15	4.8	1.9	5.06	0.7
5	509	7.40	1.15	5.2	2.0	4.39	0.7
6	610	7.51	1.16	5.8	2.1	3.90	0.8
7	710	7.63	1.17	6.2	2.1	3.52	0.8
8	810	7.51	1.18	6.5	2.2	3.13	0.9
9	911	7.78	1.18	6.6	2.1	2.75	0.9
10	1012	7.88	1.19	7.6	2.2	2.63	1.0
11	1113	8.00	1.20	8.3	2.2	2.51	1.0
12	1216	7.85	1.21	8.4	2.2	2.28	1.0
13	1317	7.96	1.22	8.1	2.2	1.95	1.0
14	1418	7.99	1.22	8.7	2.1	1.84	1.0
15	1519	7.92	1.23	9.1	2.1	1.80	1.1
16	1620	8.02	1.23	9.2	2.1	1.61	1.0
17	1724	8.08	1.23	8.4	2.0	1.33	1.0
18	1825	7.98	1.24	9.2	2.0	1.27	1.1
19	1926	8.07	1.24	9.4	2.0	1.23	1.2
20	2027	8.03	1.24	9.4	1.9	1.15	1.2
21	2128	8.11	1.24	9.9	1.9	1.13	1.1
22	2229	8.04	1.25	9.7	1.8	1.04	1.1
23	2330	8.11	1.25	9.4	1.8	0.91	1.1
24	2430	8.14	1.25	10.0	1.8	0.90	1.2
25	2531	8.09	1.26	9.9	1.8	0.83	1.1
26	2632	8.15	1.26	9.5	1.7	0.76	1.1
27	2733	8.20	1.26	9.5	1.8	0.74	1.2
28	2834	8.17	1.26	9.6	1.7	0.67	1.1
29	2934	8.14	1.27	10.2	1.7	0.69	1.2
30	3038	8.19	1.27	NA	NA	NA	NA
31	3138	8.23	1.27	9.5	1.6	0.58	1.1
32	3243	8.20	1.28	NA	NA	NA	NA
33	3343	8.24	1.28	9.6	1.6	0.53	1.1
34	3443	8.28	1.27	NA	NA	NA	NA
35	3543	8.26	1.28	9.6	1.6	0.49	1.1
36	3645	8.29	1.28	10.0	1.6	0.50	1.2
37	3746	8.31	1.28	10.0	1.5	0.47	1.2
38	3846	8.30	1.29	NA	NA	NA	NA
39	3947	8.33	1.29	9.7	1.4	0.42	1.1
40	4046.5	8.33	1.29	NA	NA	NA	NA
41	4146.5	8.32	1.29	10.1	1.4	0.41	1.2
42	4248.5	8.36	1.29	NA	NA	NA	NA
43	4350.5	8.32	1.29	9.8	1.4	0.36	1.1
44	4450.5	8.33	1.29	NA	NA	NA	NA
45	4530.5	8.36	1.29	10.5	1.4	0.37	1.2

Notes:

1) Feed solution is Maramarua CSG water (composite samples, Table 5.1) having a Na concentration of 13.2 meq/l (1000 mg/l = 43.5 meq/l) and pH= 8.57
2) Na^+, Ca^{2+}, Mg^{2+}, and K^+ concentrations were measured through Hill Laboratories
3) Ca^{2+}: 1 meq/l = 20.04 mg/l; Mg^{2+}: 1 meq/l = 12.15 mg/l; K^+:1 meq/l = 39.1 mg/l
4) Aliquot volume is ~100 ml
5) For further information about experiment setup refer to Table 5.3
6) NA = no data available

Table 5.7. Full analyses for selected samples (experiment n°7)

		Samples [1]			
	Unit	n°1	n°7	n°19	n°36
Total alkalinity	mg/l as $CaCO_3$	278	428	468	498
Bicarbonate	mg/l	339[2]	519[2]	561[2]	590[2]
Chloride	mg/l	164	151	147	149
Total Organic Carbon	mg/l	216	<0.5	27.7	30.7
Carbonate	mg/l	0.1[2]	1.5[2]	4.6[2]	8.2[2]
Dis. carbon dioxide	mg/l	390[2]	41[2]	16[2]	10[2]
Reactive silica	mg/l	25.1	27.6	27.1	25.5
Sulphate	mg/l	28.0	3.3	2.9	2.9
Total boron	mg/l	67.4	2.8	2.6	2.0
Fluoride	mg/l	0.23	0.94	1.68	1.28
Dissolved iron	mg/l	<0.02	<0.02	0.02	0.03
Total iron	mg/l	<0.4	<0.4	<0.4	<0.4
Dissolved manganese	mg/l	1.96	0.33	0.07	0.0121
Total manganese	mg/l	1.89	0.33	0.07	0.02
Total aluminium	mg/l	<0.06	<0.06	0.09	0.15
Total cobalt	mg/l	0.005	<0.004	<0.004	<0.004
Total chromium	mg/l	<0.01	<0.01	<0.01	<0.01
Total nickel	mg/l	0.02	<0.01	<0.01	<0.01
Total nitrogen	mg/l NH_4-N	0.03	NA	NA	NA
Total zinc	mg/l	0.74	0.05	0.03	<0.02

Notes:
[1] Samples analysed through Hill Laboratories, Hamilton, New Zealand
[2] Calculated using from carbonate chemistry using alkalinity and pH values

Throughout this experiment, the total sodium sorption that took place was approximately 11.3 meq/100g. According to the experimental results in Table 5.6, the first two aliquots presented higher sodium concentrations than the third one, which was the sample with the lowest sodium concentration. In any case, sodium concentration for the first two samples were still very low in comparison to the initial sodium concentration (41% and 34% for samples n°1 and n°2 respectively). From sample n°3 onwards, sodium concentrations in aliquots increased in an quasi logarithmic fashion reaching a limit of approximately 10.0 meq/l (76% of original concentration). This can be observed in

Figure 5.10, where sodium concentrations in samples throughout this experiment are represented by a logarithmic trendline (Eq 5.2) with an R^2 value of 0.87.

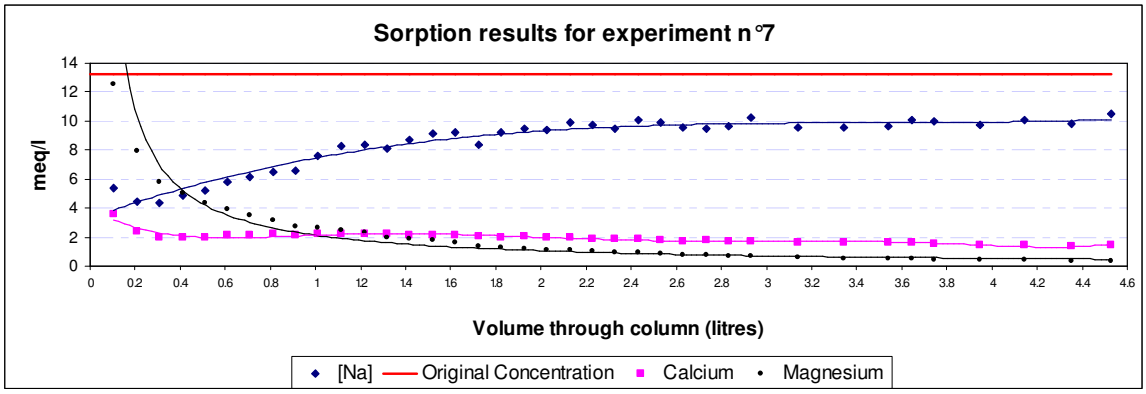

Figure 5.10

$$[\mathrm{Na}] = 1.92 \times \ln(v) + 7.61$$

where,

$[\mathrm{Na}]$ = sodium concentration in sample aliquot (meq/l)

v = volume through column in litres

Eq 5.2

The first two sample aliquots in this experiment have a higher sodium concentration than aliquots n°3 an n°4, and it will be shown later that this is a consequence of some initial zeolite dissolution. For this reason, the breakthrough curve is not perfectly logarithmic. However, as in experiment n°6, it is possible to discard these first two samples in experiment n°7 and calculate an isotherm until breakthrough is achieved (10 meq/l). This isotherm is presented in Figure 5.11, and it has a linear trendline with an R^2 value of 0.95. In this figure, the liquid phase is the change in sodium concentration in the outflow solution (minus the original concentration) divided by the maximum concentration of the outflow solution (minus the original concentration). Similarly, the solid phase is the relative change in sodium absorbance, within the zeolites, as the experiment approaches breakthrough. Figure 5.12 presents the linear relationship for this isotherm, and its calculation procedure. In this case, the separation factor (R) ranged from 0.28 to 4.7 for each of the aliquots throughout this experiment with an average of 1.5 (σ = 0.93; see Table D.15 in Appendix D).

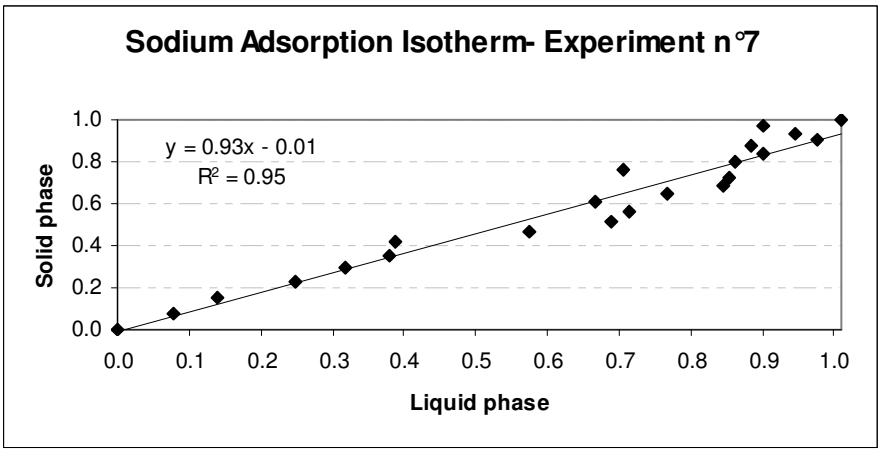

Figure 5.11. Fractional solid-concentration isotherm for experiment n°7.

$$Q = 0.93 \times C - 0.01$$

Where,

$$C = \frac{c - c'}{c'' - c'}$$

$$Q = \frac{q - q'}{q'' - q'}$$

c = outflow concentration
c'= minimum outflow concentration (first sample, 4.4 meq/l)
c'' = maximum outflow concentration (breakthrough, 10.0 meq/l)

q = sodium ion in zeolite
q' = initial zeolite sodium absorption (2.5 meq)
q'' = total zeolite absorption (at breakthrough, 13.1 meq)

Figure 5.12

Magnesium and calcium cations in samples collected throughout this experiment tended to decrease in a quasi-logarithmic manner. Magnesium concentration for the first sample was the highest recorded (12.51 meq/l), but after about 1200ml of treated feed solution were collected, magnesium concentrations were lower than 2 meq/l getting as low as 0.36 meq/l in sample n°43. On the basis of charge, calcium concentrations are not originally as high as magnesium, but these do not decrease as much. The highest calcium concentration was 3.5 meq/l and it was recorded in the first sample - subsequent samples tended to have lower calcium levels averaging around 1.8 meq/l after the third sample.

Potassium concentrations in aliquots throughout this experiment were lower than 1.2 meq/l. The initial potassium concentration was 0.7 meq/l (sample n°1), but this value

decreased to a minimum (0.6 meq/l) in the third sample. Potassium concentrations then increased in a logarithmic fashion stabilizing at around 1.1 meq/l.

Throughout this experiment, pH values increased logarithmically (Figure 5.13; $R^2 = 0.97$) starting at 6.45 and finishing at 8.36 after 4.5 litres of treated feed solution. For the first 200 ml of treated feed solution, specific conductance values were higher than in subsequent samples and higher than in the original feed solution. After the first sample, specific conductance values decreased linearly from 2.10 dS/m to 1.15 dS/m (sample n°5), and then gradually increased to a value just higher than the original specific conductance value (1.26 dS/m; Figure 5.14).

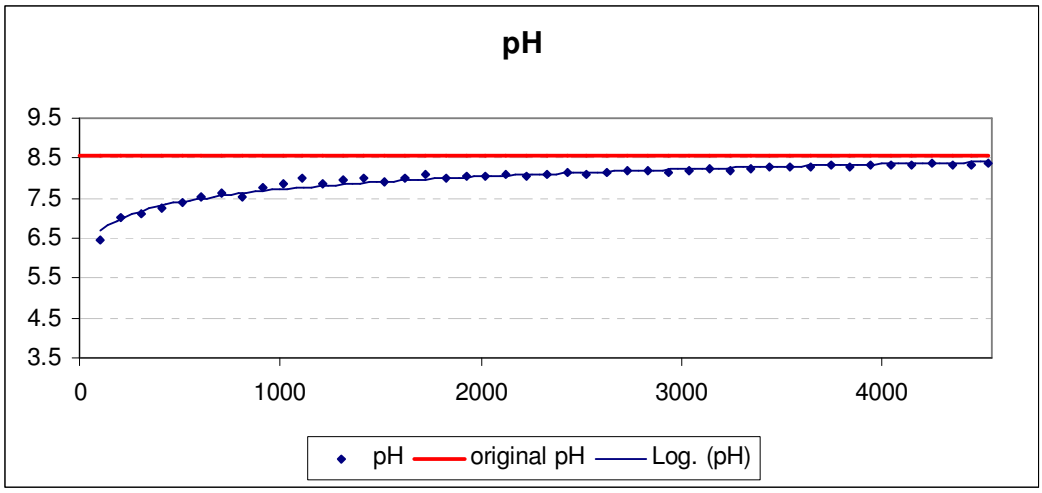

Figure 5.13

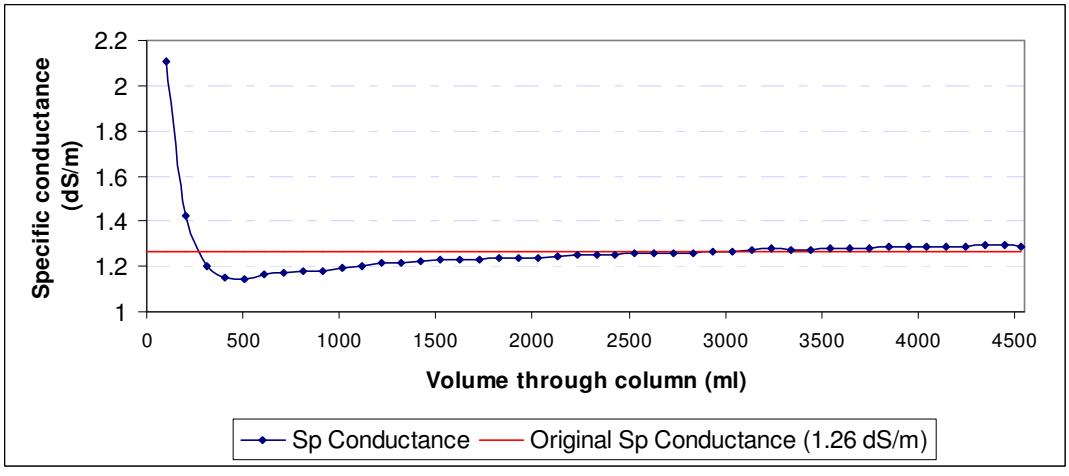

Figure 5.14

Thorough analyses for selected samples (Table 5.7) indicate increased concentrations for some of the original sample constituents in the first sample (sample

n°1), but not for the remaining samples (n°7, n°19, and n°36). For example, TOC increased from 29.2 mg/l in the original feed solution to 216 mg/l in sample n°1, while dissolved carbon dioxide increased from 5 mg/l to 390 mg/l. Sulphate increased from 2.9 mg/l to 28 mg/l, while boron increased from 2.5 mg/l to 67.4 mg/l. Other sample n°1 constituents which increased in concentrations were chloride, manganese, cobalt, nickel and zinc, but their rise in concentration was not as great in comparison to the original feed solution. In any case, for all of these constituents concentrations decreased back to original levels in samples n° 7, n°19, and n°36.

Throughout this experiment, reactive silica concentrations increased to an average of 26.3 mg/l in samples n° 1, n° 7, n°19, and n°36. This is about a 153% increase in concentration in relation to the original feed solution concentration (10.4 mg/l). In addition, aluminium concentrations showed a marked increase in samples n°19 and n°36 (from non-detectable to 0.15 mg/l), whereas fluoride concentrations decreased slightly on samples n°1 and n°7 (21% and 86% of original concentrations) but then showed some increase in samples n°19 and n°36 (153% and 116%).

Alkalinity decreased from 488 mg/l as $CaCO_3$ (original feed solution) to 278 mg/l as $CaCO_3$ in sample n°1, but subsequent values of alkalinity increased to about the same concentration as the original feed solution concentration in samples n° 7, n°19, and n°36 (Table 5.7). Consequently, bicarbonate and carbonate concentrations followed a similar trend in concentration (a decrease followed by an increase).

In some of the earlier experiments it was not possible to calculate the total sodium absorption capacity (due to lack of data), so the theoretical sodium absorption was calculated instead. This calculation consisted of integrating the trendline equation describing its breakthrough, and subtracting this value from the total sodium content over the treated volume range. This also helped to verify total sodium absorption results when it was possible to calculate these. Table 5.8 shows the theoretical sodium absorption values calculated for experiments n°1-7. This calculation procedure provides a good estimate for the missing value for total sodium absorption in experiment n°1, and it compares well with the rest of the experiments, except for experiment n°2. The latter experiment has a difference of 33% between the theoretical value and the value calculated directly from sample analyses, but these differences could be due to the highly

variable results obtained in downflow column operation (channelling and preferential flow) which might have produced a non-representative trendline.

Table 5.8. Total sodium absorption throughout column test experiments

Experiment n°	Solution concentration	total sodium absorption meq/100g	theoretical sodium absorption meq/100g
1	0.01 M NaCl 1180 µm	NA	13.4
2	0.1 M NaCl 600 µm	17.6	11.8
3	0.1 M NaCl 600 µm	40.9	42.8
4	0.1 M NaCl 300 µm	19.3	21.5
5	0.044 M NaCl 600 µm	15.9	15.0
6	0.044 M NaCl 600 µm	16.7	15.9
7	Maramarua CSG water [3)]	11.3	11.7

Notes:

1) Total sodium absorption calculated from remaining sodium concentrations in collected samples
2) Theoretical sodium absorption was calculated by integrating trendline equations and subtracting from the total original concentration over the studied range
3) Equivalent to 0.013 M NaCl

Discussion

Batch tests

Batch tests (Phases I, III, and IV) revealed that Ngakuru zeolites were capable of sorbing sodium cations from concentrated solutions of sodium. This was accompanied by the release of cations, originally contained within the zeolites, and some loss of zeolite mass. Particle size posed no significant effects on the overall process (Phase I). The process by which sodium ions were sorbed into the zeolites can be described as an ion exchange process, and the additional release of ions from the zeolite structure is mainly a dissolution process (Phase II). But, how extensive is the dissolution process in relation to the ion exchange? This question can be answered by closely examining the concentration of the different ions in solution after each batch test experiment.

First of all, there has to be an ion exchange process taking place between sodium ions in solution and cations within the zeolite. This is because sodium concentrations in the remanent solutions were lower than in the original solutions at the start of the batch tests. The ion exchange process taking place between the zeolites and the sodium solution

can be described using Figure 5.15. The arrow pointing towards the zeolite represents the cations being sorbed by the zeolite (sodium), whereas the arrow pointing away from the zeolite represents the cations being released (calcium, magnesium, potassium, and hydrogen) – if these cations are the only ones being released, then the difference (on the basis of charge) between the sodium cations being sorbed and the sum of potassium, magnesium, calcium, and hydrogen ions being released has to be zero. If this value is not zero, then that means there is a cation contribution not being accounted for, which could be explained by zeolite dissolution. Table 5.4 shows these differences for Experiment n°1 in phase IV. Here, eventhough potassium concentrations are unknown, the charge balance is zero for runs n° 1, 3, 4, and 5. Therefore, for these runs, the ions involved in the exchange were sodium (in solution) and magnesium, calcium, and hydrogen (originally in the zeolites). Since the difference in charge balance was nil, then there were no cations being released as a consequence of zeolite dissolution.

Table 5.4 also shows that there is a large mass loss (about 85%) between the first and the last experimental runs (runs n°1 and n°11). This should have produced a significant ion imbalance, particularly during the first experimental runs where dissolution was the highest (i.e. 36% after the first service run). However, cation differences (charge balance) remained low and similar experiments revealed no anion dissolution (sulphate or chloride). What could have happened was mechanical breakup of the zeolite material. That is, a given 1180 µm particle could have been broken into smaller pieces due to collisions with other particles during shaking. These particles could have kept disintegrating with increasing shaking, but absorbed cations could have still remained trapped by these smaller zeolite particles. Indeed, with increasing shaking the zeolitic solution appeared brownish in colour due to this mechanical breakup. Later, flow-through experiments (carried out without mechanical shaking) showed that, as sodium loaded solutions percolated through the zeolite column, some dissolution did take place at the beginning of each experiment (brownish colour). However, after the first couple of aliquots had been collected, the solution became clear in colour, which shows that dissolution had stopped soon after the first aliquots had gone through. Therefore, the loss of mass in batch tests is mainly due to mechanical shaking.

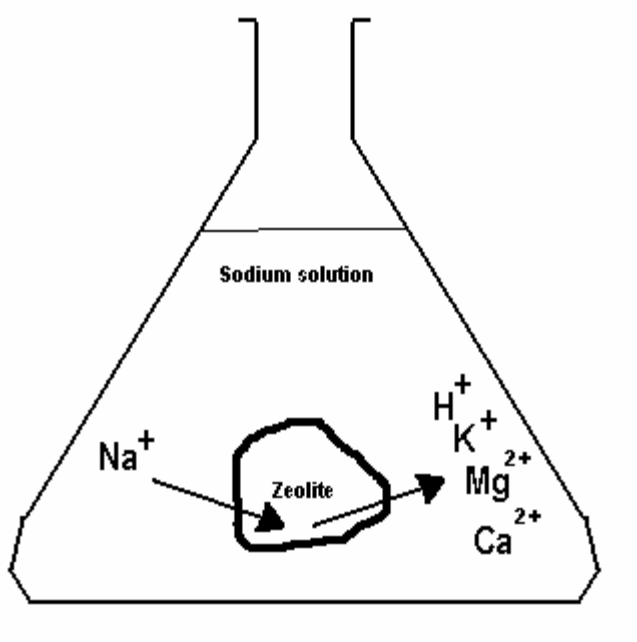

Figure 5.15. Ion exchange process with sodium solution and Ngakuru zeolites

Up to this stage it looks like there is no dissolution taking place, but anions could also be dissolving from the zeolites, and the remaining batch tests exhibited some charge balance differences. However these zeolites have an electron-deficient crystalline lattice, and they form an overall-negatively charged silicate structure which can hold positively charged salts. Also, chloride and sulphate are not dissolving as shown by runs n°4 and 5 in experiment n°1 (Phase IV). In addition, if considerable dissolution had taken place throughout these experiments, this would have been accompanied by a significant increase in specific conductance, but the experiments in phase II exhibited only a minor increase, which suggests a low level of dissolution did occur. Also, batch experiments with deionised water and a low-concentration NaCl solution (see Table D.3) suggested that the dissolution process is highly dependent on the ionic strength of the solution being treated. Therefore, it is possible that dissolution is enhanced when the zeolites are exposed to strong alkali or acid solutions, as observed in some runs during Experiment n°1 (Phase IV).

Runs n° 2, 6, and 8 in Experiment n° 1 showed important differences in charge balance (Table 5.4). However, these were regeneration runs carried with strong acid or concentrated solutions (alkali). Run n°2 showed a significant difference, but this could have been due to the release of potassium, which was not measured at the time. Most

likely, this could have been the consequence of zeolite dissolution due to the strong acid (0.1 M HCl) used for regeneration. Runs n° 6 and 8 also exhibited differences, though not as considerable as the one in run n°2; at the end of these runs, potassium concentrations were nil, which suggests these differences are a consequence of dissolution. Run n°11 was a service run, and its charge balance difference was again relatively low. Except for run n°2, in all of these cases differences in charge balance were low in comparison to the actual cations being exchanged, which suggests that an overall low level of dissolution took place.

Batch testing (Phase IV - experiments n°1-n°5 in Table 5.2) also showed that it is possible to regenerate Ngakuru zeolites for further use with different types of solution. However, repeated cycles of service/regeneration resulted in significant loss of mass, which could have practical implications for zeolite reutilisation. For example, experiment n°1 yielded good results (Table 5.4) with concentrated solutions of HCl, $CaCl_2$, and KCl, but after 11 exposures the zeolite mass was reduced by about 15%. With NaOH, sodium sorption during service runs increased from 10.8 meq/100g (no previous regeneration) to 13.1 and 21.2 meq/100g after regenerating with 0.1M HCl and 1M HCl respectively. A similar exchange capacity enhancement was noted after each regeneration cycle in experiments n°2-n°5. This exchange increase is due to the regenerant displacing sodium and other occluded salts, thus making more sites available for the exchange during the service run. Also, an increase in regenerant concentration forces more sites to become available due to a more extensive exchange during the regeneration phase. For instance, after regenerating with $CaCl_2$ in experiment n°1 (runs n° 6 and n°8) sodium sorption decreased to 5 and 8 meq/100g, however after regenerating with KCl (run n°10) this value increased to 16.6 meq/100g. This suggests that higher valence cations (for example Ca^{2+}) are more difficult to remove from the zeolite lattice than cations having the same balance (K^+ or H^+) as the cation to be exchanged in solution (in this case Na^+).

Batch absorption experiments n°1-n°5 also hint that it is possible to regenerate these zeolites virtually indefinitely. However, in experiment n°1 after 5 service/regeneration cycles, mechanical shaking reduced zeolite mass significantly (83.3%). This same effect was noted in experiment n°2 where, after 4 service/regeneration cycles, the zeolite original mass was reduced to 65.4%. Similar

results were obtained in experiments n°3 – n°5, which indicates that with more service/regeneration cycles the zeolites are increasingly exposed to mechanical wear and tear. In addition, this effect could have been exacerbated when strong acids were used for regeneration.

These experiments also showed that the major cations intervening in the exchange reactions were sodium, calcium, magnesium, and potassium (Table 5.1in the main body of this chapter and Tables D.2-D.5 in Appendix D). Once these experiments had finished, calcium, magnesium and potassium were detected in experiment samples which indicated that these salts were originally occluded within the zeolites. Low charge balance results (~0 meq/l) including sodium as the absorbed cation (Figure 5.15) corroborates this conclusion; hydrogen ions also were exchanged, but their concentration was too low to influence the final balance. In experiment n°1, the first regeneration run yielded a 13.7 meq/l charge balance difference, but it was not possible to measure potassium in the final solution resulting from the regeneration and it was suspected this difference was mainly the unmeasured potassium cation. Differences of up to 1.2 meq/l were detected in some of the samples in this experiment (runs n° 6, 8, 9, and 11 in Table 5.4), but these could be attributed to experimental errors during the measuring process. Low charge balance results were obtained in experiment n°2 (Table D.5, Appendix D). The exceptions in this experiment are runs n°3-n°6 and n°8, but these differences are explained because it was not possible to measure potassium in runs n°3, 6, and 8, and there could have been significant systematic errors while measuring sodium in runs n°4 and n°5 (sodium probe is not 100% accurate). Similar results were obtained in experiments n°3-n°5.

Throughout batch tests, the total cations being exchanged were calculated by analysing the differences in concentration between the initial solution and the final (treated) solution. Thus, for the sodium ion this capacity ranged from 5.0 to 34.3 meq/100g depending on the solution concentration and the number of times the zeolites had been regenerated. These results were later used in flow-through experiments as initial estimates of total zeolite capacity. This was useful in the design of experiments so that enough volume of sodium solutions was available to carry out these experiments. In addition, flow-through tests were designed to address the issues arising from batch test experimental results. For example, flow-tests were designed so that they gave an

indication of the kinetics of the ion exchange process, gave adequate quantification of the dissolution taking place, and provided better accuracy to confirm batch test findings.

Flow-through tests

Column tests using Ngakuru zeolites and sodium-loaded solutions confirmed these materials' ability to remove sodium cations. This was done by carrying out charge balance calculations between absorbed sodium cations and released cations in each recovered aliquot. In flow-through experiments n°1-n°5 it was not possible to measure potassium cations, and the accuracy of the sodium probe used in these experiments is not as good as the accuracy that could be obtained with an APHA certified method. Therefore, these experiments were not considered when carrying out charge balance calculations. On the other hand, samples resulting from experiments n°6 and n°7 were analysed through a certified laboratory (Hill Laboratories), which enabled accurate mass balance calculations.

Operational Issues in Experimentation

Throughout flow-through tests, a number of operational issues were observed while carrying out these experiments. For instance, in experiments n°1 and n°2 preferential flow or channelling was observed as the feed solution dripped in downflow mode into the ion exchange column. This translated into an inefficient use of the packed zeolite column, so subsequent experiments were conducted in upflow mode instead. These inefficiencies were fairly noticeable as even minor variations in flow impacted on experimental outcomes. This was evident with experiment n°3, where the 8^{th} 100 ml sample aliquot had significantly lower sodium concentrations than what could have been expected by following the experimental trendline (Figure 5.16) . This is due to an experimental error – this experiment was conducted with a cork stopper in place at the top end of the column. Fine sediment started to accumulate on the surface just over the orifice through which treated water flowed outside the column into a sampling collection bottle (Figure 5.17). To remediate this, the cork stopper was removed, but as soon as this happened, there was a sudden pressure loss, and a sudden drop in water level took place.

As a result, some of the treated solution went back into the zeolite bed so there was an overall increase in retention time which resulted in higher sodium removal.

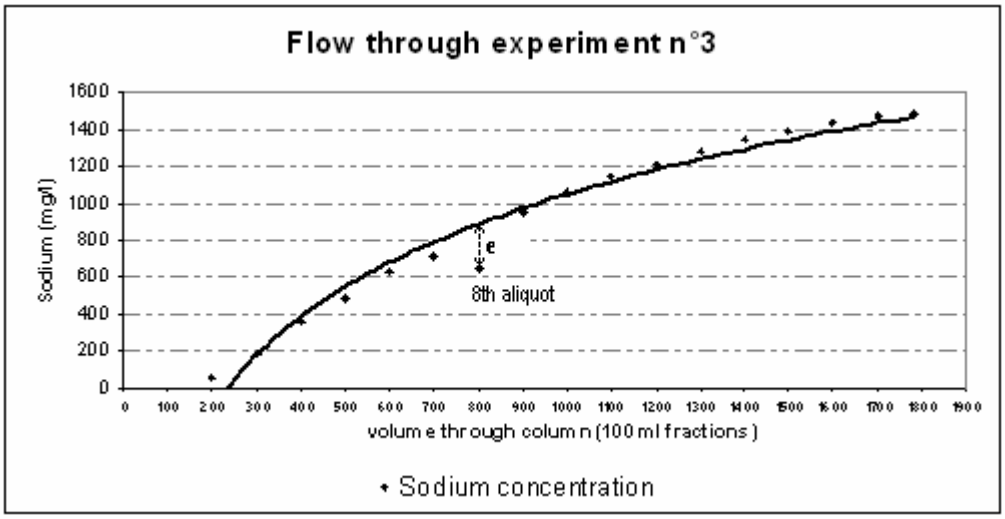

Figure 5.16.

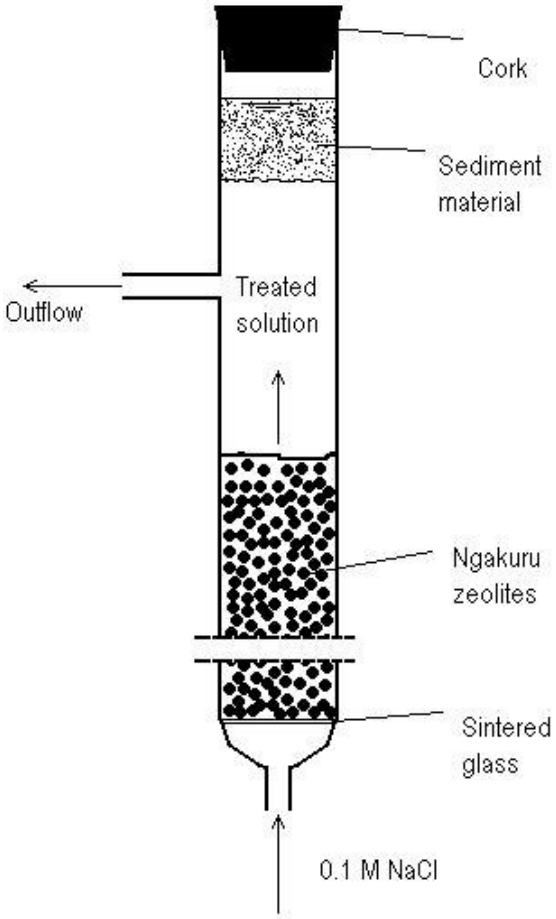

Figure 5.17. Sediment build-up in experiment n°3.

When particle size was small (<300 µm) and service rates were high enough (>15 cm^3/min), the zeolitic material inside the column became buoyant and the material exhibited fluid behaviour. This was observed in pre-trials and at the top of the ion exchange column in experiment n° 4. Mobility of zeolite material inside the column generates operational problems because, when this takes place, zeolites are carried out of the ion exchange column with the treated solution. In addition, this could reduce the contact time between the feed solution and the zeolite material generating lower exchange rates. Therefore, small particle sizes were avoided and service flow rates were kept as low as was practical given the equipment available..

Other sources of experimental errors were the first 100ml aliquots collected at the start of the experiments which had previously undergone rinsing with deionised water. These initial samples had been "contaminated" with deionised water as they contained little or no sodium, calcium, and magnesium cations. Experiments n° 3 and 4 experienced these type of problems, so the first 100 ml aliquots resulting from these experiments were discarded from further analyses (Tables D.11 and D.12, Appendix D). In addition, in experiment n°4 the original NaCl concentration was 0.1M, but this value could have increased due to water evaporation from the heated beaker. This possibility is supported by the last two outflow samples resulting from the column test experiment (Figure D.4, Appendix D) which present higher concentrations than the one corresponding to the original feed solution.

Analytical issues

Charge balance results from experiments n°6 and n°7 are presented in Figures 5.18 and 5.19. Except for the first samples (sample n°1 in experiment n°6 and samples n°2 and n°3 in experiment n°7), charge balance results are fairly low and almost within the ±1 meq/l range. These low charge balance results in recovered aliquots indicate that the main exchange processes taking place solely involve calcium, magnesium, and potassium. Hydrogen ions are also being exchanged, but their concentrations were too low to pose a significant impact in the final charge balance results. Differences in charge balance are likely to be a product of minor zeolite dissolution throughout these experiments. This was especially noticeable with sample n°1 in experiment n°6 and

samples n°1 & 2 in experiment n°7, which presented an increased net charge balance concentration for the cations being analysed (Figures 5.11 and 5.12). In addition, there was a Specific Conductance increase detected in samples n°1 & 2 in experiment n°7 (Figure 5.14), and this would have been mainly a consequence of an increased concentration of TOC, sulphate, reactive silica, and boron (Table 5.7). Because SiO_2 has no charge, TOC, sulphate, and boron would have contributed significantly to the charge imbalance throughout these experiments.

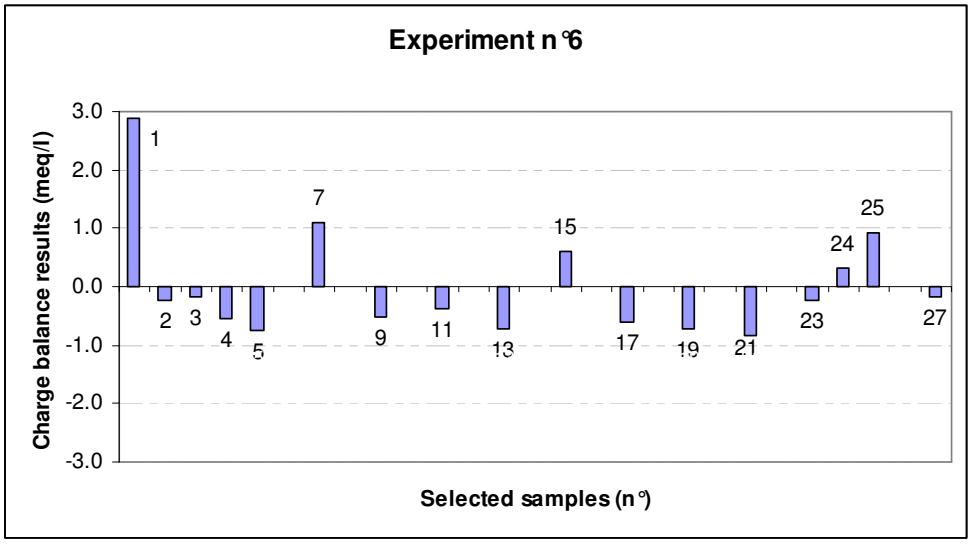

Figure 5.18. Charge balance results for selected samples in experiment n°6

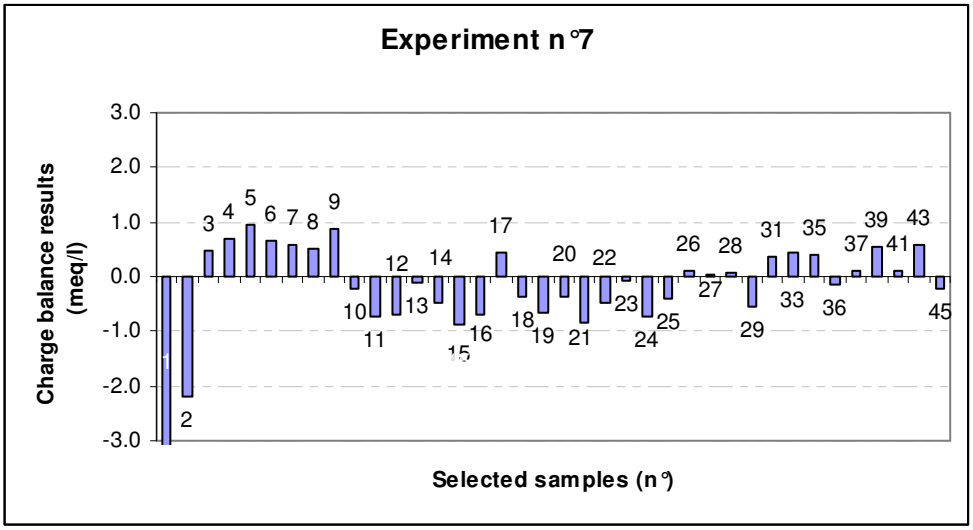

Figure 5.19. Charge balance results for selected samples in experiment n°7. Sample n°1 is off the chart with a net difference of -8.9 meq/l.

Differences within the ±1 meq/l range could have also been attributed to the accuracy of the analytical method used in the laboratory. However, the method used by Hill Laboratory was APHA 3125-B (Inductively Coupled Plasma) with very low detection limits (<0.05 mg/l) and very good accuracy, so charge balance differences are not likely attributable to the accuracy of the measuring procedure.

High potassium, calcium, and magnesium concentrations at the start of this experiment (Table 5.6) suggest dissolution of these cations along with the exchange process. Sodium could have also dissolved from the zeolites at the beginning of the experiment, and this could have generated the unusually high sodium concentrations detected in the first two 100 ml aliquots. In addition, other elements like chloride, manganese, cobalt, and nickel (Table 5.7) would have contributed with low quantities of additional ions, dissolving from the zeolites, as the feed solution passed through the ion exchange column. In experiment n°7, after 200 ml of feed solution had passed through the column, one concludes that the dissolution processes stopped almost completely as seen by a reduction in specific conductance to values nearing the original value (Figure 5.14). In addition, TOC, sulphate, boron, chloride, manganese, cobalt, and nickel concentrations were reduced to about the same ion concentrations as the ones for the original (untreated) sample (samples n° 7, 19, and 36 in Table 5.7). However, reactive silica concentrations for these samples remained higher than the original sample's concentration, which suggests that the dissolution process had not completely stopped. Fluoride and aluminium concentrations also showed some increase at the end of this experiment. In fact, a slight increase in specific conductance values is observed after the third aliquot in Figure 5.14 and, by the end of the experiment, specific conductance had surpassed the conductance for the original (untreated) CSG water.

Sodium absorption capacity

Sodium absorption from feed solutions throughout these experiments decreased almost logarithmically, with the highest sodium absorption taking place at the start of each experiment, and the lowest taking place at the very end. These breakthrough curves represent the total sodium absorbed by the zeolites, which can be expressed in terms of the zeolite mass being used, to give an indication of the total sodium absorption capacity

(Table 5.8) per 100g of zeolites (meq/100g). Sodium absorption values were generally lower than the CEC values reported by Mowatt (2000) (40-110 meq/100g), which is logical because in CEC determinations zeolite samples would typically be leached with 1M solutions of ammonium acetate and sodium chloride (Blakemore et al., 1987). As discussed in the batch absorption experiments section, the cation exchange process is highly influenced by the concentration of the leaching solution – the higher the concentration, the more extensive the cation exchange process. Since, the concentration of the feed solutions used in flow experiments n°1-7 was lower than or equal to 0.1M NaCl, the cation exchange processes would have not been as extensive as the one in a typical CEC determination. Therefore, the total sodium absorption capacity reported in these experiments is lower than reported CEC values.

The highest sodium exchange was obtained in experiment n°3 (40.9 meq/100g) which took place under a 0.1M NaCl feed solution and with prior 1M KCl regeneration. In the rest of the column test experiments, sodium absorption was in the 11-20 meq/100g range, but none of the zeolites in these experiments had undergone such a strong regeneration (i.e. 1M KCl) process. The second highest sodium absorption rate was obtained in experiment n°4, which was carried out with a heated (40°C) 0.1M NaCl solution, however the total sodium absorption obtained in this experiment was quite similar to the one obtained in experiment n°2, which was identical to n°4 except it was conducted in downflow mode and without heating the feed solution. This is not surprising because the kinetics of ion exchange processes are highly dependent on diffusion within the zeolite, which is temperature dependent in exponential form – a 30°C temperature increase would enhance diffusion by 10% (Slater, 1991). Since in this experiment the temperature was increased only by about 20°C, the effects of this increase were not significant in the overall ion exchange process.

According to results of experiments n°5 and n°6, regeneration with a weak alkali solution (0.044 M $CaCl_2$) increased the sodium absorption capacity of Ngakuru zeolites by only 5%. Although the zeolites absorption capacity did not improve significantly, the regeneration process did restore their initial sodium absorption potential for reuse.

The lowest sodium absorption was recorded with experiments n°1 and n°7, but the feed solutions in these experiments had the lowest sodium concentration although the

flow rates were different. The service flow rate in experiment n°1 was the highest service flow rate used in these experiments (78 cm^3/min), but the service flow rate in experiment n°7 was one of the lowest, therefore service flow rate does not seem to pose major implications for the studied range. This suggests that overall sodium absorption is highly dependent on feed solution concentration (Table 5.8), and this could also influence the efficiency of the regeneration process (i.e. sodium absorption capacity could be significantly enhanced if regenerating with a highly concentrated solution).

For both batch tests and flow-through experiments the total sodium absorption capacity is a function of the time of exposure (shaking time or flow rate), solution concentration, and type of solution being used (strong acid or alkali solution). However, it is possible to make some comparisons. For example, for the 0.013 – 0.044 M NaCl range, the total sodium absorption capacity ranged from 11.3 to 15.9 meq/100g (Table 5.8) for flow-through tests with no regeneration, whereas for batch tests, sodium absorption ranged from 9.6 to 16.7 meq/100g for similar concentrations (0.01M NaCl). These two range of values are quite similar for both types of experiments, which shows how batch tests can be accurate in determining total absorption values before conducting a flow-through experiment.

Kinetics of Absorption

Throughout these experiments, sodium breakthrough curves followed a logarithmic trendline; figure 5.20 shows the shape of the breakthrough curves obtained with Ngakuru zeolites compared against a typical breakthrough curve using commercial resins (Wachinski and Etzel, 1997). In this figure, the breakthrough curve for Ngakuru zeolites reaches an asymptote which is not necessarily the original feed solution concentration. This hints that, at some stage, the efficiency of the exchange decreases but it is still taking place albeit at a lesser rate. This could be due to main exchange sites within the zeolite becoming depleted, and only secluded secondary sites being available for the exchange. In addition, it was not possible to obtain a breakthrough curve for pH in experiments n°1-6, but these values were always below the initial pH, which shows that hydrogen ions also form part of the exchange process, and the final breakthrough limit has not yet been reached. However, in experiment n°7, a pH breakthrough curve (Figure

5.13) follows the same logarithmic trendline as the sodium breakthrough curve, marking the end of the experiment. The same holds true for calcium, magnesium, and potassium cations released from the zeolites (Figure 5.10). This shows that, as the availability of sites decreases, the exchange process slows down to a minimum, with less calcium, magnesium, potassium, and hydrogen ions in the zeolite being exchanged for less sodium ions in solution.

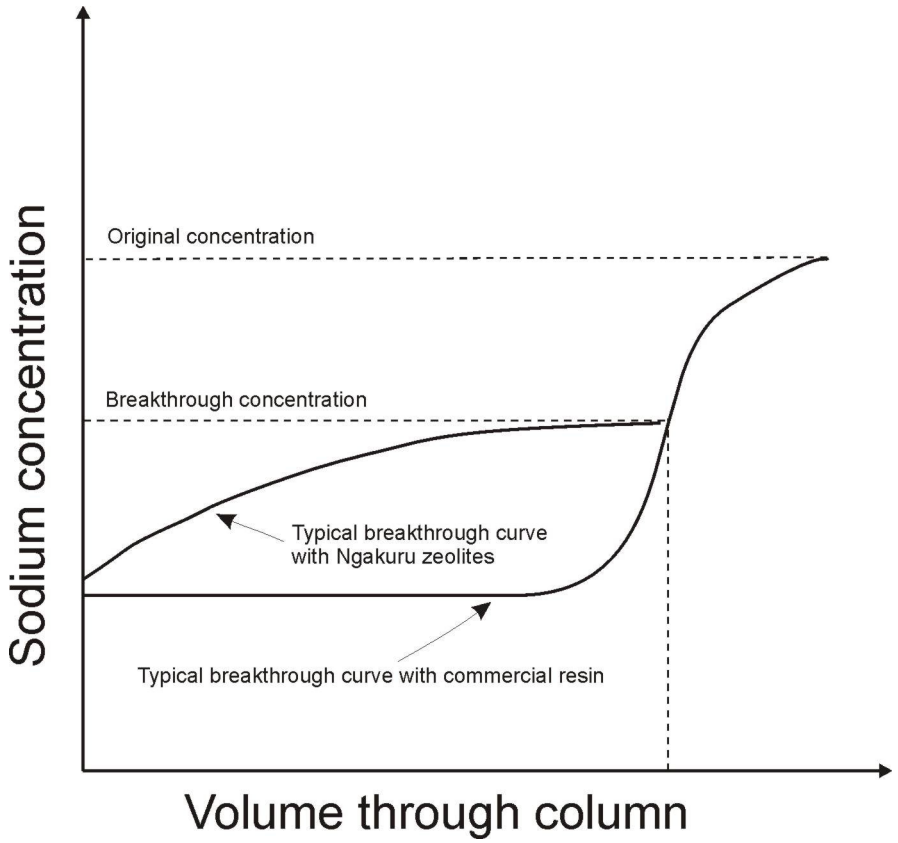

Figure 5.20. Comparison between Ngakuru zeolites and typical commercial resin breakthrough curves. Adapted from Wachinski (1997)

In addition, pH values in the flow-through experiments were about 1 to 2 pH units lower than pH values in batch experiments. Again, this could be due to exchange sites being depleted in the zeolite material once enough sodium cations are absorbed – in the case of flow through tests, the experiments were stopped before or at this point, but in batch tests the zeolites could have continued exchanging ions except, in this case, in reverse order. That is, sodium ions already within the zeolites could have been exchanged for hydrogen ions in the solution. As a consequence of this, pH in batch tests was higher than in flow-through tests.

In general, the separation factor (R) for experiments n°6 and n°7 was greater than 1 but less than 2 and, for most of the aliquots, closer to one. According to the classification of Isothermal Breakthrough Cases presented in Perry et al.(1973), this case corresponds to an *unfavorable equilibrium* (R>1), but very close to linear equilibrium (R=1). This description explains the raw breakthrough curves (meq/l vs. litres through column) obtained throughout these experiments and described in Figure 5.20 –Ngakuru zeolites are not as efficient as commercial resins for ion exchange applications involving sodium removal.

Implementation Issues

Experiment, n°7 showed that Ngakuru zeolites are able to remove sodium cations from CSG waters when operating in flow-through mode. The effectiveness of the CSG water treatment process can be evaluated by determining whether the outcome of the treatment process fits the requirements prescribed in guidelines for assessing sodicity effects. For example, according to FAO guidelines (Ayers et al., 1985), sodium toxicity effects from the treated CSG water in experiment n°7 are nil for the first five 100 ml aliquots, while treated aliquots n° 6 - 28 could induce slight to moderate effects; the last 17 samples could generate severe effects because the SAR of these values is higher than nine, which is the lower limit for severe effects.

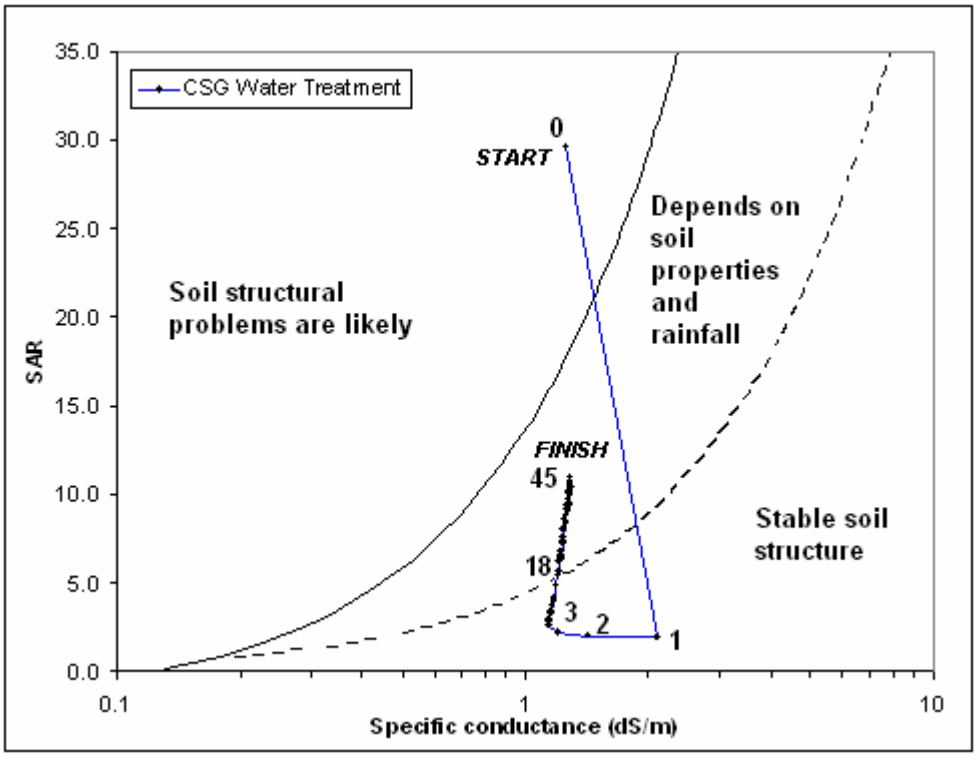

Figure 5.21. Effectiveness of zeolite treatment system for experiment n°7

In addition, the effectiveness of the zeolite treatment system to reduce infiltration problems (due to high SAR) can be assessed using the ANZECC guidelines. For this purpose, a plot of the treated effluent aliquots is presented in Figure 5.21. This plot shows that the initial value (sample n°0) is in the zone where "soils structural problems are likely", but the zeolite treatment system effectively shifts this position into the stable soil structure zone and into an intermediate zone where soil properties and rainfall play a more important role. Figure 5.21 shows that for the first 18 treated aliquots the zeolite treatment system is effective in completely eliminating potential soil infiltration problems, however for the last 27 aliquots the system starts to lose its effectiveness because the treated CSG water falls in the zone where infiltration problems "depend on soil properties and rainfall". However, according to the ANZECC soil salinity/sodicity model, the long term changes in ESP for samples n° 18-45 would be significantly reduced. For example, long term ESP values could increase as high as 34.5% if CSG water remains untreated while being disposed on the land, but with the zeolite treatment system the highest expected ESP value would be only 13% (sample n° 45).

The long term soil ESP reduction with the zeolite treatment system can also have positive effects in terms of soil salinity. For example, in experiment n°7, even aliquot n°45 would improve soil response in up to 100% for moderately sensitive crops (six soil samples in Chapter 4). In contrast, if the same soil samples were exposed to untreated CSG water (Chapter 4), one only three out of the six soil samples would be able to produce 100% yield with moderately sensitive crops according to salinity calculations (see Chapter 4).

These flow-through experiments show encouraging results for the potential treatment of CSG waters with natural zeolites. However, implementing this treatment system on site could be complicated due to operational complications (constant monitoring, specialised laboratory equipment for measuring breakthrough, and trained personnel). On the other hand, batch treatment could be more simple to implement, but the way this could be carried out would have to be after carrying out flow-through experiments to determine adequate retention times and volume of zeolite material. Therefore, a combination of these two systems would be highly effective for simplicity and ease of implementation (semi-batch operational mode). Consequently, a proposed methodology for carrying out CSG water treatment using Ngakuru zeolites is the following one:

1) Select a zeolite particle size which fits operational requirements. The recommended particle size range is 600-2360 µm. Smaller particle size would prove difficult to work with, but it is possible to work with sizes larger than 2360 µm.
2) A laboratory batch test is carried out to determine the maximum sodium absorption capacity. This results in a rough estimate of the sodium absortion capacity, which is used to design the experimental setup in step 3.
3) A flow-through experiment is carried out under laboratory conditions. This results in a more accurate determination of the sodium absorption capacity of the zeolites, while making it possible to calculate the retention time to be used with a given flow rate, mass, and zeolite

volume. Steps 2 and 3 would have to be carried out every time zeolite quality is thought to have changed (i.e. zeolites from a different quarry) and for each new well having a different CSG water quality.

4) Scale up. Zeolite mass is calculated according to a given volume of water to be treated using the calculated retention time. This can be implemented on site by digging holes in the ground, which can be lined with concrete, asphalt, or an impermeable liner. The holes are then filled with a pre-calculated amount of zeolite material (zeolite pits).

5) CSG water treatment: the calculated volume of CSG water is fed into the zeolite pits. Eventhough this is not a columnar application, it is recommended to introduce the CSG water into the zeolite pits in upflow mode, mainly to provide adequate mixing throughout.

6) Once the CSG water has been mixed and has remained in contact with the zeolites for the prescribed amount of time, the treated water can be removed from the pits either by gravity drainage (if the site topography permits it) or by using a capable pump. This water could temporarily be stored in ponds to manage its disposal. The treated water can then be used for irrigation applications or safely disposed on land, or selected rivers or streams.

7) The next step is to regenerate the zeolites, and this can be accomplished with concentrated calcium solutions following the same procedure as in steps 2-6. Alternatively, the used zeolites can be completely discarded and a fresh batch of zeolite material can be used instead. If regeneration is selected, then the concentrated wastewater resulting from this process would be of low volume, and it could be hauled to a water treatment facility or evaporated on site.

This methodology is just a framework as the ultimate treatment solution would depend on factors like CSG water quality and quantity, location, topography, regulatory requirements, and stakeholder involvement. For example, the water quality from a given site might be of very poor quality (high SAR) and extensive treatment might be required ,

prior to disposal, if the volume of co-produced CSG water is large. Extensive treatment might also be required if the local council puts this as a condition due to, for example, sensitive receiving environments downstream from CSG mining operations. Under these conditions, multiple zeolite pits could be put in service, in parallel or in series, to continuously treat large volumes of CSG waters to a desired level (i.e. quantity and quality). Site topography and location can play a very important role in disposing of the treated water. If topography permits it, receiving ponds could be built downstream from the zeolite pits so that these can be drained by gravity without having to use specialised pumps. If there is high water demand, due to nearby agricultural activities for example, then this water can be put to good use in irrigation applications. Alternatively, treated CSG water could be safely discharged into a river or stream so that downstream users can safely abstract river water.

Conclusion

This research has chosen to examine, in a broad overview, the potential for natural New Zealand zeolites to aid in the treatment of New Zealand CSG waters. The results from these preliminary experiments indicate that Ngakuru zeolites show promise in removing sodium cations from sodium-loaded solutions and Maramarua CSG waters, though it is not clear yet that they will provide a practical treatment option. Whether operating in batch or columnar mode, Ngakuru zeolites were able to absorb sodium cations from feed solutions while releasing calcium, magnesium, some potassium, and at a lesser extent hydrogen.

Some minor dissolution was detected with batch experiments, and this was later measured in a column test. Initially, zeolites will dissolve and release sulphate, boron, TOC, sodium, calcium, magnesium, potassium and reactive silica, but these dissolution processes will practically stop soon after the first batches of feed solution have passed through the column. The only exception is reactive silica dissolution which will continue throughout the ion exchange process. In any case, the increase in silica concentration was small and was not accompanied by a significant increase in aluminium concentrations.

This work did not include a detailed study of zeolite dissolution because it is not likely a dominant process occurring during any practical application of zeolite treatment of CSG water, eventhough preliminary studies indicate this dissolution would be noteworthy. It was inferred from this study that dissolution is a function of solution strength, and to fully assess zeolite dissolution, it would have been necessary to carry out zeolite dissolution experiments with different types of CSG waters (i.e. different ionic strengths) including deionised water. From a practical aspect, dissolution effects can be stopped almost completely if the zeolites are pre-washed before being used. This can be accomplished with CSG water, and the resulting wastewater will be of such low volume that it can be diluted with treated water as the treatment process continues. Further research would be needed into whether the advantages of pre-washing (e.g., removal of sediments and undesirable ions) would outweigh the disadvantages (e.g., having sediments and undesirable ions present in the first flush of treated effluent).

Although small particle size should improve reaction kinetics, in this case particle size did not pose a major impact in the cation exchange process for the studied particle size range. However, in columnar mode, small particle sizes caused some operational problems like sediment accumulation and buoyancy inside the column, and this was the overriding factor in determining the correct particle size.

The calculated sodium absorption capacity for Ngakuru zeolites under flow-through conditions without previous regeneration ranged from 11.3 meq/100g to 16.7 meq/100g. However, it was found that this value could be significantly enhanced if the zeolites were regenerated or pre-treated with a strong alkali solution (i.e. 1M KCl).

Batch absorption experiments provided a good opportunity for calculating preliminary absorption values, but these experiments gave no insight into the kinetics of the exchange process. On the other hand, flow-through experiments allowed for more accurate calculations while providing the means for monitoring the exchange process as the capacity for sodium removal was exhausted. Flow-through experiments showed that reaction kinetics are generally too low to obtain maximum removal efficiency in columnar mode (*linear* or *unfavourable*). As flow-through experiments were carried out, outflow concentrations increased logarithmically until reaching an asymptote or experimental breakthrough. Nevertheless, the benefit of carrying out flow-through treatment resides in having control of the process, while being able to discriminate between good water quality at the beginning of the treatment process, and not-so-good water quality at the end of it. This suggests that probably the best way to carrying out on-site treatment using Ngakuru zeolites is by using a semi-batch operational mode.

With Ngakuru zeolites, the rate at which the exchange takes place is highly dependent on solution concentration, and the corresponding breakthrough curve follows a quasi-logarithmic trendline reaching an asymptote having a lower concentration than the one for original feed solution. The difference between this asymptote and the original feed solution corresponds to an additional absorption capacity, which is accessible but at very slow exchange rates. In theory, the exchange rate could be improved if a finer particle size is used accompanied by lower flow rates, however this would have to be done with care to avoid operational problems. Heating the feed solution might also improve the exchange rate, but this is not practical because the feed solution would have

to be heated significantly to produce just a low improvement of the exchange rate (i.e. a 30°C increase would provide a 10% improvement).

CSG waters constitute a new wastewater in the New Zealand landscape, and they require sound local solutions for their treatment and disposal. Column test experiment n°7 showed that it is possible to treat these waters with Ngakuru zeolites. Sodium removal was accompanied by the release of calcium and magnesium from the zeolites, which had a water conditioning effect by reducing SAR values. Therefore, this treatment was successful in reducing ion toxicity issues, salinity, and infiltration problems associated with high sodium concentrations. In practical terms, in experiment n°7 180 grams of Ngakuru zeolites were able to reduce the specific sodium toxicity from "severe" to nil in the first 509 ml of CSG water undergoing zeolite treatment, and to "slight to moderate" in the next 2325 ml. Simultaneously, likely soil infiltration problems were reduced to nil in the first 1825 ml to slight (lower ESP increase) in the following 2705ml of CSG water. If the treated water is used for irrigation, reducing soil infiltration problems would reduce soil salinity, thus providing better crop yields.

Treating CSG waters with Ngakuru zeolites has the potential to transform a potential wastewater into a valuable resource. These materials are readily available in New Zealand at less than 0.5% of the cost of synthetic materials. If operated in semi-batch mode, this treatment system can be implemented with ease and with little or no specialised on site equipment if preliminary studies have previously been carried out (i.e. in a laboratory). The footprint left by this treatment system could be larger than with commercial resins, but the same facility can be used to treat CSG waters from different wells. The main advantage of treating CSG waters using natural zeolites is the reduction of SAR levels in these waters, thus making them suitable for irrigation applications. Even if the treated waters are not directly used for irrigation, the risks associated with their disposal (land or surface waters) are significantly reduced through zeolite treatment.

The exhausted zeolite bed can be regenerated for reuse using alkali solutions (i.e. $CaCl_2$); if strong concentrations are used this can even result in enhancement of the treatment system. On the other hand, the zeolites could be used only once and then discarded (without being regenerated) or used in another application. For example, the

sodium-loaded zeolite could be used in water softening or stock feed applications. In New Zealand, groundwaters are not generally hard (high calcium and magnesium), but there are isolated occurrences of hard water like, for example, waters with elevated magnesium in the Tasman District (Rosen, 2001). Sodium-loaded zeolites, a by-product of CSG water treatment, could be used at these locations to soften hard water. In this case, sodium in the zeolites would be exchanged for calcium or magnesium in the water. Resource Refineries currently sells zeolite material under the "NuFeed" brand for addition to livestock rations. In this particular application, the zeolites exchange ammonia cations in the animal digestive track for occluded salts (calcium, magnesium, and potassium) in the zeolite material. In addition, the zeolites can absorb mycotoxins and carry them safely through the digestive track. Sodium-loaded zeolites could easily be used in these sorts of applications. These "treated" zeolites would more readily exchange sodium with ammonia cations in the digestive track and would improve overall animal health by providing animals with sodium.

In sum, zeolites can be regenerated, re-used in reverse ion exchange treatment solutions, or used in agricultural applications. However, the ultimate way in which zeolite treatment solutions are implemented will depend on water quality, local regulations, and stakeholder involvement.

References

American Public Health Association., American Water Works Association., and Water Environment Federation., 1999, Standard methods for the examination of water and wastewater: Washington, D.C., American Public Health Association, 1 computer optical disc p.

ANZECC, and ARMCANZ, 2000, Australian and New Zealand Guidelines for Fresh and Marine Water Quality, ACT: Australian and New Zealand Environmental and Conservation Council (ANZECC), Agricultural and Resource Management Council of Australia and New Zealand (ARMCANZ): Canberra.

Ayers, R.S., Westcot, D.W., and Food and Agriculture Organization of the United Nations., 1985, Water quality for agriculture: Rome, Food and Agriculture Organization of the United Nations, xii, 174 p.

Blakemore, L.C., Searle, P.L., Daly, B.K., and New Zealand. Soil Bureau., 1987, Methods for chemical analysis of soils: Lower Hutt, N.Z., NZ Soil Bureau Dept. of Scientific and Industrial Research, 103 p.

Bolan, N.S., and Mowat, C., 2000, Potential value of zeolite in the removal of contaminants from wastewater stream, Water 2000, Water Conference and Expo, "Guarding the Global Resource": Auckland, NZWWA, p. 430-443.

Christie, T., Brathwaite, B., and Thomson, B., 2002, Mineral Commodity Report 23 - Zeolites, New Zealand Mining, Volume 31.

Coombs, D.S., 1959, Zeolite uses and New Zealand deposits, Fourth Triennial Mineral Conference, Volume 6, Paper 162: School of Mines and Metallurgy, Dunedin, University of Otago, p. 6.

Hach Company, 2003, Water analysis handbook : drinking water, wastewater, seawater, boiler/cooling water, ultrapure water: Loveland, Colo., Hach, 1268 p.

Mowatt, C., 2000, Preliminary investigations into the characteristics and potential uses for Ngakuru zeolites, 2000 New Zealand Minerals & Mining Conference Proceedings.

Nelson, C.R., 2005, Geologic assessment of the natural gas resources in the Powder River Basin Fort Union Formation coal seams, Proceedings - International Coalbed Methane Symposium, Volume 2005, p. 14.

Nguyen, M.L., and Tanner, C.C., 1998, Ammonium removal from wastewaters using natural New Zealand zeolites: New Zealand Journal of Agricultural Research, v. 41, p. 427-446.

NZ Natural Zeolite, 2006, What is Zeolite?, www.zeolite.co.nz.

Perry, R.H., Chilton, C.H., and Perry, J.H., 1973, Chemical engineers' handbook: Tokyo, McGraw-Hill Kogakusha, 1 v. (various pagings) p.

Rosen, M.R., 2001, Hydrochemistry of New Zealand's Aquifers, *in* Rosen, M.R., and White, P.A., eds., Groundwaters of New Zealand: Wellington, New Zealand, New Zealand Hydrological Society, p. 77-110.

Slater, M.J., 1991, Principles of ion exchange technology: Oxford [England] ; Boston, Butterworth Heinemann, xiii, 182 p.

Taulis, M., Milke, M., Trumm, D., O'Sullivan, A., Nobes, D., and Manhire, D., 2005, Characterisation of Coal Seam Gas waters in New Zealand, 2005 New Zealand Minerals Conference: Auckland, New Zealand.

Van Voast, W.A., 2003, Geochemical signature of formation waters associated with coalbed methane: Aapg Bulletin, v. 87, p. 667-676.

Wachinski, A.M., and Etzel, J.E., 1997, Environmental ion exchange : principles and design: Boca Raton, CRC/Lewis Publishers, 136 p. p.

Chapter 6

Conclusions

Throughout this thesis, a new potential environmental problem affecting the New Zealand landscape has been studied – Coal Seam Gas water. In the first chapters (Chapters 2-3), the problem was defined in terms of its cause (CSG water), while in the last chapters (Chapters 4-5) the problem itself was explained, options were evaluated, and potential solutions were considered. This research constitutes the first comprehensive study of CSG water management in New Zealand, and conclusions from this work have applicability not only for New Zealand but for CSG management worldwide.

The procedure for characterising CSG waters consists of sample analyses from co-produced waters resulting from CSG exploration and mining. Subsequently, correct interpretation of these results can provide invaluable insight into the nature of the water being abstracted. This research has instigated the acquisition of water samples from a CSG exploration well in Maramarua (NZ), and has identified this water as CSG water by comparing its quality to CSG water quality from other coal basins in the US and by using an investigative procedure known as source-rock deduction. This was complemented by isotopic analysis of this water which, in turn, validates the analytical investigation. The overall methodology has proven that the abstracted water is indeed CSG water, and this is the first time such a water quality has ever been identified in New Zealand. Consequently, researchers in New Zealand or in other countries around the world can use the same procedure for characterising water samples derived from CSG abstraction operations, and this is particularly useful at the exploration stage when limited data are available. Defining CSG water quality is not only essential for assessing future environmental implications, but it also provides opportunities in terms of resource identification and exploration.

At the exploration stage, to carry out CSG water research there needs to be close collaboration with the mining industry, which luckily has been the case throughout this thesis. However, exploration mining relies in many ways on educated guesses, which often results in sporadic data collection and incomplete data sets. For example,

discontinuous pumping caused an unequally spaced water quality data set for C-1 in Maramarua. Consequently, this has lead to using advanced methods for analysing data collected during exploration. Since analysing an unequally spaced data set using traditional statistic techniques is complicated, the Maramarua water quality data set was analysed using Factor Analysis. This study lead to the discovery of the main source of variation in CSG water quality – carbon dioxide degassing due to a change in pressure once CSG water is abstracted to the surface. About one third of sample variations are due to carbon dioxide degassing, and this process also generates calcium carbonate precipitation which was experimentally verified. In addition, Factor Analysis pinpointed other sources of variation, but these were less significant than carbon dioxide degassing. Before this work, no previous study had indicated how much variability one might expect or the underlying process controlling this variability. This knowledge has important consequences for CSG water sampling – CSG waters should be collected in such a way to minimise sample degassing and pH should be measured on-site concurrently with sample collection. In addition, samples should be kept in closed containers and handled with care to avoid sample degassing. Applying this recommendation will prevent calcium carbonate precipitation while minimising sample variations. In addition, sparging tests or geochemical modelling can be carried out to calculate the maximum calcium precipitation that will take place once CSG waters reach atmospheric equilibrium. This also has important consequences in the land disposal of CSG waters because calcium precipitation will increase SAR values.

In sum, this particular study took an in-depth look at CSG water quality once it reaches the surface. While Chapter 2 focuses more on variability between sites (within NZ and globally), Chapter 3 focuses on variability at one specific site (within NZ). But, what happens after CSG water reaches the surface? This thesis also answers this question by studying potential environmental impacts and formulating possible solutions (Chapter 5).

The potential environmental impacts related to CSG water disposal depend mainly on the receiving environment. In this case, the main receiving environments are land and surface waters, but CSG waters can also be discharged directly to the ocean or injected in deep aquifers. However, not every CSG project will be located at close

proximity to the sea, and aquifer injection is often an expensive exercise which could render CSG projects uneconomical. Therefore, assessing the potential environmental effects of disposing CSG water onto land or surface waters has been a priority throughout this thesis. When it comes to soils, the high SAR of CSG waters (high sodium, low calcium and low magnesium) will increase the sodium content of soils, thus reducing their infiltration potential. This situation occurs when CSG water is discharged on soils for prolonged periods of time – sodium in the water gets lodged to clay particles in the soil and, over time, continuous cycles of precipitation/ CSG water discharge can cause a loss of aggregation and permeability. This, in turn, causes an increase in soil salinity. A case study with Maramarua CSG water from C-1 and soils from the area, verified these effects using the ANZECC water quality guidelines. Consequently, this research has shown that land disposal of CSG waters could pose negative impacts on New Zealand soils and agricultural crops. From the conservation point of view, CSG waters could have toxic effects on some species of pants and fish, while other species could tolerate this exposure. This is due mainly to the salinity of CSG waters, which is a consequence of high bicarbonate, sodium, and sometimes chloride concentrations. In addition, sodium and chloride can be toxic to certain species of fish and plants.

So, how is it possible to prevent CSG waters from generating negative environmental impacts? One way of answering this question would be to reduce the concentration of the major ions in CSG waters (mainly sodium and chloride). Reducing these ions' concentrations could also transform CSG waters into a usable resource – irrigation water. In this research, New Zealand zeolites from Ngakuru were used to reduce sodium concentrations in CSG waters from Maramarua (Chapter 5). This process is in actual fact, the reverse process that takes place in the genesis of CSG. When CSG is being formed, sodium in clays is exchanged for calcium and magnesium cations in water flowing into the coal seam. On the other hand, Ngakuru zeolites work by doing exactly the opposite – sodium cations in the CSG water are exchanged by calcium and magnesium in the zeolites (potassium is also exchanged). This research has shown that the sodium absortion capacity for unaltered Ngakuru zeolites is about 11 to 17 meq/100g, but this exchange takes place at a moderate rate (in comparison to commercial resins for example). This has implications for the full scale use of these materials to treat CSG

waters – with these materials, a conventional flow-through treatment system may not be the most efficient mode of operation and, instead, a semi-batch operational mode is recommended for further consideration. These zeolites are cation exchangers, so chloride concentrations were not lessened. In any case, chloride is not always present in CSG waters so, in some cases, this zeolite treatment system could be all the treatment that is needed.

An important outcome of this research is a methodology for implementing on-site treatment of CSG waters using natural zeolites (Chapter 5). This can be implemented with zeolites from different quarries (around NZ and around the world) and with different CSG water qualities as long as preliminary laboratory tests are carried out. Engineers following this guideline will have the basis for carrying out on site CSG water treatment at different sites, but they will have to adapt these to local conditions and regulations. In addition, the same methodology could be applied to treat other types of wastewaters (i.e. ammonium or hardness) using natural zeolites, so wastewater engineers in general will directly benefit from this work.

This thesis has identified the potential problems associated with CSG waters in New Zealand and has suggested potential solutions. However, it is important to highlight some of its limitations. Firstly, there was limited data to work with throughout this work. This is mainly due to the novelty of CSG in New Zealand, but also due to sensitivity of this issue, which does not encourage exploration companies to share their data. Working with more water quality data from different sites would have been good in terms of characterisation and to study different scenarios, but these data were not available when this work was carried out. In addition, due to lack of funding, samples were personally analysed at the University of Canterbury Environmental Engineering Laboratory, and so the procedures used in this lab were not as rigorous as the ones that could have been used in a certified laboratory (see section A.3 in Appendix 3). In any case, laboratory procedures closely followed APHA standards, and some analyses were indeed analysed through certified labs.

This thesis has dealt with projects that are exclusively CSG. It is possible, however, that some of these mining operations will encounter a combination of gases (CSG and higher hydrocarbon gases, even oil). The water arising from these operations

could have a different chemistry to the one studied in this thesis, and if different wells produce water that go into a common reservoir, then the problem will cease to become an exclusive CSG problem. Also, throughout this thesis the quantity of water being produced has not been measured or modelled (due to lack of data related to production decisions).

In any case, this thesis has generated the basic framework for carrying out future work once CSG production takes place and CSG water samples from more sites become available. Researchers can use this work as a guide and starting point to characterise, manage, and treat CSG waters in New Zealand. More research is needed to fully characterise the impacts associated with CSG water disposal at each site where CSG projects are being developed. This has to be done on a case by case basis because of the different receiving environments and the different quantities and quality of CSG water that will be produced. This type of work will be multidisciplinary, and CSG research will need to be carried out in the following disciplines: ecology, hydrogeology, hydrology, soil science, chemical engineering, and resource planning. For example, impacts of CSG water discharge on fish communities will have to be studied using laboratory experiments and later in field trials. The same holds true for soil science – the interaction between CSG water and soils needs to be studied under laboratory conditions or in field trials with actual CSG water. These experiments will show the extent of the potential problems that could be generated in New Zealand due to CSG water discharge. In addition, further treatment options can be explored using other ion exchange materials or other techniques (i.e. reverse osmosis or electrodialysis reversal) to increase the efficiency of the sodium removal process. Once more data becomes available, it will be important to model the amount of water that could be generated out of each basin. This can be done with dual porosity models which simulate both Darcy flow from the coal cleats and diffusion from the coal matrix. However, this modelling work will have to be done once CSG production plans are formulated (to account for the correct number and distribution of wells in each basin).

Appendix A

A.1 Laboratory methods

pH and Specific Conductance. These measurements were conducted with calibrated meters according to the APHA 4500-pH Value B and APHA 2510 B standards.

Total Dissolved Solids (TDS). TDS measurements were carried out using APHA standard 2540 C in which samples are dried in an oven at 180°C. In addition, measurements with a calibrated meter were carried out for verification purposes.

Alkalinity. Alkalinity was determined at the EEL (University of Canterbury) using APHA 2320 B titration method. In this method, a sample is titrated with a 0.01N HCl^- solution until reaching a pH in the 4.3-4.7 range (usually 4.5).

Hardness. Hardness was determined at the EEL (University of Canterbury) using APHA 2340 C method (American Public Health Association. et al., 1999). This method consists of preparing a sample with a 2 mL ammonia buffer solution and then adding 1 or 2 drops of EBT indicator. After the EBT is added, the sample turns red because this is the colour of the EBT-Mg complex. The sample is then titrated using a standard EDTA solution. The EDTA reacts with Ca^{2+} and Mg^{2+} ions to form stronger complexes than the ones formed with EBT. However, the Ca^{2+} ions are the first ones to react because the reaction rate constant for the Ca^{2+} reaction is higher than the one for Mg^{2+}. While the EDTA is being added, the sample remains red until all of the Ca^{2+} and Mg^{2+} ions have reacted with the EDTA. Once all the Mg^{2+} ions have reacted, the sample turns from red to blue, which is the colour of the uncomplexed EBT indicator. APHA reports a good precision with this methodology, capable of attaining a RSD of 2.9% and a relative error of 0.8%.

Calcium. The method for calcium determination at the EEL (University of Canterbury) was APHA 3500-Ca A. This method is similar in principle to the Hardness method but instead of using an EBT indicator, a Murexide indicator is used and the endpoint colour difference is from pink to purple. A NaOH buffer solution is used to drive the process at a pH between 12 and 13.

Magnesium. Unfortunately, the equipment required to measure magnesium (atomic absorption or inductively coupled plasma) was not available at the EEL. However, it was possible to calculate this value by subtracting calcium from hardness concentrations taking care of using the same units (mg/l as $CaCO_3$).

Chloride. It was not possible to determine chloride concentrations at the EEL using APHA standards. However, it was possible to determine these values using HACH method 8225 (Hach Company., 2003). This method allows the determination of chloride concentrations in the range of 0 to 25,000 mg/l. This method consists on diluting a 50 ml sample with 50 ml of deionised water. A powder pillow of potassium chromate is used as an indicator and the sample turns yellow. The sample is then titrated using a 0.0141N silver nitrate solution until the colour changes from yellow to red-brown.

Sulphate. Sulphate concentrations were determined at the EEL (University of Canterbury) using HACH 8051 method.

Sodium. Sodium concentrations were determined with a Cole-Parmer sodium ion electrode. The sodium electrode was calibrated each time before being used and every two hours using three NaCl standard solutions (10 ppm, 100 ppm, and 1000 ppm). The electrode was rinsed with a dilute electrode rinse solution every time before dipping it into a standard. Once the readings for each standard were recorded, these were plotted in a semi-logarithmic plot with sodium concentrations in the x-axis and electrode potential in the y-axis. From this plot, the slope and y-intercept values were used in a linear regression calculation to correlate sodium concentrations with electrode potential. Once the electrode was calibrated, it was used to measure the sodium concentration of samples, which had to be adjusted with 2 ml of an Ionic Strength Adjuster solution. When the meter was not being used, it was stored in a 5 M NaCl sodium electrode storage solution.

Carbonate species. Bicarbonate, carbonate, carbonic acid, and carbon dioxide were calculated using carbonate equilibrium equations along with the measured values for alkalinity and pH. The carbonate system is well documented in Snoeyink and Jenkins (1980) and Stumm and Morgan (1996), and its equations are presented in Chapter 3. For thorough calculations, activity coefficients were considered, and these were calculated from ionic strength values and using the Güntelberg approximation of the DeBye-Hückel

theory (Eq A.1). These values were in turn calculated using specific conductance measurements (Eq A.2).

$$-\log \gamma_i = \frac{0.5 \cdot Z_i^2 \cdot \mu^{\frac{1}{2}}}{1 + \mu^{\frac{1}{2}}}$$

where,

Z_i = charge of species i

μ = ionic strength of sample

Eq A.1. Güntelberg approximation of the DeBye-Hückel theory in Snoeyink and Jenkins (1980)

$$\mu = 1.6 \cdot 10^{-5} \cdot specific\ conduct.\ (\mu S / cm)$$

Eq A.2. (Russell, 1976)

A.2 CSG exploration in New Zealand

A.2.1 Ashers-Waituna

The Ashers-Waituna Lignite Deposit is located south east of Invercargill off Provincial State Highway 92. This deposit consists of lignite type B coals with moderate sulphur content. The maximum cumulative seam thickness for this deposit can be up to 30m, with and individual maximum thickness of 18.2m. On March 15th 2004, exploration hole AW2 was completed in this deposit; this hole targeted several layers of coal (of approximately 5m in thickness) between 70-100m deep (Pope, 2004a). On the 13th and 14th of March two groundwater samples from this well were collected when some artesian pressure was encountered in the midst of drilling operations. These samples were then analysed for major ions in the EEL (University of Canterbury). It was feared from the start that these samples would not be representative of CSG waters because the borehole was not cased to coal, and because it was impossible to purge the hole before collecting the sample. Thus, it is likely that these samples could have been contaminated by drilling fluids and mixed with waters from other formations (sands). However, the samples were collected and analysed to provide a point of comparison for future sampling rounds. It is necessary to point out that these samples were inadequate and unacceptable for the purposes of this research. However, they were analysed in the laboratory to

present a case to the mining company carrying out the exploration work, for carrying out proper well development and using better sampling collection techniques.

Table A.1. Ashers-Waituna (AW2) water samples

		Sample date	
		13/3/2004	14/3/2004
pH		7.11	6.47
Specific Conductance	µS/cm	NA	271
Alkalinity	mg/l as $CaCO_3$	79	57.5
TDS	mg/l	198	260
Hardness	mg/l as $CaCO_3$	89	92
Calcium (Ca^{2+})	mg/l	23.3	22.5
Magnesium (Mg^{2+})	mg/l	7.5 [(a)]	8.7 [(a)]
Sodium (Na^{+})	mg/l	34.3 [(b)]	28.3 [(b)]
Chloride (Cl^{-})	mg/l	60	60
Sulphate (SO_4^{2-})	mg/l	<2	11
Bicarbonate (HCO_3^{-})	mg/l	96.14 [(c)]	70.08 [(c)]
Carbonate (CO_3^{2-})	mg/l	0.07 [(c)]	0.01 [(c)]
Carbon dioxide ($CO_{2\,(aq)}$)	mg/l	26.9 [(c)]	85.9 [(c)]

Notes:

[(a)] calculated from known hardness and calcium concentrations
[(b)] calculated assuming zero electro neutrality and neglecting minor ions and K^{+}
[(c)] calculated from carbonate equilibrium using known alkalinity and pH

In both of these samples (Table A.1), pH levels are neutral, but calcium and magnesium concentrations are high in comparison to other ions (sodium and chloride for example). Sulphate levels are low (<11 mg/l in both cases), and Alkalinity values are low enough to produce low bicarbonate concentrations. The Schoeller diagram of Figure A.1 shows these values compared against each other. Here, sulphate levels are low in both cases (0.01 mg/l has been adopted in the 13/3/2004 sample just for plotting this point in the graph), but the rest of the ions are not too far away from the 1 meq/l value. This signature does not fit the geochemical signature for CSG waters presented by Van Voast (Van Voast, 2003). Figure A.2 shows a Piper diagram plotting these samples and showing the major ions composition (high sodium, calcium, and magnesium), but this figure also shows the high degree of variability between samples. This is not expected for samples taken on two consecutive days from the same well, but in this case there are too

many factors that contribute to the reliability of samples. For example, the hole was not cased down to the coal seams (open hole configuration) allowing for a variable flow of water from other formations. Also, there was no purging of stagnant water before collection, therefore this sample could have been contaminated by drilling fluids. These factors become even more important in this situation because the hole is shallow (<100m) and has sandy cap rocks which allow water flow from other units. It is interesting to note, however, that desorption results from core canisters indicated low gas content, a result that matches the hypothesis that these water samples do not correspond to CSG water.

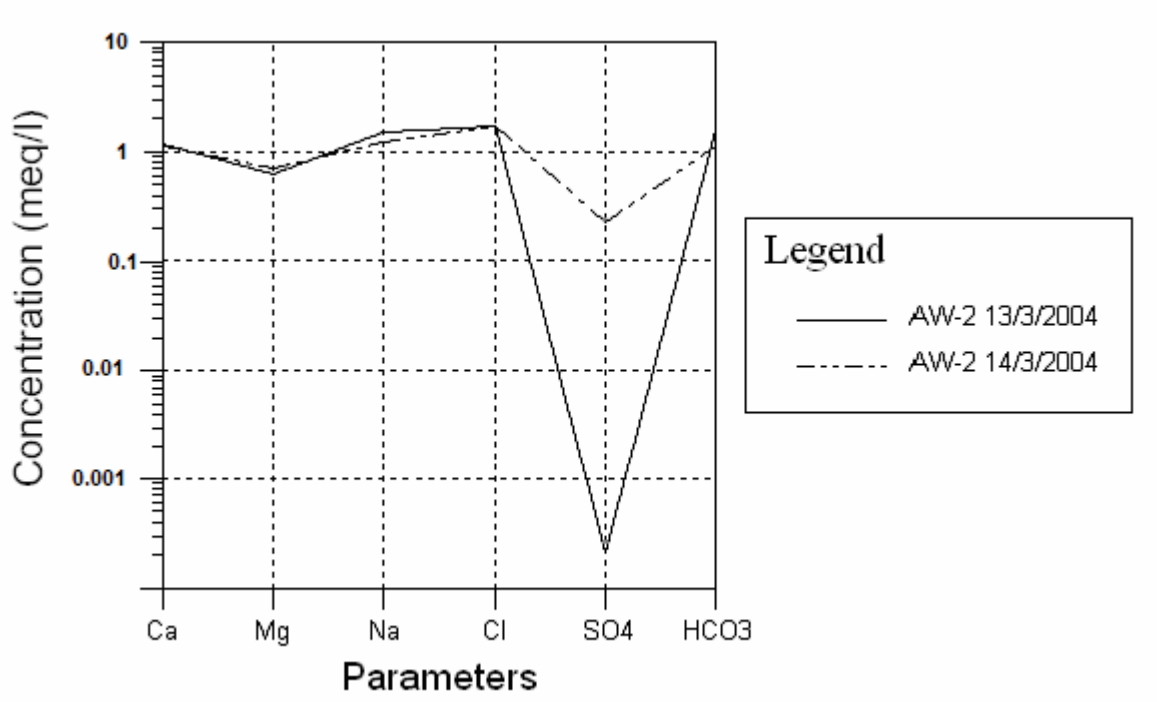

Figure A.1. Schoeller diagram for Ashers-Waituna samples

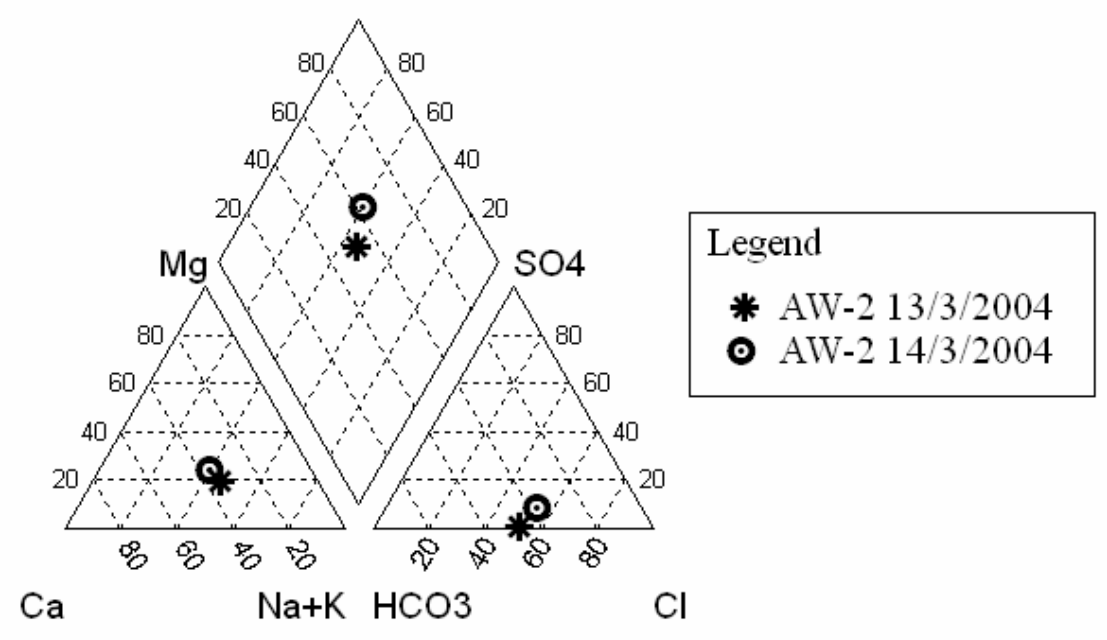

Figure A.2. Piper diagram for Ashers-Waituna samples

A.2.2 Reefton

In April 2004, drill hole RSE-1 was completed in the Reefton Coalfield. Here, CSG exploration targeted the Eocene Brunner Coal Measures which consists of high volatile bituminous C rank coal (low to high ash and sulphur contents). The drill penetrated through several layers of carbonaceous mudstones, sandstones, and thin layers of coal before reaching a total of 15.6m of coal at a depth between 215 and 252m. Four water samples were collected as the drilling process continued. Again, these samples could have been contaminated by drilling fluids and mixed with water from other formations (the well was not cased to coal). These samples were analysed at the EEL (University of Canterbury) and results are presented in Table A.2. Results from this analysis show samples of varying water quality with significant variations in pH and Specific Conductance (parameters which should remain constant before collecting samples). Alkalinity also shows significant variations through sampling reaching variations of up to 26%. Also, these waters have negative electro neutrality which makes it impossible to calculate sodium concentrations by this option. Furthermore, this is an indication of problems with the samples in relation to the chosen analytic procedure.

These limiting factors make it impossible to plot these samples on Schoeller and Piper diagrams, but some conclusions can still be drawn from these analyses. For instance, bicarbonate and sulphate variations suggest that methanation could have been present in the first sample but not in subsequent samples. This suggests that methanation could have occurred as a localised phenomenon, and water could have been impeded to flow through the low-porosity bituminous Brunner Coal Measures. These samples do not match the chemical signature of CSG waters presented by Van Voast (2003). This was further corroborated by low CSG desorption results obtained by CRL Energy.

Table A.2. Reefton water samples, April 2004

		Samples 2004			
		18/4	20/4	21/4	23/4
pH		6.56	6.15	6.06	6.74
Specific Conductance	µS/cm	897	681	603	NA
Alkalinity	mg/l as $CaCO_3$	335	245	185	210
TDS	mg/l	580	420	NA	334
Hardness	mg/l as $CaCO_3$	562	408	344	378
Calcium (Ca^{2+})	mg/l	82.6	73.0	68.14	60
Magnesium (Mg^{2+})	mg/l	86.59 [(a)]	54.91 [(a)]	42.28 [(a)]	55.53 [(a)]
Chloride (Cl^-)	mg/l	30	NA	NA	35
Sulphate (SO_4^{2-})	mg/l	<2	NA	NA	30
Bicarbonate (HCO_3^-)	mg/l	408 [(b)]	299 [(b)]	226 [(b)]	256 [(b)]
Carbonate (CO_3^{2-})	mg/l	0.10 [(b)]	0.03 [(b)]	0.02 [(b)]	0.09 [(b)]
$CO_{2\,(aq)}$	mg/l	386 [(b)]	737 [(b)]	688	164

Notes:

[(a)] calculated from known hardness and calcium concentrations
[(b)] calculated from carbonate equilibrium using known alkalinity and pH

A.2.3 Kaitangata

The Kaitangata Coalfield (Southland) has a history of methane gas occurrence that dates back to 1879, when a naked flame within the Kaitangata mine works caused a gas explosion causing major losses of life. The coal rank in this sector varies from Lignite to Sub-bituminous B. In February 2004, CRL Energy and L&M Mining drilled borehole K2 in the Kaitangata sector. The drill went through several layers of high ash lignites

before the well had to be abandoned due to technical difficulties. Desorption results from this hole yielded low CSG results.

Before borehole K2 was abandoned, one water sample was collected when an artesian burst of water was registered. This burst quickly died out and it is suspected that this water could have come from an old mine shaft. Therefore this sample cannot be used as a CSG water sample but it does provide a useful point of comparison to present a case for proper well completion and sample collection techniques, to the mining companies carrying out exploration work. Results from the analyses carried out at the EEL (University of Canterbury) are presented in Table A.3.

Table A.3. Water analyses results for K2 borehole

		01/02/2004
pH		6.21
Specific Conductance	µS/cm	518
Alkalinity	mg/l as $CaCO_3$	60
TDS	mg/l	312
Hardness	mg/l as $CaCO_3$	124
Calcium (Ca^{2+})	mg/l	27.2
Magnesium (Mg^{2+})	mg/l	13.6 [(a)]
Chloride (Cl^-)	mg/l	99
Bicarbonate (HCO_3^-)	mg/l	73 [(c)]
Carbonate (CO_3^{2-})	mg/l	0.01 [(c)]
$CO_{2\,(aq)}$	mg/l	159 [(c)]
Sulphate (SO_4^{2-})	mg/l	>70
Sodium (Na^+)	mg/l	<68.3 [(b)]

Notes:
[(a)] calculated from known hardness and calcium concentrations
[(b)] calculated assuming zero electro neutrality and neglecting minor ions
[(c)] calculated from carbonate equilibrium using known alkalinity and pH

Piper (Figure A.3) and Schoeller (Figure A.4) diagrams for this water analysis indicated that this water is not CSG water. Calcium and Magnesium levels are high in relation to other ions and bicarbonate levels are low. There is a certain degree of uncertainty surrounding the sulphate measurement because this parameter was out of range for the chosen analytic procedure. However, sulphate levels are higher than ever

recorded (and could be even higher), which is not a good indication. This has implications in the possible values for sodium, which were calculated assuming zero electro neutrality. Hence, a maximum value of 68.3mg/l is suggested (not high enough to have resulted from ion exchange processes).

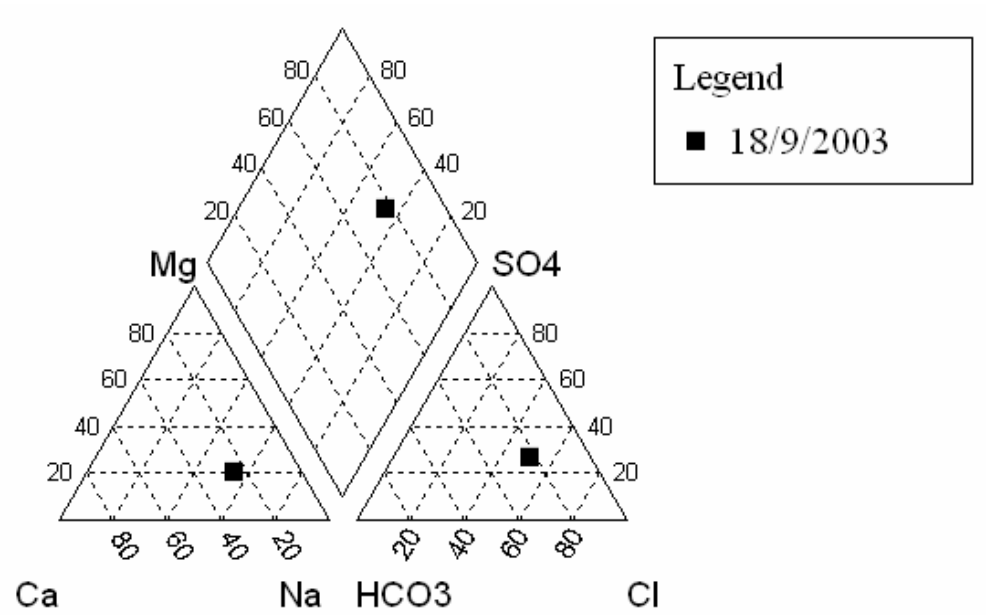

Figure A.3. Piper diagram for K2 water sample

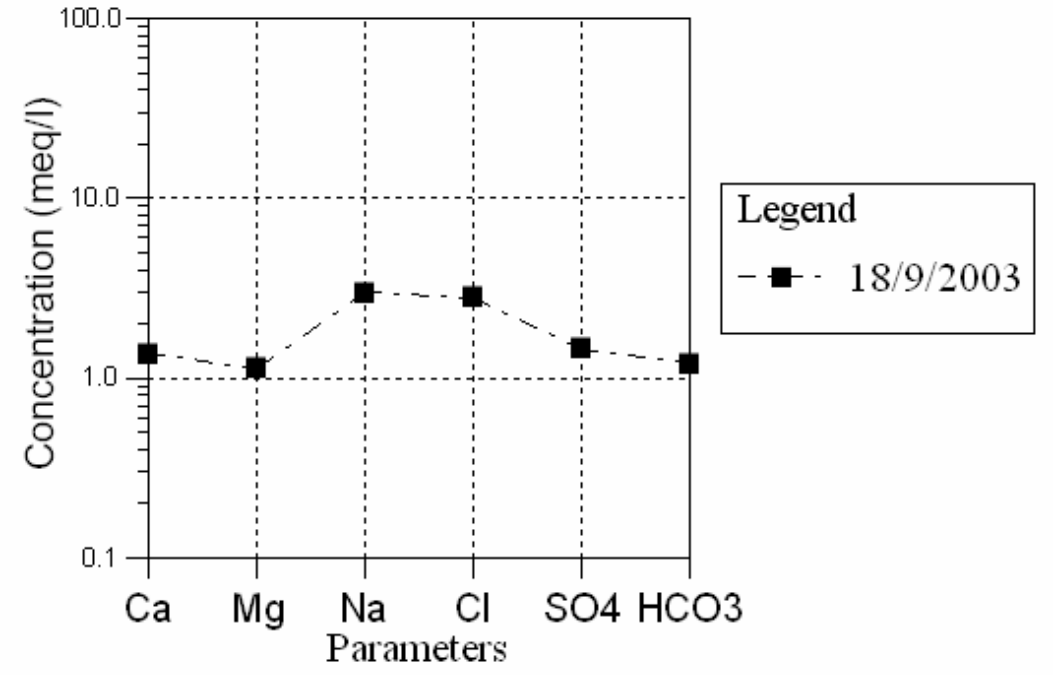

Figure A.4. Schoeller diagram for K2 sample

A.2.4 Hawkdun

The Hawkdun coalfield is located in Central Otago between the Hawkdun range and the St. Bathans range (Figure A.5). The coal from this field is classified as moderate to high ash, low sulphur, and having a lignite B rank (Pope, 2004b). The Hawkdun coalfield had been previously studied in 1986 by the Liquid Fuels Trust Board to determine the mine water discharge for a future open-cast mine (LFTB Study Group., 1986). In this study, a series of piezometers were installed into major water-bearing units to determine specific aquifer properties (permeability and transmisivity) within the Hawkdun coalfield. This study concluded that high artesian flows are likely to develop below the coal seams, while low pressure flows would tend to develop in the fractures within the seams themselves. The data from this study also suggested that there could be significant variation in water flow from these units. The set of lignite seams comprising the Hawkdun coalfield is referred to as the Manuherikia Group. At the top of this deposit lies a layer of low permeability clay or silt, which acts as a confining layer for any groundwater present beneath the coal seams. Below the top layer, lies the Middle Manuherikia group deposits which consists of lignite units overlapped by carbonaceous mudstones. The 1986 LFTB study indicated that these seams are most likely to be hydraulically connected and may contain significant quantities of groundwater in fractures within the lignites. The Lower Manuherikia group consists of silts with paleo channels filled with gravel, which, according to the LFTB report, can contain significant quantities of groundwater.

Between November 2002 and December 2004 Kenham Holdings and CRL Energy conducted CSG exploration of the Hawkdun Lignites in Central Otago (Pope, 2004b). Three boreholes were drilled to retrieve important data for the assessment of CSG potential. The first one of these boreholes (H2; Figure A.5) was drilled directly into the Manuherikia group, penetrating through a relatively thin gravel layer. The top of the Manuherikia group for this hole consists of a thick layer of low permeability silty clay capable of restricting water flow from any underlying units. Beneath the silty clay layer lies a carbonaceous mudstone layer with some coal lenses followed by a very thick

mudstone with minor interbedded silt and sand. The H2 borehole then penetrates through four lignite layers (middle Manuherikia group) overlapping carbonaceous mudstones of varied thickness. The drillers reached a depth of about 108 m before they had to abandon this borehole due to excessive artesian flow of water coming from the four lignite seams within the middle Manuherikia group. Groundwater from this borehole flowed right to the surface, thus offering a great opportunity for collecting samples. Unlike the H2 borehole, the other two Hawkdun drill holes did not have enough artesian pressure to facilitate water sampling.

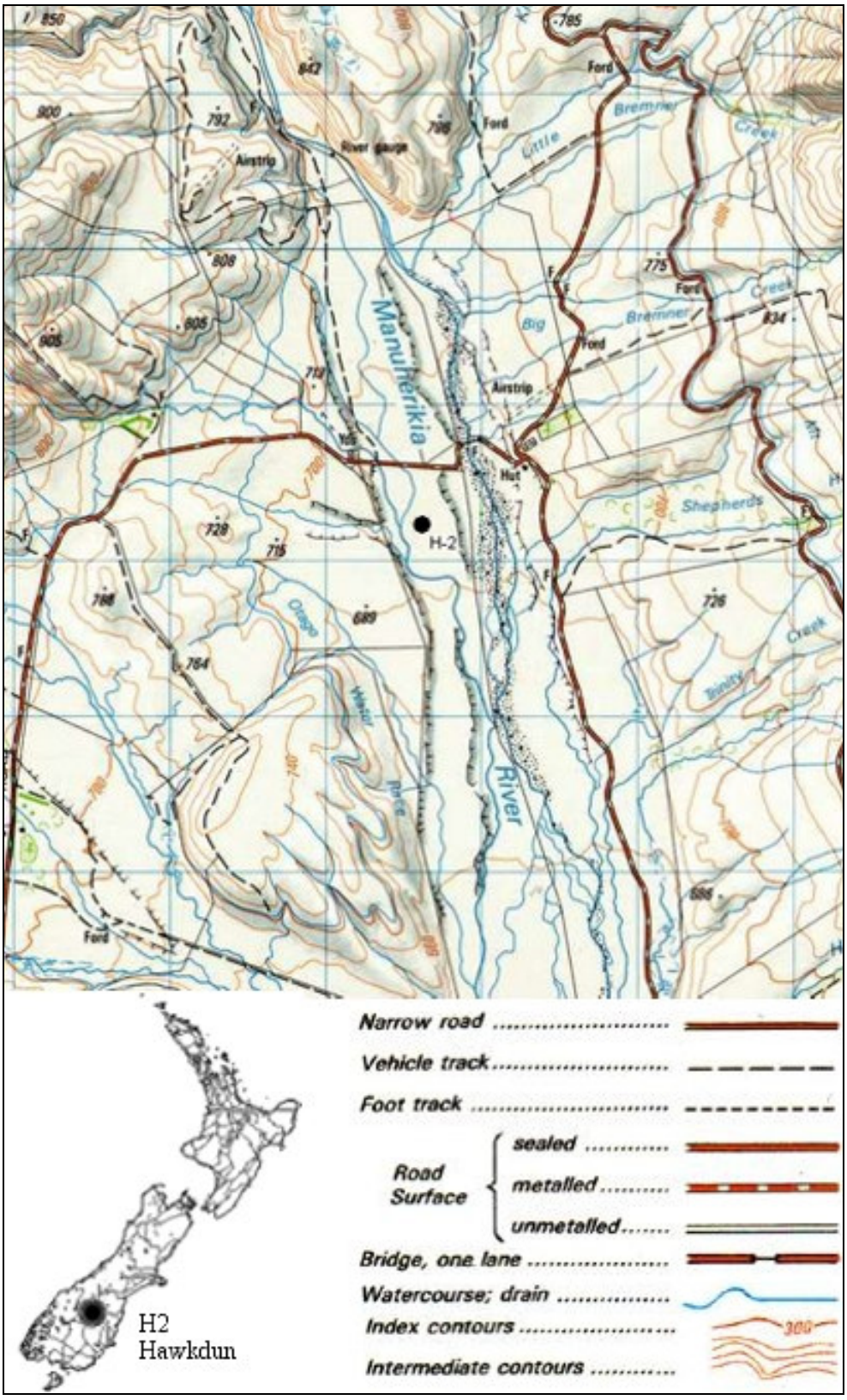

Figure A.5. Location of borehole H2

Table A.4. Drill hole summary for borehole H2

From (m)	To (m)	Thickness (m)	Lithology		
0.00	2.60	2.60	Gravels		
2.60	17.20	14.60	Silty clay	UPPER	MANUHERIKIA GROUP
17.20	24.00	6.80	Carbonaceous mudstone with coal lenses		
24.00	72.00	48.00	Blue/green mudstone with minor interbedded silt and sand		
72.00	74.68	2.68	Carbonaceous mudstone	MIDDLE	
74.68	74.98	0.30	Brown/black lignite, with carbonaceous mudstone partings		
74.98	75.58	0.60	Carbonaceous mudstone		
75.58	86.83	11.25	Brown/black lignite, with carbonaceous mudstone partings		
86.83	86.91	0.08	Carbonaceous mudstone		
86.91	101.90	14.99	Brown/black lignite, with carbonaceous mudstone partings		
101.90	102.32	0.42	Carbonaceous mudstone		
102.32	108.13	5.81	Brown/black lignite, with carbonaceous mudstone partings		

Adapted from Pope (Pope, 2004b)

Sampling of the H2 borehole was conducted following groundwater monitoring guidelines related to purging and stabilisation parameters (Nielsen, 1990). Therefore, before taking each sample sufficient time was allowed for the hole to purge itself and the sample was taken after pH, temperature and specific conductance were stable. Unfortunately, this borehole was not cased down to coal, which means that groundwater from the lignites was mixing with waters from other units (i.e. carbonaceous mudstones). Also, there is the possibility for these waters to dissolve minerals and/or exchange ions with other exposed units (mudstones, silty clay, and gravels). This becomes more important with time when the borehole walls start to collapse and the vertical flow of water becomes even more erratic.

Water samples were collected from the H2 hole on the 3/12/2002, 28/7/2003, and 25/11/2004.These samples were analysed at Hill Laboratories, the CRL Energy Laboratory, and the EEL (University of Canterbury); results are presented in Table A.5. The Hawkdun samples exhibit a consistent progression of values that fall within the range of what could be expected for coal seam gas waters; the pH of these samples is fairly

neutral (6.8-7), with low calcium and magnesium concentrations, relatively high sodium and bicarbonate, and low sulphate content (Figure A.7). Therefore, the water type for these samples is the sodium bicarbonate type which is a common characteristic of CSG waters (Figure A.6).

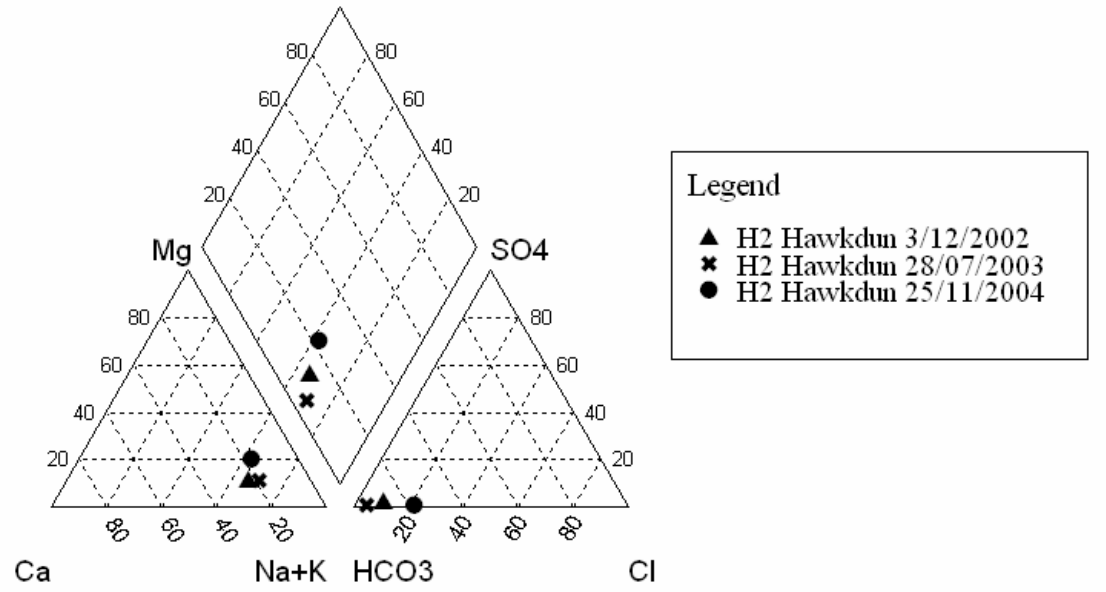

Figure A.6. Piper diagram for Hawkdun, H2.

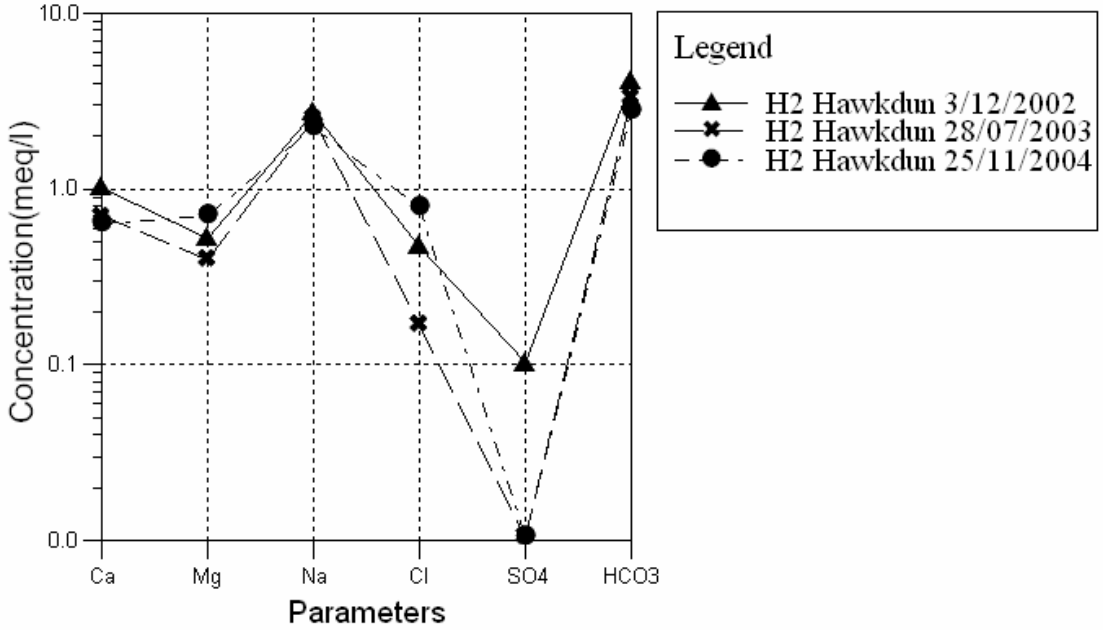

Figure A.7. Schoeller diagram of chemical quality for Hawkdun, H2.

The sulphate content for these samples (SO_4^{2-} < 5 mg/l) is one hundred times lower than the upper limit for the likelihood of methane production (SO_4^{2-} < 500 mg/l)

presented by Van Voast (2003). This, along with the relatively high bicarbonate concentrations (250 mg/l, 202 mg/l, and 170 mg/l) suggests sulphate reduction is taking place. The methane bearing potential of the Hawkdun lignites was confirmed with CSG desorption results of core canisters which produced significant quantities of methane gas. This confirms the assumption that sulphate reduction is taking place within the coal seams. Alkalinity and bicarbonate levels decrease at about the same rate across the three samples. This suggests initial bicarbonate concentrations could have been higher for the first sample because some of this bicarbonate could have originated from the carbonaceous mudstones overlapping the coal seams within the Manuherikia group. This could be observed as foam like bubbles when this groundwater first flowed to the surface (Figure A.8). As vertical flow continued, the mudstones along the edge of the borehole could have been washed away leaving just the coal seams exposed within the borehole. The coal seams could have then subsided one on top of the other thus restricting the flow of water from the carbonaceous units. Therefore, subsequent samples might better resemble what could be expected from pure CSG waters. The same analysis holds true for the dissolved carbon dioxide in water samples.

For this borehole, dissolved metals concentrations (arsenic, iron, manganese, chromium, mercury, and zinc) are low in comparison to what could be expected from an acid mine drainage situation. This is because there is no oxidation taking place and the water pH is fairly neutral. Total iron and manganese concentrations are just over the maximum acceptable values specified in the NZ drinking water standards (0.02 mg/l for iron and 0.05 mg/l for manganese), but these values are still fairly low in comparison to waters arising from other operations (i.e. AMD).

Figure A.8. Bubbly flow from the H2 borehole on 2/12/2002 (3:30pm).

The three H2 samples plotted in Figure A.6 represent the percentage of major ions in each of the water samples being analysed. Sample points in this figure do not coincide; this shows the extent of variations in major ion composition. However, in a situation like the one in borehole H2, these variations could be expected mainly because the hole is not cased. Consequently, the hole is subjected to changes in water flow from unconfined units; therefore, this hole may be subjected to seasonal variations and changes in water quality.

Table A.5. Hawkdun H2 samples

		Sample date		
		3/12/2002	28/07/2003	25/11/2004
pH	pH units	6.8	7	6.9
Specific Conductance (T=25ºC)	µS/cm	386	342	401
TDS	mg/l	309	262	336
Hardness	mg/l as $CaCO_3$	76.5 [(a)]	54.7 [(a)]	67
Alkalinity	mg/l as $CaCO_3$	205	166	140
Bicarbonate (HCO_3^-)	mg/l	250 [(b)]	202 [(b)]	170 [(b)]
Carbonate (CO_3^{2-})	mg/l	0.09 [(b)]	0.12 [(b)]	0.08 [(b)]
Carbon dioxide ($CO_{2\,(aq)}$)	mg/l	141 [(b)]	73 [(b)]	77 [(b)]
Calcium (Ca^{2+})	mg/l	20.2	14	12.8
Magnesium (Mg^{2+})	mg/l	6.32	4.8	8.5 [(c)]
Sodium (Na^+)	mg/l	62.2	57.3	51.7 [(d)]
Potassium (K^+)	mg/l	10.4	6	NA
Chloride (Cl^-)	mg/l	16.6	6	28
Sulphate (SO_4^{2-})	mg/l	4.9	<0.5	<2
Zinc (Zn^{2+})	mg/l	<0.001	0.04	NA
Fluoride (F)	mg/l	NA	0.38	NA
Boron (B)	mg/l	NA	0.3	NA
Silica (SiO_2)	mg/l	NA	58.9	NA
Dissolved Organic Carbon	mg/l	NA	8.8	NA
Total Iron (Fe)	mg/l	NA	3.7	NA
Manganese (Mn)	mg/l	NA	0.29	NA
Arsenic (As)	mg/l	NA	<0.02	NA
Barium (Ba^{2+})	mg/l	NA	<0.002	NA
Chromium (Cr^{2+})	mg/l	NA	<0.01	NA
Mercury (Hg)	mg/l	NA	<0.002	NA
Selenium (Se)	mg/l	NA	<0.02	NA

Notes:

NA= Not Available.
3/12/2002 sample analysed through Hill Laboratories.
28/07/2003 sample analysed through CRL Energy and Hill laboratories.
25/11/2004 sample analysed at the EEL (University of Canterbury).

[(a)] Calculated from calcium and magnesium concentrations
[(b)] Calculated from carbonate equilibrium using known alkalinity and pH
[(c)] Calculated from known hardness and calcium concentrations
[(d)] Calculated assuming zero electro neutrality and neglecting minor ions. This value also includes K^+ ions.

A.3 Sample collection methods

Background information

In 2002 CRL Energy Ltd and L&M Mining Ltd applied for research funds for a PhD, through The University of Canterbury, to the New Zealand Foundation for Research Science and Technology (FRST). These funds were granted taking the form of a Technology for Industry Fellowship (TIF) to fund living expenses, enrolment costs, and some study-related costs associated with this PhD work. Although it was intended that CRL Energy and L&M Mining would pay all drilling, sampling, and analysis costs of the research, no funds were made explicitly available to fund the work itself. Instead, contractual provisions were made by these companies, to meet all programme expenses for the successful completion of the work. In the long run, this proved to be a considerable problem. The CRL Energy Ltd manager who devised the project left to work for a CSG competitor, and L&M Mining Ltd took much longer than anticipated to choose sites for drilling work investigations. In addition, L&M Mining Ltd were more interested in assessing the CSG resource than in sampling CSG water, so they concentrated their efforts on drilling as many holes as possible to assess the quality of coal and CSG potential, and gave low priority to the collection of CSG water samples. Consequently, these companies were reluctant to spend money to properly case wells and acquire high water quality pumps to sample CSG waters from the wells they were drilling. In addition, they decided they were not going to fund a sampling programme to regularly collect samples, and they were not going to spend money ensuring high quality data were collected from field investigations. Instead, they were going to supply these data themselves when the opportunity presented itself. They did, however, commit to procuring small funds for simple laboratory analyses, and eventually purchased a multi-metre to use in site investigations.

At this stage, there was little that could be done from the point of view of designing a proper sampling collection programme, and the methodology adopted in carrying out this work had to take into account a considerable degree of uncertainty and lack of control.

Methods

The methods for collecting water samples varied depending on different site conditions, equipment available, and the person collecting the samples. As mentioned earlier (background information) there was little control over how this was done, but some basic provisions were taken to try to ensure good quality samples were collected. For example, clean sample bottles were ordered from certified laboratories (CRL Energy Ltd and Hill Laboratories) and, in some instances, specific measurements like pH and Specific Conductance were monitored to ensure that they remained constant prior to taking the sample. This was to try to make sure that actual aquifer water (and not stagnant water) was sampled.

The EEL (University of Canterbury) had limited equipment to analyse water samples. The basic equipment at this laboratory included pH and conductivity meters, ovens, HACH spectrophotometers, basic reagents, and laboratory equipment. An ICP or Atomic Absorption machine was not available at the EEL, so it was not possible to achieve a high degree of accuracy when analysing water samples. Eventually, a sodium selective electrode was purchased for the purposes of measuring this ion's concentration in CSG water, and provisions were made to analyse some of the samples using Atomic Absorption equipment at the Chemistry Department (University of Canterbury). It was not straight forward to use the Chemistry Department each time - university policy forces its different departments to operate as entirely different entities, thus charging money for services rendered.

The inadequacies of the methods discussed here are clearly evident to the author and include: the lack of good quality samples from cased boreholes at different sites, inadequate well purging prior to sample collection, the lack of sample field blanks to validate the sampling, and not being able to analyse all of the samples through certified laboratories. Whenever samples were analysed at the EEL (University of Canterbury), accuracy was compromised due to lack of resources. For example, chloride and sulphate were measured using HACH methods (see section A.1), and sodium was measured with a sodium ion electrode; when this instrument was not available, it was necessary to assume zero electroneutrality to estimate sodium concentrations. These methods are generally not

considered accurate methods for estimating analyte concentrations, but they were used here due to lack of resources.

Ashers-Waituna, Reefton, and Kaitangata

As described by on-site personnel, water from these boreholes was collected when "artesian conditions" where encountered while the drilling was taking place. These "artesian conditions" could have been due to air pumped into the borehole by the drillers to clear the hole and push water out of the well. It was unfortunate that no further descriptions accompanied the origin of these samples, so these samples were always treated with caution as to their origins and future use. In any case, these samples were analysed to provide a future point of comparison, and to present a case for carrying out good quality sampling to the mining companies doing the exploration work.

Samples were collected in 1000ml clean plastic bottles supplied by the CRL Energy Ltd laboratory. The samples were completely filled with water taking care there were no air gaps when closing their lids; no on-site measurements were taken in this case, but the samples were sent (via courier or delivered by personnel) in containers packed with ice. These samples were received at the CRL Energy Ltd offices in Christchurch to analyse at the EEL within 48 hours of collection, where they were analysed for major ions composition following the methods specified in section A.1

Hawkdun

In this case, true artesian conditions were encountered when the drill bit penetrated into the lignite seams of the Manuherikia group on 2/12/2002 (section A.2.4). The well was left opened with water flowing right to the surface for 24 hours before samples were collected personally on 3/12/2002. At the time of collection, pH and specific conductance were measured using a calibrated meter, and these data are presented in Table A.6. The samples were collected in 1000ml bottles (untreated), 250ml bottles (treated with HNO_3), and 750ml glass bottles to preserve different constituents before analyses were carried out. Once again, samples were collected whilst taking care not to leave any air gaps inside the bottle and, in case of bottles containing HNO_3, taking care not to spill any of the treatment solutions. After the drilling investigation was completed, the well was capped with a closed tap to stop the water flow. On 28/07/2003 this tap was opened to collect a

second sample. Groundwater started flowing to the surface after a few minutes of opening the tap, and it was left running for 45min before collecting the sample. In addition, while water was flowing to the surface, pH and specific conductance were monitored approximately every 15min, and these data are presented in Table A.6. Samples were collected in plastic bottles using the same procedure used on the previous sampling collection event (3/12/2002). A final sample was collected from this borehole on 25/11/2004. In this instance, a sample was collected by CRL Energy Ltd personnel in a 1000ml plastic bottle, but without monitoring pH or specific conductance. The sample was then couriered to Christchurch where it was analysed at the EEL (University of Canterbury).

Table A.6. Monitoring of pH and Specific Conductance prior to sample collection.

Sample	Time	pH	Specific Conductance(μS/cm)
3/12/2002	13:00	6.96	383
28/7/2003	13:13	6.62	361
28/7/2003	13:30	6.88	357
28/7/2003	13:48	6.94	358
28/7/2003	13:59	6.94	360

Maramarua

When C-1 was first drilled in Maramarua, the uncased borehole was sampled using a subcontractor (DJ Phelps & Co Ltd) with the aid of a special submersible pump. This subcontractor collected the samples only after the solution chemistry of the groundwater being pumped had stabilised using temperature, pH, and conductivity as indicators. Table A.7 presents the field parameters being monitored at the time of collecting this first sample on 18/09/2003. The sample was collected in a 500ml untreated bottle for Organics, a 250ml bottle treated with HNO_3 for dissolved metals, a 250ml glass bottle to test for TPH, a 250ml bottle (sulphuric acid preserved), and a 100ml glass bottle for TOC. Once this sample was collected it was packed in an ice-box and sent to Hill Laboratories, where it was analysed.

Table A.7. Groundwater sampling record for sample collected on 18/9/2003 (9am)

Water level cm	Volume pumped litres	Temperature °C	pH	Specific Conductance µS/cm
25	0	NA	NA	NA
NA	20	15.2	7.2	950
NA	20	15.1	7.5	970
NA	40	15.1	7.5	960
NA	20	15.1	7.5	970
NA	40	15.1	7.5	970
NA	40	15.1	7.5	960
NA	20	15.1	7.5	960
NA	40	15.1	7.5	960
NA	20	15.1	7.5	970
NA	40	15.1	7.5	960
NA	40	15.1	7.5	960
1698	40	15.1	7.5	970

After C-1 was re-drilled and cased in 2004, subsequent samples were collected from this well. Samples were collected in 1000ml (unpreserved) plastic bottles supplied by the CRL Energy Ltd Laboratory. In a few instances, the samples were collected personally and on-site measurements were carried out on these occasions (Table A.8). However, for the most part, the samples were collected by an on-site operator, who followed basic sample collection methods. Samples were collected after the pump had been dewatering the well for some time, and care was taken not to leave any air gaps in the sample bottles. Samples were then packed in containers with ice, and couriered to the CRL Energy Ltd offices in Christchurch for analyses at the EEL (University of Canterbury).

Table A.8. Groundwater monitoring prior to sample collection

Date and time	Water level m	Temperature °C	Specific Conductance µS/cm	pH
12/9/2004, 17:22	64.8	19.2	1471	7.72
13/9/2004, 14:16	90.6	19.6	1462	7.79
14/9/2004, 9:30	100	18.3	1478	7.85

Note:
These measurements were taken only while monitoring pumped water (after 15 minutes) to ensure that these properties remained constant.

On 19/8/2004 a sample was collected by the field operator in 1000ml bottles (untreated), 250ml bottles (treated with HNO_3), and 750ml glass bottles. The sample was then packed in an ice-box and sent to Hill Laboratories for a full analysis.

A.4 References

American Public Health Association., American Water Works Association., and Water Environment Federation., 1999, Standard methods for the examination of water and wastewater: Washington, D.C., American Public Health Association, 1 computer optical disc p.

Hach Company., 2003, Water analysis handbook : drinking water, wastewater, seawater, boiler/cooling water, ultrapure water: Loveland, Colo., Hach, 1268 p.

LFTB Study Group., 1986, South Island Phase II Lignite Site Selection Studies Programme. Resource definition, geotechnical, hydrology, and mine planning studies. Hawkdun deposit.: Wellington, N.Z., Liquid Fuels Trust Board.

Nielsen, D., 1990, Practical handbook of ground-water monitoring: Chelsea, MI, Lewis Publishers, x, 717 p.

Pope, S., 2004a, 2004 Coal Seam Gas Exploration Results: Ashers-Waituna Lignite Deposit, PEP 38-217, Southland.: Christchurch, CRL Energy Ltd, p. 41.

—, 2004b, Coal Seam Gas Exploration Results: Hawkdun Coalfield, Central Otago, 2002-2004.: Christchurch, CRL Energy Ltd, p. 42.

Russell, L.L., 1976, Chemical aspects of groundwater recharge with wastewaters: Berkeley, University of California.

Snoeyink, V.L., and Jenkins, D., 1980, Water chemistry: New York, Wiley, xiii, 463 p.

Stumm, W., and Morgan, J.J., 1996, Aquatic chemistry : chemical equilibria and rates in natural waters: New York, Wiley, xvi, 1022 p.

Van Voast, W.A., 2003, Geochemical signature of formation waters associated with coalbed methane: Aapg Bulletin, v. 87, p. 667-676.

Appendix B

B.1 Sodium calculations and corrections

Sodium concentrations were measured through the chemistry department (University of Canterbury). The analytical method used at this laboratory, was APHA 3500 Na-B which uses an atomic absorption spectrophotometer in the flame emission mode. Unfortunately, due to budget constraints, not all of the samples were measured like this. Therefore, the rest of the sodium concentrations, in the rest of the samples, were measured using a sodium probe or determined from zero electroneutrality. The sodium probe used at the EEL was a Cole-Parmer Sodium Ion Electrode which, if properly calibrated, is capable of achieving a ±2% reproducibility. The probe manufacturer recommends calibrating the probe using standards of similar composition and ionic strength. Therefore, this probe was calibrated against sample values of known sodium concentrations (previously determined using method 3500 Na-B).

The atomic absorption method and the sodium probe were not available from the start of the project, therefore some samples were consumed before they could be analysed. For these samples, the method of zero electroneutrality was used to calculate sodium concentrations. In this method, the difference between anions and cations (in meq/l) is calculated for the samples for which sodium concentrations are known from APHA 3500 Na-B (Eq B.1). The differences should be zero (or close to zero) but, because of accumulated systematic errors, there is a sizeable difference (Δ = 52.84 mg/l on average). The next step is to calculate the difference between anions and cations in the samples for which sodium concentrations are unknown. These differences include the unknown (the sodium cation) plus a value associated with the accumulated systematic errors. Consequently, to obtain an estimate of their sodium concentrations, the previously calculated difference (52.84 mg/l) is added to their final value (Eq B.2). An example of this calculation procedure is presented in Table B.1.

$$\Delta_{average} = \frac{\sum_{i=1}^{13} \left| \sum anions_i - \sum cations_i \right|}{13}$$

Eq B.1

$$Na^{+}_{sample} = \left| \sum anions_{sample} - \sum cations_{sample} \right| + \Delta_{average}$$

Eq B.2

Table B.1. Sodium calculations assuming zero electroneutrality

Sample	Sodium Atomic Absorption	Zero electroneutrality(1)	Sum Cations	Sum Anions	Anions-Cations	Corrected(2)
	mg/l	mg/l	meq/l	meq/l	mg/l	mg/l
1/08/2004		272.8				325.7
6/08/2004		273.8				326.6
7/08/2004		272.3				325.1
8/08/2004		273.4				326.2
9/08/2004	**315.7**		14.25	12.44	-42.093	
10/08/2004		268.7				321.5
16/08/2004		262.8				315.6
20/08/2004		259.4				312.2
12/09/2004		257.8				310.6
13/09/2004		255.2				308.1
14/09/2004		254.6				307.5
17/09/2004		256.4				309.2
18/09/2004 (1)		257.4				310.2
18/09/2004 (2)		262.8				315.6
18/09/2004 (3)		258.0				310.9
19/09/2004		258.3				311.1
20/09/2004		262.5				315.4
21/09/2004	**319.5**		14.55	11.97	-60	
4/10/2004	**317.6**		14.43	11.79	-61.395	
5/10/2004		263.8				316.6
20/10/2004		260.7				313.5
21/10/2004		265.0				317.9
22/04/2005	**289.2**		13.61	11.86	-40.698	
23/04/2005	**297.0**		13.72	11.62	-48.837	
25/04/2005	**312.7**		14.17	11.4	-64.419	
27/04/2005	**313.2**		14.07	11.57	-58.14	
29/04/2005	**307.9**		13.87	11.75	-49.302	
3/05/2005	**307.4**		13.74	11.71	-47.209	
10/05/2005	**313.7**		14.05	11.69	-54.884	
23/05/2005	**312.4**		13.93	11.7	-51.86	
24/05/2005	**305.7**		13.9	11.64	-52.558	
10/06/2005	**312.9**		14.09	11.7	-55.581	
$Corrected^{(2)} = 52.84 + Zero\ electroneutrality^{(1)}$				Average	-52.84	

B.2 Precision and accuracy

Whenever possible, repetitions were carried out to obtain a true value (approximated by the average) for the population of measurements being carried out. This procedure also yields an implicit error (relative standard deviation, standard deviation of the mean, and relative error) associated with each measured value. Unfortunately, it is not always possible to carry out many repetitions when sample volumes are limited (see Appendix G), and CSG waters undergo changes when exposed to normal atmospheric conditions. Nevertheless, these errors should already be low if the APHA standards are followed carefully.

pH and Specific Conductance. Meters were calibrated on a regular basis and two sets of meters were used from time to time to verify their accuracy. In the case of specific conductance it was found that there is some discrepancy between terminologies that sometimes leads to confusion among meter users. The term "conductivity" refers to the ability of a solution to conduct an electric current. This value is measured in μS/cm or μmho/cm and varies with temperature; it is necessary to define a standard temperature as a baseline to carry out comparisons. Therefore, the term "specific conductance" has been defined as the conductivity of a sample measured at 25°C. This value is often expressed in mS/m, but it can be expressed in any units as long as the property being measured is adequately specified (in terms of name or temperature). The pH meter used at the EEL was an EDT Instruments meter model number RE 357, and its accuracy was ±0.02 pH units (±0.05 with just one significant figure). For specific conductance measurements, a WTW LF325 Tetracon meter was used, and its accuracy was ±0.5% of the measured value with a variation of ±1 digit.

Total Dissolved Solids (TDS). There are three ways of carrying out TDS measurements. The first one involves drying a sample in an oven at a designated temperature, and the second one consists of measuring all of the dissolved ions and calculating the TDS value analytically. The third method, which is an estimate, involves taking these measurements with a calibrated Specific conductance meter.

Measuring TDS with a meter is not a precise way of determining this parameter because meters use a basic estimation of TDS based on specific conductance

measurements. Eq B.3 presents the relationship relating TDS and specific conductance. The value of A ranges from 0.54 to 0.96, but usually assumes values between 0.55 and 0.76 depending on the water being analysed (Hounslow, 1995). For the particular case of the Maramarua CSG samples, A ranged from 0.51 to 0.63.

$$\text{TDS (mg/l)} = A \cdot \text{Specific Conductance } (\mu S/cm)$$

Eq B.3 (Hounslow, 1995)

If the value of A is unknown, measuring TDS using a meter would lead to a considerable degree of uncertainty. Therefore, the TDS values measured at the EEL were determined by drying a known volume of sample water in an oven following APHA standards. Again, there seems to be some confusion to the correct application of APHA standards. APHA specifies different measuring procedures for total solids, total suspended solids, and total dissolved solids (TDS). It specifies drying temperatures of 103°-105° C for total solids and total suspended solids, but 180°C for TDS. This is because when the sample is dried up, CO_2 and H_2O are lost and bicarbonates are converted to carbonates (Eq B.4). However, at temperatures below 180°C Eq B.4 may not go to completion, hence APHA specifies a drying temperature of 180°C. This is particularly important when analysing CSG waters because of the high bicarbonate content present in these waters. APHA reports on the precision of this procedure by single-laboratory analyses of 77 samples of a known 293 mg/l TDS concentration which yielded a standard deviation of differences of 21.20 mg/l.

$$2HCO_3^- \rightarrow CO_3^{2-} + CO_2 + H_2O$$

Eq B.4 (Hounslow, 1995)

It was discovered that most laboratories around the world are relaxed about the drying temperature for TDS and often use 103°-105° C instead of 180°C. The EEL is no exception. This generally would pose no problems in low bicarbonate waters but with CSG waters overestimation of TDS is definitely a possibility. Therefore, the preferred temperature used for drying the samples at the EEL was 180° C. Getting the oven to a temperature of 180° C sometimes was a problem as this lab is shared with other users. Under these circumstances the samples were originally dried at 103°-105° C; later, when

the oven was available, the TDS analyses were repeated but at a temperature of 180°C. It was discovered that TDS values decreased in 14 out of 19 Maramarua C-1 samples when using 180°C. The relative differences in the 14 samples which yielded lower results were about 6% on average and up to 10% in some cases. The remaining 5 samples yielded higher results possibly due to random errors, but the relative differences were low anyway (-1.4% on average). Therefore, this comparison provided an important lesson in terms of determining TDS values in CSG waters.

Another way of determining TDS is by conducting a full ion analysis and then calculating TDS analytically by adding all the ions plus the silica while taking care of subtracting the amount of water and carbon dioxide that would be lost in the evaporation process. Applying stochiometry to Eq B.4, the amount of H_2O and CO_2 that is lost due to evaporation is $0.5082 \cdot HCO_3^-$. Therefore, this amount needs to be deducted from the sum of all the ions (including bicarbonate) plus silica contained in solution. In this way, Eq B.5 presents the relationship for calculating TDS in this fashion. All of these ions and the silica (SiO2) are expressed in mg/l, so the end result (TDS) also has these units. It was not possible to calculate TDS values in this way at the EEL because this would have required a complete ion determination. However, it is important to keep in mind this calculation procedure as some laboratories do not follow this convention, not compensating for the amount of carbon dioxide and water that would be lost due to evaporation (Van Voast, 2003).

$$\text{TDS (mg/l)} = \sum \text{ions (mg/l)} + \text{SiO2 (mg/l)} - [HCO_3^- \text{ (mg/l)} \cdot 0.5082]$$

Eq B.5 (Hounslow, 1995)

Alkalinity. According to APHA, when the alkalinity is due entirely to bicarbonate and carbonate (10-500 mg/l), a standard deviation of 1 $mgCaCO_3/L$ can be achieved, but an experimental value of 5 $mgCaCO_3/L$ is normally obtained (American Public Health Association. et al., 1999). For the Maramarua analysis, the chosen sample volume was 100ml, and 2-3 repetitions were carried out in 10 of samples. The relative standard deviation (RSD) for these samples ranged from 0.45% to 3.17%, which is a good indication of the precision of these results.

Hardness. To apply the APHA 2340 C method, a 25ml sample was diluted with deionised water to 50ml. It was later discovered that this water was not as deionised as originally thought so these measurements were corrected to take this effect into account; the analysis was then onwards carried out with 50ml but with no dilution. Consequently, 2-4 repetitions were carried out in 23 of the Maramarua C-1 samples, which produced an average RSD of 13.46%. This high error percentage is attributed to the difficulties in measuring low hardness concentration in CSG waters (<33 mg$CaCO_3$/L), and to possible variations due to calcium carbonate precipitation after the sample is exposed to normal atmospheric conditions.

Coal Seam Gas waters are subjected to high pressures while in the coal aquifer. At these pressures the partial pressure of CO_2 gas is significantly high (about 0.1 atm), which allows CO_2 gas to stay dissolved in the aquifer water. Once water is pumped up to the surface, the lower atmospheric pressure causes a lower CO_2 partial pressure (about 0.0003 atm). At a lower partial pressure, the dissolved CO_2 gas will slowly start to abandon its dissolved form and will form part of air under normal atmospheric conditions. This process is not instantaneous and may require anywhere from a few hours to a few days depending on the degree of agitation and aeration to which the sample is subjected. As CO_2 gas leaves the water samples, the carbonate equilibrium changes in the samples. Bicarbonate (HCO_3^-) concentrations decrease in the sample, while carbonate (CO_3^{2-}) and pH values increase. As this takes place Ca^{2+} precipitates as $CaCO_3$, Mg^{2+} precipitates as dolomite $CaMg(CO_3)_2$, and zinc precipitates as smithsonite ($ZnCO_3$) or hydrozinite $Zn5(CO_3)_2(OH)_6$. This has direct consequences in the analytical determination of calcium, magnesium, and zinc ions dissolved in the water sample. If samples are left for too long they will degas and their chemistry will change. In addition, there can be a significant differences between repetitions from the same sample depending on the amount of time that has elapsed between measurements and the degree of agitation to which each sample has been exposed. However, if precautions are taken, these effects can be minimized and their importance is only relevant to the time elapsed since the CSG water has been abstracted from the aquifer and the time of sample collection. If care is taken not to leave any air gaps in the sample bottle, degassing will be minimum. However, once the sample bottle is opened, degassing can take place again,

but at a very slow rate because the surface tension of the water prevents CO_2 gas from leaving the bottle at once. This process explains the high averaged RSD values (13.46%) in repetitions taken from hardness measurements of Maramarua samples. A good approach for solving this problem would be to wait until the sample has been degassed (or to aerate the sample to accelerate this process) and then measure the dissolved constituents (after precipitation). This method would produce more stable results but would ignore the actual concentrations present in the sample before sparging.

Calcium. The precision for this methodology (APHA 3500-Ca A) reported by APHA yields a RSD of 9.2% and a relative error of 1.9%. As for hardness, calcium determinations had a similar approach, with some errors being made at the beginning because 25ml of sample was diluted with 25ml of not-so-deionised water. However, as with hardness, these measurements were corrected and 50ml of sample volume with no dilutions were used instead. In this way, 2-5 repetitions were carried out in 23 of the samples producing an average RSD of 17.32%. Again, this apparently large error is attributed to the difficulties in measuring small calcium concentrations (<8mg/l) and $CaCO_3$ precipitation once the sample bottle is opened exposing it to the atmosphere.

Chloride. HACH method 8225 was used to measure chloride. This involves titrating the sample until there is a colour change from yellow to red-brown. However, this endpoint is not very clear because while titrating the sample the colour change goes from yellow to dark orange and finally to red-brown. During this colour sequence, yellow clusters are present and, as the sample is being stirred, the sample colour seems lighter than it truly is. Hence, a biased is introduced and a larger amount of titrant than necessary is added to the sample. However, this error is systematic which means that measurements carried out using this method can be compared against each other. The HACH manual does not mention how to correct for this bias or how to calibrate the measuring method against other systematic errors. Consequently, original chloride measurements where about 23% greater than the chloride concentration from the sample analysed through the CRL Energy laboratory (19/8/2004). Therefore, HACH method 8225 was calibrated against known chloride concentrations. The result of this produced a linear regression formula (Figure B.1) with an excellent coefficient of determination (R^2=0.9957). In this

way, chloride measurements where corrected using the linear regression equation presented in Figure B.1.

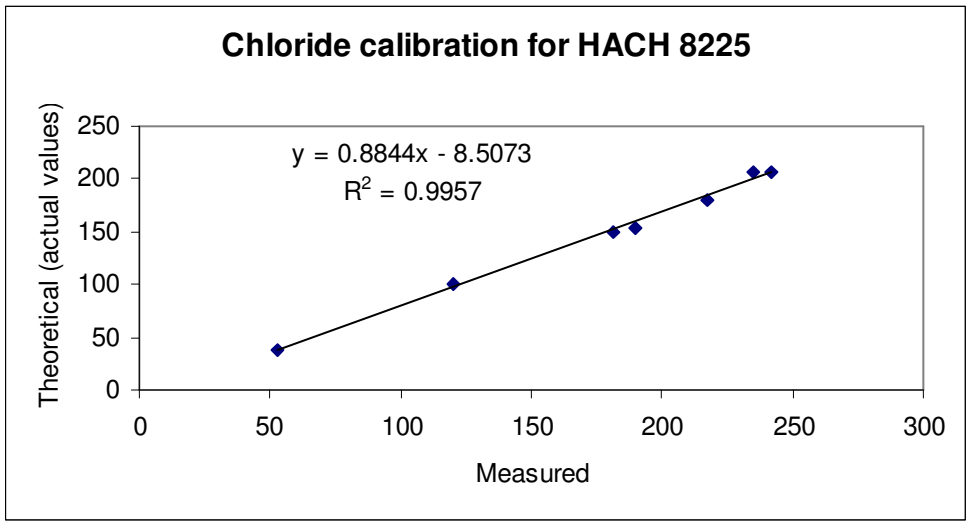

Figure B.1. Calibration of HACH method 8225

On average, chloride concentrations analysed at the EEL were 144 mg/l, while the value measured at the CRL Energy laboratory (19/8/2004 sample) was 146 mg/l. Since CRL Energy uses an ion chromatography (APHA 4110 B) this value should be more precise than the HACH titration method (with calibration). Consequently, the relative error using HACH is 1.44%. To determine an associated error, 2-5 repetitions were carried out in 18 on the Maramarua samples being analysed. The average RSD obtained using this methodology was 1.41%.

HACH method 8225 does not include an estimate of its precision, but it does provide guidelines to test the accuracy of the additions and solutions. For example, the standard 0.0141N silver nitrate solution decomposes with light, so it was tested regularly using a sodium chloride standard solution of 1000mg/l as Cl^-.

Sulphate. The HACH 8051 method used for measuring sulphate, works only for the range of values from 2 to 70 mg/l and uses a digital spectrophotometer device to carry out the sulphate determination. Its sensitivity is reported within a 1 mg/l of SO_4^{2-} range (Hach Company., 2003), and the methodology leaves little room for random errors. In 31 out of the 33 Maramarua C-1 samples analysed using this procedure, sulphate concentrations were below the detectable range of values (<2 mg/l). This was confirmed

with the 19/8/2004 sample analysed at the CRL Energy laboratory which uses ion chromatography (APHA 4110 B) and which reported a value of 0.7 mg/l.

Carbonate equilibrium. The uncertainty associated with the different carbonate species was calculated using error propagation techniques as described in Meyer (1975). For the bicarbonate concentrations of the Maramarua C-1 samples, the average relative standard deviation (RSD) is 20.4% (9.2% min and 23.8% max); for carbonate, the average RSD is 18.4% (8.3% min and 21.6% max); for dissolved carbon dioxide the average RSD was 25.5% (11.5% min and 29.4% max).

Precision and accuracy - discussion

The values for New Zealand CSG water presented in this document correspond to the average of measurement repetitions performed on collected samples. It was possible to store some of these samples in sealed bottles to avoid $CaCO_3$ precipitation. However, after a period of approximately 4 weeks, a white sediment was observed in some of these bottles. This could have been $CaCO_3$ precipitation which could have been produced if CO_2 gas came out of solution under lower partial pressure conditions (this gas could have left the bottle through the cap or could have remained trap in an air gap inside the bottle). Another possibility is that this $CaCO_3$ could have precipitated through a slow diffusion process. Therefore, it was decided not to use these samples to produce more repetitions on the measured parameters. This is a valid objection because the error of the mean is directly proportional to the error of a single observation. Thus, "a reduction by a factor of 10 in the average error of individual measurements produces the same improvement in the precision of the mean as do 100 repetitions" (Meyer, 1975). Consequently, a calcium titration performed on a sample in which $CaCO_3$ was allowed to precipitate would introduce a bias when averaging this value along previous titrations performed on the sample with no $CaCO_3$ precipitation.

Because there is uncertainty in the analytical methods used, it is necessary to clarify a few points. First of all, sulphate concentrations for most of the Maramarua (C-1) 2004/2005 samples analysed at the EEL (University of Canterbury) are unknown, but lower than 2 mg/l (<0.0420 meq/l). Therefore, in order to plot these values in the Piper and Schoeller diagrams (Chapter 3 - figures 3.6, 3.7, and 3.8), a nominal value of 0.02

meq/l was chosen for these samples. Secondly, the methods for calculating magnesium in these samples could give way to error generation. This is because magnesium is calculated by measuring hardness and calcium, and then subtracting calcium from hardness. However, hardness is not only given entirely by magnesium and calcium because other elements like strontium, barium, and some heavy metals can add to the hardness of samples (Hounslow, 1995). This can be observed with the full analysis (CRL Energy laboratory) from the 19/8/2004 which indicated the presence of some heavy metals and barium; its Schoeller diagram (Chapter 3 – figure 3.8) shows the magnesium concentration for this sample below the calculated concentrations for 2004 and 2005 samples. However, the main source of errors is given by the combination of errors when determining both hardness and calcium, which translates into error amplification. For example, some random errors could have been made when measuring hardness (errors in judgement, ambient fluctuations, etc.), thereby producing a result which already contains an associated error. When measuring calcium, a different set of random errors associated with the calcium values is generated and, when combined with the hardness values, these yield even wider fluctuations. It is possible to observe graphically (Chapter 3 – figure 3.8) this phenomenon by inspecting the variations of the 2004/2005 samples measured at the EEL (University of Canterbury). Here, the variations for these samples are lower for calcium than for magnesium. The same analysis holds true for sodium values, which have been calculated in the 2004/2005 samples by assuming zero electro neutrality in the water samples analysed at the EEL. However, in this case because sodium values are much higher than calcium or magnesium values, these differences are not noticeable when taking their logarithm. Hence sodium values appear with practically no variation.

B.3 Time plots for parameters

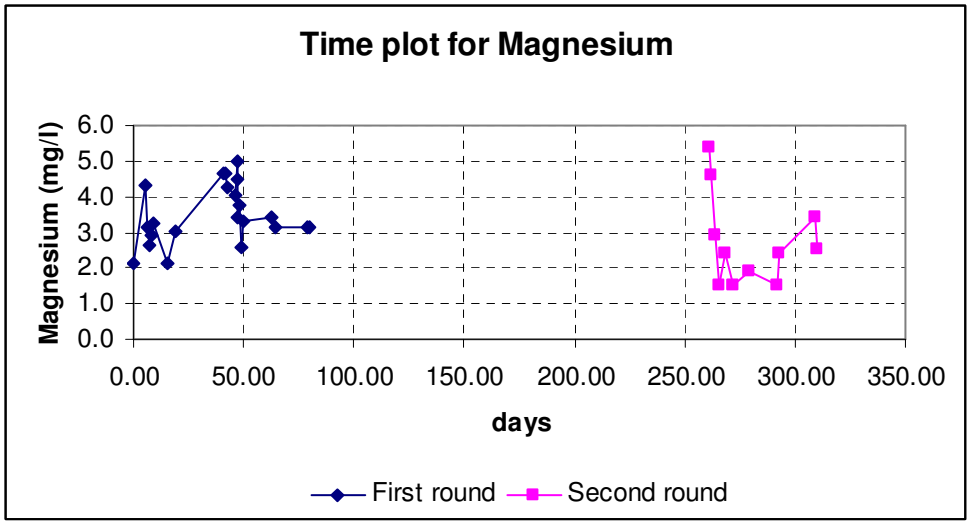

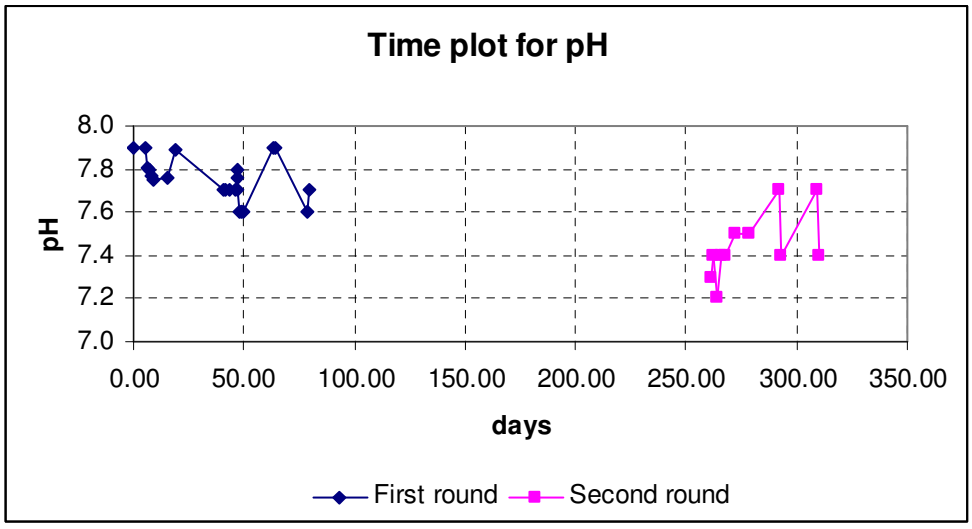

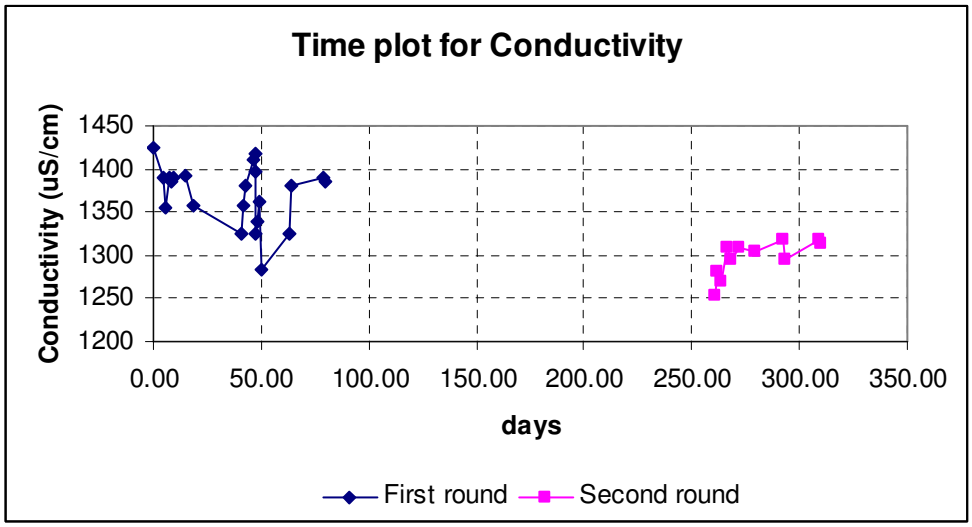
Time plot for Conductivity
Conductivity (uS/cm)
1450
1400
1350
1300
1250
1200
0.00
50.00
100.00
150.00
200.00
250.00
300.00
350.00
days
First round
Second round

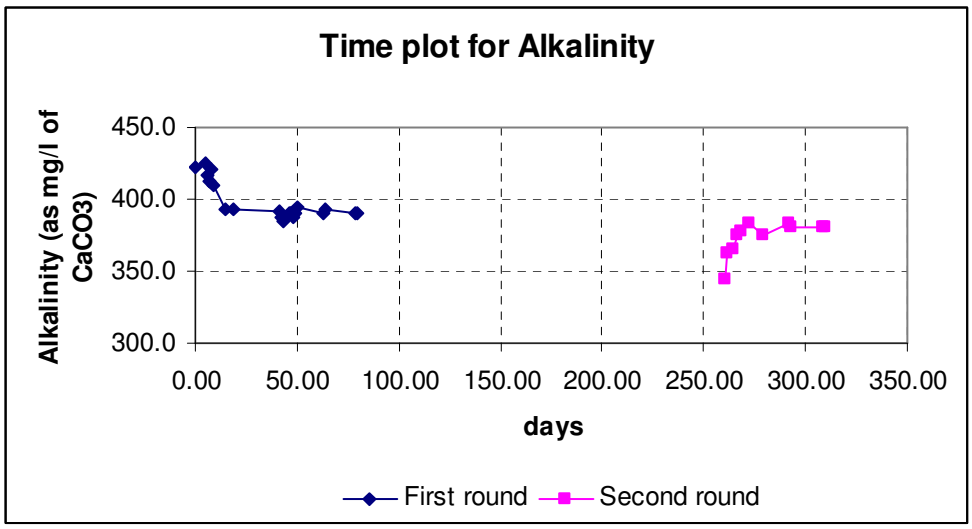
Time plot for Alkalinity
Alkalinity (as mg/l of CaCO3)
450.0
400.0
350.0
300.0
0.00
50.00
100.00
150.00
200.00
250.00
300.00
350.00
days
First round
Second round

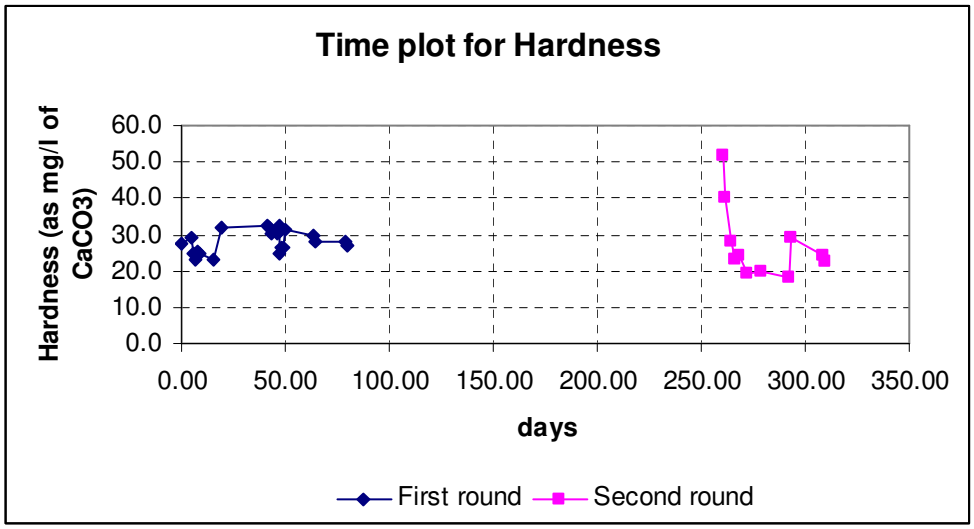
Time plot for Hardness
Hardness (as mg/l of CaCO3)
60.0
50.0
40.0
30.0
20.0
10.0
0.0
0.00
50.00
100.00
150.00
200.00
250.00
300.00
350.00
days
First round
Second round

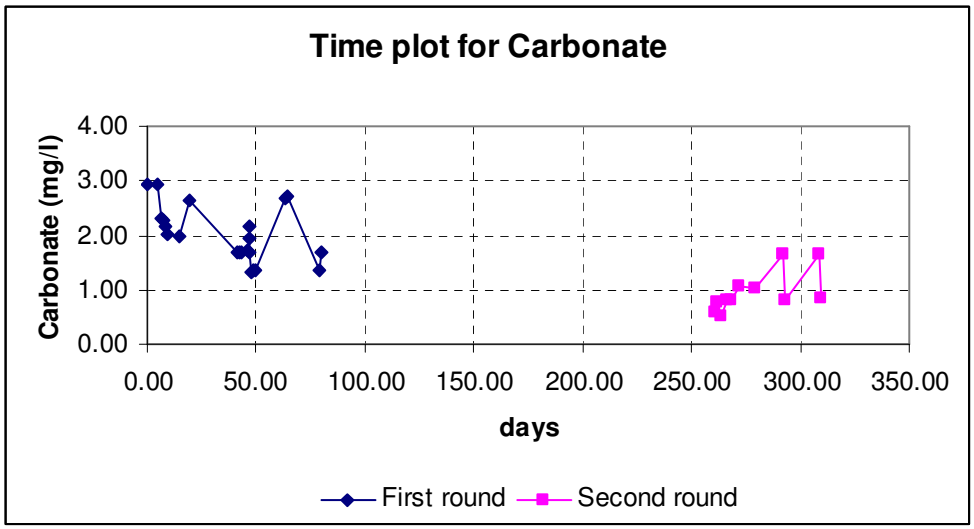
Time plot for Carbonate
Carbonate (mg/l)
4.00
3.00
2.00
1.00
0.00
0.00
50.00
100.00
150.00
200.00
250.00
300.00
350.00
days
First round
Second round

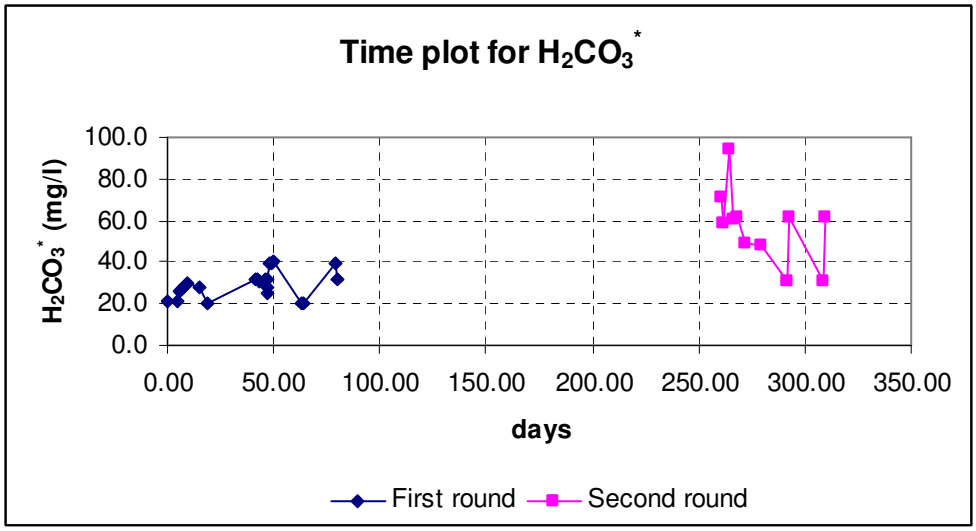
Time plot for H2CO3*
H2CO3* (mg/l)
100.0
80.0
60.0
40.0
20.0
0.0
0.00
50.00
100.00
150.00
200.00
250.00
300.00
350.00
days
First round
Second round

B.4 Principal components analysis

Principal components analysis is a technique that focuses on the eigenvectors of a variance-covariance or a correlation matrix (Davis, 2002). It works as a transformation of the original data thus allowing the reduction of the number of variables involved without significant loss of information. PCA applications in geology are numerous because these allow one to better delineate the principal structure conveyed in geological data. For example, a PCA using the conductivities and γ-ray activities of downhole geophysical logs from the New York State Finger Lakes, has allowed a straightforward and objective definition of the underlying units (Nobes and Schneider, 1996).

Although there are no explicit requirements for the nature of the original data set, the US EPA recommends the data to be normally distributed (US Environmental Protection Agency, 2004).

Let X and Y be two variables representing characteristics of a particular process (Eq B.6 and Eq B.7). In the case of CSG water these variables might be pH and calcium concentrations of a series of samples.

$$X = \{x_1, x_2, ..., x_n\}$$

Eq B.6

$$Y = \{y_1, y_2, ..., y_n\}$$

Eq B.7

$$\left[\sigma^2\right] = \begin{bmatrix} \sigma_x^2 & \sigma_{xy} \\ \sigma_{yx} & \sigma_y^2 \end{bmatrix}$$

Eq B.8

Let $[\sigma^2]$ be a variance-covariance matrix calculated using variables *X* and *Y* (Eq B.8), where σ_x^2 and σ_y^2 are variances of variables *X* and *Y*, and σ_{xy} (= σ_{yx}) their covariance. Then it is possible to represent this matrix graphically by taking its rows as vector coordinates to be plotted on a Cartesian system. In Figure B.2, “Vector 1”

represents the first row of matrix [σ^2], while "Vector 2" represents its second row. The eigenvectors of [σ^2] will have the same slope as the principal axes (I and II) of the ellipse in Figure B.2; the eigenvalues (λ_I and λ_{II}) represent the length of its principal semi axes. It is important to note that the eigenvectors of [σ^2] are mutually orthogonal, and the sum of its eigenvalues is equal to the sum of the elements in its diagonal ($\sigma_x^2 + \sigma_y^2$) with each variable making its own contribution to the total variance.

The sum of the principal semi axes' length represent the total variance associated with [σ^2], but their individual lengths correspond to the calculated eigenvalues and not to the individual variances. Therefore, each eigenvalue contributes to the total variance, however the proportion at which this takes place is different to the contribution of individual variances. This time the major principal semi axis (I) will be responsible for most of the variance, while the secondary principal semi axis (II) will only account for a small contribution.

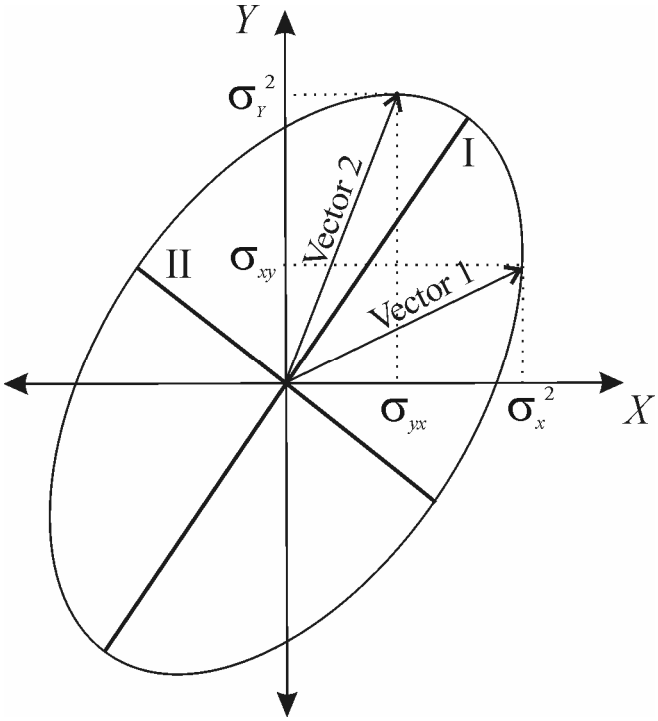

Figure B.2. Graphic representation of a variance-covariance matrix.

It is possible to project the original set of data on to the principal semi axis (I and II) through a transformation defined by a linear combination of eigenvalues. Let A be the matrix of eigenvalues of $[\sigma^2]$, and A_I and A_{II} matrix vectors of A (Eq B.9). If α_1 and α_2 are the components of A_I, and β_1 and β_2 are the components of A_{II}, then the transformation of the original data set, X and Y, into the principal component space, XZ and YZ, will be of the form presented in Eq B.10. This transformation is presented in matrix notation in Eq B.11.

$$A = \begin{bmatrix} A_I & A_{II} \end{bmatrix} = \begin{bmatrix} \begin{bmatrix} \alpha_1 \\ \alpha_2 \end{bmatrix} & \begin{bmatrix} \beta_1 \\ \beta_2 \end{bmatrix} \end{bmatrix}$$

Eq B.9

$$\begin{aligned} XZ_1 &= x_1 \cdot \alpha_1 + y_1 \cdot \alpha_2 & YZ_1 &= x_1 \cdot \beta_1 + y_1 \cdot \beta_2 \\ XZ_2 &= x_2 \cdot \alpha_1 + y_2 \cdot \alpha_2 & YZ_2 &= x_2 \cdot \beta_1 + y_2 \cdot \beta_2 \\ &\vdots & &\vdots \\ XZ_n &= x_n \cdot \alpha_1 + y_n \cdot \alpha_2 & YZ_n &= x_n \cdot \beta_1 + y_n \cdot \beta_2 \end{aligned}$$

Eq B.10. Principal components space transformations

$$Z = \begin{bmatrix} XZ & YZ \end{bmatrix} = \begin{bmatrix} x_1 & y_1 \\ x_2 & y_2 \\ \cdot & \cdot \\ \cdot & \cdot \\ \cdot & \cdot \\ x_n & y_n \end{bmatrix} \cdot \begin{bmatrix} \alpha_1 & \beta_1 \\ \alpha_2 & \beta_2 \end{bmatrix} = \begin{bmatrix} [X] & [Y] \end{bmatrix} \cdot A$$

Eq B.11

The new data set, Z, is referred to as the "principal components scores" or simply "scores", whereas the matrix of eigenvalues, A, is referred to as the "principal components loadings" or "loadings"(Davis, 2002). The scores, XZ and YZ, will be uncorrelated because the principal semi axes on to which these are projected are mutually orthogonal. What's more, the variance of the first new data set, XZ, will be equal to the first eigenvalue, and the variance of the second new data set, YZ, will be equal to the second one. Thus, the new data sets will contain the same total variance as the original

data set, but the partial distribution of variance will fall on each separate data set, *XZ* or *YZ*, which will be equal to their corresponding eigenvalues.

The analysis can be extended to more than just two sets of variables, so a large number of properties or characteristics can be included; plotting the scores on principal components space becomes complicated and sometimes impossible but the validity of the analysis still holds. In theory, there is no restriction regarding the minimum number of observations to carry out a principal components analysis. However, variances and covariances need a large sample size before stabilising, and for 2 or less observations ($n \leq 2$) it is not possible to calculate these values. To deal with incommensurate units, it is possible to standardize the original data by subtracting the average and dividing by the standard deviation for each data point. In this case, the variance-covariance matrix becomes the correlation matrix, [*R*], and the PCA is carried out using the latter. A straight forward way of computing the correlation matrix is by transposing the original data set and multiplying it by itself, the result is then divided by *n*-1 to avoid bias (Eq B.12). In this case, the diagonal of [*R*] will contain ones, and the sum of these will be equal to the number of vector columns (properties or characteristics).

$$[R] = \frac{1}{n-1}[G]^t \cdot [G]$$

where
[*G*] is a matrix containing the original data set in vector columns
n is the total number of samples or observations
Eq B.12

The analysis of principal components usually focuses on analysing the effect that each variable (property or characteristic) has on the total variation. In addition, the analysis can solely focus on those eigenvectors whose eigenvalues account for the majority of the variance, which simplifies the problem. By concentrating on analysing the loadings it is possible to determine which characteristics are relevant within each eigenvector. This process sometimes is referred to as “reification”(Davis, 2002). If the studied phenomenon has several characteristics (in the case of CSG water these could be pH, calcium concentration, alkalinity, etc.) then a PCA could determine which of these characteristics is responsible for the most variation in the data set. Furthermore, a closer

examination of the loadings responsible for the highest contribution of variance can provide important information about the processes involved in shaping this variation. PCA is a powerful technique; however it is not straightforward because it works by interpreting the *transformed* data and its components, and not the actual data set. Also, in PCA the number of principal components (eigenvalues of *A*) is always equal to the number of variables, which can complicate the scrutiny of results if there are too many variables or if their eigenvalues are similar in magnitude. A different variation of PCA, factor analysis, deals with these issues and proves quite effective in describing the processes involved.

B.5 Factor analysis

Given a $[G]_{nxm}$ data matrix, the objective of factor analysis is to select p-variates from a total of m-variates, and to express the data matrix of p-variates into common factors (common to all the p variables) and unique factors (unique to each of the p variables) (Haan, 1977). This decomposition can be expressed using algebraic notation for each of the n rows of matrix $[G]_{nxm}$, in the following way:

$$G_j = \sum_{r=1}^{p} a_{jr} \cdot f_r \quad + \quad \varepsilon_j \qquad\qquad j = 1.....m$$

$$p < m$$

Eq B.13 (Davis, 2002).

In Eq B.13, a_{jr} are the factor loading coefficients, f_r, are the common factors, and ε_j are the unique factors representing the random variation unique to G_j. Common applications of factor analysis in hydrology, however, are normally carried out by ignoring the unique factors, ε_j (Matalas and Reiher, 1967; Wallis, 1967).

To simplify the analysis, it is possible to express the factor loading coefficients and the common factors in matrix notation. In this way, $[A^R]$ will be an *mxp* matrix of factor loadings and [*F*] will be an *nxp* matrix of common factors. The different values of G_j are assumed to be multivariate and normally distributed. Therefore the variance/covariance matrix can be calculated by multiplying $[A^R]$ by its transpose and

then adding the independent variations (Eq B.14) (Davis, 2002). If the unique factors are ignored, Eq B.14 can be further simplified. Also, if the data are standardised using Eq B.12, then the variance/covariance matrix becomes the correlation coefficient matrix, [*R*].

$$\left[\sigma^2\right] = \left[A^R\right] \cdot \left[A^R\right]^t + \left[\text{var } \varepsilon_{jj}\right]$$

Eq B.14 (Davis, 2002).

The analysis then focuses not on calculating the actual factor decomposition of G_j, but rather on calculating the loading matrix, $[A^R]$, and the matrix of factor scores, $[S^R]$. As in the case of PCA, the analysis of the factor loading matrix can provide insight in determining the most relevant processes involved in shaping a particular data set. However, this time the analysis focuses on analysing the loadings of an actual factor *decomposition* rather than a factor *transformation*.

Before outlining the Factor Analysis procedure, it is necessary to consider the number of factors to be extracted. Originally, there are *m* number of variates, and the challenge is to extract a fewer number (*p*) of these without significant loss of information. Determining the number of factors to be extracted is not straight forward and requires some subjectivity. The simplest strategy for selecting the number of factors to be extracted, is to decide on the value of *p* before carrying out the analysis (Davis, 2002). This can be done if there is some hint on the number of possible factors for a particular problem. Some researchers recommend extracting only two or three factors because this is the maximum number of factors that can be displayed on a diagram (Davis, 2002). Another approach in selecting the number of factors to be extracted is to select only those factors that are responsible for most of the variance, which is reflected by the corresponding eigenvalues. For example, an “elbow” in a scree plot (a plot of the eigenvalues against their corresponding factor numbers) shows the maximum number of factors to extract (UCLA Academic Technology Services). Figure B.3 shows an example of such an elbow configuration in a scree plot - in this case only 8 factors should be extracted.

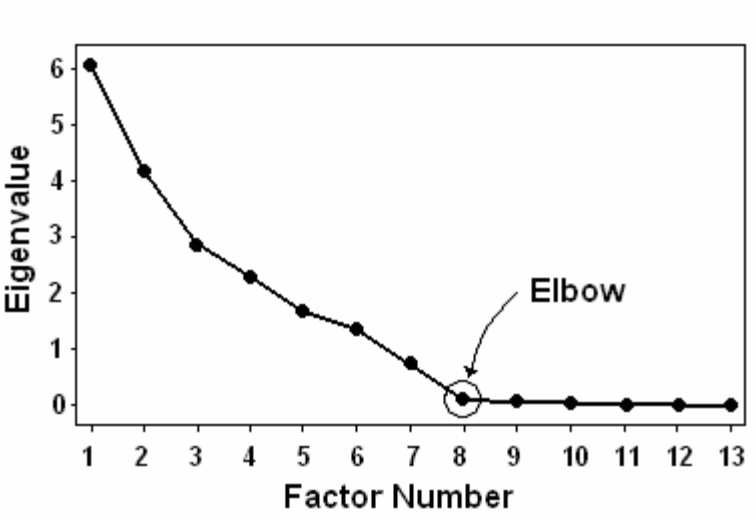

Figure B.3. Example of a typical scree plot with an elbow configuration

In factor analysis, $[A^R]$ is calculated by multiplying the *mxp* matrix of eigenvectors, $[U]$, by a diagonal *pxp* matrix containing the square root of the corresponding eigenvalues $[\Lambda]$ (Eq B.15, Eq B.16, and Eq B.17). This analysis is normally referred to as *R*-mode factor analysis because it is carried out using the eigenvectors of the correlation coefficient, $[R]$ (Eq B.12). It is also possible to carry out a similar analysis by calculating the eigenvectors of $[Q]$, which is calculated in the same way as $[R]$ was calculated (using Eq B.12), but this time the matrix of original observations $[G]$ is multiplied by its transpose rather than the transpose being multiplied by the matrix. This analysis is known as *Q*-mode factor analysis; in this case the factor loadings signify the proportion that must be allocated to each individual observation in order to project the variates onto the factor axes (Davis, 2002). *R*-mode factor analysis, on the other hand, focuses on representing the weighting that is assigned to each variate so that the observations are projected onto the factor axes (Davis, 2002). Since the aim of this particular study focuses on analysing the processes involved in shaping Maramarua data, the analysis used will be *R*-mode factor analysis.

$$[U]=\begin{bmatrix} \alpha_1 & \beta_1 & \cdot & \cdot & \psi_1 \\ \cdot & \cdot & \cdot & \cdot & \cdot \\ \cdot & \cdot & \cdot & \cdot & \cdot \\ \cdot & \cdot & \cdot & \cdot & \cdot \\ \alpha_m & \beta_m & \cdot & \cdot & \psi_m \end{bmatrix}_{mxp}$$

where,

the columns of $[U]$ are the eigenvectors of $[\sigma^2]$ or $[R]$

Eq B.15

$$[\Lambda]=\begin{bmatrix} \sqrt{\lambda_1} & 0 & 0 & 0 & 0 \\ 0 & \sqrt{\lambda_2} & 0 & 0 & 0 \\ 0 & 0 & \cdot & 0 & 0 \\ 0 & 0 & 0 & \cdot & 0 \\ 0 & 0 & 0 & 0 & \sqrt{\lambda_p} \end{bmatrix} = [I]\cdot\left[\sqrt{\lambda}\right]^t$$

where,

$\lambda = p$ eigenvalues of $[\sigma^2]$ or $[R]$

$[I] = pxp$ identity matrix

Eq B.16

$$\left[A^R\right]=[U]\cdot[\Lambda]=\begin{bmatrix} a_{11} & a_{12} & \cdot & \cdot & \cdot & a_{1p} \\ a_{21} & \cdot & \cdot & \cdot & \cdot & \cdot \\ \cdot & \cdot & \cdot & \cdot & \cdot & \cdot \\ \cdot & \cdot & \cdot & \cdot & \cdot & \cdot \\ a_{m1} & \cdot & \cdot & \cdot & \cdot & a_{mp} \end{bmatrix}$$

Eq B.17

The factor loadings in Eq B.17 have the same direction as the eigenvectors and their magnitudes are given by the square roots of their eigenvalues. For example, if just the first two factors are selected (first two columns of matrix $[A^R]$ in Eq B.17) and m=2 then the two factors can be represented in a two dimensional coordinate system (Figure B.4). Here, the first two factors are orthogonal and their coordinates are given by their corresponding factor loadings (in vector columns); their magnitudes are in fact the square roots of their eigenvectors. In this way, the eigenvalues represent the proportion of the total variance accounted for by the eigenvectors. The sums of the squared factor loading coefficients for each row of the matrix in Eq B.17 are referred to as “communalities”, and these represent the amount of each variable’s variance retained throughout the factors. If

no factors are extracted ($p = m$) then the communalities are equal to the original variances (if working with raw data) or to 1 (if working with standardised data; Eq B.18) (Davis, 2002). Therefore if $p<m$ factors are extracted, the communalities provide a measurement of the efficiency of the factor extraction process.

$$If\ \ p = m\ and\ i = 1..m \quad \Rightarrow \quad \sum_{j=1}^{p} a_{ij}^2 = 1$$

Eq B.18

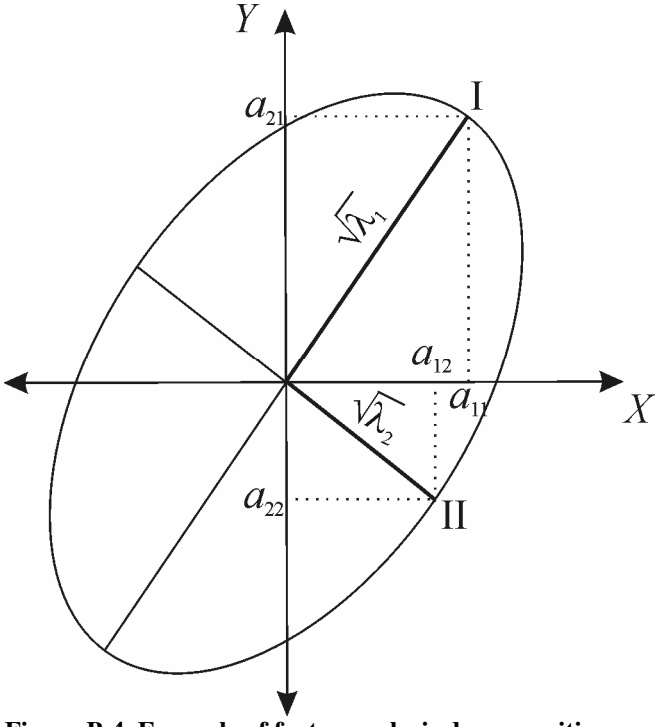

Figure B.4. Example of factor analysis decomposition

As with PCA, it is possible to compute the matrix of factor scores, $[S^R]$, but this time the original data is multiplied by the factor loading matrix, $[A^R]$ (Eq B.19).

$$[S^R] = [G] \cdot [A^R]$$

Eq B.19

However, the original factor decomposition (Eq B.13) also takes into account the unique factors (ε_j). Therefore, the factor scores calculated in this way contain the variance/covariance structure of the original m values as well as the variance/covariance structure of the selected p factors. To account for this difference, the unique part of the original m values has to be divided out of the factor scores resulting in a matrix of "true"

factor scores (Davis, 2002). This is done by pre multiplying the factor loadings by the inverse of the variance/covariance matrix [σ^2] or correlation matrix [R] (Eq B.20). The matrix of factor score coefficients, [B], is defined by Eq B.21 further simplifying Eq B.20 into Eq B.22.

$$[S^R_{True}] = [G] \cdot [R^{-1}] \cdot [A^R]$$
Eq B.20

$$[B] = [R^{-1}] \cdot [A^R]$$
Eq B.21

$$[S^R_{True}] = [G] \cdot [B]$$
Eq B.22

In this way, the analysis of the matrix of factor score coefficients, [B], allows determining the variates with the highest influence, and the possible interrelationships or processes involved in shaping the data. In addition, a plot of the scores could provide insight into the influence of selected factors on selected properties inherent to the original data set. Consequently, a factor analysis transformation can be a powerful tool when determining which processes have the highest impact on a final outcome shaping a particular data set. Sometimes, however, it is not possible to determine which factors have the highest or lowest impacts as these appear to have very similar weights. In these instances, it is possible to force the analysis into exaggerating these differences thus making it easier to interpret factor analyses results.

The factor loading matrix contains the correlations between the loadings and the original variables. Therefore, the factors plot in axes that are orthogonal to each other in p space. There are, however, m-p axes that have been removed, and it is possible to further rotate the remaining p axes. Such a procedure is normally referred to as “factor rotation”. There are several rotation techniques, but the most popular one is the “varimax” scheme first defined by Kaiser (1958). In this technique, the factor axes are rotated so that the projection of each loading onto the axes is either near the origin or far away from it. Therefore, the factor loading matrix is rotated by multiplying it to an orthogonal matrix, [T] (Eq B.23), so that the correlations between the loadings and the original variables is

changed - the factor loadings will be either close to ±1 or ~0 (Davis, 2002). Matrix [*T*] is calculated by maximizing the variance of the loadings on the factors. This variance is defined by Eq B.24, and the quantity to maximize is *V* (Eq B.25). The new factor score coefficients will be given by Eq B.26 and the rotated true factor scores will be given by Eq B.27. Because the axes have been rotated to accentuate differences, it is possible to interpret the factor score coefficients more easily.

$$[A^{R}_{Rotated}] = [A^{R}] \cdot [T]$$

Eq B.23

$$s_k^2 = \frac{p \cdot \sum_{j=1}^{m} (a_{jp}^2 / h_j^2)^2 - (\sum_{j=1}^{m} a_{jp}^2 / h_j^2)^2}{p^2}$$

where,
s_k^2= the variance of the loading on the *k*th factor
p = the number of factors
m= the number of original variables
a_{jp}= the loading of variable *j* on factor *p*
h_j^2= the communality of the *j*th variable

Eq B.24 (Davis, 2002)

$$V = \sum_{k=1}^{p} s_k^2$$

Eq B.25

$$[B_{Rotated}] = [R^{-1}] \cdot [A^{R}_{Rotated}]$$

Eq B.26

$$[S^{R}_{True,\ Rotated}] = [G] \cdot [B_{Rotated}]$$

Eq B.27

There is no formal restriction on the minimum number of observations to carry out a factor analysis. However, the factor analysis procedure uses correlations, which usually require a large number of observations before they stabilise. Many researchers give subjective recommendations on the minimum number of observations to carry out factor analyses. Comrey (1992), for example, advises that 50 is a very poor number, 100

is poor, 200 is fair, 300 is good, 500 is very good, and 1000 or more is excellent. Hatcher (1994) recommends that the number of observations should be either five times the number of variables or 100, whichever is larger. On the other hand, Bryant and Yarnold (1995) recommend that the ratio between number of observations and variables should be 5 or larger. During CSG exploration, these recommendations are hard to implement simply because the number of samples is always limited. Therefore additional precautions have to be taken when dealing with a small number of observations. For example, the data can be checked for outliers and tested for normality prior to carrying out the analysis. Also, once the factor analysis is carried out, it should be checked that the communalities are close to 1.

B.6 Implementing Factor Analysis using MINITAB

MINITAB is a computer program designed to carry out advanced statistical calculations. It was originally developed in 1972 by faculty members of The Pennsylvania State University to aid in the teaching of statistics at university level. The main feature in MINITAB is its user-friendliness and versatility- this program is now established as a bench mark program in statistical analysis, and is used in a variety of applications including research, industry, and science. The latest release is version 14, and its features include regression analysis, analysis of variance, reliability/survival analysis, time-series and forecasting, and multivariate analysis to mention a few (MINITAB Inc, 2005). The multivariate analysis techniques in MINITAB include PCA and Factor Analysis. However, the calculation procedure is not explained in the software manuals, and the technical language is verbal rather than mathematical which can become confusing at times. For example, the terms “scores” and “coefficients” are loosely used in MINITAB indistinctly on whether the analysis being carried out is PCA or Factor Analysis. The correct terminology would be to use the terms “principal component scores” and “principal component loadings” when carrying out PCA, and to use the terms “factor scores” and “factor score coefficients” when performing a factor analysis. However, once the user gets used to this terminology PCA and Factor Analyses are easy to implement and the user can focus his or her attention in interpreting results rather than

on performing tedious calculations. Therefore, the analysis of Maramarua CSG water quality data was carried out using MINITAB v14. Prior to carrying out the analysis it was necessary to test the data for normality and, in cases where the data did not follow a normal distribution, transformations were duly applied. MINITAB does not require a predefined number of observations to carry out factor analyses. However, it does require more observations than variables to carry out the calculations.

B.7 Data transformation for factor analysis

The test of normality used in this analysis was the *W* test developed by Shapiro and Wilk(1965). This procedure tests the H_0 null hypothesis "the population has a normal distribution" versus the H_A hypothesis "the population does not have a normal distribution". To do this, the two most extreme values are subtracted and multiplied by a constant (this constant reflects the tendency of extreme values in normal distributions (Milke and Huitric, 1993)). This process is carried out with subsequent extreme values, and the final result (*W*) is then summed, squared, and divided by the sum of the squared deviations of the original data set. The *W* value is then compared against a known W_α value which has been developed by Shapiro and Wilk(1965) using Monte Carlo simulations. If $W<W_\alpha$,the null hypothesis (H_0) is rejected and H_A is accepted. In this test, the significance level (α) reflects the probability of inadvertently rejecting the null hypothesis when it is in fact true. Therefore, small values of α are more conservative than larger ones; for this analysis, a 1% significance level (99% confidence) was employed to select a W_α value for testing the null hypothesis. If the null hypothesis was false using this significance level (H_A), then a transformation was applied to the data set so that the hypothesis was not false anymore (H_0). The transformations used for this purpose were selected using the MINITAB software which is able to calculate the optimal transformation to normalise data that do not follow a normal distribution. Table B.2 shows the normalised parameters and their selected transformations (if any) passing the *W* test, and the original data vs. the transformed data are plotted in figures 5-7.

Table B.2. Normalised parameters and their selected transformations (if any) after W test (α=0.1%)

Parameter	Transformation	Mean/transformed mean	Std. dev./ transformed std. dev.
pH	NTR	7.7	0.18
TDS	NTR	773	24.13
Alkalinity	$x^{1/2}$	19.8	0.37
Hardness	NTR	26.7	4.03
Calcium	NTR	5.6	1.03
Chloride	$1.8 + 1.18 \cdot Log\left[\frac{x - 139.48}{159.63 - x}\right]$	1.04	0.42
Carbonate	NTR	1.72	0.66
Carbon dioxide	$-1.18 + 1.03 \cdot \text{asinh}\left[\frac{x - 23.90}{5.75}\right]$	-0.03	1.08
Sodium	NTR	314.1	5.71
Water column	NTR	101.86	42.65

NTR = No transformation required

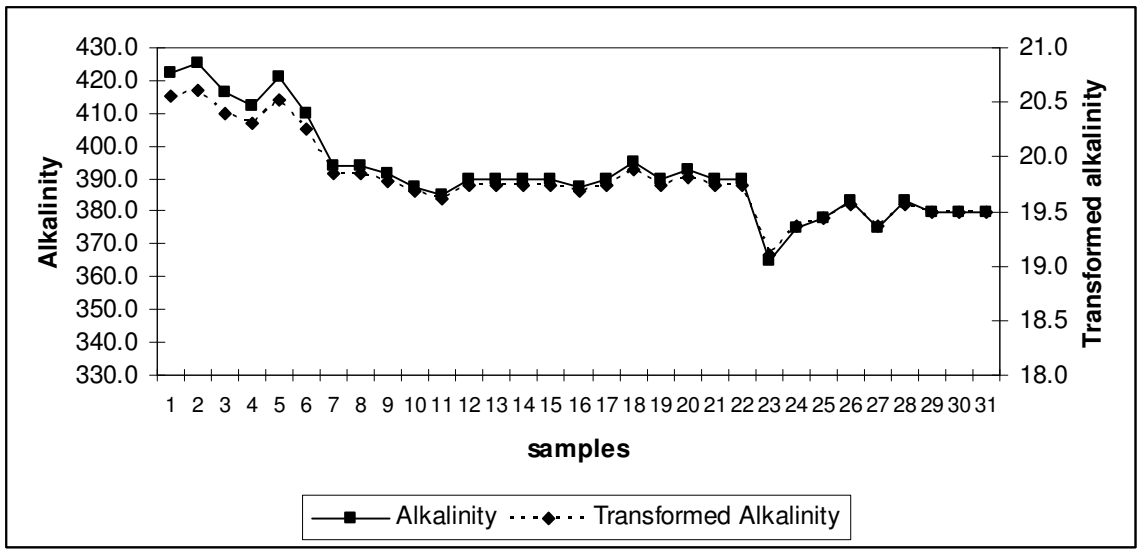

Figure B.5. Original alkalinity data plotted against transformed alkalinity data

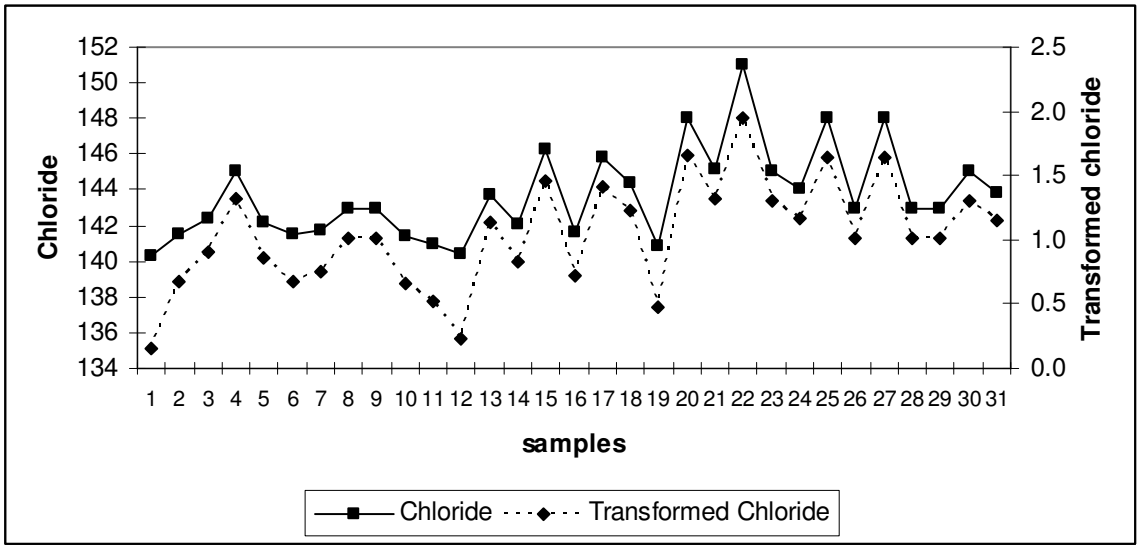

Figure B.6. Original chloride data plotted against transformed chloride data

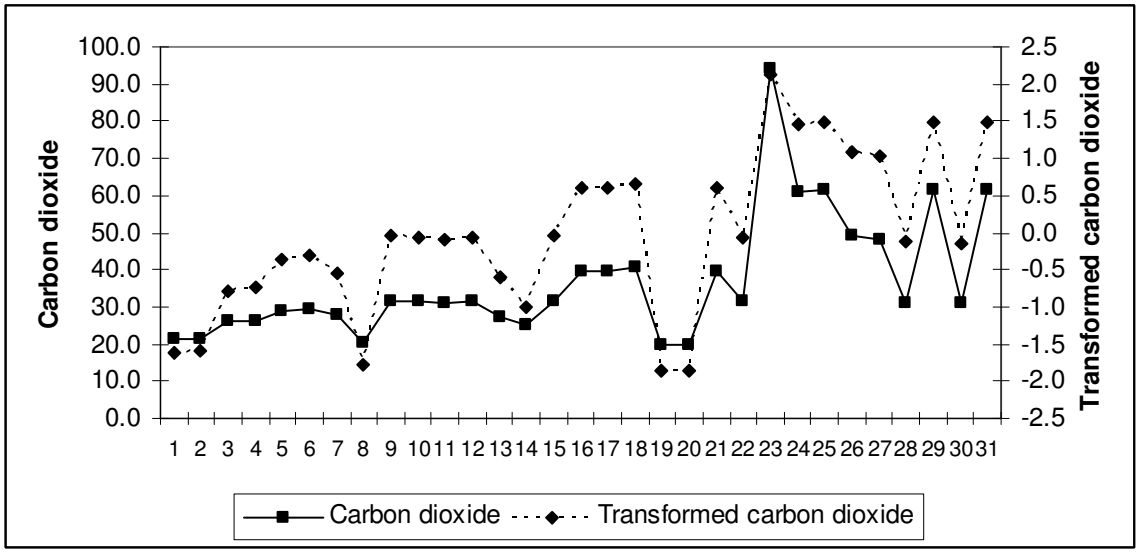

Figure B.7. Original carbon dioxide data plotted against transformed carbon dioxide data.

B.8 References

American Public Health Association., American Water Works Association., and Water Environment Federation., 1999, Standard methods for the examination of water and wastewater: [Washington, D.C.], American Public Health Association, 1 computer optical disc p.

Bryant, F.B., and Yarnold, P.R., 1995, Principal components analysis: Thousand Oaks, CA, Sage Publications.

Comrey, A.L., and Lee, H.B., 1992, A first course in factor analysis: Hillsdale, N.J., L. Erlbaum Associates, xii, 430 p.

Davis, J.C., 2002, Statistics and data analysis in geology: New York, J. Wiley, xvi, 638 p.

Haan, C.T., 1977, Statistical methods in hydrology: Ames, Iowa State University Press, xv, 378 p.

Hach Company., 2003, Water analysis handbook : drinking water, wastewater, seawater, boiler/cooling water, ultrapure water: Loveland, Colo., Hach, 1268 p.

Hatcher, L., 1994, A step-by-step approach to using the SAS system for factor analysis and structural equation modeling: Cary, N.C., SAS Institute, xiv, 588 p.

Hounslow, A., 1995, Water quality data : analysis and interpretation: Boca Raton, Lewis Publishers, 397 p.

Kaiser, H.F., 1958, The Varimax Criterion for Analytic Rotation in Factor-Analysis: Psychometrika, v. 23, p. 187-200.

Matalas, N.C., and Reiher, B.J., 1967, Some Comments on Use of Factor Analyses: Water Resources Research, v. 3, p. 213-&.

Meyer, S.L., 1975, Data analysis for scientists and engineers: N.Y., Wiley, 513 illus. p.

Milke, M.W., and Huitric, R.L., 1993, Simulating Errors in Statistical Tests of Leachate-Impacted Groundwater Quality: Ground Water, v. 31, p. 645-653.

MINITAB Inc, 2005, MINITAB, Volume 2005: Pennsylvania.

Nobes, D.C., and Schneider, G.W., 1996, Results of downhole geophysical measurements and vertical seismic profile from the Canandaigua borehole of New York State Finger Lakes: Special Paper - Geological Society of America, v. 311, p. 51-63.

Shapiro, S.S., and Wilk, M.B., 1965, An Analysis of Variance Test for Normality (Complete Samples): Biometrika, v. 52, p. 591-&.

US Environmental Protection Agency, 2004, Statistical Primer, Volume 2005, p. web page.

UCLA Academic Technology Services, Factor Analysis Using SAS PROC FACTOR, *in* Services, U.A.T., ed., Volume 2005: Los Angeles, p. Web page.

Van Voast, W.A., 2003, Geochemical signature of formation waters associated with coalbed methane: Aapg Bulletin, v. 87, p. 667-676.

Wallis, J.R., 1967, When Is It Safe to Extend a Prediction Equation - an Answer Based Upon Factor and Discriminant Function Analysis: Water Resources Research, v. 3, p. 375-&.

Appendix C

C.1 Infiltration risk model

Introduction

Discharge of high-SAR water, such as CSG water, on to the land can result in soil infiltration problems resulting from soil dispersion and loss of aggregation. The parameters that influence the chemical dispersion phenomenon are: soil salinity, sodicity (ESP), clay content, organic matter content, cation exchange capacity (CEC), and soil drainage.

Materials and Methods

A GIS study using ArcMap was carried out using the Fundamental Soil Data Layer (FSDL) obtained from Landcare Research New Zealand Ltd (Landcare Research New Zealand Ltd, 2000). This database contains information on CEC, soiltype, salinity, organic matter, and drainage for New Zealand soils. The soiltype included references to the soils' main texture type, but this information had to be summarized into broader categories (clay, sand, loam, sand, silt, and gravels) to determine clay percentage (which plays an important role in assessing soil dispersion).

CEC and clay content were considered to be properties which contribute to soil dispersion potential, while salinity, organic matter, and drainage were assumed to be attenuating properties. All of these properties, but soiltype, were already subdivided into 5 categories in the FSDL, however some of these had to be reclassified so that the scoring system was consistent throughout (1-5 with 1 the best score and 5 the worst). As previously mentioned, soiltype was rearranged into main texture format, and a scoring system which reflected the clay percentage was developed - a score of 3 was assigned to clay, 2 to loam, 1 to silt, -2 to peat, and 0 to everything else. These scores, along with the class scores for the rest of the properties being analysed, were added or subtracted to

produce an Infiltration Problem Potential (IPP) index (Table C.1 and Eq C.1). This results in a model for assessing infiltration potential problems from the soil point of view. That is, this model aims at assessing soil response to prolonged leaching with high SAR water, for example, but assuming that this exposure will take place in the long term. Therefore, rainfall or potential evapotranspiration will not influence the final result, which is unavoidable in the long-term.

Table C.1. Salinity categories used in IPP model

CEC class	Salinity	Texture (Clay %)	Organic matter C	Drainage
1: very low	1: very low	-2: peat	1: very low	1: very poor
2: low	2: low	0: sand and gravels	2: low	2: poor
3: medium	3: medium	1 silt (up to 25% clay)	3: medium	3: imperfect
4: high	4: high	2: loam	4: high	4: moderately well
5: very high	5: very high	3: clay	5: very high	5: well

$$IPP = CEC\ class + Texture\ class - Salinity\ class - Organic\ matter - 0.5 \cdot Drainage + 14.5$$ Eq C.1

All of the scores, which are added or subtracted in Eq C.1, are weighted in the same manner except for drainage. Drainage was assigned a weight of 0.5 because this value was derived from in situ visual interpretations of the soil profile, while the rest of the values were obtained using analytical techniques. It is important to note that some terms (salinity, organic matter, and drainage) in Eq C.1 are being subtracted from the *IPP*. This is because these properties can actually enhance soil permeability. For example, salinity can provide aggregation and soil stability (Oster, 1979), and adequate drainage helps maintain good soil stability. Similarly, organic matter can provide bonding agents which helps maintain good soil structure (Cameron, 2003). A value of 14.5 is added to the final IPP value to avoid negative values which could arise when dealing with soils with low CEC, low clay percentage, high peat content, high salinity, high organic matter, and high drainage. The final model was calibrated assuming Central Otago (Allen et al., 1998) soils would have serious infiltration problems (alkali soils), and soils from

Clandeboye (Cameron et al., 2003) would have moderate infiltration problems when irrigated with high-SAR water.

Results

All of the properties affecting soil infiltration under high-SAR irrigation regimes were plotted in various graphs with their different categories. CEC class and Organic Matter content have already been presented in Chapter 3 (Ch. 3: Figures 1 and 2), and salinity class, texture class, and drainage class plots are presented in Figures 1, 2, and 3 in this appendix. However, the main result of this analysis is the IPP index classification as presented in Figure 3 (Chapter 3). This figures' analysis has been presented in Chapter 3.

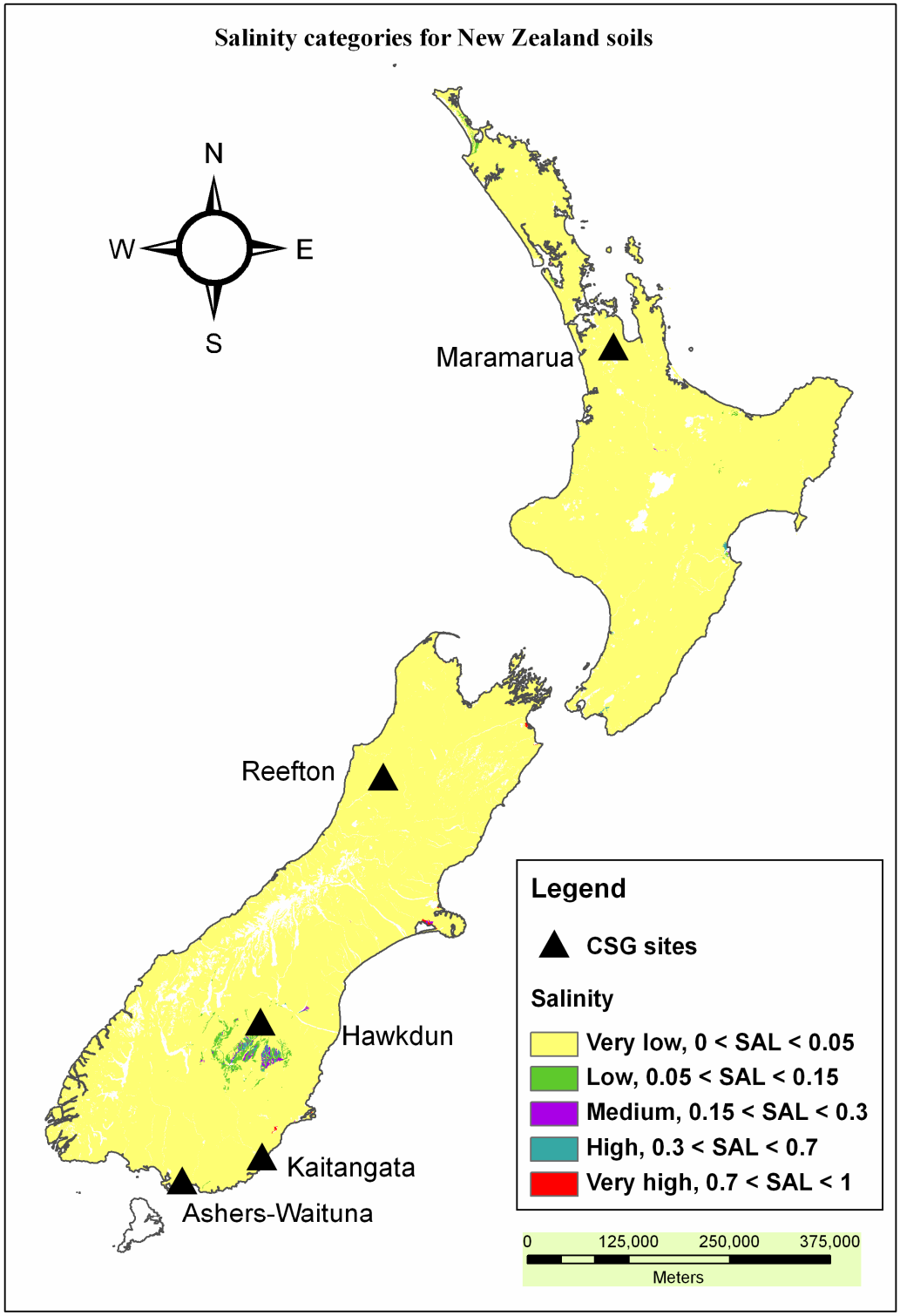

Figure C.1. Salinity classes for New Zealand soils.

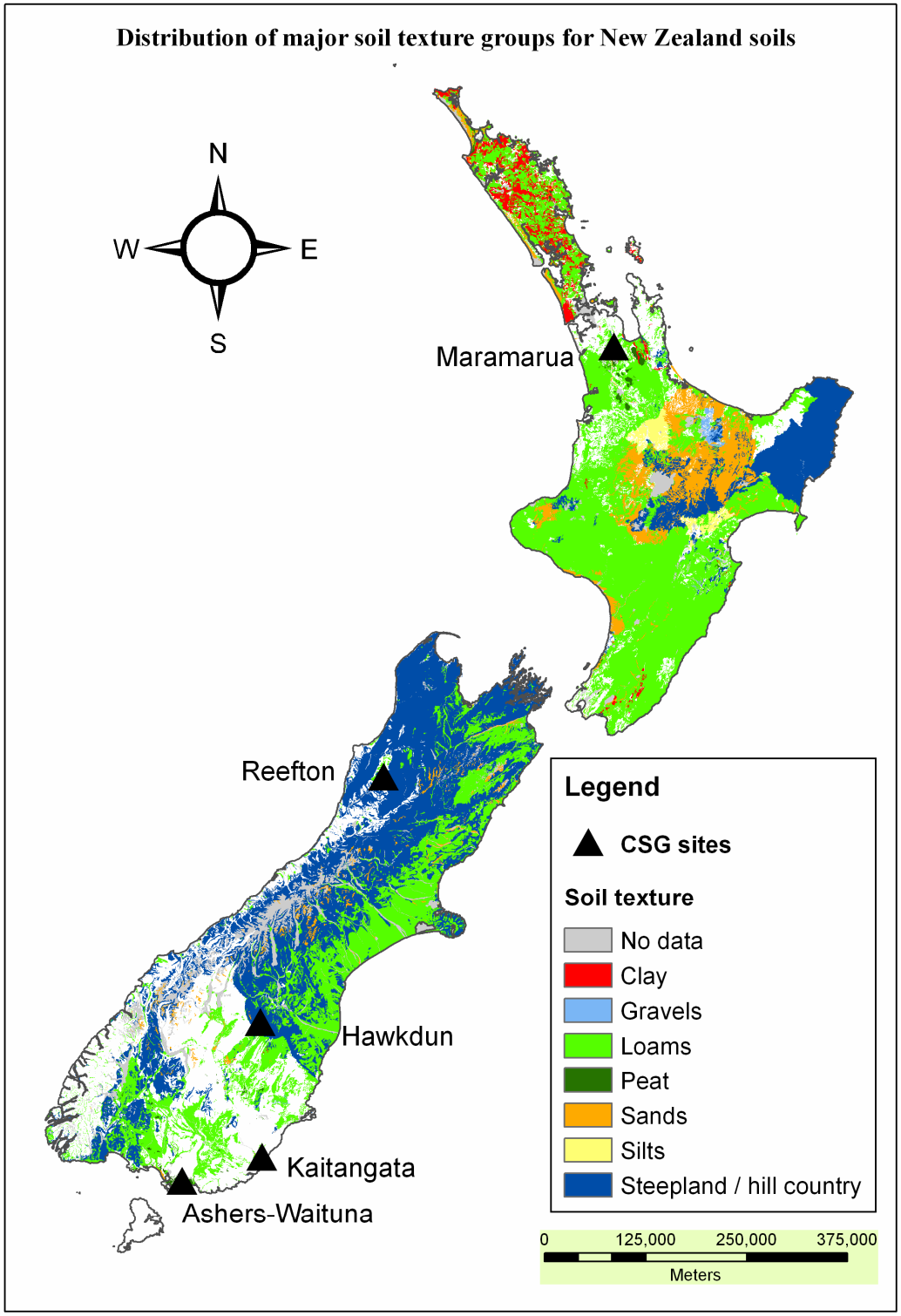

Figure C.2. Main soil texture distribution for New Zealand soils.

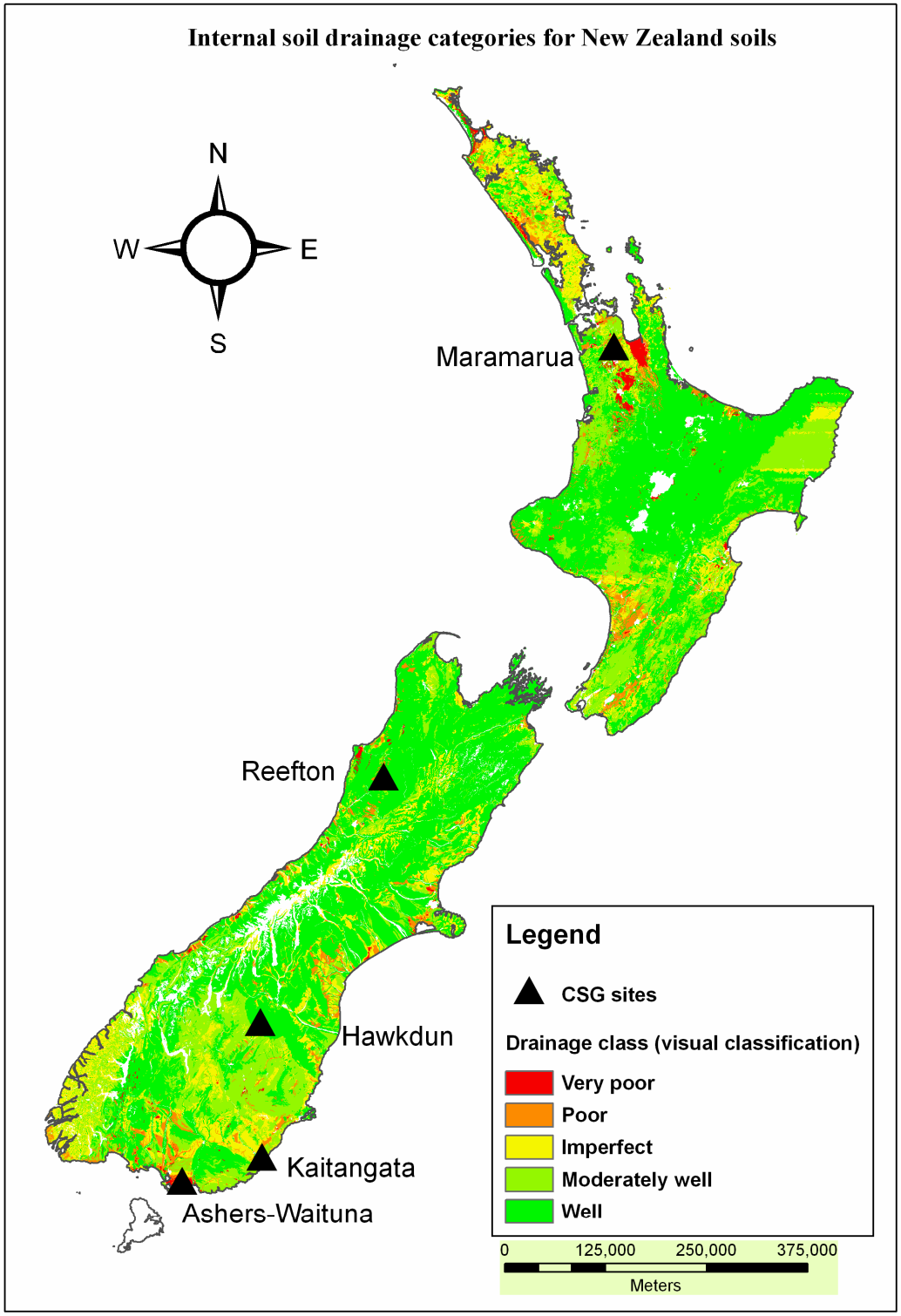

Figure C.3. Drainage classes for New Zealand soils.

C.2 Soil Salinity calculations

Soil salinity assessment calculations were carried out in accordance to the salinity model presented in the ANZECC guidelines. Water quality (EC, SAR) and soil properties (clay%, CEC, and ESP) were considered along with rainfall and irrigation to calculate the relevant leaching fraction. Once this was done, an average root zone salinity was calculated, and this gave an indication of the crop tolerance and plant response for a given salinity. The model is presented as follows:

Leaching fraction under rain fed conditions

The leaching fraction (*LF*) is the proportion of water leaching below the root zone, and this is an essential parameter used for the estimation of salinity and infiltration problems. The basis of this approach is a salt mass balance approach after equilibrium conditions are reached. Consequently, the *LF* can be estimated by calculating the ratio between input salinity (rainfall) and output salinity (drainage).

$$CCR\ (mmolc/100g) = \frac{CEC(mmolc/100g)}{Clay\%}$$

Eq C.2. From ANZECC (2000)

where,

CCR = Clay mineralogy which is expressed in mmolc/100g

CEC = Cation exchange capacity expressed in mmolc/100g

Clay % = number from 1-100 expressing the percentage of clay in relation to sand and loam materials

Note: 1 mmolc/100g is equivalent to 1 meq/100g, but mmolc is used here to be consistent with ANZECC guidelines notation.

The electrical conductivity of the soil saturation extract (EC_{SE}) is then calculated using the rainfall depth, soil ESP, and parameters depending on the soil CCR.

$$EC_{SE} = 10^{\left(a+b\cdot\log\frac{EC_r\cdot D_r}{ESP}\right)}$$

Eq C.3 (Shaw, 1996, as cited in ANZECC and ARMCANZ 2000) .

where,

EC_r = the electrical conductivity of rain which is assumed to be 0.03 dS/m

D_r = rainfall depth in mm/year for the area being analysed.

ESP is the Exchangeable sodium percentage of the soil calculated using Eq C.4 where both Na and CEC are in meq/100g

Parameters *a* and *b* are obtained from Table 9.2.8 in the ANZECC guidelines(2000) using soil CCR and Clay %

$$ESP = \frac{[Na]}{CEC} \times 100$$

Eq C.4

It is now possible to calculate the leaching fraction (LFr) under rain-fed conditions:

$$LF_r = \frac{EC_r}{2.2 \cdot EC_{SE}}$$

Eq C.5 (Shaw, 1996, as cited in ANZECC and ARMCANZ 2000).

where $2.2*EC_{SE}$ is an estimative value for the electrical conductivity of the drainage water below the root zone (ANZECC, 2000).

This LFr is the amount of water draining below the root zone under rain-fed conditions, and it is an indication of soil infiltration as affected by salinity. However, in this case rainfall has low salinity. In the next section a similar analysis is explained, but this time the water used in this assessment has high salinity.

Land application (irrigation) of CSG waters

When irrigating with high-SAR values, over prolonged periods of time, ESP values will increase and thus need to be adjusted. This adjustment uses the SAR of the water and a relationship between ESP and SAR, which was developed from soil samples taken from 9 western states in the US (US Salinity Laboratory Staff, 1954).

$$ESP = \frac{100 \cdot (-0.0126 + 0.01475 \cdot SAR_d)}{1 + (-0.0126 + 0.01475 \cdot SAR_d)}$$

Eq C.6 (US Salinity Laboratory Staff, 1954)

Where the SARd value is the adjusted SAR value which accounts for calcium carbonate precipitation. The SARd value is calculated using the RNa procedure formulated by Suarez (Suarez, 1981, as cited in Ayers and Westcot 1985).

To assess the salinity hazard prior to irrigating with CSG waters of known quality, it is necessary to calculate the leaching fraction with the corrected ESP values. For this purpose, the electrical conductivity (EC_i) of the irrigation water needs to be calculated while considering rain or other sources (surface waters for example).

$$LF_f = LF_r \cdot \left[2.65 \cdot \sqrt{\frac{EC_i}{EC_r}} - 1.35 \right]$$

Eq C.7 (ANZECC and ARMCANZ, 2000)

where,

LF_r = leaching fraction under rain-fed conditions (Eq C.5)

EC_i = Weighted EC of input water from irritation and rainfall in dS/m

Eq C.7 must be applied with care. In the case of leaching under rain-fed conditions (with no ESP correction) this value often exceeds 100%. However, by definition, the leaching fraction cannot exceed 100%, so when calculation of LF_r produces a result larger 100% the leaching fraction would correspond to the maximum (100%).

The average root zone leaching fraction is then calculated using the following relationship:

$$LF_{av} = \left(0.976 \cdot LF_f + 0.022\right)^{0.625}$$

Eq C.8 (Rhoades, 1982 and Shaw et al., 1987, as cited in ANZECC and ARMCANZ 2000)

The predicted root zone salinity is then calculated using the following relationship:

$$EC_{SE} = \frac{EC_i}{2.2 \cdot LF_{av}}$$

Eq C.9 (Shaw, 1996, as cited in ANZECC and ARMCANZ 2000).

The value of EC_{SE} can then be compared to the values on tables 4.2.4 and 9.2.10 from the ANZECC water quality guidelines.

Calculations for Maramarua

Table C.2. Kopuku Wetland sample

Specific Conductance	pH	TDS	DO	Alkalinity	Cl^-	Hardness	Ca^{2+}	SO_4^{2-}
µm/cm	pH units	mg/l	mg/l	mg/l CaCO3	mg/l	mg/l CaCO3	mg/l	mg/l
273	6.59	188	0.41	52.5	47	70	12.8	9

Notes:
Sampled using standard calibrated meters and titrations according to APHA standards at the Environmental Engineering Laboratory.
This sample presented a yellow /brown colour which is typical of swamp water containing humic material.

According to the findings of Chapter 2, an increase in SAR of approximately 23% could take place once CSG water is pumped to the surface and equilibrates with atmospheric pressure. However, in this case the SAR adjustment procedure developed by Suarez (1981, as cited in Ayers et al., 1985) was used instead. This produced a SAR value of 36.5 (Table 2) which corresponds to an 8.6% increase. These differences are attributed to changes in pressure and water quality (pH and [Ca2+]) between the samples used in Chapter 2 and the analytical data used in the SAR adjustment methodology.

Table C.3. SAR adjustment calculations (SARd)

Maramarua C-1 water quality					Suarez, 1981, as cited in Ayers and Westcot 1985		
EC µS/cm	Na meq/l	Ca meq/l	Mg meq/l	SAR	HCO3/Ca	Table 11	Adj RNa
1310	14.5	0.30	0.074	33.6	24.02	0.243	36.5

Table C.4. Clay %, CCR, and *a* and *b* parameters calculations

Sample	Pit #	Depth mm	pH	Specific Conductance µS/cm	CEC meq/100g	Na meq/100g	ESP %	Clay %	CCR meq/100g	Table 9.2.8 ANZECC guid. a	b
1	1	0-150	5.5	79.9	10	0.12	1.20%	16	0.63	0.44	-0.934
2	1	150-450	5.1	76	10	0.14	1.40%	24	0.42	0.33	-0.857
3	2	0-150	5.6	34	13	0.17	1.31%	13	1.00	-0.559	-0.067
4	2	150-450	5.1	57.7	11	0.21	1.91%	28	0.39	0.411	-0.936
5	3	0-150	6.1	41.9	14	0.08	0.57%	27	0.52	0.411	-0.936
6	3	150-450	5.1	36.6	7	0.025	0.36%	32	0.22	0.147	-0.672

Note: Rainfall from closest weather station (Maramarua Forest, 1947-1980) is 1263 mm/year

Table C.5. Land disposal with 100% CSG water

	Long term effects Without ESP correction							**Long term effects with ESP correction**							
sample		leaching under rain-fed			leaching under irrigation			Long term effects with ESP correction		Leaching under rain fed conditions					
					Prediction		Long-term				rain	irrig water			
#	Pit #	EC_{SE} dS/m	LFr %	ECi dS/m	LFf	LF_{av}	EC_{SE} dS/m	SAR	ESP %	EC_{SE} dS/m	LFr %	ECi dS/m	LFf %	LF_{av} %	EC_{SE} dS/m
1	1	0.110	12.4%	1.31	100%	99.9%	0.60	36.5	34.5%	2.5	0.5%	1.31	9%	24.8%	2.4
2	1	0.127	10.8%	1.31	100%	99.9%	0.60	36.5	34.5%	2.0	0.7%	1.31	11%	28.1%	2.1
3	2	0.220	6.2%	1.31	100%	99.9%	0.60	36.5	34.5%	0.3	5.0%	1.31	80%	87.4%	0.7
4	2	0.157	8.7%	1.31	100%	99.9%	0.60	36.5	34.5%	2.4	0.6%	1.31	9%	25.6%	2.3
5	3	0.051	26.8%	1.31	100%	99.9%	0.60	36.5	34.5%	2.4	0.6%	1.31	9%	25.6%	2.3
6	3	0.061	22.3%	1.31	100%	99.9%	0.60	36.5	34.5%	1.3	1.0%	1.31	17%	34.9%	1.7

Table C.6. Crop salinity assessment with 100% CSG water

Plant salt tolerance groupings. Criteria based on EC_{SE} and Table 4.2.4 from ANZECC (2000)							EXAMPLES			Ayers and Westcot (1985)
Sample	Pit	Sensitive crops	Moderately sensitive crops	Moderately tolerant crops	Tolerant crops	Very tolerant crops	Generally too saline	White Clover (NZ) Sensitive	Barley, forage Very tolerant	Salinity assessed on the basis of EC of irrigation water
#	#	Very low	Low	Medium	High	Very High	Extreme	Yield	Yield	Degree of restriction on use
1	1	Low yield	Low yield	100% yield	100% yield	100% yield	100% yield	86%	100%	Slight to moderate
2	1	Low yield	Low yield	100% yield	100% yield	100% yield	100% yield	89%	100%	Slight to moderate
3	2	100% yield	100% yield	100% yield	100% yield	100% yield	100% yield	100%	100%	Slight to moderate
4	2	Low yield	Low yield	100% yield	100% yield	100% yield	100% yield	87%	100%	Slight to moderate
5	3	Low yield	Low yield	100% yield	100% yield	100% yield	100% yield	87%	100%	Slight to moderate
6	3	Low yield	100% yield	100% yield	100% yield	100% yield	100% yield	93%	100%	Slight to moderate

Table C.7. Land disposal with 70% CSG water and 30% rain water

		Long term effects without ESP correction						**Long term effects with ESP correction**							
		Leaching under rain-fed			leaching under irrigation			Long term effects with ESP correction		Leaching under rain fed conditions					
					Prediction		Long-term				rain	irrig water			
Sample	Pit	EC_{SE}	LFr	ECi	LFf	LF_{av}	EC_{SE}	SAR	ESP	EC_{SE}	LFr	ECi	LFf	LF_{av}	EC_{SE}
#	#	dS/m	%	dS/m			dS/m		%	dS/m	%	dS/m	%	%	dS/m
1	1	0.110	12.4%	0.93	99.9%	100%	0.42	25.5	26.7%	2.0	0.7%	0.93	9%	25.4%	1.7
2	1	0.127	10.8%	0.93	99.9%	100%	0.42	25.5	26.7%	1.6	0.9%	0.93	12%	28.5%	1.5
3	2	0.220	6.2%	0.93	83%	89%	0.47	25.5	26.7%	0.3	5.1%	0.93	68%	78.7%	0.5
4	2	0.157	8.7%	0.93	99.9%	100%	0.42	25.5	26.7%	1.9	0.7%	0.93	10%	26.3%	1.6
5	3	0.051	26.8%	0.93	99.9%	100%	0.42	25.5	26.7%	1.9	0.7%	0.93	10%	26.3%	1.6
6	3	0.061	22.3%	0.93	99.9%	100%	0.42	25.5	26.7%	1.1	1.2%	0.93	16%	34.5%	1.2

Table C.8 Crop salinity assessment with 70% CSG water and 30% rain water

Plant salt tolerance groupings. Criteria based on ECSE and Table 4.2.4 from ANZECC (2000)								EXAMPLES		Ayers and Westcot (1985)
Samples	Pit	Sensitive crops	Moderately sensitive crops	Moderately tolerant crops	Tolerant crops	Very tolerant crops	Generally too saline	White Clover (NZ) Sensitive	Barley, forage Very tolerant	Salinity assessed on the basis of EC of irrigation water
#	#	Very low	Low	Medium	High	Very High	Extreme	Yield	Yield	Degree of restriction on use
1	1	Low yield	100% yield	100% yield	100% yield	100% yield	100% yield	93%	100%	Slight to moderate
2	1	Low yield	100% yield	100% yield	100% yield	100% yield	100% yield	95%	100%	Slight to moderate
3	2	100% yield	100% yield	100% yield	100% yield	100% yield	100% yield	100%	100%	Slight to moderate
4	2	Low yield	100% yield	100% yield	100% yield	100% yield	100% yield	94%	100%	Slight to moderate
5	3	Low yield	100% yield	100% yield	100% yield	100% yield	100% yield	94%	100%	Slight to moderate
6	3	Low yield	100% yield	100% yield	100% yield	100% yield	100% yield	98%	100%	Slight to moderate

Table C.9. Land disposal with 50% CSG water and 50% rain water

		Long term effects Without ESP correction						**Long term effects with ESP correction**							
		leaching under rain-fed		leaching under irrigation				Long term effects with ESP correction	Leaching under rain fed conditions						
					Prediction		Long-term				rain	irrig water			
Sample #	Pit #	EC_{SE} dS/m	LFr %	ECi dS/m	LFf	LF_{av}	EC_{SE} dS/m	SAR	ESP %	EC_{SE} dS/m	LFr %	ECi dS/m	LFf %	LF_{av} %	EC_{SE} dS/m
1	1	0.110	12.4%	0.67	99.9%	100%	0.30	18.2	20.4%	1.5	0.9%	0.67	10%	26.3%	1.2
2	1	0.127	10.8%	0.67	99.9%	100%	0.30	18.2	20.4%	1.3	1.1%	0.67	12%	29.3%	1.0
3	2	0.220	6.2%	0.67	79.8%	80%	0.38	18.2	20.4%	0.3	5.1%	0.67	58%	71.4%	0.4
4	2	0.157	8.7%	0.67	98.0%	98%	0.31	18.2	20.4%	1.4	0.9%	0.67	11%	27.3%	1.1
5	3	0.051	26.8%	0.67	99.9%	100%	0.30	18.2	20.4%	1.4	0.9%	0.67	11%	27.3%	1.1
6	3	0.061	22.3%	0.67	99.9%	100%	0.30	18.2	20.4%	0.9	1.5%	0.67	16%	34.6%	0.9

Table C.10. Crop salinity assessment with 50% CSG water and 50% rain water

Sample	Pit	Plant salt tolerance groupings. Criteria based on ECSE and Table 4.2.4 from ANZECC (2000)						EXAMPLES		Ayers and Westcot (1985)
		Sensitive crops	Moderately sensitive crops	Moderately tolerant crops	Tolerant crops	Very tolerant crops	Generally too saline	White Clover (NZ) Sensitive	Barley, forage Very tolerant	Salinity assessed on the basis of EC of irrigation water
#	#	Very low	Low	Medium	High	Very High	Extreme	Yield	Yield	Degree of restriction on use
1	1	Low yield	100% yield	100% yield	100% yield	100% yield	100% yield	98%	100%	None
2	1	Low yield	100% yield	100% yield	100% yield	100% yield	100% yield	100%	100%	None
3	2	100% yield	100% yield	100% yield	100% yield	100% yield	100% yield	100%	100%	None
4	2	Low yield	100% yield	100% yield	100% yield	100% yield	100% yield	99%	100%	None
5	3	Low yield	100% yield	100% yield	100% yield	100% yield	100% yield	99%	100%	None
6	3	100% yield	100% yield	100% yield	100% yield	100% yield	100% yield	100%	100%	None

Table C.11. Comparison of leaching fractions with or without ESP correction.

		No ESP correction			With ESP correction		
Sample #	Pit #	LFr %	LF_{av} %	LF Increase	LFr %	LF_{av} %	LF Increase %
1	1	12.4%	99.9%	87.4%	0.5%	24.8%	24.2%
2	1	10.8%	99.9%	89.1%	0.7%	28.1%	27.4%
3	2	6.2%	99.9%	93.7%	5.0%	87.4%	82.4%
4	2	8.7%	99.9%	91.2%	0.6%	25.6%	25.1%
5	3	26.8%	99.9%	73.0%	0.6%	25.6%	25.1%
6	3	22.3%	99.9%	77.5%	1.0%	34.9%	33.8%
1	1	12.4%	99.9%	87.4%	0.7%	25.4%	24.7%
2	1	10.8%	99.9%	89.1%	0.9%	28.5%	27.7%
3	2	6.2%	89.0%	82.8%	5.1%	78.7%	73.7%
4	2	8.7%	99.9%	91.2%	0.7%	26.3%	25.5%
5	3	26.8%	99.9%	73.0%	0.7%	26.3%	25.5%
6	3	22.3%	99.9%	77.5%	1.2%	34.5%	33.3%
1	1	12.4%	99.9%	87.4%	0.9%	26.3%	25.4%
2	1	10.8%	99.9%	89.1%	1.1%	29.3%	28.2%
3	2	6.2%	79.8%	73.6%	5.1%	71.4%	66.3%
4	2	8.7%	98.0%	89.3%	0.9%	27.3%	26.3%
5	3	26.8%	99.9%	73.0%	0.9%	27.3%	26.3%
6	3	22.3%	99.9%	77.5%	1.5%	34.6%	33.1%

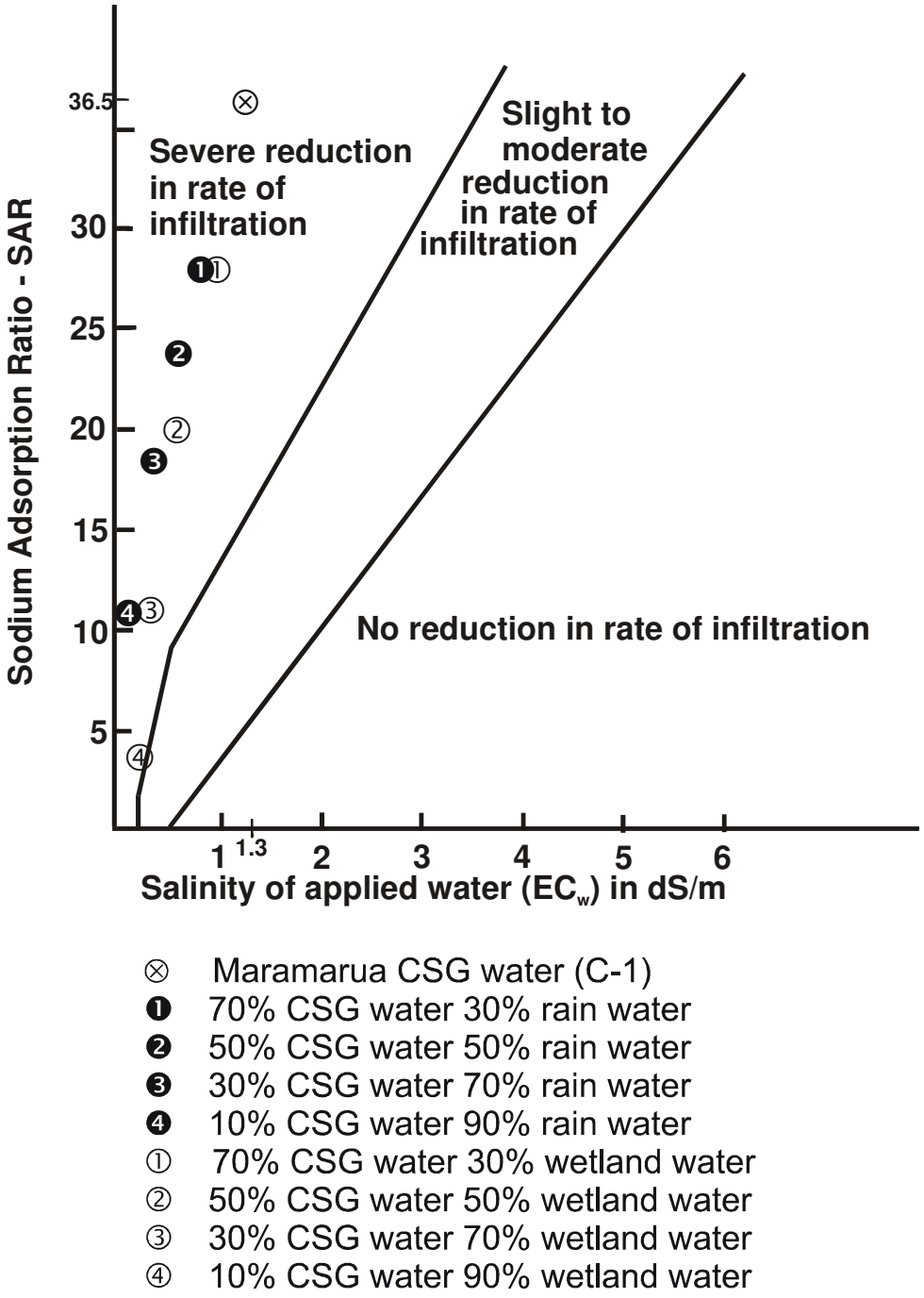

Figure C.4. Soil infiltration problem assessment using Maramarua CSG water after Ayers (1985)

Table C.12. Crop tolerance to sodium and chloride toxicity associated with Maramarua CSG water

Ion	CSG Water mg/l	Sensitive	Moderately sensitive	Moderately tolerant	Tolerant
Chloride	146	OK	OK	OK	OK
Sodium	334	Not OK	Not OK	May be OK	OK

Notes:

CSG water from Maramarua C-1 (19/8/2004 sample, see Chapter 1)

Sensitive crops: almond, apricot, citrus, plum, grape
Moderately sensitive: pepper, potato, tomato
Moderately tolerant: barley, maize, cucumber, lucerne, safflower, sesame, sorghum
Tolerant: cauliflower, cotton, sugar beet, sunflower

C.3 References

Allen, R.B., McIntosh, P.D., and Wilson, J.B., 1998, The distribution of plants in relation to pH and salinity on inland saline/alkaline soils in Central Otago, New Zealand. (vol 35, pg 517, 1997): New Zealand Journal of Botany, v. 36, p. 153-153.

ANZECC, and ARMCANZ, 2000, Australian and New Zealand Guidelines for Fresh and Marine Water Quality, ACT: Australian and New Zealand Environmental and Conservation Council (ANZECC),

Agricultural and Resource Management Council of Australia and New Zealand (ARMCANZ): Canberra.

Ayers, R.S., Westcot, D.W., and Food and Agriculture Organization of the United Nations., 1985, Water quality for agriculture: Rome, Food and Agriculture Organization of the United Nations, xii, 174 p.

Cameron, K.C., Di, H.J., Anwar, M.R., Russell, J.M., and Barnett, J.W., 2003, The "critical" ESP value: does it change with land application of dairy factory effluent?: New Zealand Journal of Agricultural Research, v. 46, p. 147-154.

Landcare Research New Zealand Ltd, 2000, The New Zealand National Soils Database Spatial Extension, Soil Fundamental Data Layers: Lincoln, Landcare Research New Zealand Ltd.

Rhoades, J.D., 1982, Reclamation and management of salt-affected soils after drainage. In Rationalisation of water

and soil research and management, Proceedings of the First Annual Western Provincial Conference: Lethbridge, Canada, p. 123–197.

Shaw, R.J., 1996, A unified soil property and sodicity model of salt leaching and water movement [PhD thesis], University of Queensland.

Shaw, R.J., Thorburn, P.J., and Dowling, A.J., 1987, Principles of landscape, soil and water salinity: Processes and management options, Proceedings of Brisbane Region Salinity

Workshop: Part A, in Landscape, soil and water salinity: Brisbane, Queensland Department of Primary Industries.

Suarez, D.L., 1981, Relationship between pHc and sodium adsorption ratio (SAR) and an alternative method of
estimating SAR of soil or drainage waters: Soil Science Society of America Journal, v. 45, p. 469-475.

US Salinity Laboratory Staff, 1954, Diagnosis and improvement of saline and alkali soils: [Washington,, US Govt. Print. Off.], vii, 160 p. p.

Appendix D

D.1 Description and calculation of separation factor

The reaction between the zeolite material and a concentrated solution (i.e. Na^+) can be described using the following relationship(Amphlett, 1964):

$$\overline{A}^+ + B^+ \Leftrightarrow A^+ + \overline{B}^+$$

Where,

$\overline{A}^+$ is the solid phase material or zeolite material which contains occluded cations (i.e. Ca^{2+}, Mg^{2+}, or K^+)

B^+ is the liquid phase or orginal concentrated solution (i.e. Na^+ feed solution in flow through experiments)

A^+ is the liquid phase after the exchange has taken place (i.e. the solution containing K^+, Mg^{2+}, or Ca^{2+})

$\overline{B}^+$ is the solid phase after the exchange (i.e. the zeolite material containing Na^+ ions)

Then, the equilibrium constant governing this ion exchange reaction can be defined as:

$$K = \frac{\{A^+\}\cdot\{\overline{B}^+\}}{\{\overline{A}^+\}\cdot\{B^+\}} = \frac{[A^+]\cdot[\overline{B}^+]}{[\overline{A}^+]\cdot[B^+]} \times \frac{\Gamma_B}{\Gamma_A} \times \frac{\gamma_A}{\gamma_B} \quad \text{(Amphlett, 1964)}$$

where the symbols { } denote activity, [ ] concentration, Γs are the individual ion activity coefficients in the solid phase, and γs are the activity coefficients for the liquid phase.

Then it is possible to define the separation factor *r* as:

$$r = \frac{[A^+]\cdot[\overline{B}^+]}{[\overline{A}^+]\cdot[B^+]} = \frac{c_A \cdot q_B}{q_A \cdot c_B} = \frac{\frac{c_A}{c_o}\cdot\frac{q_B}{Q}}{\frac{c_B}{c_o}\cdot\frac{q_A}{Q}} = \frac{x_A \cdot y_B}{x_B \cdot y_A} = \frac{x_A \cdot (1-y_A)}{y_A \cdot (1-x_A)}$$

Where,

$$c_A = [A^+] \quad q_A = [\overline{A}^+] \quad x_A = \frac{c_A}{c_o} \quad y_A = \frac{q_A}{Q} \qquad \text{(Perry et al., 1973)}$$

$$c_B = [B^+] \quad q_A = [\overline{B}^+]$$

c_o = *original concentration in solution* $\quad Q$ = *total ions in zeolites*

It is possible to work with one section of the isotherm (fractional) and define the separation factor in terms of the fractional isotherm:

$$X = \frac{c - c'}{c'' - c'}$$

$$Y = \frac{q - q'}{q'' - q'}$$

Where,

c' = the initial concentration in solution

q' = initial quantity of ions within the zeolite

c'' = final concentration in solution

q'' = final quantity of ions within the zeolite

Then the separation factor for the fractional isotherm is defined as:

$$R = \frac{X_A \cdot (1 - Y_A)}{Y_A \cdot (1 - X_A)}$$

(Perry et al., 1973)

D.2 Batch absortion experiment results

Phase I.

Table D.1. Effect of particle size on ion exchange processes using Ngakuru zeolites (first experiment)

	Wwet	Wdry	Moisture	Zeolite weight	NaCl 1M	pH	Spec. Cond. (T=25°C)	Calcium mg/l as CaCO3	Calcium	Hardness mg/l as CaCO3
	g	g	%	g	ml		mS/cm	CaCO3	mg/l	CaCO3
Passing 150 µm	3.7	3.6	3.1%	1.0074	50	5.5	85.9	235	94	NA
150 µm	3.5	3.3	4.4%	1.0026	50	5.6	85.3	224	89.6	300
300 µm	7.8	7.5	4.0%	1.0016	50	5.4	84.2	196	78	250
600 µm	13.4	12.8	4.5%	1.0019	50	5.1	85.4	196	78	275
1180 µm	25.3	24.3	3.9%	1.0048	50	5.4	86	248	99	320
2360 µm	1.3	1.3	3.4%	1.0013	50	5.3	85.7	248	99	330
Kitty litter	27.1	25.6	5.3%	1.0051	50	4.5	85.9	115	46	NA

Notes:
Original solution concentration : NaCl 1M
Original pH = 7.2
Original specific conductance = 85.7 mS/cm
Shanking time: 1 hour 45 min

Table D.2. Effect of particle size on ion exchange processes using Ngakuru zeolites (second experiment)

	Zeolite weight	NaCl 1M	pH	Cond (T=25°C)	Calcium	Calcium	Hardness mg/l as CaCO3	Mg
	g	ml		mS/cm	mg/l as CaCO3	mg/l		mg/l
Passing 150 µm	1.0032	53	5.1	75	248	99.2	315	16
150 µm	1.0019	53	5.4	76.2	244	97.6	320	19
300 µm	1.0026	53	5.4	76.4	236	94	295	14
600 µm	1.0013	53	5.4	76.5	248	99	315	16
1180 µm	1.0034	53	5.4	76.4	264	106	340	19
2360 µm	1.0009	53	5.7	76.7	309	124	NA	

Notes:
Original solution concentration : NaCl 1M
Original pH = 6.3
Original specific conductance = 75.4 mS/cm
Shanking time: 8 hours

Phase II.

Table D.3. Experiments to determine dissolution potential of Ngakuru zeolites

	Zeolite mass	Vol.	pHi	pHf	SPi	SPf	Ca	Ca	Hardness	Mg
	g	ml			µS/cm	µS/cm	mg/l CaCO3	mg/l	mg/l CaCO3	mg/l
NaCl 0.005M	2.0059	100	6.2	5.5	538	546	20	8	32	3
Deionised Water	1.0031	53	~7	6.4	1.9	41.8	8	3.2	4.17	NA

Notes:
9.5 hours shaking time
Zeolite particle size: 1180 µm
pHi = initial pH
pHf = final pH
Spi =initial Specific Conductance @ T=25°C
Spf = final Specific Conductance @ T=25°C

Phase III.

Table D.4. Effect on solution characteristics on ion exchange processes using Ngakuru zeolites

Solution type	concentration	weight zeolites	initial pH	final pH	calcium	magnesium	absorbed sodium
	M	g			meq/g	meq/g	meq/g
NaCl	1	2.0018	7.20	5.51	0.21	0.79	0.915
NaCl	0.1	2.0018	7.65	6.46	0.14	0.38	0.267
NaCl	0.01	2.0045	7.30	6.39	0.03	0.18	0.096
NaOH	0.01	2.0006	11.52	10.81	0.00	0.00	0.227

Notes:
1) Selected volume was 0.12 litres in all cases
2) Zeolite particle size was 600 µm

Phase IV.

Experiment n°2

After 4 service/regeneration cycles the zeolites were still absorbing sodium ions (21.6 meq/100g in n°9), however there was a 65.4% reduction in mass. In this case, the first service run showed that the cations originally contained within the zeolite are calcium, magnesium, and potassium. Hydrogen ions, however, were absorbed during this first service run (pH increase from 6.34 to 7.47), but in subsequent runs these ions were released. The first service run yielded a natural sodium exchange capacity of 10.4 meq/100g, but this value tended to increase after each regeneration run, reaching a

maximum of 21.6 meq/100g in the last service run. Overall, the exchange process took place with very small charge balance differences (~0 meq/100g; Table D.5).

Throughout the course of this experiment, the zeolites kept releasing occluded calcium, magnesium, and potassium cations. Runs n°1-n°3 show calcium cations being released, but it is not possible to determine where the calcium cations are coming from in subsequent runs because of regeneration with a strong $CaCl_2$ solution in run n°4. Similarly, magnesium cations kept being released throughout, but sometimes their release was undetected (n° 5, 7, and 9).

Due to budget constraints, it was not possible to measure potassium throughout. However, run n°1 indicated 0.6 meq/l of potassium cations originally in the zeolites, and potassium was released in run n° 5 (0.07 meq/l). The last run (n°9) resulted in high potassium levels, but this is due to previous regeneration with KCl.

Table D.5. Experiment n°2. Batch sorption experiments with 600µm zeolites

n°	Reaction type	zeolite weight	sample volume	Sol. type	initial pH	final pH	final Na^+	final Ca^{2+}	final Mg^{2+}	final K^+	trapped cations	released cations	charge balance	main cation exchange
		g	litres				meq/l	meq/l	meq/l	meq/l	meq/l	meq/l	meq/l	meq/100g
1	Service	4.02	0.225	0.01M NaCl	6.34	7.47	8.1	0.52	0.28	0.60	1.9	1.4	0.5	10.4
2	Regeneration	2.72	0.125	1M HCl	0.25	0.25	7.7	2.4	0.40	NA	10.5	10.5	0.0	35.4
3	Service	2.08	0.125	0.01M NaCl	6.34	2.81	6.5	0.16	0.08	NA	3.5	1.96	1.5	21.1
4	Regeneration	1.88	0.125	0.09M $CaCl_2$	5.32	5.32	0.7	173.7	6.00	0.00	2.0	6.8	4.8	4.9
5	Service	1.76	0.125	0.01M NaCl	6.34	3.13	8.0	0.32	0.00	0.07	2.0	1.21	0.8	14.1
6	Regeneration	1.66	0.125	0.01M $CaCl_2$	6.62	4.60	0.4	17.9	0.28	NA	2.1	0.67	1.5	2.7
7	Service	1.56	0.125	0.01M NaCl	6.34	3.53	8.6	0.30	0.00	NA	1.4	0.63	0.7	11.0
8	Regeneration	1.45	0.125	0.1M KCl	6.76	3.32	3.5	0.40	0.20	NA	NA	4.80	4.8	30.4
9	Service	1.39	0.125	0.01M NaCl	6.34	5.67	7.6	0.20	0.00	2.23	2.4	2.43	0.0	21.6

Notes:

1. NA = not available
2. main cation exchange = meq of main cation intervening in the exchange reaction per 100g of zeolites

Experiment n°3 – 5

Table D.6. Batch absorption experiments with 1180µm zeolites

n°	Reaction type	zeolite weight	sample volume	Sol. type	initial pH	final pH	final Na^+	final Ca^{2+}	final Mg^{2+}	final K^+	TC	RC	CB	main cation exchange
		g	litres				meq/l	meq/l	meq/l	meq/l	meq/l	meq/l	meq/l	meq/100g
1	Service	2.04	0.125	0.01M NaCl	6.34	6.48	7.3	0.56	0.3	0.51	2.7	1.39	1.3	16.7
2	Regeneration	1.21	0.125	0.09M $CaCl_2$	5.32	5.61	3.2	175.6	0.0	NA	NA	3.2	NA	33.0
3	Service	0.96	0.125	0.01M NaCl	6.34	6.91	7.7	0.8	0.0	0.28	2.3	1.07	1.2	29.7
4	Regeneration	0.79	0.125	0.01M $CaCl_2$	6.62	6.45	0.6	17.8	0.0	NA	2.0	0.6	NA	9.3
5	Service	0.65	0.125	0.01M NaCl	6.34	6.27	8.2	0.54	0.0	NA	1.8	0.54	NA	34.3
6	Regeneration	0.55	0.125	0.1M KCl	6.76	6.67	2.1	1.7	0.1	NA	0.0	2.2	NA	47.1

Notes:

1. NA = not available
2. main cation exchange = meq of main cation intervening in the exchange reaction per 100g of zeolites
3. TC = trapped cations; RC = released cations; CB = charge balance

Table D.7. Batch absorption experiments with 1180µm zeolites

n°	Reaction type	zeolite weight	sample volume	Sol. type	initial pH	final pH	final Na^+	final Ca^{2+}	final Mg^{2+}	final K^+	TC	RC	CB	main cation exchange
		g	litres				meq/l	meq/l	meq/l	meq/l	meq/l	meq/l	meq/l	meq/100g
1	Service	2.00	0.125	0.01M NaCl	6.34	6.55	7.8	0.7	0.2	0.48	2.2	1.38	0.8	13.8
2	Regeneration	0.99	0.125	0.01M $CaCl_2$	6.62	6.48	0.9	17.1	0.5	NA	3.0	1.4	NA	11.0
3	Service	0.83	0.125	0.01M NaCl	6.34	6.28	8.0	0.6	0.0	0.26	2.0	0.86	1.1	30.0
4	Regeneration	0.69	0.125	0.1M KCl	6.76	5.74	2.3	1.8	0.3	NA	NA	2.6	NA	41.7

Notes:
1) NA = not available
2) main cation exchange = meq of main cation intervening in the exchange reaction per 100g of zeolites
3) TC = trapped cations; RC = released cations; CB = charge balance

Table D.8. Batch absorption experiments with 1180µm zeolites

n°	Reaction type	zeolite weight	sample volume	Sol. type	initial pH	final pH	final Na^+	final Ca^{2+}	final Mg^{2+}	final K^+	TC	RC	CB	main cation exchange
		g	litres				meq/l	meq/l	meq/l	meq/l	meq/l	meq/l	meq/l	meq/100g
1	Service	2.14	0.125	0.01M NaCl	6.34	6.39	7.7	0.6	0.2	0.52	2.3	1.32	0.9	13.2
2	Regeneration	1.16	0.125	0.1M KCl	6.76	5.87	3.6	2.8	2.4	NA	NA	4.0	NA	39.0

Notes:
1) NA = not available
2) main cation exchange = meq of main cation intervening in the exchange reaction per 100g of zeolites
3) TC = trapped cations; RC = released cations; CB = charge balance

D.3 Experimental results for flow-through tests

Experiment n°1

Experiment n°1 showed that zeolites were able to absorb sodium cations under flow-through conditions; aliquot concentrations increased in an almost logarithmic fashion starting at 98 mg/l and finishing at 180 mg/l after 10.1 litres of 0.01 M NaCl (223 mg/l) feed solution had gone through the column (Table D.9 and Figure D.1). It was not possible to directly calculate the total sodium absortion taking place in experiment n°1 because only 7 out of 21 samples were analysed for sodium. However, it was possible to calculate a theoretical value by analysing the trendline characterising the 7 sample points. As a result, the calculated theoretical sodium absorption in this experiment was 12.8 meq/100g.

Experiment n°2

Experiment n°2 indicated that Ngakuru zeolites were able to absorb sodium cations from a 0.1 M (about 2299 mg/l) NaCl feed solution in a logarithmic fashion. Initial sodium concentrations in aliquots started at 1582 mg/l and finished at 2072 mg/l, while pH values consistently stayed below the 6.03 original value at an average pH of about 3.98 (Table D.10 and Figure D.2). The total sodium exchange capacity measured in this experiment was 17.6 meq/100g. In addition, calcium and hardness concentrations were measured for three of the aliquots. The first sample (taken after 100 ml of feed solution) had calcium concentrations of 259 mg/l and magnesium concentrations of 81 mg/l. Calcium concentrations seemed to remain the same for the 4^{th} sample (after 400 ml through the column) with 236 mg/l, but magnesium concentrations almost doubled (157mg/l). However, after 1700 ml of feed solution had gone through the column (sample 17), calcium concentrations decreased to 136 mg/l and magnesium decreased to 34 mg/l.

Table D.9. Absortion results for experiment n°1

Sample n°	volume through column (litres)	Na^+ concentration in sample (mg/l)
1	0.1	98
3	1.1	103
5	2.1	123
9	4.1	145
15	7.1	160
20	170.5	171
21	10.1	180

Notes:

1) Na^+ concentrations were measured with Cole-Parmer sodium probe
2) Aliquot volume is 100 ml
3) For further information about experiment setup refer to Table 5.3 in Chapter 5

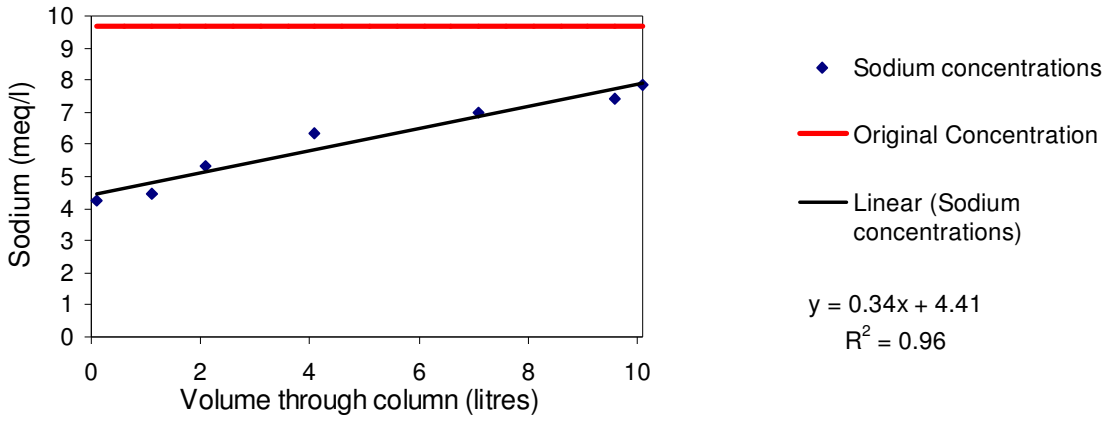

Figure D.1. Plot of experimental results for experiment n°1

Table D.10. Absortion results for experiment n°2

Sample n°	volume through column (ml)	Na^+ concentration in sample (mg/l)	pH pH units
1	100	1582	4.08
2	200	1682	3.88
3	300	1767	3.89
4	400	1811	3.94
5	500	1886	3.91
6	600	1933	3.89
7	700	1997	4.03
8	800	1910	3.92
9	900	1933	3.95
10	1000	2006	4.04
11	1100	2047	3.97
12	1200	2081	3.96
13	1300	2115	3.98
14	1400	2106	3.97
15	1500	2141	4.14
16	1600	2124	4.01
17	1700	2132	4.02
18	1800	2072	3.99

Notes:

1) Na^+ concentrations were measured with Cole-Parmer sodium probe
2) Aliquot volume is 100 ml
3) For further information about experiment setup refer to Table 5.3 in Chapter 5

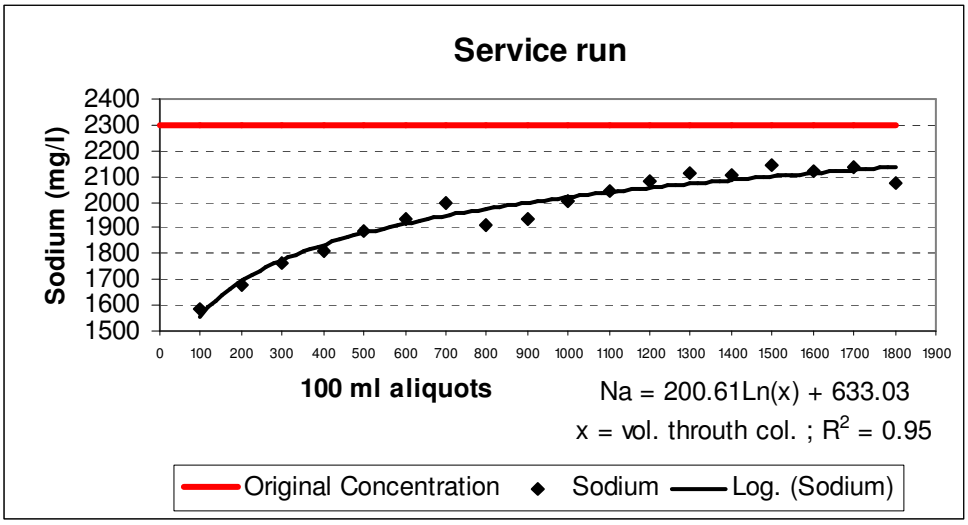

Figure D.2. Plot of experimental results for experiment n°2

Experiment n°3

Sodium concentrations in Figure D.3 increase in a linear fashion until approximately 1100 ml of feed solution had run through the column, and it then increases logarithmically to approximately 1500 mg/l. Eq 1 provides the best fit for this set of points with R^2 =0.97.

Calcium and hardness concentrations were measured for samples n°1, 10, and 15. From these values, magnesium concentrations were calculated. Sample n°1 (first 100ml) presented calcium and magnesium concentrations of 32 mg/l and 16 mg/l respectively. After 1000ml of feed solution had gone through (sample n°10), calcium concentrations increased to 58 mg/l and magnesium decreased to 10 mg/l. On the other hand, sample n°15 presents lower calcium and magnesium concentrations (36 mg/l and 4 mg/l) than sample n°10, which shows that the cation exchange rate is decreasing as volume flows through the column.

pH values (Table 7) through out this column test were consistently lower than the original pH value of 5.8, which shows that hydrogen ions are also being exchanged for sodium ions. Sample n°1 had the highest pH but, as mentioned earlier, it is possible that this sample was contaminated with deionised water. For the rest of this experiment, values for pH were as low as 4.38 reaching a maximum of 4.96 at the end of the test (last sample).

Table D.11. Results for experiment n°3

Sample n°	vol. through ml	pH pH units	Na^+ mg/l	Ca^{2+} mg/l	Mg^{2+} mg/l
1	100*	5.02	8	32	16
2	200	4.53	60	NA	NA
3	300	4.38	191	NA	NA
4	400	4.41	364	NA	NA
5	500	4.44	504	NA	NA
6	600	4.42	653	NA	NA
7	700	4.48	733	NA	NA
8	800	4.63	671	NA	NA
9	900	4.46	981	NA	NA
10	1000	4.53	1093	58	10
11	1100	4.5	1174	NA	NA
12	1200	4.51	1247	NA	NA
13	1300	4.52	1319	NA	NA
14	1400	4.54	1389	NA	NA
15	1500	4.58	1434	36	4
16	1600	4.58	1481	NA	NA
17	1700	4.6	1516	NA	NA
18	1780	4.96	1529	NA	NA

Notes

1) Feed solution is a 0.1 M NaCl solution with pH= 5.8
2) Na^+ concentrations were measured with Cole-Parmer sodium probe
3) Aliquot volume is 100 ml
4) For further information about experiment setup refer to Table 5.3 in Chapter 5
5) NA = no data available
6) * this aliquot might have been contaminated with deionised water

$$[\mathrm{Na}] = 32.44 \cdot \ln(v) + 47.08$$

where,

$[\mathrm{Na}]$ = sodium concentration in sample aliquot (meq/l)

v = volume through column in litres

Eq D.1

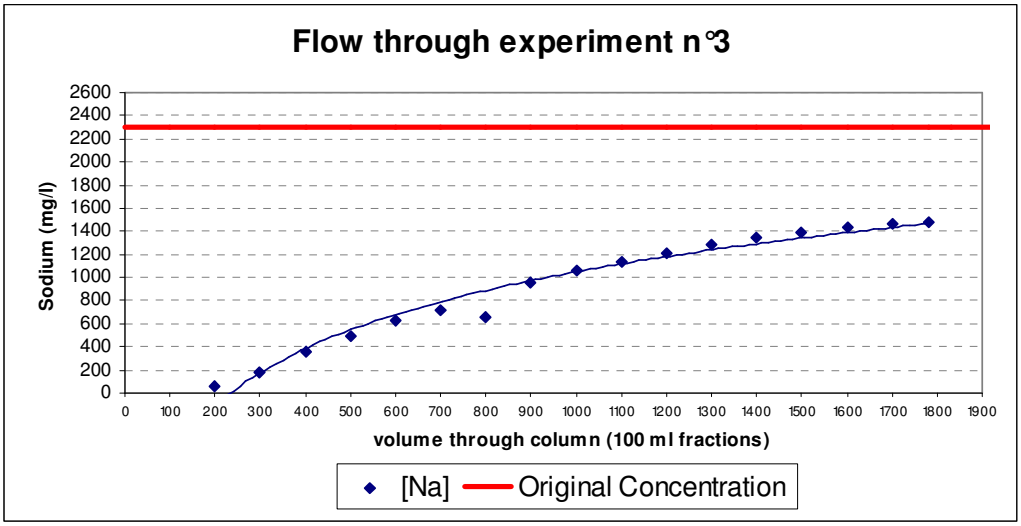

Figure D.3. Plot of sodium concentration vs. feed solution flow through column test in experiment n°3

Experiment n°4

Table D.12. Results for experiment n°4

Sample n°	vol. through ml	pH pH units	Na^+ mg/l	Ca^{2+} mg/l	Mg^{2+} mg/l
1	100*	6.3	25	12	15
2	200	5.38	220	NA	NA
3	300	4.49	642	824	302
4	400	4.13	880	NA	NA
5	500	4.07	1108	NA	NA
6	600	4.09	1302	NA	NA
7	700	4.08	1476	NA	NA
8	800	4.13	1607	NA	NA
9	900	4.11	1707	NA	NA
10	1000	4.16	1814	376	49
11	1100	4.13	1927	NA	NA
12	1200	4.17	2056	NA	NA
13	1300	4.13	2184	NA	NA
14	1400	4.16	2311	NA	NA
15	1500	4.26	2387	292	41

Notes

1) Feed solution is a 0.1 M NaCl solution with pH= 5.85
2) Solution entered column at ~ 40°C
3) Na^+ concentrations were measured with Cole-Parmer sodium probe
4) Aliquot volume is 100 ml
5) For further information about experiment setup refer to Table 5.3 in Chapter 5
6) NA = no data available
7) * this aliquot might have been contaminated with deionised water

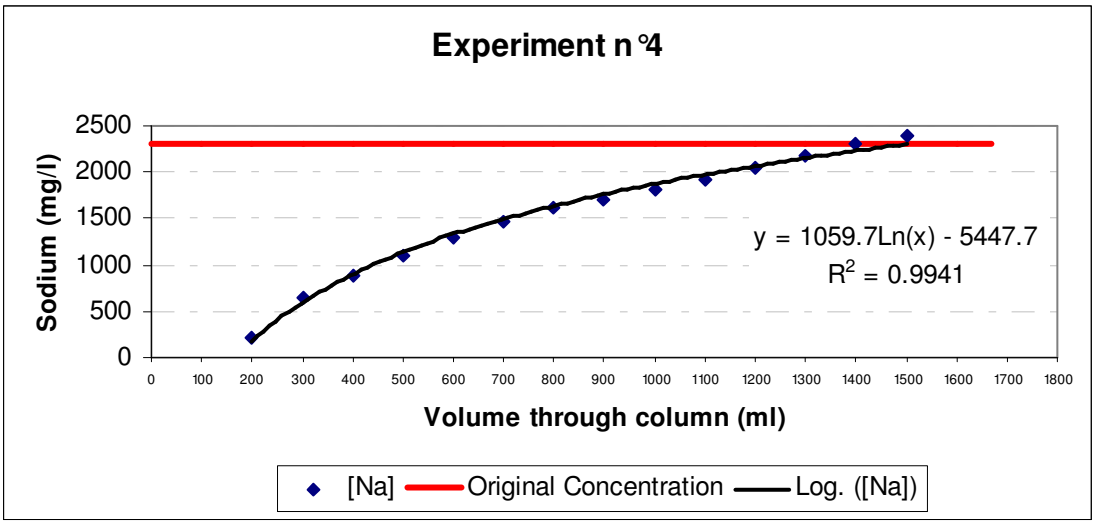

Figure D.4. Plot of sodium concentration vs. feed solution flow (40°C) through column test in experiment n°4

Experiment n°5

Table D.13. Results for experiment n°5

Sample n°	vol. through ml	pH pH units	Na^+ meq/l	Ca^{2+} meq/l	Mg^{2+} meq/l
1	100	4.79	14.5	10.7	14.3
2	200	4.69	15.2	11.6	14.3
3	300	4.76	16.7	12.4	11.8
4	400	4.68	18.5	12.7	7.2
5	500	4.57	20.4	12.8	7.4
6	600	4.49	22.3	12.6	5.8
7	700	4.6	24.1	11.6	4.8
8	800	4.49	25.1	NA	NA
9	900	4.45	26.4	NA	NA
10	1000	4.47	27.5	10.0	3.3
11	1100	4.46	28.2	NA	NA
12	1200	4.48	29.3	NA	NA
13	1300	4.63	30.3	8.5	2.2
14	1400	4.53	31.0	NA	NA
15	1500	4.49	32.2	NA	NA
16	1600	4.52	32.5	7.0	1.9
17	1700	4.51	34.3	NA	NA
18	1800	4.53	34.6	NA	NA
19	1900	4.52	34.9	6.0	1.6
20	2000	4.53	35.4	NA	NA
21	2100	4.51	35.6	NA	NA
22	2200	4.55	35.9	5.2	1.4
23	2300	4.52	36.8	NA	NA
24	2400	4.55	37.1	NA	NA
25	2500	4.53	37.5	4.8	1.1
26	2600	4.56	38.0	NA	NA
27	2700	4.62	38.4	NA	NA

Notes

1) Feed solution is a 0.044 M NaCl solution with pH= 6.35
2) Original Na^+ concentration is 0.044 M (1000 mg/l = 43.5 meq/l)
3) Na^+ concentrations were measured with Cole-Parmer sodium probe
4) Ca^{2+} : 1 meq/l = 20.04 mg/l ; Mg^{2+} : 1 meq/l = 12.15 mg/l
5) Aliquot volume is 100 ml
6) For further information about experiment setup refer to Table 5.3 in Chapter 5
7) NA = no data available

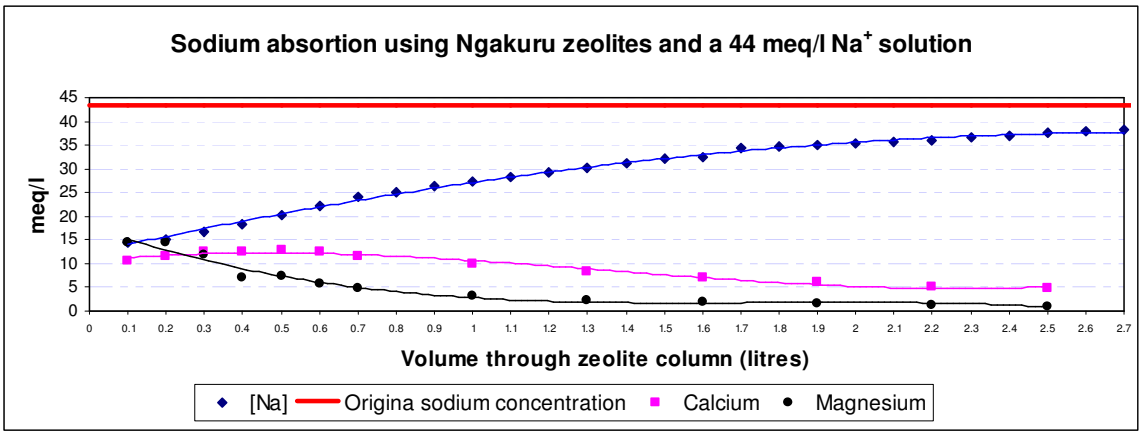

Figure D.5. Experiment #5: sodium absorption and cation release using Ngakuru zeolites

$$[\mathrm{Na}] = 8.7 \cdot \ln(v) + 28.6$$

where,

$[\mathrm{Na}]$ = sodium concentration in sample aliquot (meq/l)

v = volume through column in litres

$R^2 = 0.95$

Eq D.2

Experiment n°6

Table D.14. Fractional isotherm and separation factor for experiment n°6

Solution (c-c')/(c''-c') X	Solid (q-q')/(q''-q') Y	Separation factor *R*
0.00	0.09	
0.19	0.17	1.116
0.24	0.25	0.982
0.33	0.32	1.074
0.41	0.38	1.148
0.48	0.50	0.919
0.65	0.60	1.238
0.73	0.69	1.229
0.83	0.77	1.508
0.84	0.84	1.050
0.93	0.90	1.434
0.97	0.95	1.449
1.00	1.00	

Experiment n°7

Table D.15. Fractional isotherm and separation factor for Experiment n°7

Solution (c-c')/(c''-c') X	Solid (q-q')/(q''-q') Y	Separation factor *R*
0.0	0.0	
0.1	0.1	0.978
0.1	0.2	0.884
0.2	0.2	1.139
0.3	0.3	1.135
0.4	0.4	1.117
0.4	0.4	0.888
0.6	0.5	1.528
0.7	0.5	2.103
0.7	0.6	1.976
0.7	0.6	1.308
0.8	0.6	1.807
0.8	0.7	2.523
0.9	0.7	2.242
0.7	0.8	0.738
0.9	0.8	1.534
0.9	0.8	1.758
0.9	0.9	1.122
1.0	0.9	4.696
0.9	0.9	1.227
0.9	1.0	0.278
1.0	1.0	

D.4 References

Amphlett, C.B., 1964, Inorganic ion exchangers: Amsterdam, New York,, Elsevier Pub. Co., x, 141 p. p.

Perry, R.H., Chilton, C.H., and Perry, J.H., 1973, Chemical engineers' handbook: Tokyo, McGraw-Hill Kogakusha, 1 v. (various pagings) p.

Appendix E

X-ray diffraction results provided by the Geology Department, University of Canterbury

Name: Mauricio Taulis

1180µm FIRST BATCH

Sample: 1

The crystalline material present in this sample has been identified as:

Component	Colour on scan	Percentage*
Mordenite	yellow	75
Sanidine	green	25

SANIDINE → Potassium Aluminium Silicate Feldspar

Potassium Feldspar

*Estimate only.

S#1/1180/B1

Name: Mauricio Taulis

1180µm SECOND BATCH

Sample: 2

The crystalline material present in this sample has been identified as:

Component	Colour on scan	Percentage*
Mordenite	yellow	75
Sanidine	green	25

→K Feldspar

*Estimate only.

S#2/1180/B2

Name: Mauricio Taulis

THIRD BATCH (collected)

Sample: 3 600 µm

The crystalline material present in this sample has been identified as:

Component	Colour on scan	Percentage*
Mordenite	yellow	70
Sanidine	green	30

*Estimate only.

S#3/600/B3

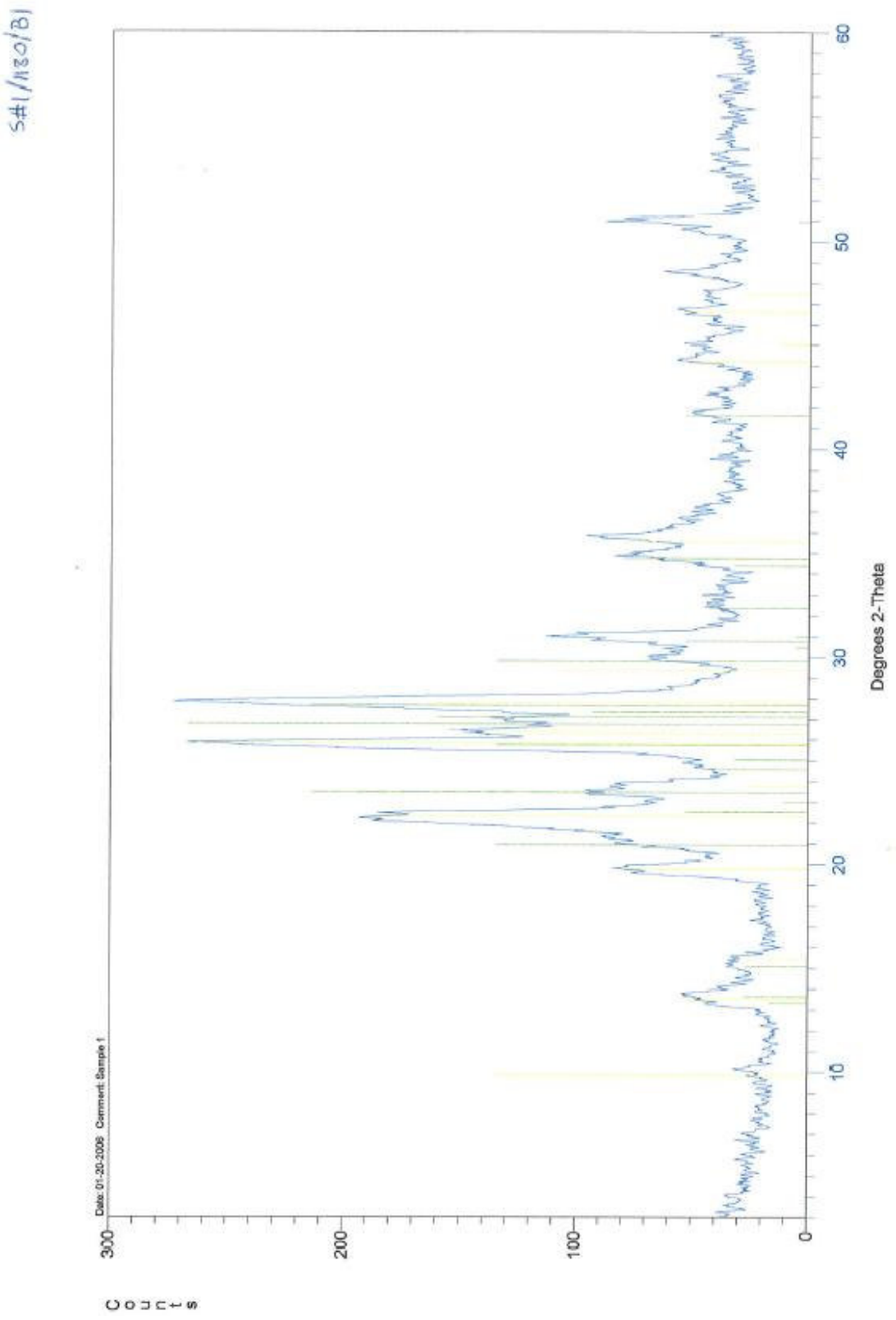
S#1/1820/B1
Date: 01-20-2006 Comment: Sample 1
Counts
300
200
100
0
10
20
30
40
50
60
Degrees 2-Theta

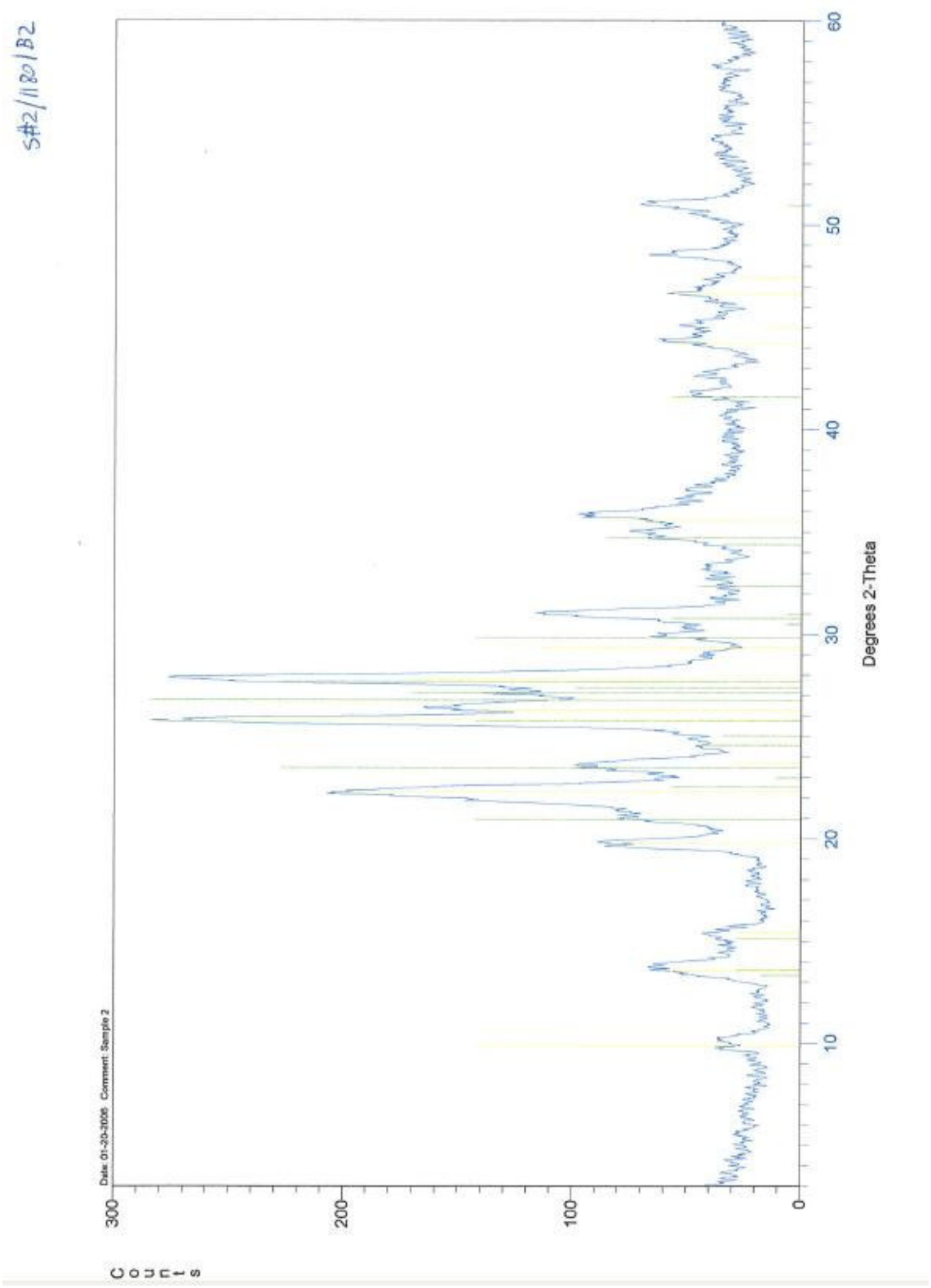
S#2/1180/B2
Date: 01-20-2006 Comment: Sample 2
Counts
300
200
100
0
10
20
30
40
50
60
Degrees 2-Theta

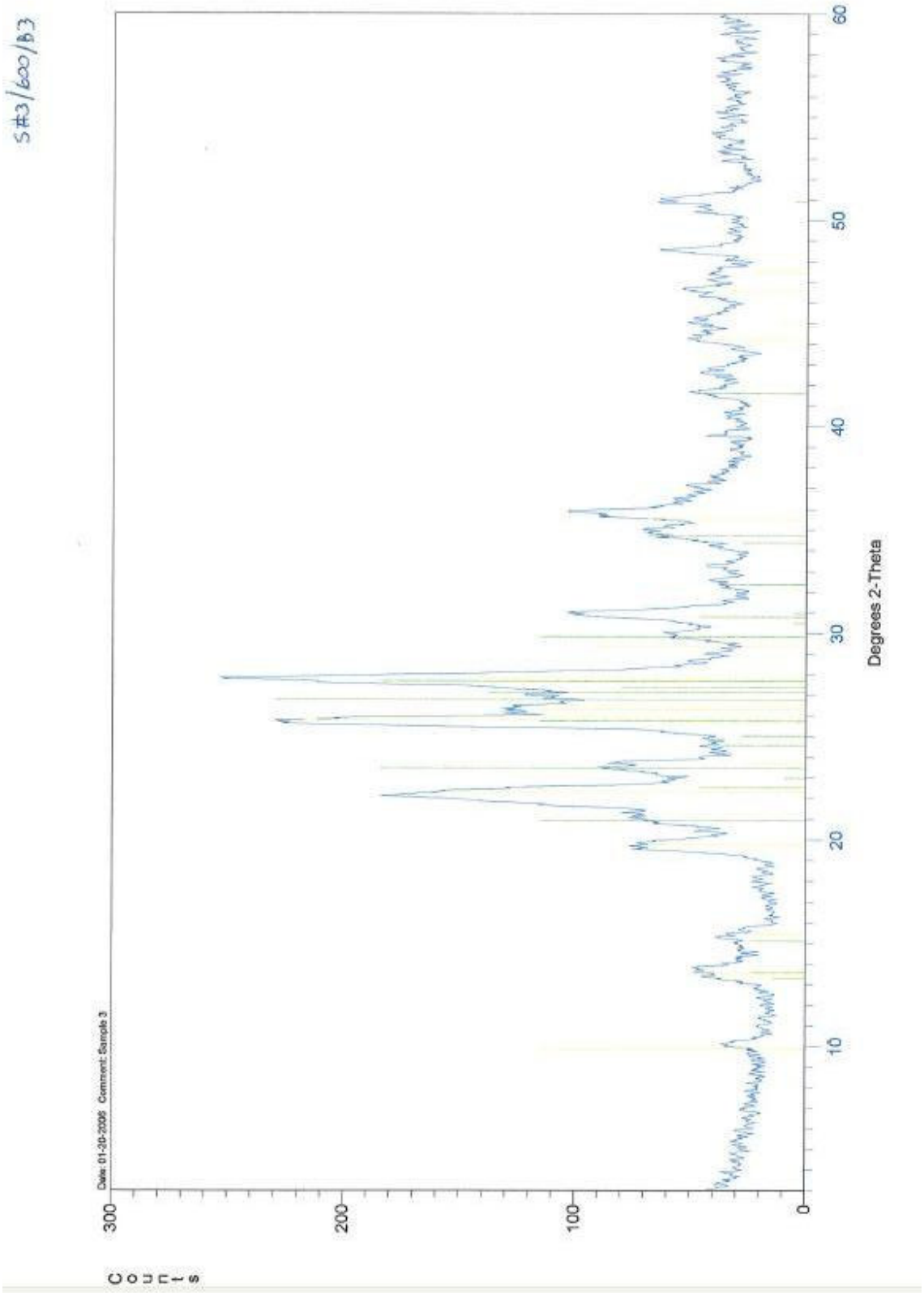
S#3/600/B3
Data: 01-30-2006 Comment: Sample 3
Counts
300
200
100
0
10
20
30
40
50
60
Degrees 2-Theta

Appendix F

Glossary of Terms

Absorption. The "process whereby a chemical is incorporated into the interior of a solid" (Reddi and Inyang, 2000). A broader definition of absorption is "the process of taking up and internalizing of a substance by another substance through chemical or molecular action (e.g. a gas absorbed by a liquid)" (Dooley JJ , 1999).

Accuracy, A measure of the degree of systematic errors being carried out when conducting a measurement. In this way, small systematic errors produce results of high accuracy.

Adsorption. The "process of attraction of chemicals to the surface of a solid" (Reddi and Inyang, 2000). It has also been defined as the accumulation of a chemical at the interface (Adamson, 1990) of a solid.

Aerobic respiration. A process by which microorganisms consume the electrons generated by an oxidation reduction reaction in the presence of oxygen. The process is controlled by the reaction (Snoeyink and Jenkins, 1980):

$O_{2(g)} + 4H^+ + 4e^- \rightarrow 2H_2O$

Anaerobic respiration. An anoxic process by which microorganisms consume the electrons generated as reduction reactions take place. Some of the common anaerobic reactions controlling this process are (Snoeyink and Jenkins, 1980):

Denitrification	$2NO_3^- + 12H^+ + 10e^- \rightarrow N2_{(g)} + 6H_2O$
Nitrate reduction	$NO_3^- + 10H^+ + 8e^- \rightarrow NH_4^+ + 3H_2O$
Fermentation	$CH_2O + 2H^+ + 2e^- \rightarrow CH_3OH$
Sulphate reduction	$SO_4^{2-} + 9H^+ + 8e^- \rightarrow HS^- + 4H_2O$
Methane fermentation	$CO_{2(g)} + 8H^+ + 8e^- \rightarrow CH_{4(g)} + 2H_2O$

Cation Exchange Capacity (CEC). The CEC of a soil (or material) is "defined by the amount of a cation (such as NH4+, Ba2+) that a soil can hold when a buffered or unbuffered salt solution is leached through the soil" (Blakemore, 1987).

Cleat. Natural fracture occurring in coal which defines the basic matrix structure of coal. Cleats form an orthogonal system in coal and are divided into face cleats (dominant cleats parallel to the maximum compressive stress) and butt cleats (parallel to the fold axis).

Conductivity (electrical conductivity). This is the ability of a solution to conduct an electrical current. An electrical current is conducted through a solution by the movement of ions in solution. The higher the dissolved ions concentrations, the higher the conductivity. It is temperature dependent (see specific conductance) and measured in mhos/cm or μS/cm (Snoeyink and Jenkins, 1980).

Darcy's Law. An empirical law discovered by Henry Darcy in 1856 which describes flow through a porous media (Freeze and Cherry, 1979). Darcy's law can be defined by the following equation:

$$v = -K \cdot \frac{\Delta h}{\Delta l}$$

where $\Delta h = h_2 - h_1$ or the difference in hydraulic head between two given points

$\Delta l = l_2 - l_1$ or the distance between two given points

$-K$ = constant inherent to the porous media and know as hydraulic conductivity (L/T)

v = the speed of liquid flow through the porous media (L/T)

Desorption. The reverse process of Sorption (Reddi and Inyang, 2000).

Diffusion. "The process whereby ionic or molecular constituents move under the influence of their kinetic activity in the direction of their concentration gradient" (Freeze and Cherry, 1979).

Exchangeable Sodium Percentage (ESP). This is the ratio (%) of sodium cations to the total CEC in a given soil. It can be calculated using the following equation:

$$ESP = \frac{Na \cdot 100}{CEC}$$

where Na and CEC are the sodium content and cation exchange capacity of the soil both generally expressed in meq/100g.

Fick's Law (or Fick's first Law). The law governing the diffusion process: "the mass of diffusing substance passing through a given cross section per unit time is proportional to the concentration gradient" (Freeze and Cherry, 1979). This law is generally expressed by:

$$F = -D \cdot \frac{dC}{dx}$$

where F = the mass flux (M/L^2T)

D = the diffusion coefficient (L^2/T)

C = the solute concentration (M/L^3)

dC/dx = concentration gradient (negative quantity in the direction of diffusion)

Gas flow test. A pilot operation for CSG well desorption. This involves pumping water out of a selected well for an extended period of time (months) to obtain relevant data (i.e. pressure for gas flow, water quality data, and aquifer properties) for CSG extraction.

Hydraulic conductivity (*K*). As defined in Darcy's Law definition, *K* is a measure of the rate at which a liquid can flow through a porous media. *K* has "high values for sand and gravel and low values for clay and most rocks" (Freeze and Cherry, 1979).

Hydraulic gradient. The differential form of $\Delta h/\Delta l$ (= dh/dl) as defined in Darcy's Law definition.

Ion exchange. The process of cation substitution in solids, therefore it is often considered a special case of absorption (Reddi and Inyang, 2000).

Precision. A measure of the extent of random errors being committed. For example, high precision relates to small random errors.

Random errors. Random fluctuations in measurements that are of a non-deterministic nature. These fluctuations could originate due to errors of judgment, ambient fluctuations, mechanical vibrations, and intrinsical random processes to mention a few (Meyer, 1975).

Relative error. A measurement of the deviation generated when measuring a property which has a true value which is known or inferred.

Relative error = $\delta x = \Delta x/x$

$\Delta x = x_o - x$

where,

x = true value

x_o = measured value

Δx = absolute error

Relative Standard Deviation (RSD). This is also known as the fractional standard deviation and is the standard deviation sample population divided by its average. Often expressed in percentage units.

Salinity. Is the total salt concentration found in water. It can be measured using TDS (mg/l) or specific conductance (dS/m).

SAR. This is the Sodium Adsortion Ratio and can be calculated for the irrigation water or for the soil-water solution itself. General guidelines, however, are based on the SAR of the irrigation water. The SAR value can be calculated using the following equation with concentrations in meq/l:

$$SAR = \frac{[Na]}{\sqrt{\frac{[Ca]+[Mg]}{2}}}$$

The SAR value needs to be adjusted for calcium precipitation specially in the presence of bicarbonate (Ayers, 1985).

Sorption. The term commonly used to include all the processes responsible for mass transfer: absorption, adsorption, and ion exchange (Reddi and Inyang, 2000). The word "sorbed" can be used to describe how CSG is held in the micropores of coal. That is, CSG is sorbed when it is contained within the coal micropores, and it is said to be "desorbed"when it is released by lowering of the piezometric pressure.

Specific conductance (specific conductivity or conductance). Is the conductivity of a solution measured at a reference temperature of 25°C. This value is usually expressed in mS/m (Hounslow, 1995).

Systematic errors. Errors of deterministic nature such as calibration errors, biased errors of judgment, varying efficiencies in observations and experimental conditions (Meyer, 1975).

References

Adamson, A.W., 1990, Physical chemistry of surfaces: New York, Wiley, xxi, 777 p.

Ayers, R.S., Westcot, D.W., and Food and Agriculture Organization of the United Nations., 1985, Water quality for agriculture: Rome, Food and Agriculture Organization of the United Nations, xii, 174 p.

Blakemore, L.C., Searle, P.L., Daly, B.K., and New Zealand. Soil Bureau., 1987, Methods for chemical analysis of soils: Lower Hutt, N.Z., NZ Soil Bureau Dept. of Scientific and Industrial Research, 103 p.

Dooley JJ , and http://energytrends.pnl.gov/index.htm, E.T.s., 1999, Glossary - Energy R&D, Global Trends in Policy and Investment., Volume 2005.

Freeze, R.A., and Cherry, J.A., 1979, Groundwater: Englewood Cliffs, N.J., Prentice-Hall, xvi, 604 p.

Hounslow, A., 1995, Water quality data : analysis and interpretation: Boca Raton, Lewis Publishers, 397 p.

Meyer, S.L., 1975, Data analysis for scientists and engineers: N.Y., Wiley, 513 illus. p.

Reddi, L.N., and Inyang, H.I., 2000, Geoenvironmental engineering : principles and applications: New York, Marcel Dekker, xii, 494 p.

Snoeyink, V.L., and Jenkins, D., 1980, Water chemistry: New York, Wiley, xiii, 463 p.

Bibliography

Adamson, A.W., 1990, Physical chemistry of surfaces: New York, Wiley, xxi, 777 p.

Alabama State Oil and Gas Board (AOGB), 2003, Coalbed Methane Resources of Alabama http://www.ogb.state.al.us, Volume 2005.

Alabaster, J.S., Lloyd, R., European Inland Fisheries Advisory Commission. Working Party on Water Quality Criteria for European Freshwater Fish., and European Inland Fisheries Advisory Commission. Working Party on Toxicity Testing Procedures., 1980, Water quality criteria for freshwater fish: London, Butterworths by arrangement with the Food and Agriculture Organization of the United Nations, xviii, 297 p.

ALL-Consulting, 2003, Handbook on Coal Bed Methane Produced Water: Management and Beneficial Use Alternatives.: Tulsa, Oklahoma, Ground Water Protection Research Foundation, US Department of Energy, National Petroleum Technology Office, Bureau of Land Management.

ALL-Consulting, and Montana Board of Oil and Gas Conservation, 2004, Coal Bed Methane primer. New Source of Natural Gas–Environmental Implications. Background and Development in the Rocky Mountain West: Tulsa, Oklahoma, US Department of Energy, National Petroleum Technology Office.

Allen, R.B., McIntosh, P.D., and Wilson, J.B., 1998, The distribution of plants in relation to pH and salinity on inland saline/alkaline soils in Central Otago, New Zealand. (vol 35, pg 517, 1997): New Zealand Journal of Botany, v. 36, p. 153-153.

American Public Health Association., American Water Works Association., and Water Environment Federation., 1999, Standard methods for the examination of water and wastewater: Washington, D.C., American Public Health Association, 1 computer optical disc p.

Amphlett, C.B., 1964, Inorganic ion exchangers: Amsterdam, New York,, Elsevier Pub. Co., x, 141 p. p.

ANZECC, and ARMCANZ, 2000, Australian and New Zealand Guidelines for Fresh and Marine Water Quality, ACT: Australian and New Zealand Environmental and Conservation Council (ANZECC), Agricultural and Resource Management

Council of Australia and New Zealand (ARMCANZ): Canberra.

Ayers, R.S., Westcot, D.W., and Food and Agriculture Organization of the United Nations., 1985, Water quality for agriculture: Rome, Food and Agriculture Organization of the United Nations, xii, 174 p.

Bartos, T.T., Ogle, K.M., Wyoming. State Engineer's Office., United States. Bureau of Land Management., and Geological Survey (US), 2002, Water quality and environmental isotopic analyses of ground-water samples collected from the Wasatch and Fort Union formations in areas of coalbead methane development : implications to recharge and ground-water flow, eastern Powder River Basin, Wyoming, Water-resources investigations report ; 02-4045: Cheyenne, Wyo; Denver, CO, US Dept. of the Interior US Geological Survey, Branch of Information Services distributor, p. vi, 88 , (4 folded).

Bauder, J., 2001, Quality and Characteristics of Saline and Sodic Water Affect Irrigation Suitability: MSU, Bozeman, MT, p. http://waterquality.montana.edu.

Blakemore, L.C., Searle, P.L., Daly, B.K., and New Zealand. Soil Bureau., 1987, Methods for chemical analysis of soils: Lower Hutt, N.Z., NZ Soil Bureau Dept. of Scientific and Industrial Research, 103 p.

Bodger, F., 2005, The use of coal seam gas waters in New Zealand to treat acid mine drainage, Civil Engineering: Christchurch, University of Canterbury, p. 44.

Boelter, A.M., Lamming, F.N., Farag, A.M., and Bergman, H.L., 1992, Environmental effects of saline oil-field discharges on surface waters: Environmental Toxicology and Chemistry, v. 11, p. 1187-1195.

Bolan, N.S., and Mowat, C., 2000, Potential value of zeolite in the removal of contaminants from wastewater stream, Water 2000, Water Conference and Expo, "Guarding the Global Resource": Auckland, NZWWA, p. 430-443.

Bresler, E., McLean, B.L., and Carter, D.L., 1982, Saline and sodic soils: Principles-dynamics-modeling., Advanced series in agricultural sciences., Volume 10: New York, NY, Springer-Verlag.

Bryant, F.B., and Yarnold, P.R., 1995, Principal components analysis: Thousand Oaks, CA, Sage Publications.

Burkett, W.C., McDaniel, R., and Hall, W.L., 1991, The Evaluation and Implementation

of a Comprehensive Production Water Management Plan, Coalbed Methane Symposium: Tuscaloosa, Alabama.

Cameron, K.C., Di, H.J., Anwar, M.R., Russell, J.M., and Barnett, J.W., 2003, The "critical" ESP value: does it change with land application of dairy factory effluent?: New Zealand Journal of Agricultural Research, v. 46, p. 147-154.

Carothers, W.W., and Kharaka, Y.K., 1980, Stable carbon isotopes of HCO3- in oil-field waters--implications for the origin of CO2: Geochimica et Cosmochimica Acta, v. 44, p. 323-332.

Cavanagh, J., and Coakley, J., 2005, An introduction to policy on metal contaminants, *in* Moore, T.A., Black, A., Centeno, J.A., Harding, J.S., and Trumm, D.A., eds., Metal Contaminants in New Zealand, Volume In Press, Corrected Proof: Christchurch, resolutionz press, p. 5-23.

Cave, M., 2002, Turning a coalbed methane project into a co-producing hydrocarbon project, 2002 New Zealand Petroleum Conference proceedings: Wellington, N.Z., New Zealand Crown Minerals, p. 13.

Cave, M., and Syme, A., 2002, Impact of Operational and Environmental Issues on the development of Coalseam Gas in New Zealand, 2004 New Zealand Petroleum Conference proceedings: Wellington, N.Z., New Zealand Crown Minerals, p. 11.

Chapelle, F., 2001, Ground-water microbiology and geochemistry: New York, N.Y., Wiley, xvii, 477 p.

Chatfield, C., 1996, The analysis of time series : an introduction: London, Chapman & Hall, xii, 283 p.

Christie, T., Brathwaite, B., and Thomson, B., 2002, Mineral Commodity Report 23 - Zeolites, New Zealand Mining, Volume 31.

Clark, I.D., and Fritz, P., 1997, Environmental isotopes in hydrogeology: Boca Raton, FL, CRC Press/Lewis Publishers, 328 p. p.

Claypool, G.E., and Kaplan, I.R., 1974, The origin and distribution of methane in marine sediments: Marine Science, v. 3, p. 99-139.

Collier, K.J., Ball, O.J., Graesser, A.K., Main, M.R., and Winterbourn, M.J., 1990, Do organic and anthropogenic acidity have similar effects on aquatic fauna?: Oikos, v. 59, p. 33-38.

Colorado Oil and Gas Conservation Comission, 2001, Webpage database for production.

Comrey, A.L., and Lee, H.B., 1992, A first course in factor analysis: Hillsdale, N.J., L. Erlbaum Associates, xii, 430 p.

Coombs, D.S., 1959, Zeolite uses and New Zealand deposits, Fourth Triennial Mineral Conference, Volume 6, Paper 162: School of Mines and Metallurgy, Dunedin, University of Otago, p. 6.

Curtin, D., Steppuhn, H., and Selles, F., 1994, Structural Stability of Chernozemic Soils as Affected by Exchangeable Sodium and Electrolyte Concentration: Canadian Journal of Soil Science, v. 74, p. 157-164.

Davies-McConchie, F., McConchie, D., Clark, M., Lin, C., Pope, S., and Ryffel, T., 2002, A new approach to the treatment and management of sulphidic mine tailings, waste rock and acid mine drainage: New Zealand Mining, v. 31, p. 7-15.

Davis, H.A., Simpson, T.E., Lawrence, A.W., Miller, J.A., and Anonymous, 1993, Coalbed methane produced water management strategies in the Black Warrior Basin of Alabama: Proceedings - International Coalbed Methane Symposium, v. 1993, p. 317-338.

Davis, J.C., 2002, Statistics and data analysis in geology: New York, J. Wiley, xvi, 638 p. p.

Davis, W.N., Bramblett, R.G., and Zale, A.V., 2006, The effects of coalbed natural gas activities on fish assemblages: a review of the literature: Bozeman, Montana State University, p. 48.

—, 2006, Effects of coalbed natural gas activities on fish assemblages in the Powder River Basin, 2005, *in* Montana Cooperative Fishery Research Unit, ed.: Bozeman, Montana State University, p. 3.

Decker, A.D., Klusman, R., Horner, D.M., and Anonymous, 1987, Geochemical techniques applied to the identification and disposal of connate coal water: Proceedings - International Coalbed Methane Symposium, v. 1987, p. 229-242.

Deffeyes, K.S., 1965, The Deffeyes diagram for 25°C: Limnology and Oceanography, v. 10, p. 412.

Deidre B. Boysen, J.E.B., Jessica A. Boysen, 2002, Strategic produced water management and disposal economics in the Rocky Mountain Region, Ground

water protection council.

Department of Conservation, 2006, New Zealand map service, DOCgis GeoSpatial Information Platform, p. http://extranet.doc.govt.nz/bip/.

—, 2006, New Zealand's Wetlands of International Significance: Whangamarino, http://www.doc.govt.nz/Conservation/Wetlands/.

Detmer, E., 2005, Zeolite water conditioning system: Sheridan, p. Personal conversation.

Dooley JJ , and http://energytrends.pnl.gov/index.htm, E.T.s., 1999, Glossary - Energy R&D, Global Trends in Policy and Investment., Volume 2005.

Edbrooke, S.W., Sykes, R., and Pocknall, D.T., 1994, Geology of the Waikato Coal Measures, Waikato Coal Region, New Zealand., Institute of Geological & Nuclear Sciences Monograph, p. 236.

Eisler, R., 1991, Cyanide Hazards to Fish, Wildlife, and Ivertebrates, US Fish and Wildlife Service.

Energy Information Administration, 2004, Advance Summary: US Crude Oil, Natural Gas, and Natural Gas Liquids Reserves 2003 Annual Report: Washington, DC 20585, Office of Oil and Gas, US Department of Energy, p. 18.

Environment Waikato, 2002, Waikato Regional Plan - Proposed plan and maps on CD-ROM as amended by decisions (appeals version), *in* Waikato Regional Council, ed.: Hamilton, Waikato Regional Council,.

Environment Waikato, 2006, River Levels and Rainfall. Whangamarino Wetland. Levels at Ropeway on Island Block Road, Meremere, Volume 2006: Hamilton, Environment Waikato, p. web page and online database system.

Eser, P., and Rosen, M.R., 2000, Effects of artificially controlling levels of Lake Taupo, North Island, New Zealand, on the Stump Bay wetland: New Zealand Journal of Marine and Freshwater Research, v. 34, p. 217-230.

Freeze, R.A., and Cherry, J.A., 1979, Groundwater: Englewood Cliffs, N.J., Prentice-Hall, xvi, 604 p.

Gamson, P.D., Beamish, B.B., and Johnson, D.P., 1993, Coal Microstructure and Micropermeability and Their Effects on Natural-Gas Recovery: Fuel, v. 72, p. 87-99.

—, 1996, Coal Microstructure and Micropermeability and Their Effects on Natural-Gas

Recovery, *in* Gayer, R.A., and Harris, I.H., eds., Coalbed methane and coal geology: London, Geological Society, p. 165-179.

Gas Technology Institute, 2002, http://www.gastechnology.org/.

Gayer, R.A., and Harris, I.H., 1996, Coalbed methane and coal geology: London, Geological Society, viii, 344 p.

Gilbert, R.O., 1987, Statistical methods for environmental pollution monitoring: New York, Van Nostrand Reinhold Co., x, 320 p.

Gillard, G., Trumm, D., Manhire, D., Taulis, M., and Muckle, F., 2003, Final Report Exploration Permit 40 396 Hawkdun: Christchurch, CRL Energy Ltd, p. 51.

GRI (Gas Research Institute), 2000, Coalbed Methane Potential of the US Rocky Mountain Region, p. 3pp.

Haan, C.T., 1977, Statistical methods in hydrology: Ames, Iowa State University Press, xv, 378 p.

Hach Company, 2003, Water analysis handbook : drinking water, wastewater, seawater, boiler/cooling water, ultrapure water: Loveland, Colo., Hach, 1268 p.

Hagmaier, J.L., 1971, Groundwater flow, hydrogeochemistry, and uranium deposition in the Powder River Basin, Wyoming [Ph.D thesis]: Grand Forks, University of North Dakota, Department of Geology.

Hamilton, T.M., 1970, Groundwater flow in part of the Little Missouri River Basin, North Dakota [Ph.D thesis]: Grand Forks, University of North Dakota, Department of Geology.

Hatcher, L., 1994, A step-by-step approach to using the SAS system for factor analysis and structural equation modeling: Cary, N.C., SAS Institute, xiv, 588 p.

Hem, J.D., 1985, Study and interpretation of the chemical characteristics of natural water, U. S. Geological Survey Water-Supply Paper, p. 263.

Higgins, C.L., and Wilde, G.R., 2005, The role of salinity in structuring fish assemblages in a prairie stream system: Hydrobiologia, v. 549, p. 197-203.

Hoffman, R.D., and Animated Software Company., 2004, Internet glossary of pumps: [California], Animated Software Co.

Hounslow, A., 1995, Water quality data : analysis and interpretation: Boca Raton, Lewis Publishers, 397 p.

IEA Coal Industry Advisory Board., 1994, Global methane and the coal industry : a two-part report on methane emissions from the coal industry and coalbed methane recovery and use: Paris.Washington, D.C., OECD; OECD Publications and Information Centre distributor, 67 p.

Jenden, P.D., and Kaplan, I.R., 1986, Comparison of microbial gases from the Middle America Trench and Scripps Submarine Canyon: implications for the origin of natural gas: Applied Geochemistry, v. 1, p. 631-646.

Jensen, M.E., 1983, Design and operation of farm irrigation systems: St. Joseph, Mich., American Society of Agricultural Engineers, xi, 829 p. p.

Ji, Z.-G., 2005, Water quality models: chemical principles: Hoboken, New Jersey., John Wiley and Sons, Inc.

Johnson, K.C., 2004, The New Zealand coal seam gas scene, 2004 New Zealand Petroleum Conference proceedings: Wellington, N.Z., New Zealand Crown Minerals, p. 7.

Kaiser, H.F., 1958, The Varimax Criterion for Analytic Rotation in Factor-Analysis: Psychometrika, v. 23, p. 187-200.

Karassik, I.J., 1986, Pump handbook: New York, McGraw-Hill, 1 v. (various pagings) p.

Kirkpatrick, A., Pearson, K., and Bauder, J., 2003, The Use of Coal Bed Methane Product Water to Enhance Wetland Function: MSU, Bozeman, MT, p. 11.

Kirkpatrick, A.D., 2005, Assessing constructed wetlands for beneficial use of saline-sodic water: Bozeman, Montana State University,.

Kjeldsen, P., Barlaz, M.A., Rooker, A.P., Baun, A., Ledin, A., and Christensen, T.H., 2002, Present and Long-Term Composition of MSW Landfill Leachate: A Review: Critical Reviews in Environmental Science and Technology, v. 32, p. 297-336.

Knight, R.L., 1997, Wildlife habitat and public use benefits of treatment wetlands: Water Science and Technology, v. 35, p. 35-43.

Krevelen, D.W.v., 1961, Coal: typology, chemistry, physics, constitution: Amsterdam, New York,, Elsevier Pub. Co., xviii, 514 p.

Kristin, K., Bauder, J., and Wheaton, J.R., 2006, http://waterquality.montana.edu/docs/methane/cbmfaq.shtml, Water quality and Irrigation Management, Volume 2006: Bozeman, Montana State University.

Kuuskraa, V.A., 1989, Coalbed Methane Sparks a New Energy Industry: Oil & Gas Journal, v. 87, p. 49-&.

Landcare Research New Zealand Ltd, 2000, The New Zealand National Soils Database Spatial Extension, Soil Fundamental Data Layers: Lincoln, Landcare Research New Zealand Ltd.

—, 2000, New Zealand Land Resource Inventory (NZLRI): Lincoln, Landcare Research New Zealand Ltd.

Law, B.E., and Rice, D.D., 1993, Hydrocarbons from coal: Tulsa, Okla., USA, American Association of Petroleum Geologists, viii, 400 p.

Lee, R.W., 1981, Geochemistry of water in the Fort Union Formation of the northern Powder River Basin, southeastern Montana, U. S. Geological Survey Water-Supply Paper.

Lee-Ryan, P.B., Fillo, J.P., Tallon, J.T., and Evans, J.M., 1991, Evaluation of management options for coalbed methane produced water, Coalbed methane symposium: Tuscaloosa, Alabama, The University of Alabama,, p. 31-41.

LFTB Study Group., 1986, South Island Phase II Lignite Site Selection Studies Programme. Resource definition, geotechnical, hydrology, and mine planning studies. Hawkdun deposit.: Wellington, N.Z., Liquid Fuels Trust Board.

Main, M.R., 1988, Factors influencing the distribution of kokopu and koaro (Pisces: Galaxiidae) : a thesis submitted in partial fulfilment of the requirements for the degree of Master of Science in Zoology in the University of Canterbury, 127 leaves, [36] leaves of plates p.

Maloszewski, P., and Zuber, A., 1982, Determining the Turnover Time of Groundwater Systems with the Aid of Environmental Tracers .1. Models and Their Applicability: Journal of Hydrology, v. 57, p. 207-231.

Matalas, N.C., and Reiher, B.J., 1967, Some Comments on Use of Factor Analyses: Water Resources Research, v. 3, p. 213-&.

McBeth, I., Reddy, K.J., and Skinner, Q.D., 2003, Chemistry of trace elements in coalbed methane product water: Water Research, v. 37, p. 884-890.

McBeth, I.H., Reddy, K.J., and Skinner, Q.D., 2003, Coalbed methane product water chemistry in three Wyoming watersheds: Journal of the American Water

Resources Association, v. 39, p. 575-585.

McIntosh, A., and McDowall, R., 2004, Fish Communities in rivers and streams, *in* Harding, J.S., New Zealand Hydrological Society., and New Zealand Limnological Society., eds., Freshwaters of New Zealand: [Wellington, N.Z.], New Zealand Hydrological Society ; New Zealand Limnological Society, p. 17.1-17.9.

McLaren, R.G., and Cameron, K.C., 1990, Soil science : an introduction to the properties and management of New Zealand soils: Auckland, N.Z., Oxford University Press, viii, 294 , 8 of plates p.

Menneer, J.C., McLay, C.D.A., and Lee, R., 2001, Effects of sodium-contaminated wastewater on soil permeability of two New Zealand soils: Australian Journal of Soil Research, v. 39, p. 877-891.

Meyer, S.L., 1975, Data analysis for scientists and engineers: N.Y., Wiley, 513 illus. p.

Milke, M.W., and Huitric, R.L., 1993, Simulating Errors in Statistical Tests of Leachate-Impacted Groundwater Quality: Ground Water, v. 31, p. 645-653.

MINITAB Inc, 2005, MINITAB, Volume 2005: Pennsylvania.

Montana Board of Oil and Gas Conservation, 2005, On-Line Data, http://bogc.dnrc.state.mt.us.

Montana State University, 2006, Frequently Asked Questions Coal Bed Methane (CBM), Volume 2006: Bozeman, Montana State University, p. Web page http://waterquality.montana.edu/docs/methane/cbmfaq.shtml.

—, 2006, Coal Bed Methane Water Treatment System, http://waterquality.montana.edu/docs/methane/cbm-wts.shtml, Montana State University., p. Drake Engineering Inc. Water Treatment System.

Montgomery, S.L., 1999, Powder River Basin, Wyoming: An expanding coalbed methane (CBM) play: Aapg Bulletin-American Association of Petroleum Geologists, v. 83, p. 1207-1222.

Montgomery, S.L., Tabet, D.E., and Barker, C.E., 2001, Upper Cretaceous Ferron Sandstone: Major Coalbed Methane Play in Central Utah: AAPG Bulletin, v. 85, p. 199-219.

Moore, T.A., Manhire D.A., Flores R.M., 2002, Coalbed Methane opportunities in New Zealand: Similarities with the Powder River Basin coalbed methane paradigm, AusIMM Conference: Auckland, New Zealand.

Moore, T.A., and Shearer, J.C., 2003, Peat/coal type and depositional environment - Are they related?: International Journal of Coal Geology, v. 56, p. 233-252.

Mount, D.R., Drottar, K.R., Gulley, D.D., and Fillo, J.P., 1993, Use of Laboratory Toxicity Data for Evaluating the Environmental Acceptability of Produced Water Discharge to Surface Waters, v. 46, p. 175.

Mount, D.R., O'Neil, P.E., and Evans, J.M., 1993, Discharge of coalbed product water to surface waters: assessing, predicting, and preventing ecological effects: Quarterly Review of Methane from Coal Seams Technology, v. 11, p. 18-25.

Mowatt, C., 2000, Preliminary investigations into the characteristics and potential uses for Ngakuru zeolites, 2000 New Zealand Minerals & Mining Conference Proceedings.

Nelson, C.R., 2005, Geologic assessment of the natural gas resources in the Powder River Basin Fort Union Formation coal seams, Proceedings - International Coalbed Methane Symposium, Volume 2005, p. 14.

New Mexico Oil Conservasion Division, New Mexico Energy, Minerals and Natural Resources Department - OCD Webpage, Development RBDMS.

New Zealand. Mines Division., Longworth McKenzie Cole., and Worley Consultants Ltd., 1983, New Zealand coal resources survey : preliminary mining and environmental constraints assessment pilot study : Maramarua coalfield: [Wellington, N.Z.], Mines Division Ministry of Energy, 2 v. p.

New Zealand. Ministry of Health., and New Zealand. National Drinking-Water Standards Review Expert Working Group., 2000, Drinking-water standards for New Zealand, 2000: Wellington, N.Z., Ministry of Health, xiii, 130 p.

Nguyen, M.L., and Tanner, C.C., 1998, Ammonium removal from wastewaters using natural New Zealand zeolites: New Zealand Journal of Agricultural Research, v. 41, p. 427-446.

Nielsen, D., 1990, Practical handbook of ground-water monitoring: Chelsea, MI, Lewis Publishers, x, 717 p.

NIWA, 2006, NIWA Atlas of New Zealand Freshwater Fishes, Common smelt (Retropinna retropinna), http://www.niwascience.co.nz/rc/freshwater/fishatlas/species/common_smelt, Volume 2006, NIWA.

—, 2006, NZFFD, New Zealand Freshwater Fish Database, NIWA, p. http://fwdb.niwa.co.nz/.

Nobes, D.C., and Schneider, G.W., 1996, Results of downhole geophysical measurements and vertical seismic profile from the Canandaigua borehole of New York State Finger Lakes: Special Paper - Geological Society of America, v. 311, p. 51-63.

Nuccio, V.F., 2002, Coalbed Methane- What is it? Where is it? And why all the fuss?, Coalbed methane of North America, II Rocky Mountain Association of Geologists, 2002: Denver, Colo., The Rocky Mountain Association of Geologists, p. 6.

NZ Natural Zeolite, 2006, What is Zeolite?, www.zeolite.co.nz.

O'Neil, P.E., Harris, S.C., and Mettee, M.F., 1989, Stream Monitoring of Coalbed Methane Produced Water from the Cedar Cove Degasification Field, Alabama, The 1989 Coalbed Methane Symposium: Tuscaloosa, Alabama, The University of Alabama,.

O'Neil, P.E., Harris, S.C., Mettee, M.F., McGregor, S.W., and Shepard, T.E., 1991, Long-term biomonitoring of a product water discharge from the Cedar Cove degasification field, Alabama, Geological Survey of Alabama (Bulletin), Tuscaloosa, Volume 141.

Oremland, R.S., Marsh, L.M., and Polcin, S., 1982, Methane Production and Simultaneous Sulfate Reduction in Anoxic, Salt-Marsh Sediments: Nature, v. 296, p. 143-145.

Oster, J.D., and Schroer, F.W., 1979, Infiltration as Influenced by Irrigation Water-Quality: Soil Science Society of America Journal, v. 43, p. 444-447.

Perry, R.H., Chilton, C.H., and Perry, J.H., 1973, Chemical engineers' handbook: Tokyo, McGraw-Hill Kogakusha, 1 v. (various pagings) p.

Pope, S., 2004, Coal Seam Gas Exploration Results: Hawkdun Coalfield, Central Otago, 2002-2004.: Christchurch, CRL Energy Ltd, p. 42.

—, 2004, 2004 Coal Seam Gas Exploration Results: Ashers-Waituna Lignite Deposit, PEP 38-217, Southland.: Christchurch, CRL Energy Ltd, p. 41.

Pope, S., and Trumm, D., 2004, Coal Seam Gas Desorption Results: Drill Holes C1, K1 and K3, Maramarua Coalfield, Waikato, 2003.: Christchurch, CRL Energy Ltd, p. 27.

PTTC, 2000, Coal bed methane strategraphic traps in the ferron coals of east-central Utah, PTTC Rocky Mountain Newsletter, Volume September.

Ralph J. Haefner, and US Geological Survey, 2002, Water Quality at an Abandoned Coal Mine Reclaimed with PFBC By-Products: Columbus, Ohio, US Geological Survey, p. 37.

Reddi, L.N., and Inyang, H.I., 2000, Geoenvironmental engineering : principles and applications: New York, Marcel Dekker, xii, 494 p.

Rhoades, J.D., 1982, Reclamation and management of salt-affected soils after drainage. In Rationalisation of water

and soil research and management, Proceedings of the First Annual Western Provincial Conference: Lethbridge, Canada, p. 123–197.

Rice, C.A., and Anonymous, 1999, Waters co-produced with coalbed methane from the Ferron Sandstone in east-central Utah; chemical and isotopic composition, volumes, and impacts of disposal: Abstracts with Programs - Geological Society of America, v. 31, p. 385.

Rice, C.A., and Bartos, T.T., 2001, Nature and Characteristics of Water Co-Produced with Coalbed Methane with emphasis on the Powder River Basin, USGS Coalbed Methane Field conference May 9-10, 2001., Volume Open File Report 01-235: Casper, Wyoming., USGS.

Rice, C.A., Breit, G.N., Hills, F.A., and Anonymous, 1993, Variations of Mg, Sr, and K in sulfate minerals from the Paradox Formation, Utah; clues to the composition of depositional and diagenetic brines: Abstracts with Programs - Geological Society of America, v. 25, p. 253.

Rice, C.A., Ellis, M.S., and Bullock, J.H., Jr., 2000, Water co-produced with coalbed methane in the Powder River Basin, Wyoming: preliminary compositional data: Open-File Report - U. S. Geological Survey.

Rice, D.D., 1992, Controls, habitat, and resource potential of ancient bacterial gas, *in* Vially, R., ed., Bacterial gas : proceedings of the conference held in Milan, September 25-26, 1989: Paris, Editions Technip, p. 91-118.

—, 1993, Composition and origin of coalbed gas, *in* Law, B.E., and Rice, D.D., eds., Hydrocarbons from coal, Volume AAPG Studies in Geology, American Association of Petroleum Geologists, p. 159-184.

Rice, D.D., and Claypool, G.E., 1981, Generation, accumulation, and resource potential of biogenic gas: AAPG Bulletin, v. 65, p. 5-25.

Robb, M.R., 2000, Information on water allocation in New Zealand, Lincoln Environmental Client Report 4375/1, Ministry for the Environment, p. 180.

Robinson, K.M., 2003, Effects of saline-sodic water on EC, SAR, and water retention: Bozeman, Montana State University.

Rosen, M.R., 2001, Hydrochemistry of New Zealand's Aquifers, *in* Rosen, M.R., and White, P.A., eds., Groundwaters of New Zealand: Wellington, New Zealand, New Zealand Hydrological Society, p. 77-110.

Rosen, M.R., and White, P.A., 2001, Groundwaters of New Zealand: Wellington, N.Z., New Zealand Hydrological Society, xiii, 498 p.

Russell, L.L., 1976, Chemical aspects of groundwater recharge with wastewaters: Berkeley, University of California.

Salmon, J.E., and Hale, D.K., 1959, Ion exchange; a laboratory manual: London,, Butterworths Scientific Publications, 136 p. p.

Sanders, F., Gustin, S., and Pucel, P., 2001, Natural treatment of CBM produced water: field observations., CBM Associates Inc.,, Funded by Marathon Oil Company.

Scarsbrook, M.R., and National Institute of Water and Atmospheric Research (N.Z.), 2003, A guide to the groundwater invertebrates of New Zealand: Wellington [N.Z.], Niwa, 59 p.

Schoell, M., 1980, The hydrogen and carbon isotopic composition of methane from natural gases of various origins: Geochimica et Cosmochimica Acta, v. 44, p. 649-661.

Schwochow, S.D., Nuccio, V.F., Rocky Mountain Association of Geologists., Gas Research Institute., and Petroleum Technology Transfer Council (US), 2002,

Coalbed methane of North America, II Rocky Mountain Association of Geologists, 2002: Denver, Colo., The Association, vi, 108 p.

Settle, T., Mollock, G.N., Hinchman, R.R., and Negri, M.C., 1998, Engineering the use of green plants to reduce produced water disposal volume., Society of Petroleum Engineers: Inc. Devon Energy Corporation, Oklahoma City, OK. Argonne National Laboratory, Argonne IL.

Shainberg, I., and Letey, J., 1984, Response of Soils to Sodic and Saline Conditions: Hilgardia, v. 52, p. 1-57.

Shapiro, S.S., and Wilk, M.B., 1965, An Analysis of Variance Test for Normality (Complete Samples): Biometrika, v. 52, p. 591-&.

Shaw, R.J., 1996, A unified soil property and sodicity model of salt leaching and water movement [PhD thesis], University of Queensland.

Shaw, R.J., Thorburn, P.J., and Dowling, A.J., 1987, Principles of landscape, soil and water salinity: Processes and management options, Proceedings of Brisbane Region Salinity

Workshop: Part A, in Landscape, soil and water salinity: Brisbane, Queensland Department of Primary Industries.

Skaar, D., Farag, A., and Harper, D., 2005, National pollution discharge elimination system. Toxicity of the major salt (sodium bicarbonate) from coalbed methane production to fish in the Tongue and Powder river drainages in Montana, Semi-annual progress report prepared for US Environmental Protection Agency: Helena.

Skaar, D., Morris, B., and Farag, A., 2004, National pollution discharge elimination system. Toxicity of the major salt (sodium bicarbonate) from coalbed methane production to fish in the Tongue and Powder river drainages in Montana, Progress report prepared for US Environmental Protection Agency: Helena.

Slater, M.J., 1991, Principles of ion exchange technology: Oxford [England] ; Boston, Butterworth Heinemann, xiii, 182 p.

Snoeyink, V.L., and Jenkins, D., 1980, Water chemistry: New York, Wiley, xiii, 463 p.

Soil Improvement Committee, 1995, Western fertilizer handbook: Danville, Ill., Interstate Publishers, xiii, 338 p., [12] p. of plates p.

Stach, E., 1982, Stach's textbook of coal petrology: Berlin, Borntraeger, 535 p.

Stumm, W., and Morgan, J.J., 1996, Aquatic chemistry : chemical equilibria and rates in natural waters: New York, Wiley, xvi, 1022 p.

Suarez, D.L., 1981, Relationship between pHc and sodium adsorption ratio (SAR) and an alternative method of

estimating SAR of soil or drainage waters: Soil Science Society of America Journal, v. 45, p. 469-475.

Sumner, M.E., 1992, The electrical double layer and clay dispersion, *in* Sumner, M.E., and Stewart, B.A., eds., Soil crusting: chemical and physical processes, Volume Adv. Soil Sci.: Boca Raton, FL, Lewis Publishers.

Tabachnick, B.G., and Fidell, L.S., 2001, Using multivariate statistics: Boston, Allyn and Bacon, xxvi, 966 p.

Taulis, M., Milke, M., Trumm, D., O'Sullivan, A., Nobes, D., and Manhire, D., 2005, Characterisation of Coal Seam Gas waters in New Zealand, 2005 New Zealand Minerals Conference: Auckland, New Zealand.

The Seacreast Group, 2003, Water quality data collected from water wells in the Raton basin, Colorado: Denver, Colorado, Colorado Oil and Gas State Conservation Comission.

Todd, D.K., 1980, Groundwater hydrology: New York, Wiley, xiii,535 p.

Trumm, D., Black, A., Gordon, K., Cavanagh, J., O'Halloran, K., and de Joux, A., 2005, Acid mine drainage assessment and remediation at an abandoned West Coast coal mine, Metal Contaminants in New Zealand: Christchurch, resolutionz.

US Environmental Protection Agency, 2004, Evaluation of Impacts to Underground Sources of Drinking Water by Hydraulic Fracturing of Coalbed Methane Reservoirs, US Environmental Protection Agency.

US Environmental Protection Agency, 2004, Statistical Primer, Volume 2005, p. web page.

US Environmental Protection Agency, 2004, 2005, Exposure Assessment Models, US Environmental Protection Agency, p. web page.

US Environmental Protection Agency, and Advanced Resources International, 2002, Enhanced CBM Recovery, US Environmental Protection Agency.

US Geological Survey, 2000, Coal bed methane: potential and concerns, USGS Fact

Sheet FS-123-00.

—, 2000, Water Produced with Coal-Bed Methane, USGS Fact Sheet FS-156-00.

US Salinity Laboratory Staff, 1954, Diagnosis and improvement of saline and alkali soils: [Washington,, US Govt. Print. Off.], vii, 160 p. p.

UCLA Academic Technology Services, Factor Analysis Using SAS PROC FACTOR, *in* Services, U.A.T., ed., Volume 2005: Los Angeles, p. Web page.

Van Voast, W.A., 2003, Geochemical signature of formation waters associated with coalbed methane: Aapg Bulletin, v. 87, p. 667-676.

Van Voast, W.A., and Anonymous, 1991, Hydrogeologic aspects of coal-bed methane occurrence, Powder River Basin: AAPG Bulletin, v. 75, p. 1142-1143.

Van Voast, W.A., and Hedges, R.B., 1975, Hydrogeologic aspects of existing and proposed strip coal mines near Decker, Southeastern Montana.: Bulletin - Montana Bureau of Mines and Geology, v. 97, p. 31.

Vially, R., Azienda generale italiana petroli., International Union of Geological Sciences., and Institut franðcais du pâetrole., 1992, Bacterial gas : proceedings of the conference held in Milan, September 25-26, 1989: Paris, Editions Technip, x, 242 p.

Wachinski, A.M., and Etzel, J.E., 1997, Environmental ion exchange : principles and design: Boca Raton, CRC/Lewis Publishers, 136 p. p.

Wallis, J.R., 1967, When Is It Safe to Extend a Prediction Equation - an Answer Based Upon Factor and Discriminant Function Analysis: Water Resources Research, v. 3, p. 375-&.

Wesolowski, D.J., 1992, Aluminum speciation and equilibria in aqueous solution: I. The solubility of gibbsite in the system Na-K-Cl-OH-Al(OH)4 from 0 to 100[deg]C: Geochimica et Cosmochimica Acta, v. 56, p. 1065-1091.

West, D.W., Boubée, J.A.T., and Barrier, R.F.G., 1997, Responses to pH of nine fishes and one shrimp native to New Zealand freshwaters: New Zealand Journal of Marine and Freshwater Research, v. 31, p. 461-468.

Wheaton, J.R., Bobst, A.L., Donato, T.A., and Anonymous, 2004, Ground-water monitoring in the Powder River Basin, southeastern Montana: Abstracts with Programs - Geological Society of America, v. 36, p. 187.

Wheaton, J.R., and Donato, T.A., 2004, COALBED-METHANE BASICS: Powder River Basin, Montana: Butte, Montana Bureau of Mines and Geology, p. 20.

Whiticar, M.J., Faber, E., and Schoell, M., 1986, Biogenic methane formation in marine and freshwater environments: CO2 reduction vs. acetate fermentation--Isotope evidence: Geochimica et Cosmochimica Acta, v. 50, p. 693-709.

Williams, W.D., 2001, Anthropogenic salinization of inland waters: Hydrobiologia, v. 466, p. 329-337.

Williams. B, 2001, Personal communication between Mr. Williams/ V.P., Redstone and Dr. Langhus/ALL-LLC. March 23, 2001.

Woltemate, I., Whiticar, M.J., and Schoell, M., 1984, Carbon and hydrogen isotopic composition of bacterial methane in a shallow freshwater lake: Limnology and Oceanography, v. 29, p. 985-992.

Wyoming State Engineers Office, and Wyoming State Geological Survey, 2005, The Coal Section.